LATE QUATERNARY HISTORIES OF LAKES HURON AND MICHIGAN: A STABLE ISOTOPE INVESTIGATION OF SEDIMENT CORES AND MODERN BIOGENIC CARBONATES

(Spine title: The Late Quaternary Histories of Lakes Huron and Michigan)

(Thesis format: Integrated Article)

by

Rebecca A. Macdonald

Graduate Program in Geology

A thesis submitted in partial fulfillment
of the requirements for the degree of
Doctor of Philosophy

The School of Graduate and Postdoctoral Studies
The University of Western Ontario
London, Ontario, Canada

THE UNIVERSITY OF WESTERN ONTARIO
SCHOOL OF GRADUATE AND POSTDOCTORAL STUDIES

CERTIFICATE OF EXAMINATION

Supervisor	Examiners
Dr. Fred J. Longstaffe	Dr. T. Kurtis Kyser
Supervisory Committee	Dr. Katrina Moser
Dr. Stephen R. Hicock	Dr. Elizabeth Webb
Dr. Robert Schincariol	Dr. Avner Ayalon

The thesis by

Rebecca Amy Macdonald

entitled:

Late Quaternary Histories of Lakes Huron and Michigan: A Stable Isotope Investigation of Sediment Cores and Modern Biogenic Carbonates

is accepted in partial fulfillment of the
requirements for the degree of
Doctor of Philosophy

Date____________________________

Chair of the Thesis Examination Board

ABSTRACT

Late Quaternary histories are investigated here for sediment cores from Lakes Huron and Michigan, using the oxygen- and carbon-isotope compositions of biogenic carbonates and the oxygen- and hydrogen-isotope compositions of porewater. Age models for these cores are based on sedimentological information, and where possible, radiocarbon and pollen dates. The Michigan Basin cores provide a thick record of the late Pleistocene, whereas the Huron Basin cores primarily record Holocene deposition. Taken together, the histories recorded in biogenic carbonates from these sediments provide a clear account of lakewater isotopic changes – and their significance – over much of the history of the Great Lakes Basin.

Biogenic carbonates, and ostracodes in particular, serve as excellent recorders of lakewater $\delta^{18}O$ values. Modern specimens from Lake Huron have been used to assess non-equilibrium oxygen- and carbon-isotope fractionation effects during shell formation within this setting. This information provides improved ability to calculate the oxygen-isotopic compositions of paleolakewater using fossil biogenic carbonates from the cores. The fossil shell compositions indicate intervals characterized by low $\delta^{18}O$ meltwater originating from the retreating Laurentide Ice Sheet and/or associated proglacial lakes, and periods dominated by higher $\delta^{18}O$ water that are more reflective of regional precipitation, runoff and climatic conditions. Differences in the oxygen- and carbon-isotope compositions of deep- versus shallower-water ostracode species in the Michigan Basin cores suggest isotopic stratification of its lakewater during the late Pleistocene. Results for previously unstudied parts of the Huron Basin suggest that sub-basins acquired different oxygen-isotope compositions during periods of very low lake levels, reflecting different water sources and/or different conditions at such times. Early Holocene influxes of glacial meltwater into the Huron Basin, and to a lesser extent the Michigan Basin, correlate with major global climate perturbations that were likely triggered by release of large volumes of glacial meltwater into the Arctic and/or North Atlantic Oceans.

Porewater did not preserve original lakewater $\delta^{18}O$ and δD values. These compositions are largely controlled by downward diffusion of modern lakewater.

Keywords: Lake Huron, Lake Michigan, sediment cores, Pleistocene, Holocene, stable isotopes, paleolimnology, ostracodes, bivalves, porewater, glacial meltwater

EPIGRAPH

There was an advisor named Fred,
Who got it into his head
To study some cores
From the Great Lakes' floors
With isotopes, to see where it led

"Life is like a piston core, you never know what you're going to get!"

- Fred Longstaffe

ACKNOWLEDGEMENTS

I would like to first and foremost thank my supervisor, Fred, for his tremendous guidance and encouragement throughout my (lengthy) period of study. Fred was always available for both intellectual and emotional support, and I am truly grateful for his financial support during the many months after I ceased to be a 'fundable' student. I will forever be grateful for Fred's unique teaching style that captivated my interests in the final year of my undergraduate degree.

Funding for this project was provided by the Canada Foundation for Innovation and NSERC research grants to Fred Longstaffe. I would additionally like to thank the Ontario Graduate Scholarship in Science and Technology (OGSST) and The University of Western Ontario for personal financial support during my studies.

I have been extremely lucky to have had tremendous assistance throughout my research: Lisa Munro, Alana Iutzi, Alexandra Carter, Ayumi Hyodo, Matt Longstaffe and Sam Russell were instrumental in sediment core processing. Ryan Libbey was tremendously helpful with ostracode processing and counting; I know that I will never be able to repay my debt of asking Ryan to count thousands upon thousands of ostracode valves. Kim Law was always encouraging and willing to discuss any problems that had arisen, and amazingly manages the schedules of so many students and researchers with ease. Li Huang provided much assistance with the many mass spectrometers used in this study. I am very grateful for the numerous times she talked me through reviving the Optima after its many near-death experiences during my evening and weekend Multiprep marathons. Brandon Curry and Allison Smith were helpful with ostracode identification, and Gerry Mackie was brilliantly helpful with clam identification.

I wish to thank the Captain and crew of the *CCGS Limnos* and Environment Canada's Technical Operations staff for collecting the sediment cores and water samples used in this study. I am very grateful for Allan Crowe's assistance with arranging the collection of all these crucial materials. John King provided the sediment core images.

Ayumi Hyodo, Ryan Hladyniuk and Mike Lewis provided many stimulating Great Lakes-centric conversations.

I would like to acknowledge many dear friends who have since moved on from Western but who easily demonstrated that research and fun could indeed co-exist, as least some of the time, including but not limited to Greg Wanger, Kim Dalby, Kebbi Hughes, Tyler Hayes and Lyndsay Moore. I would also like to mention my former office mates, Deana Schwartz and Andrea Prentice, who both encouraged and distracted me in just about the right proportions. My family has been truly encouraging throughout this endeavor. Most importantly, I would like to acknowledge the tremendous impact that Sam has had on many aspects of this work. His incredible support throughout the past many years has been a blessing and his endless passion for all things isotopic is impressive and motivating.

TABLE OF CONTENTS

CHAPTER 1: INTRODUCTION

CHAPTER 2: OXYGEN- AND CARBON-ISOTOPE FRACTIONATIONS BETWEEN MODERN LAKE HURON BIOGENIC CARBONATES AND LAKE HURON WATER

CHAPTER 3: LATE PLEISTOCENE AND HOLOCENE HISTORY AND OXYGEN AND CARBON ISOTOPIC EVOLUTION OF LAKE MICHIGAN

CHAPTER 4: LATE PLEISTOCENE AND HOLOCENE HISTORY AND OXYGEN AND CARBON ISOTOPIC EVOLUTION OF LAKE HURON

CHAPTER 5: THE OXYGEN- AND HYDROGEN-ISOTOPE COMPOSITIONS OF POREWATER FROM HURON AND MICHIGAN BASIN SEDIMENTS

CHAPTER 6: CONCLUSIONS

LIST OF TABLES

LIST OF FIGURES

LIST OF APPENDICES

CHAPTER 1

Introduction

1.1 RESEARCH OBJECTIVES

Lake cores have long been used as an archive of past climatic and environmental conditions and their relative fluctuations through time. This thesis uses paleolimnology, the study of lake sediments, to investigate evolution for the North American Great Lakes Basin. The first proglacial lakes in the Great Lakes Basin formed approximately 16,000 years ago (Larson and Schaetzl 2001). Cores available from different regions of the Great Lakes invariably capture different segments of this history but can be considered collectively to acquire a more complete picture of the late Pleistocene and Holocene intervals of geological time. The Michigan and Huron Basins are perfectly situated within the Great Lakes Basin; their central placement has allowed them to act as flow-through basins during major floods originating from upstream Lake Superior and/or glacial Lake Agassiz at various times during their histories. Cores obtained from Lakes Michigan and Huron comprise the heart of this thesis, and are used – principally through the stable isotopic analysis of ostracodes, but also through the analysis of other shelly fauna and porewater – to investigate the passage of glacial meltwater through this system following the Glacial Maximum.

Specially, the goals of this study are: (1) to assess the accuracy of using biogenic carbonates (e.g. ostracodes, bivalves, gastropods) to reconstruct the isotopic compositions of water present during shell formation; (2) to investigate whether deep- and shallow-water ostracode species can be used to identify periods of isotopic stratification in the water column; (3) to identify times when the Michigan and Huron Basins were inundated with waters of a glacial origin, which may have been directly sourced from the ice sheet or from upstream proglacial lakes; (4) to compare the oxygen-isotope records of the Michigan and Huron Basins to that of the other Great Lakes in order to identify periods of connectivity and to obtain a sense of changes in inflow/outflow pathways; (5) to examine variations in the carbon-isotope compositions of biogenic carbonates and to assess the information provided concerning source waters and primary productivity within the basins; and (6) investigate the effects of changing late Pleistocene and Holocene climates on the oxygen- and carbon-isotope compositions of waters (including dissolved inorganic carbon content) in the Michigan and Huron Basins.

The evolutionary history of the Great Lakes has been the subject of many studies. Continued investigation of these basins adds to our knowledge and understanding of their histories, owing largely to advancements in age control, archive resolution, and geochemical analyses. The cornerstone of this dissertation lies in the isotopic archives preserved in sediment cores from the Great Lakes. These provide insight into the continuous reconfigurations of water pathways, as well as the effects of regional and global climate changes, within the Great Lakes Basin at the end of the last glacial period. Recognizing how the Great Lakes responded to major climatic shifts is crucial to predicting how lake levels, water chemistry and quality, fisheries and overall health of the Great Lakes Basin may be affected by current or future climate change. Background information critical to this investigation includes the origin and evolution of Lake Agassiz and the Great Lakes, and their role in late Pleistocene and Holocene climate change, the use of oxygen isotope compositions to trace glacial meltwater movement, and the causes and controls of oxygen and carbon isotope fractionations in fresh (meteoric) water and biogenic carbonate minerals. A brief summary of these topics is given below.

1.2 LAKE AGASSIZ, MOVEMENT OF GLACIAL MELTWATER AND LATE PLEISTOCENE CLIMATE CHANGE

Numerous globally significant climate changes occurred during the late Pleistocene to mid-Holocene. Large and sudden inputs of freshwater to both the North Atlantic and Arctic oceans have been implicated in interfering with the normal thermohaline circulation patterns of the oceans, which play a major role in regulating climate in the Northern Hemisphere. Specifically, it is believed that the sudden dilution of ocean surface water caused by the addition of large volumes of freshwater reduced the production of North Atlantic Deep Water (NADW). Reduction (or cessation) of the NADW would have greatly attenuated northward movement of the warm Gulf Stream, which delivers heat to the subpolar region, resulting in the cooling of high latitude regions around the North Atlantic, especially Northern Europe (Rooth 1982; Boyle and Keigwin 1987; Broecker et al. 1989; Broecker 1991; Alley et al. 1997; Barber et al. 1999; Rahmstorf 2006; Peltier 2007). Meltwater sourced directly from the retreating Laurentide Ice Sheet (LIS) and/or outflows from Lake Agassiz, a massive proglacial lake that existed from ~11.7 – 7.7 ka [13,600 – 8,450 cal] BP (Fig 1.1), are the two possible sources of such sufficiently large volumes of freshwater.

The Bølling-Allerød (BOA) warm interval (~12.5 – 11 ka [14,600 – 12,900 cal] BP) affected much of the Northern Hemisphere, including Greenland (Broecker 1992; Dansgaard et al. 1993; Grootes et al. 1993; North Greenland Ice Core Project 2004), Europe (von Grafenstien et al. 1999; Zolitschka et al. 2000; McKenzie 2010) and North America (Yu and Eicher 1998, 2001; Obbink et al. 2010). The BOA period ended abruptly with the onset of the Younger Dryas (YD) cold interval (11 – 10 ka [12,900 – 11,500 cal] BP). Drastic decreases in Lake Agassiz water levels appear to be coincident with major climate cooling events during the late Pleistocene and Holocene, including the YD, an unnamed event at ~8.3 ka [9300 cal] BP and the ‘8.2 ka [calendar] event’ (~7.7 ka [8,450 cal] BP; Rooth 1982; Alley et al. 1997; Broecker et al. 1988, 1989; Alley 2000; Clark et al. 2001; Fisher et al. 2002; Teller et al. 2002; Ebbesen and Hald 2004; Teller and Leverington 2004; Rasmussen et al. 2006; Daley et al. 2009; Murton et al. 2010; Yu et al. 2010).

Lake Agassiz drained south to the Gulf of Mexico via the Mississippi River during its Lockhart phase (11.7 – 11.0 ka [13,600 – 12,900 cal] BP; Teller and Thorleifson 1983; Fisher 2003, 2007; Teller and Leverington 2004). Until recently, it was largely accepted that continued northward retreat of the LIS opened Lake Agassiz’s eastern outlets in the Thunder Bay region during its Moorhead phase (~11.0 – 10.0 ka [12,900 – 11,500 cal] BP) allowing drainage to shift to the Great Lakes Basin at ~11 ka and triggering the YD cooling event in the North Atlantic Ocean (Rooth 1982; Teller 1985; Broecker et al. 1989; Lewis and Anderson 1989; Lewis et al. 1994; Teller and Leverington 2004). However, channels or deposits expected from such a large release of

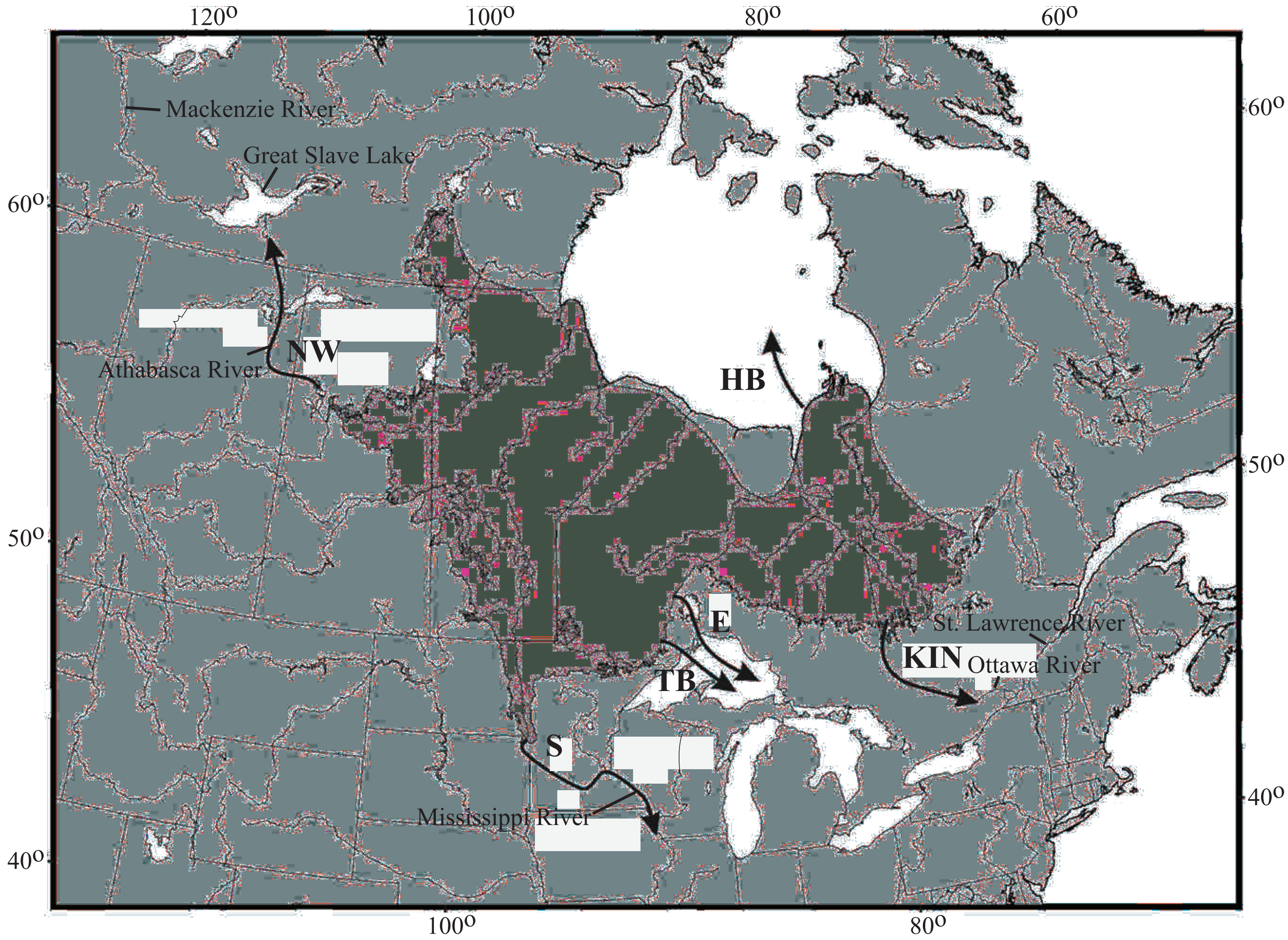

Figure 1.1. Maximum extent of Lake Agassiz over the course of its existence from ~11.7 – 7.7 ka [13,600 – 8,200 cal] BP. Main outlets are indicated by letters and arrows; NW = northwestern outlet, S = southern outlet, TB = multiple eastern outlets through the Thunder Bay region, E = eastern outlet through the Nipigon Basin, KIN = Kinojévis outlet, HB = Hudson Bay route of final drainage (modified from Teller et al. 2005)

water in the region west of Thunder Bay have yet to be discovered (Lowell et al. 2005; Teller et al. 2005). Additionally, various studies report a lack of evidence for large volumes of freshwater passing through the St. Lawrence River on route to the North Atlantic Ocean near the onset of the YD (Rodrigues and Vilks 1994; Keigwin and Jones 1995; DeVernal et al. 1996). Recently it has been suggested that large outpourings of freshwater into either the North Atlantic or Arctic Oceans would have been equally capable of disrupting ocean circulation patterns (Peltier 2007). As such, focus on identifying the various pathways of Lake Agassiz floods, which has been the subject of many debates, has expanded beyond the Great Lakes Basin. New evidence of a massive flood from the Agassiz Basin through the Mackenzie River Valley (the NW outlet; Fig. 1.1) on route to the Arctic Ocean between ~11.1 – 10.8 ka [13,000 – 12,800 cal] BP is garnishing much attention (Teller et al. 2005; Murton et al. 2010). The initial passage of Lake Agassiz outflow eastwards through the Great Lakes Basin may have occurred at ~10.8 ka, as suggested by the distinctive Wilmette Bed in the Michigan Basin (Teller 1985; Colman et al. 1994c; Teller and Leverington 2004; Teller et al. 2005). Some researchers, however, believe that eastwards drainage routes through the Great Lakes Basin did not open until ice retreat in the Lake Nipigon region commenced Lake Agassiz's Nipigon phase (9.5 – 8.2 ka [10,700 – 9,100 cal] BP; Lowell et al. 2005, 2009; Teller et al. 2005; Fisher et al. 2008). This topic is still hotly debated in the literature.

Evidence suggests that the Marquette glacial advance into the Superior Basin at ~10 ka [11,500 cal] BP redirected Lake Agassiz outflow through its northwestern outlet to the Arctic Ocean until ~9.5 ka [10,700 cal] BP (Emerson phase; Smith and Fisher 1993; Fisher and Smith 1994; Fisher et al. 2002; Fisher 2003, 2007; Teller and Leverington 2004; Lowell et al. 2005; Couch and Eyles 2008; Murton et al. 2010). A brief diversion of southward flow to the Gulf of Mexico may have occurred before eastward drainage through the Great Lakes Basin resumed at 9.5 ka (Fisher 2003; Boyd 2007). This marks the beginning of Lake Agassiz's Nipigon phase (9.5 – 8.1 ka [10,700 – 9,000 cal] BP) during which flow through the Great Lakes Basin was at times catastrophic (Teller and Thorleifson 1983; Teller 1985; Lewis and Anderson 1989; Colman et al. 1994a; Lewis et al. 1994; Teller et al. 2002, 2005; Fisher 2003; Teller and

Leverington 2004; Breckenridge and Johnson 2009; Breckenridge et al. 2010). By 9.0 ka [10,200 cal] BP the LIS had fully retreated from the Great Lakes watershed (Karrow et al. 2000; Larson and Schaetzl 2001). Further northward retreat of the LIS allowed Lakes Agassiz and Ojibway to join together in the Hudson Bay lowlands area at ~8.1 ka [9,000 cal] BP; the combined drainage of this massive proglacial lake was diverted away from the Great Lakes Basin through the Kinojévis outlet into the Ottawa and St. Lawrence Rivers before reaching the North Atlantic Ocean (Fig. 1.1; Lewis and Anderson 1989; Lewis et al. 1994; Bajc et al. 1997; Barber et al. 1999; Teller and Leverington 2004).

A massive flood from Lake Agassiz at ~7.7 ka [8,450 cal] BP, brought on by the collapsing LIS, flowed into Hudson Bay and onto the North Atlantic Ocean (Barber et al. 1999), again disrupting regular ocean currents (Stuiver et al. 1995; Hughen et al. 1996; Alley et al. 1997; Barber et al. 1999; Flesche Kleiven et al. 2008; Daley et al. 2009). This short perturbation, known as the '8.2 ka [calendar] event', is believed to have mostly affected the North Atlantic region, leading to a brief climate transition from warm to cold to warm again (Shuman et al. 2002).

1.3 THE GREAT LAKES BASIN

The basins occupied by today's North American Great Lakes were carved from areas of relatively weaker bedrock by ice movement during the most recent (Wisconsin) glaciation (Hough 1958; Cvancara and Melik 1961; Wold et al. 1981; Larson and Schaetzl 2001). The Last Glacial Maximum peaked at ~20 ka [24,000 cal] BP, after which the LIS retreated northward into the Great Lakes Basin where it repeatedly advanced and retreated for a few thousand years (Larson and Schaetzl 2001). The earliest lakes in the Great Lakes Basin formed as water was impounded against the retreating LIS. The first lakes in the Michigan and Huron Basins were known as Lake Milwaukee (~15.5 ka [18,800 cal] BP; Schneider and Need 1985) and Lake Maumee (~14.4 ka; Eschman and Karrow 1985; Lewis et al. 1994), respectively. The early lake phases in both basins changed rapidly during the latter portions of the Pleistocene (~15 – 10 ka) as the LIS changed positions numerous times – each time opening and closing different inlets and outlets to and from the basins (Eschman and Karrow 1985; Hansel et al. 1985; Lewis and Anderson 1989). Isostatic uplift maintained a major role in the evolution of the Great Lakes by continuing to exert control over the lakes' inlets and outlets even after the final retreat of the LIS north of Lake Superior at ~9 ka [10,200 cal] BP (Hough 1958; Larson and Schaetzl 2001). The histories of the Michigan and Huron Basins are summarized in Figures 1.2 and 1.3 respectively.

The specific histories of the Michigan and Huron Basins most relevant to this study begin at ~12.5 ka [14,700 cal] BP during the Port Huron glacial advance (Eschman and Karrow 1985; Lewis et al. 1994). Early Lake Algonquin was present in the Huron Basin at this time. Initially, Early Lake Algonquin drained to the south through the Port Huron outlet until retreat of the glacier opened the Fenelon Falls outlet to the east (Fig. 1.4) shortly before 12 ka [13,850 cal] BP. This marked the low-level Kirkfield-Algonquin phase as the lake drained through the Simcoe Basin (Eschman and Karrow 1985; Finamore 1985; Lewis et al. 1994). The Lake Chicago phase was present in the Michigan Basin until retreat from the Port Huron advance opened the Straits of Mackinac, allowing one confluent body of water to form within the Michigan and Huron Basins, which drained through the Fenelon Falls outlet (Fig. 1.4).

The Two Rivers/Greatlakean ice advance (11.8 – 11.2 ka [13,700 – 13,000 cal] BP) closed the Straits of Mackinac, shifting drainage in the Michigan Basin once again to the outlet at Chicago (Chicago II, Fig. 1.2; Hansel et al. 1985), while water in the Huron Basin continued to drain through the Fenelon Falls outlet (Lewis et al. 1994). Around this time, glacial Lake Agassiz developed (~11.7 ka [13,600 cal] BP) as the LIS retreated northward into the Hudson Bay watershed (Clayton 1983).

The Straits of Mackinac were reopened by retreat of the Two Rivers/Greatlakean ice advance, once again joining the waters in the Michigan and Huron Basins. The Main Lake Algonquin phase (11 – 10.3 ka [12,900 – 12,100 cal] BP) was initiated as continued uplift shifted drainage from the Fenelon Falls outlet to Port Huron (Hansel et al. 1985) and continued retreat of the LIS allowed expansion of this phase into the Superior Basin

Figure 1.2. Chronology of the Michigan Basin from 15.0 ka [18,500 cal] BP to present. Post Alg. represents the Post Algonquin drawdown phase, a time of rapidly dropping lake levels. Blue shaded regions indicate flooding events originating from the Lake Agassiz Basin. Grey shaded regions indicate times when inlets and outlets were active. *a:* The Upper Peninsula refers to all inlets passing over the Upper Michigan Peninsula; e.g., rivers into Green Bay and the Au Train-Whitefish channel. *b:* Represents the Straits of Mackinac, which connect the Michigan and Huron Basins. *c:* In shallow regions of the lake the boundary between the Lower and Upper units is marked by the Chippewa unconformity (10.3 ka [12,100 cal] BP). *d:* One previously-examined Michigan core indicated a flood synchronous with the Mattawa I flood in the Huron Basin. *e:* The Au Train-Whitefish channel may have been open during the Marquette advance in the Superior Basin. The occurrences of both *d* and *e* are examined in Chapter 3 (this thesis). *f:* Inputs to modern Lake Michigan consist of precipitation and runoff. *hc:* Indicates periods when the Michigan Basin was hydrologically closed; i.e., water level was below the outlet height. (Modified from Hansel et al. 1985; Schneider and Need 1985; Hansel and Mickelson 1988; Colman et al. 1990, 1994b, 1994c; Forester et al. 1994; Lewis et al. 1994, 2005, 2007; Safarudin and Moore 1999; Miller et al. 2000; Odegaard et al. 2003; Breckenridge and Johnson 2009; Breckenridge et al. 2010; Fisher et al. 2010)

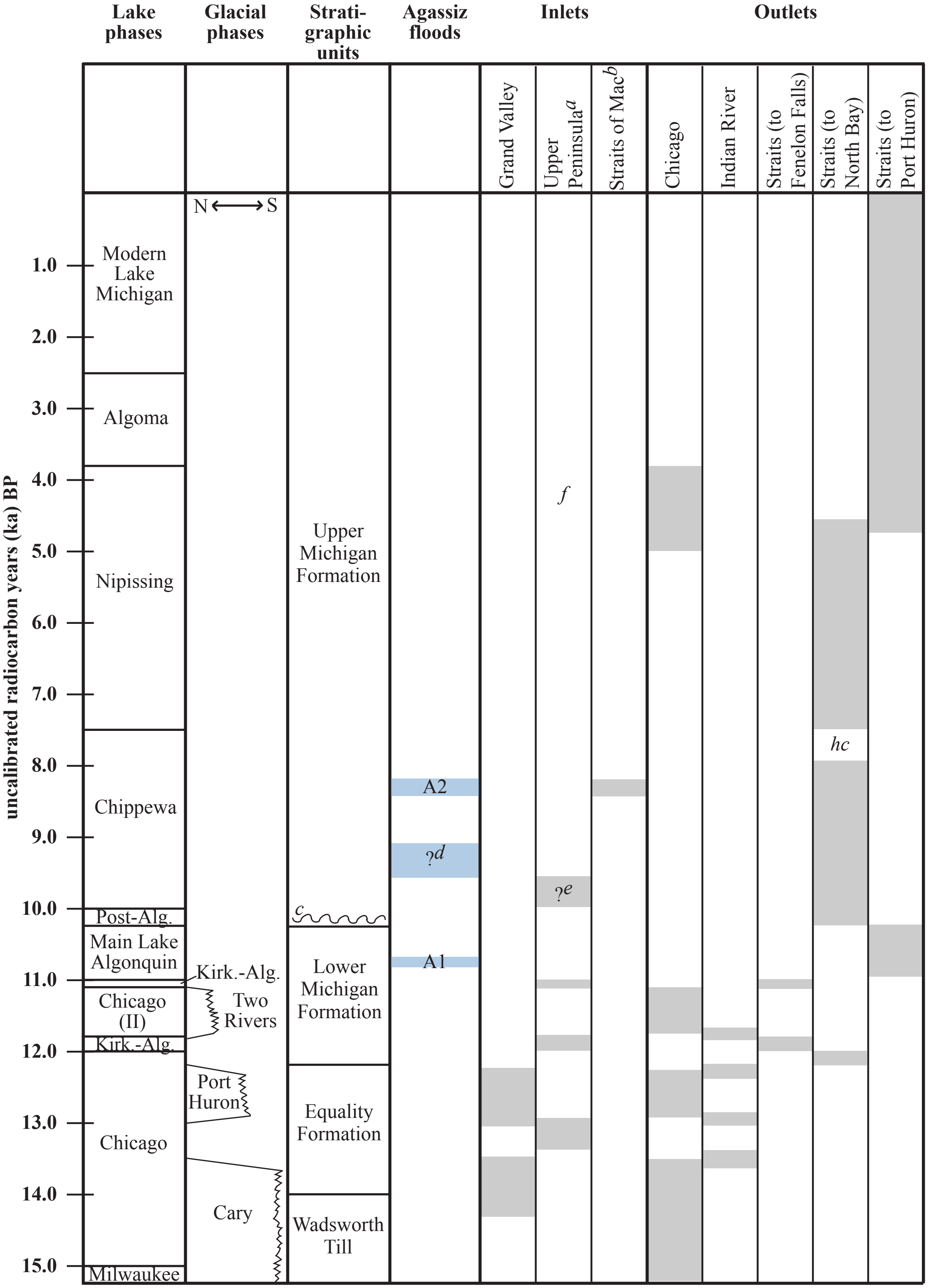

Figure 1.2. Chronology of the Michigan Basin (full caption is on the previous page).

Figure 1.3. Chronology of the Huron Basin from 15.0 ka [18,500 cal] BP to present. Post Alg. represents the Post Algonquin drawdown phase, a time of rapidly dropping lake levels. Blue shaded regions indicate flooding events originating from the Lake Agassiz Basin. Grey shaded regions indicate times when inlets and outlets were active. *a:* Lake water from the Superior Basin may have been diverted northwards over the interval from 8.9 - 8.4 ka [10,000 - 9,450 cal] BP. *b:* Some early periods of the Huron Basin received only direct inflows of meltwater. *hc:* Indicates periods when the Huron Basin was hydrologically closed; i.e., water level was below the outlet height (Eschman and Karrow 1985; Finamore 1985; Lewis and Anderson 1989; Colman et al. 1994c; Lewis et al. 1994, 2005, 2007; Moore et al. 1994, 2000; Rea et al. 1994a; Dobson et al. 1995; Godsey et al. 1999; Karrow et al. 2000; Larson and Schaetzl 2001; Odegaard et al. 2003; Breckenridge and Johnson 2009; Breckenridge et al. 2010; Brooks et al. 2010; Brooks and Medioli 2010).

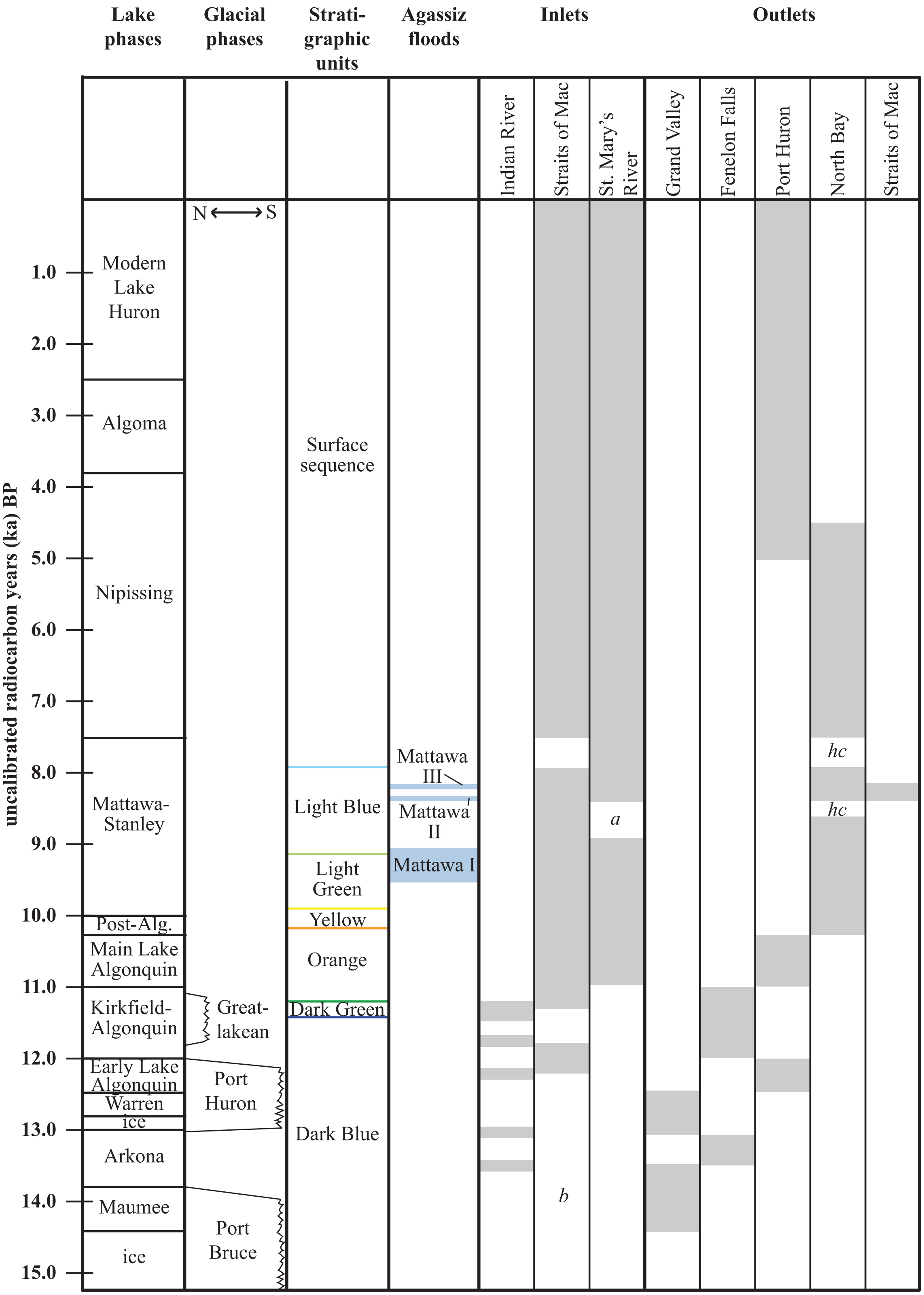

Figure 1.3. Chronology of the Huron Basin (full caption is on the previous page).

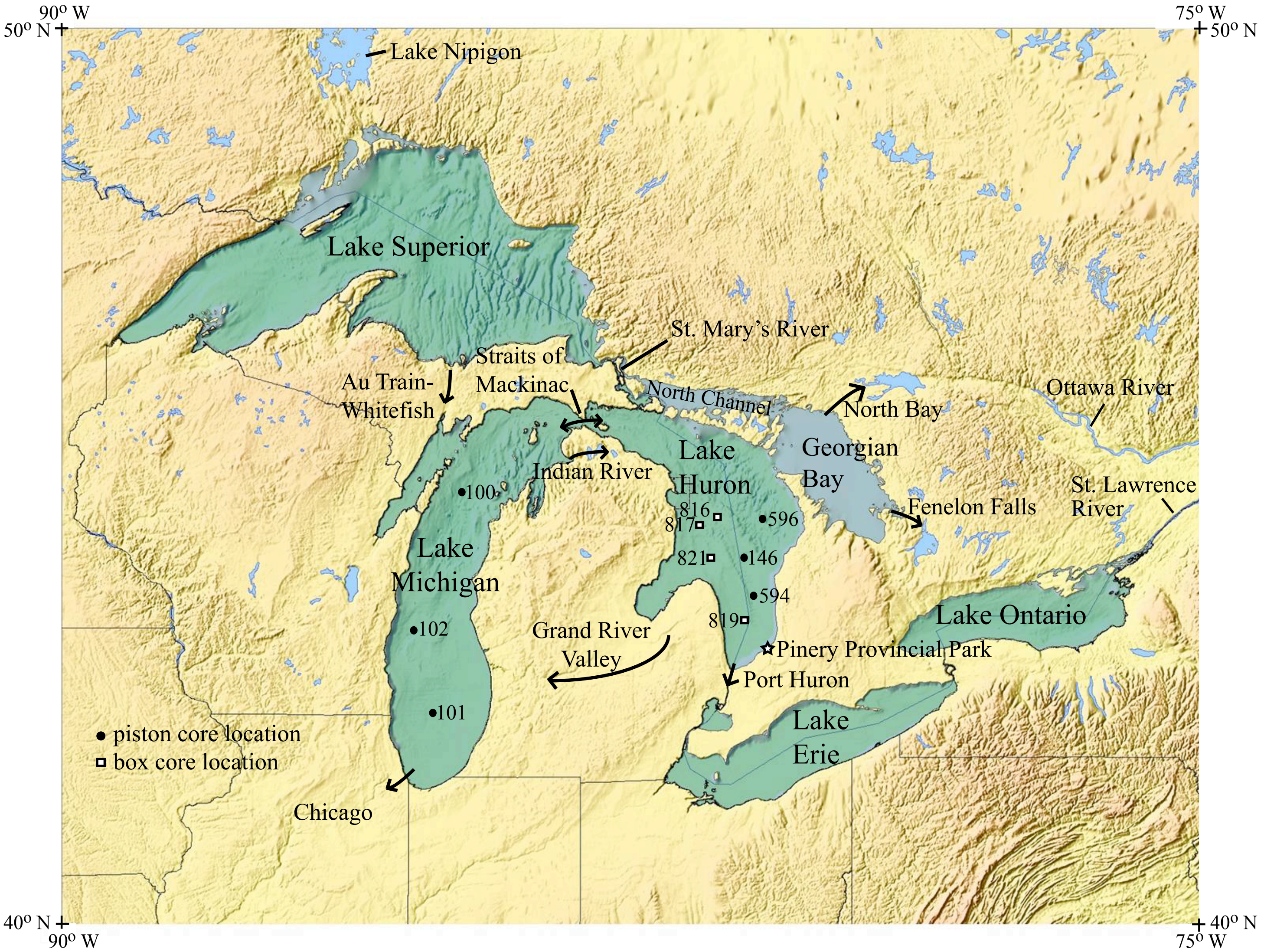

Figure 1.4. Map of the Great Lakes Basin showing core locations, major inlets and outlets.

(Lewis et al. 1994). Outflow from the Agassiz Basin may have been directed eastwards to Lake Superior and onwards through the Great Lakes system as early as ~10.8 ka [12,800 cal] BP (Clayton 1983; Teller 1985; Leverington et al. 2000; Teller and Leverington 2004). Deposition of the Wilmette Bed, a massive grey clay within a very thick red glaciolacustrine unit found in Michigan Basin sediments, has been attributed to this inflow from Lake Agassiz (Colman et al. 1994c).

The Marquette ice readvance into the Superior Basin at ~10 ka [11,500 cal] BP redirected Lake Agassiz water through its northwestern outlet and away from the Great Lakes Basin (Fig. 1.1; Teller and Thorleifson 1983). This diversion, together with the opening of the North Bay outlet in northeast Georgian Bay (Fig. 1.4), drained the waters of the Main Lake Algonquin phase until low lake levels were established shortly after 10 ka (Lewis and Anderson 1989; Lewis et al. 1994). Retreat from the Marquette ice advance initiated the Nipigon phase of Lake Agassiz (~9.5 – 8.2 ka [10,700 – 9,100 cal] BP), which drained eastwards through the Great Lakes Basin and onwards to the Atlantic Ocean (Clayton 1983; Teller and Thorleifson 1983; Farrand and Drexler 1985; Lewis and Anderson 1989).

Oscillating water levels in the Michigan and Huron Basins between ~10 – 7.5 ka [11,500 – 8,350 cal] BP were largely dependant on influxes of water from the upstream Agassiz ± Superior Basins. Generally, this interval is referred to as the Mattawa-Stanley phase in the Huron Basin, where Mattawa refers to periods of high water levels and Stanley, low water levels. In the Michigan Basin this interval is referred to as the Chippewa phase, and distinctions have not been made between periods of high and low water levels.

At ~8.1 ka [9,050 cal] BP, Lakes Agassiz and Barlow-Ojibway merged north of the Great Lakes in the Hudson Bay Lowlands (Barber et al. 1999). Outflow from this conjoined lake was directed into the Ottawa River Valley, bypassing the Great Lakes, which led to the final lowstand phases in the Michigan and Huron Basins from 7.9 – 7.5 ka [8,650 – 8,350 cal] BP (Lewis and Anderson 1989; Teller and Leverington 2004).

These lowstands were hydrologically closed, a result of decreased water inputs as well as a dry climate that affected much of the mid-Holocene (Dorale et al. 1992; Kutzbach and Webb 1993; Dean et al. 1996; Edwards et al. 1996; Yu et al. 1997; Lovan and Krishnamurthy 2011). These lowstand phases ended gradually as the North Bay outlet was uplifted, causing lake levels to rise. The Nipissing transgressive phase in the Huron Basin peaked at ~5 ka [5,730 cal] BP when the outlets from the Michigan and Huron Basins shifted to Chicago and Port Huron, respectively (Lewis et al. 2007). With continued erosion of the Port Huron outlet, the Chicago outlet was abandoned at ~3.8 ka [4,160 cal] BP; lakewater in the Michigan Basin has since drained through the Straits of Mackinac into Lake Huron (Eschman and Karrow 1985; Hansel et al. 1985; Larson 1985).

1.3.1 Late Pleistocene and Holocene climate variation in the Great Lakes Basin

Climate archives from central and eastern North America, including the Great Lakes Basin, suggest that the late Pleistocene and much of the Holocene were drier than present (Webb et al. 1993; Dean et al. 1996; Edwards et al. 1996; Shuman et al. 2002; Williams et al. 2010; Shuman and Plank 2011). During these periods, climate in the Great Lakes region resembled that of modern high-latitude regions with a strong temperature gradient present immediately south of the LIS (COHMAP 1988; Webb et al. 1993; Levesque et al. 1997). The dominant controls on moisture balance in these regions were high summer insolation, continental ice coverage and associated changes in atmospheric circulation patterns (COHMAP 1988; Guiot et al. 1993; Rensenn et al. 2009; Williams et al. 2010; Shuman and Plank 2011).

Regional temperatures increased at the onset of the Holocene (Edwards et al. 1996; Yu and Eicher 1998, 2001; Yu 2000) and were particularly warm during the Holocene Hypsithermal (~8 – 4 ka [9,000 – 4,400 cal] BP), which affected much of North America (Bartlein et al. 1984; Dorale et al. 1992; Kutzbach and Webb 1993; Krishnamurthy et al. 1995; Dean et al. 1996; Edwards et al. 1996; Yu et al. 1997; Lovan and Krishnamurthy 2011). The combination of a dry climate during the early Holocene and the warm Holocene Hypsithermal caused large decreases in water levels in the Great Lakes Basin such that Lakes Michigan and Huron (and likely others) became hydrologically closed (Lewis et al. 2007). Moisture levels in the Great Lakes region increased sharply following the collapse of the ice sheet (~7.7 ka [8,450 cal] BP) as changes in atmospheric circulation allowed subtropical moisture to travel northwards (COHMAP 1988; Webb et al. 1993; Bartlein et al. 1998; Shuman et al. 2002).

1.3.2 Oxygen-isotope compositions of Great Lakes water

The various water sources that have fed the Great Lakes can be identified using their oxygen-isotope compositions, particularly because unmodified glacial meltwater is characterized by significant depletion of ^{18}O relative to most other water sources. As a proxy for water compositions, many investigators have measured the $\delta^{18}O$ values of small shelly organisms, mainly ostracodes and bivalves, preserved in sediment cores from the Great Lakes (Colman et al. 1990, 1994a, 1994b; Lewis and Anderson 1992; Forester et al. 1994; Last et al. 1994; Lewis et al. 1994; Rea et al. 1994a, 1994b; Dettman et al. 1995; Tevesz et al. 1998; Godsey et al. 1999; Moore et al. 2000; Macdonald and Longstaffe 2008; Breckenridge and Johnson 2009). These data allow researchers to identify the various sources of water that have traveled through the Great Lakes Basin at different times.

Co-existing benthic and pelagic proxies for water composition (cellulose, ostracodes and porewater) from Lake Agassiz have been used to suggest that its surface and bottom waters had different oxygen-isotope compositions for much of its history (Last et al. 1994; Remenda et al. 1994; Buhay and Betcher 1998; Birks et al. 2007). Such putative isotopic stratification adds great complexity to interpretation of ostracode oxygen-isotope records, and has major implications for identifying the pathways of Lake Agassiz outflows. During the Lockhart (11.7 – 11.0 ka [13,600 – 12,900 cal] BP) and Emerson (10.0 – 9.5 ka [11,500 – 10,700 cal] BP) phases of Lake Agassiz, which drained southward through the Mississippi River to the Gulf of Mexico and northwestward through the Mackenzie Valley to the Arctic ocean, respectively (Teller and Thorleifson

1983), surface waters may have been enriched in ^{18}O by ~6 ‰ relative to bottom waters (Birks et al. 2007). Likewise, during the Moorhead phase (~11.0 – 10.0 ka [12,900 – 11,500 cal] BP), which likely drained northwest towards the Arctic Ocean (Murton et al. 2010; Teller et al. 2005) before being rerouted eastwards through the Great Lakes Basin at ~10.8 ka [12,800 cal] BP (Colman et al. 1994a; Teller and Leverington 2004; Teller et al. 2005), surface waters may have been enriched in ^{18}O relative bottom waters by ~7 ‰ (Birks et al. 2007). By the Nipigon phase (9.5 – 8.2 ka [10,700 – 9,100] BP) when drainage was again eastwards through the Great Lakes Basin, precipitation, which is generally enriched in ^{18}O relative to glacial meltwater, likely had become a dominant source of water draining into the Agassiz Basin. Climate warming and associated evaporation is thought to have caused these precipitation-derived surface waters to become further enriched in ^{18}O by as much as 18 ‰ relative to bottom waters (Birks et al. 2007; Lewis et al. 1994; Buhay and Betcher 1998).

Early studies of Huron Basin sediment cores led to two prominent hypotheses relating lake levels to the oxygen-isotope composition of the lakewater. The first model, which was proposed by Lewis and Anderson (1989), suggested that large inflows from upstream Lake Agassiz would substantially raise lake levels and lower the oxygen-isotope compositions of the lakewater. This model was somewhat revised by Lewis et al. (1994) after evidence linked highstand phases to water with higher oxygen-isotope compositions and lowstand phases to lower oxygen-isotope compositions. This model suggested that highstands were caused by hydraulic damming at outlets during periods of high flow and shorter water residence times, and that lowstands were periods of lower flow and longer water residence times. This hypothesis suggests that highstands contained waters released from Lake Agassiz, often as immense floods. When Agassiz waters were diverted elsewhere, the ensuing lowstands were fed by a modest and more or less continuous input of meltwater originating either from the ice-marginal environment north of the Nipigon Basin or by backflooding from glacial Lake Ojibway discharge as it drained through the Ottawa River Valley (Fig. 1.4; Lewis et al. 1994). Lewis et al. (1994) noted surprise at the unexpected finding that the oxygen-isotope compositions of Lake Agassiz outflows were not characteristic of meltwater. This model is in agreement with evidence for ^{18}O-rich Lake Agassiz surface waters (Buhay and Betcher 1998; Birks et al. 2007).

The second model, proposed by Rea et al. (1994a), suggests that highstands were the result of high outlets impounding lakewater, which led to increased residence times in the basins and allowed for significant accumulation of local precipitation and runoff, as well as evaporative enrichment. In this scenario, lowstands were characterized by large surges of meltwater; low outlets during lowstands allowed unrestricted flow through the lake basins, resulting in shorter water residence times during these phases (Rea et al. 1994a, 1994b; Dettman et al. 1995).

Within the Michigan Basin, periods characterized by low-^{18}O waters have consistently been attributed to floods originating from the Agassiz Basin and/or more directly from the ice sheet (Colman et al. 1990, 1994a, 1994b, 1994c; Forester et al. 1994; Miller et al. 2000; Breckenridge and Johnson 2009). To investigate the discrepancies between the histories of the Michigan and Huron Basins, Breckenridge and Johnson (2009) recalibrated the chronologies of Michigan and Huron Basin cores based on paleomagnetic secular variation records and grain size measurements. They found that many of the radiocarbon dates from the Huron Basin on which the above two theories were established were unreliable and demonstrated that the association of high lake levels to high δ^{18}O values (or conversely low lake levels to low δ^{18}O values) is inaccurate. These findings are in agreement with more recent studies in the Huron Basin that correlate periods of low-^{18}O values to the Mattawa floods, which likely originated from Lake Agassiz, as per the original model of Lewis and Anderson (1989) (Lewis et al. 2005, 2007, 2008; Breckenridge and Johnson 2009; Breckenridge et al 2010; Brooks et al. 2010; Brooks and Medioli 2010).

1.4 STABLE ISOTOPE SYSTEMATICS OF METEORIC WATER AND BIOGENIC CARBONATES

Isotopes of a given element contain the same number of protons and electrons but a different number of neutrons, which gives these isotopes different masses and accounts for minor but measurable differences in their reactivity rates and thus their concentrations amongst different substances. Stable isotope abundances are expressed as the ratio of the heavy (rare) to light (common) isotopes within a substance relative to an international standard using the δ (delta) notation in units of ‰ (permil, or parts per thousand):

$$\delta\ (‰) = [(R_{sample}/R_{standard}) - 1] \tag{1.1}$$

where R is the isotopic ratio (e.g. $^{18}O/^{16}O$) in the sample or standard (Coplen 2011). A positive δ-value indicates that the sample is enriched in the heavy isotope relative to the standard and a negative δ-value indicates that the sample is depleted of the heavy isotope relative to the standard. The international standard for hydrogen is VSMOW and for carbon is VPDB. The international standards for oxygen are Vienna Standard Mean Ocean Water (VSMOW; used for most substances) and Vienna PeeDee Belemnite (VPDB; used for carbonate minerals in some circumstances). The oxygen-isotope VSMOW and VPDB scales are related by the equation (Coplen et al. 1983):

$$\delta^{18}O_{VPDB} = 0.97002 * \delta^{18}O_{VSMOW} - 29.98 \tag{1.2}$$

Different isotopes of an element are distributed among various phases by a process called fractionation, which can occur under equilibrium or kinetic (non-equilibrium) conditions (Clark and Fritz 1997). Kinetic fractionation occurs when one isotope reacts more rapidly than another in an irreversible system or in a system where the products are removed from the reactants before equilibrium is reached. This type of fractionation is commonly associated with diffusion and biological processes. Equilibrium fractionation occurs in reversible systems that are in chemical equilibrium, causing one isotope to become preferentially concentrated in some phases over others in the same system. As a general rule of equilibrium fractionation, heavy isotopes are concentrated in the phase with stronger bonds. Lighter isotopes are thus concentrated in the phase with weaker bonds and as a result are more reactive.

Equilibrium fractionation reactions are temperature-dependant. The fractionation factor α, which indicates the degree to which isotopes are fractionated during reactions, is defined as:

$$\alpha = R_a/R_b \tag{1.3}$$

where R_a is the isotopic ratio in phase a and R_b is the isotopic ratio is phase b. The fractionation factor (α) is inversely related to temperature. Fractionation is greatest at low temperatures, resulting in the widest spread of δ-values between reactant(s) and product(s). Conversely, fractionation decreases at high temperatures, yielding products with isotopic compositions approaching those of the reactants.

1.4.1 Meteoric waters – oxygen and hydrogen isotopes

The oxygen- and hydrogen-isotope compositions of precipitation have long been used to study the meteoric water cycle. The water cycle more or less begins with evaporation from the surface of the oceans at low latitudes. Evaporation of water (and formation of vapour) involves both kinetic and equilibrium fractionation (Dansgaard 1964; Gonfiantini 1986). These fractionations produce vapour that is enriched in the lighter isotopes of oxygen and hydrogen relative to its liquid water source. This is a result of the slightly different partial pressures of the different molecules of water (called isotopologues); the molecule with both the light isotopes of oxygen and hydrogen ($H_2{}^{16}O$; mass 18 amu) evaporates more readily than $HD^{16}O$ (mass 19 amu), which in turn evaporates more readily than $H_2{}^{18}O$ (mass 20 amu; other isotopologues of water are very rare). At the opposite end of the water cycle, during condensation, water molecules that contain the heavier isotopes preferentially condense first (i.e., $H_2{}^{18}O > HD^{16}O > H_2{}^{16}O$). The isotopic composition of precipitation is additionally affected by the composition of its source, temperature, latitude, altitude and continental effects (Dansgaard 1964; Rozanski et al. 1993; Clark and Fritz 1997; Jouzel et al. 1997). Generally, when vapour sources formed near the equator travel towards the poles, earlier precipitation events (i.e.

those that occur at low latitudes in warmer regions) will have higher δ^{18}O and δD values than later precipitation events (i.e. those that occur at high latitudes in colder regions; Dansgaard 1964; Rozanski et al. 1993). This relationship of the global distribution of oxygen and hydrogen isotopes in precipitation is described by the Global Meteoric Water Line (GMWL; Craig 1961):

$$\delta D = 8 * \delta^{18}O + 10 \tag{1.4}$$

Water sourced from glacial ice would have had characteristically low δ^{18}O values, typical of precipitation at high latitudes/altitudes and low temperatures; it is believed that the LIS produced meltwater with δ^{18}O values of ~ -30 ‰ (Dansgaard and Tauber 1969; Rozanski et al. 1993; Sima et al. 2006). Lakes directly abutted against the LIS (e.g. proglacial lakes such as Lake Agassiz) and lakes that received direct inflows of meltwater would therefore also have had low δ^{18}O values although addition of relatively ^{18}O-rich precipitation would serve to increase the isotopic composition of the body of water.

1.4.2 Biogenic carbonates – oxygen and carbon isotopes

The carbon- and oxygen-isotope compositions of biogenic carbonates normally record local environmental conditions at the time of shell formation. Thus biogenic carbonates, and ostracodes in particular in the realm of the Great Lakes, have proven themselves to be useful for paleoenvironmental reconstruction. Ostracodes are small (~0.5 – 2 mm) aquatic, bivalved crustaceans composed of low-Mg calcite (Turpen and Angell 1971). Gastropods (snails) and most bivalves (clams) precipitate shells made of aragonite. Under equilibrium conditions, the δ^{18}O values of these organisms' valves/shells are controlled by water temperature and the oxygen isotopic composition of its host water. The following equations describe oxygen-isotope fractionation between low-Mg calcite and aragonite, respectively, and the water from which they form under equilibrium conditions:

$$1000 \ln \alpha_{calcite\text{-}H2O} = 2.78 * 10^6/T^2 \text{ (K)} - 2.89 \quad (1.5)$$

(O'Neil et al. 1969, revised by Friedman and O'Neil 1977)

$$1000 \ln \alpha_{aragonite\text{-}H2O} = 18.45 * 10^3/T \text{ (K)} - 32.54 \quad (1.6)$$

(Böhm et al. 2000)

Many biogenic carbonates precipitate from solution under equilibrium conditions, and so their oxygen-isotope compositions can be accurately predicted using the above equations. Of those biogenic carbonates that do not precipitate at equilibrium, most have lower-than-expected $\delta^{18}O$ values – a result of kinetic fractionation (McConnaughey 1989a, 1989b). However, for reasons as yet unknown, ostracodes valves and perhaps also some bivalves precipitate valves/shells enriched in ^{18}O relative to equilibrium compositions.

Within lacustrine environments, the effects of temperature on the $\delta^{18}O_{shell}$ values are commonly masked by large temporal variations in $\delta^{18}O_{lakewater}$ values (Holmes and Chivas 2002; Leng and Marshall 2004). For example, bottom waters in the Great Lakes become thermally stratified during the summer months and temperatures do not fluctuate beyond ~1 – 4 °C (Dettman et al. 1995). Accordingly, the $\delta^{18}O_{shell}$ value of any ostracode living in these deep regions of the lakes (e.g. *C. subtriangulata*) will only change with variations in $\delta^{18}O_{lakewater}$ values.

Ostracodes often have narrow environmental and temperature preferences for viability and usually will only molt and precipitate new valves when condition requirements (e.g. temperature) are met (Boomer 2002). Ostracodes molt new carapaces eight to nine times during their lifetime, typically during the summer (Kesling 1951; Xia et al. 1997; Boomer 2002). Ostracodes form their shells within hours to days (Rosenfeld 1982; Chivas et al. 1986), so their valves offer a snapshot of environmental conditions for very narrow moments in time. Given that many ostracode species have specific ecological requirements, changes in fossil assemblages through time can provide information on changes in environmental conditions (Boomer 2002).

Calculating the amount of isotopic fractionation between two phases, such as the calcite carapace of an ostracode and lakewater, can be useful to studies concerned with the compositions of paleolakewater if the species form their valves over a very narrow temperature range. The growing temperature range of *C. subtriangulata*, the most common ostracode species in the Great Lakes, is well known. Dettman et al. (1995) calculated a fractionation factor (α-value) of 1.0358 between the oxygen-isotope compositions of modern *C. subtriangulata* valves and modern Lake Huron water. They then applied this fractionation factor to valves of *C. subtriangulata* as well as to another *Candona* species isolated from Huron Basin sediment cores to calculate the oxygen-isotope composition of paleolakewater present during valve formation. The growing temperature ranges of other common ostracode species present in the Great Lakes are largely undocumented. Since calculated $\delta^{18}O_{lakewater}$ values vary by 0.24 ‰ per °C (equation 1.5) and various ostracode species present in Great Lakes sediment cores likely have different optimum growth temperatures, the determination of specific fractionation factors for each species is required.

The $\delta^{13}C$ values of biogenic carbonates are largely controlled by the carbon isotope composition of dissolved inorganic carbonate (DIC). The DIC pool in the Great Lakes is dominated by bicarbonate (HCO_3^-) but other biological and abiological factors, such as primary productivity, decay of organic matter, exchange with atmospheric CO_2, and dissolution of carbonate minerals in the watershed can also influence the composition of this pool (Kerr-Lawson et al. 1992; Dettman et al. 1995; Leng and Marshall 2004). The carbon-isotope systematics of biogenic carbonates from the Great Lakes Basin is poorly understood, and only a few studies have attempted to interpret these records (e.g., Hladyniuk and Longstaffe 2011).

The $\delta^{13}C$ values of inorganic carbonates formed from a DIC source do not show significant temperature dependence at low temperatures (10 – 40 °C) and are enriched in ^{13}C by 1 ‰ for calcite and ~ 3 ‰ for aragonite relative to DIC (Romanek et al. 1992; Holmes and Chivas 2002). Hence, the carbon-isotope compositions of valves/shells formed at equilibrium with DIC can be predicted. Commonly, however, the $\delta^{13}C$ values of biogenic carbonates are lower than predicted for equilibrium. This outcome may be the result of kinetic isotope fractionation effects, or may stem from the addition of metabolic (i.e. dietary) carbon to the internal carbon pool from which the valve/shell has formed (McConnaughey 1989a, 1989b).

1.4.3 Porewater – oxygen and hydrogen isotopes

Another record of the oxygen- and hydrogen-isotope compositions of ancient lakewater can be provided by the porewater contained in sediment cores. With continuous deposition of sediments on the lake floor, lakewater becomes trapped in the void (pore) spaces between sediment grains. Fine-grained sedimentary deposits such as the lacustrine clays in the Great Lakes region generally have very low intrinsic permeability and hence have the potential to retain original lakewater entrapped during sedimentation (Desualniers et al. 1981; Kolak et al. 1999; McIntosh and Walter 2006). For example, porewaters extracted from early Holocene glaciolacustrine clays in the Agassiz Basin had very low $\delta^{18}O$ values reflective of the meltwater-rich content of Lake Agassiz at the time of sediment deposition (Remenda et al. 1994; Birks et al. 2007).

1.5 RESEARCH SAMPLE

In May 2003, two piston cores were collected from one site in the Goderich sub-basin of Lake Huron (core 146-1: 44° 14' 55" N and 82° 15' 16" W; water depth 92.4 m; core length 14.84 m; and core 146-2: 44° 14' 42" N and 82° 15' 48" W; water depth, 92.4 m; core length, 11.88 m) (Fig. 1.4). The cores were collected within 17 m of each other. The first core retrieved was found to have a crack in the core liner mid-way down its ~15 m-length and so a second ~12 m-long core was collected at the same site. Together these cores comprise core 146; the shorter core makes up the majority of core 146 from the top of the sediment surface (core depth 0 m) to a depth of 11.88 m. Only a small portion of the longer (cracked) core is used, from a core depth of 12.14 to 14.8 m. There is a ~ 26 cm gap between sediment of the two cores. In May 2004, two more cores were collected from Lake Huron, one again from the Goderich sub-basin (core 594: 43° 48' 02" N and 82° 06' 57" W; water depth, 88.5 m; core length 15.0 m) and one from the Manitoulin sub-basin (core 596: 44° 41' 13" N and 81° 54' 42" W; water depth, 120 m; core length, 12.0 m). All piston cores from Lake Huron and Lake Michigan (see below) examined in this study were collected with the assistance of the Captain, crew and staff of the *CCGS Limnos.*

In May-June 2006, three piston cores were collected from Lake Michigan (Fig. 1.4). One core each was taken from the Chippewa sub-basin (core 100: 45° 07’ 00” N and 86° 42’ 33” W; water depth, 164 m; core length, 16.0 m), the Milwaukee sub-basin (core 102: 43°30’ 59” N and 87° 28’ 05” W, water depth, 140 m; core length, 14.73 m), and the South Chippewa sub-basin (core 101: 42° 33’ 53” N and 87° 13’ 54” W; water depth, 134 m; core length, 16.6 m).

In June 2007, four box cores were collected from Lake Huron from the Alpena sub-basin (box core 816: 44° 47’ 01” N and 82° 45’ 47” W; box core 817: 44° 41’ 35” N and 82° 52’ 57” W), the Port Huron sub-basin (box core 819: 43° 31’ 41” N and 82° 14’ 17” W), and the Saginaw sub-basin (box core 821: 44° 25’ 21” N and 82° 44’ 59” W) (Fig. 1.4). These box cores provided modern deep-water ostracodes and clams, and were collected by the Captain, crew and staff of the *CCGS Griffon*. Modern biogenic carbonates were also collected from strand-line deposits along the beach in Pinery Provincial Park on the southwestern shores of Lake Huron.

1.6 STRUCTURE OF THE DISSERTATION

Chapter 2 lays the foundation for the thesis by testing whether common Great Lake ostracodes and molluscs form their shells in isotopic equilibrium with lakewater or if they exhibit isotopic vital effects for which correction is necessary. Modern specimens of ostracodes, bivalves and gastropods were collected from both deep and shallow environments of Lake Huron. Many of these species commonly occur in Great Lake sediment cores and many researchers have used the isotopic compositions of their shells to identify changes in lakewater composition through time (Colman et al. 1990, 1994a, 1994b; Lewis and Anderson 1992; Forester et al. 1994; Last et al. 1994; Lewis et al. 1994; Rea et al. 1994a, 1994b; Dettman et al. 1995; Tevesz et al. 1998; Godsey et al. 1999; Moore et al. 2000; Macdonald and Longstaffe 2008; Breckenridge and Johnson 2009). In this chapter, the oxygen- and carbon-isotope compositions of these shells are compared to average Lake Huron $\delta^{18}O$ (water) and $\delta^{13}C$ (DIC) values. The oxygen-isotope values of the shells and Lake Huron water are used to measure the carbonate-water oxygen-isotope fractionation typical of each species. These measurements are then used to calculate the oxygen-isotope compositions of paleolakewater for ostracodes and bivalve samples from Lakes Michigan and Huron sediment cores (Chapters 3 and 4). Growing temperature ranges have been previously documented for only the most common ostracode species in Great Lakes cores. The data obtained in Chapter 2 are also used to assess the average (and likely optimum) growth temperatures for species typically present in sediments from Lake Huron.

Chapter 3 examines the history of Lake Michigan, as recorded in one core each from the South Chippewa, Milwaukee and Chippewa sub-basins (cores 101, 102 and 100, respectively, Fig. 1.4). The lithologies in each core are described within the context of their depositional environments and respective lake phases, and efforts are made to infer the ages of these sediments. The oxygen-isotope compositions of several ostracode and clam species from these cores are examined to characterize the water that fed the Michigan Basin over the intervals represented in these sediments. These data are also used to assess connectivity to adjacent basins as the hydrology of the Great Lakes system evolved during the late Pleistocene and early to mid Holocene. The carbon-isotope compositions of the biogenic carbonates are used to investigate the dominant controls on the DIC pool, which relate primarily to changes in source water and primary productivity. A comparison of the oxygen- and carbon-isotope compositions of shallow- versus deep-water ostracodes and clams is used to test for isotopic stratification of lakewater during the time period represented by these sediments.

Chapter 4 describes the history of the Huron Basin, as captured by the oxygen and carbon isotopic compositions of biogenic carbonates preserved in three sediment cores, two from the Goderich sub-basin (cores 146 and 594) and one from the Manitoulin sub-basin (core 596). These regions of the Huron Basin have not been previously examined in this way; these cores provide a more complete picture of source water variations within the Huron Basin. The sedimentary sequences recognized in these cores are combined with radiocarbon and pollen information to develop age models for the sediments. The $\delta^{18}O_{paleolakewater}$ values, together with bulk mineralogical data, are used to identify periods when the Huron Basin was inundated with glacial meltwater. The $\delta^{13}C$ values of the biogenic carbonates are used to identify the dominant factors controlling the lakewater DIC pool at various times; variations in these values are shown to relate to changes in productivity and water sources to the Huron Basin during its late Pleistocene and Holocene history.

Chapter 5 assesses the usefulness of porewater extracted from sediments as a proxy for the oxygen- and hydrogen-isotope compositions of ancient lakewater in the Huron and Michigan Basins. Comparisons with lakewater oxygen-isotope compositions based on biogenic carbonates are made to determine the extent to which porewater isotopic compositions are modified by post-entrapment advection- and diffusion-dominated transport.

Chapter 6 summarizes the major conclusions of this thesis concerning: (i) the usefulness of proxy measurements for water sources and organic productivity during the late Pleistocene and Holocene histories of the Michigan and Huron Basins, (ii) the extent and timing of major flooding events within these basins, and (iii) implications for local, regional and global climate change during this critical transitional stage of North American geological history. Research areas most in need of future investigation, and why they are important, are also summarized.

The appendices provide supplementary taxonomic and ecological information for the ostracode, bivalve and gastropod species, and serve as a repository for the stable isotopic data collected during this investigation.

1.7 REFERENCES

Alley RB, Mayewski PA, Sowers T, Stuiver M, Taylor KC, Clark PU (1997) Holocene climatic instability: A prominent, widespread event 8200 yr ago. Geology 25: 483-486

Alley RB (2000) The Younger Dryas cold interval as viewed from central Greenland. Quat Sci Rev 19: 213-226

Bajc AF, Morgan AV, Warner BG (1997) Age and paleoecological significance of an early Postglacial fossil assemblage near Marathon, Ontario, Canada. Can J Earth Sci 34: 687-698

Barber DC, Dyke A, Hillaire-Marcel C, Jennings AE, Andrews JT, Kerwin MW, Bilodeau G, McNeely R, Southon J, Morehead MD, Gagnon J-M (1999) Forcing of the cold event of 8,200 years ago by catastrophic drainage of Laurentide lakes. Nature 400: 344-348

Bartlein PJ, Webb T III, Fleri E (1984) Holocene climatic change in the northern Midwest: Pollen-derived estimates. Quat Res 22: 361-374

Bartlein PJ, Anderson PM, Anderson KH, Edwards ME, Thompson RS, Webb RS, Webb III T, Whitlock C (1998) Paleoclimate simulations for North America for the past 21,000 years: Features of the simulated climate and comparisons with paleoenvironmental data. Quat Sci Rev 17: 549-585

Birks SJ, Edwards TWD, Remenda VH (2007) Isotopic evolution of Glacial Lake Agassiz: New insights from cellulose and porewater isotopic archives. Palaeogeogr Palaeoclimatol Palaeoecol 246: 8-22

Boyle EA, Keigwin LD (1987) North Atlantic thermohaline circulation during the past 20,000 years linked to high-latitude surface temperature. Nature 330: 35-40

Breckenridge A, Johnson TC (2009) Paleohydrology of the upper Laurentian Great Lakes from the late glacial to early Holocene. Quat Res 71: 397-408

Breckenridge A, Lowell TV, Fisher TG, and Yu S (2010) A late Lake Minong transgression in the Lake Superior basin as documented by sediments from Fenton Lake, Ontario. J Paleolimnol DOI 10.1007/s10933-010-9447-z

Broecker WS (1991) The great ocean conveyor. Oceanography 4: 79-89

Broecker WS (1992) Defining the boundaries of the late-glacial isotope episodes. Quat Res 38: 135-138

Broecker WS, Anree M, Wolfli W, Oeschger H, Bonani G, Kennett J, Peteet D (1988) The chronology of the last deglaciation: Implications to the cause of the Younger Dryas event. Paleoceanography 3: 1-19

Broecker WS, Kennett JP, Flower BP, Teller JT, Trumbore S, Bonani G, Wolfli W (1989) Routing of meltwater from the Laurentide Ice Sheet during the Younger Dryas cold episode. Nature 341: 318-321

Brooks GR, Medioli BE (2010) Sub-bottom profiling and coring of sub-basins along the lower French River, Ontario: insights into depositional environments within the North Bay outlet. J Paleolimnol DOI 10.1007/s10933-010-9414-8

Brooks GR, Medioli BE, Telka AM (2010) Evidence of early Holocene closed-basin conditions in the Huron-Georgian basins from within the North Bay outlet of the upper Great Lakes. J Paleolimnol DOI 10.1007/s10933-010-9408-6

Böhm F, Joachimski MM, Dullo W-C, Eisenhauer A, Lehner H, Reitner J, Worheid G (2000) Oxygen isotope fractionation in marine aragonite of coralline sponges. Geochim Cosmochim Acta 64: 1695-170

Boomer I (2002) Environmental applications of marine and freshwater ostracoda. In: Haslett SK (ed) Quaternary Environmental Micropalaeontology. Arnold, London, pp 115-138

Boyd M (2007) Early postglacial history of the southeastern Assiniboine Delta, glacial Lake Agassiz basin. J Paleolimnol 37: 313-329

Buhay WM, Betcher RN (1998) Paleohydrologic implications of ^{18}O-enriched Lake Agassiz water. J Paleolimnol 19: 285-296

Chivas AR, De Deckker, P. and Shelley, J.M.G. (1986) Magnesium content of nonmarine ostracod shells: A new palaeosalinometer and palaeothermometer. Palaeogeogr Palaeoclimatol Palaeoecol 54: 43-61

Clark ID, Fritz P (1997) Environmental Isotopes in Hydrogeology. CRC Press/Lewis Publishers, Boca Raton, Florida

Clark P, Marshall SJ, Clarke GKC, Hostetler SW, Licciardi JM, Teller JT (2001) Freshwater forcing of abrupt climate change during the last glaciation. Science 293: 283-287

Clayton L (1983) Chronology of Lake Agassiz drainage to Lake Superior. In: Teller JT,

Clayton L (eds) Glacial Lake Agassiz, Geol Assoc Canada Spec Paper 26, pp 291-307

COHMAP Members (1988) Climatic changes of the last 18,000 years: observations and model simulations. Science 241: 1043-1052

Colman SM, Keigwin LD, Forester RM (1994a) Two episodes of meltwater influx from glacial Lake Agassiz into the Lake Michigan basin and their climatic contrasts. Geology 22: 547-550

Colman SM, Jones GA, Forester RM, Foster DS (1990) Holocene paleoclimate evidence and sedimentation rates from a core in southwestern Lake Michigan. J Paleolimnol 4: 269-284

Colman SM, Clark JA, Clayton L, Hansel AK, Larsen CE (1994b) Deglaciation, lake levels, and meltwater discharge in the Lake Michigan basin. Quat Sci Rev 13: 879-890

Colman SM, Forester RM, Reynolds RL, Sweetkind DS, King JW, Gangemi P, Jones GA, Keigwin LD, Foster DS (1994c) Lake-level history of Lake Michigan for the past 12,000 years: the record from deep lacustrine sediments. J Great Lakes Res 20: 73-92

Coplen TC (2011) Guidelines and recommended terms for expression of stable-isotope ratio and gas-ratio measurement results. Rapid Commun Mass Spectrom 25: 2538-2560

Coplen TB, Kendall C, Hopple J (1983) Comparison of stable isotope reference samples. Nature 302: 236-238

Couch AG, Eyles N (2008) Sedimentary record of glacial Lake Mackenzie, Northwest Territories, Canada: Implications for Arctic freshwater forcing. Palaeogeogr Palaeoclimatol Palaeoecol 268: 26-38

Craig H (1961) Standard for reporting concentrations of deuterium and oxygen-18 in natural waters. Science 133: 1833-1834

Cvancara AM, Melik JC (1961) Bedrock Geology of Lake Huron. Programs and Abstracts of the 4th Conference on Great Lake Research, pp 116-125

Daley TJ, Street-Perrott FA, Loader NJ, Barber KE, Hughes PDM, Fisher EH, Marshall JD (2009) Terrestrial climate signal of the "8200 yr B.P. cold event" in the Labrador Sea region. Geology 37: 831-834

Dansgaard W (1964) Stable isotopes in precipitation. Tellus 16: 436-468

Dansgaard W, Tauber H (1969) Glacier oxygen-18 content and Pleistocene ocean temperature. Science 166: 499-502

Dansgaard W, Johnsen S, Clausen H, Dahl-Jensen D, Gundestrup N, Hammer C, Hvidberg C, Steffensen J, Sveinbjornsdottir A, Jouzel J, Bong G (1993) Evidence for general instability in past climate from a 250 kyr ice-core record. Nature 364: 218-220

Dean WE, Ahlbrandt TS, Anderson RY, Bradbury JP (1996) Regional aridity in North America during the middle Holocene. The Holocene 6: 145-155

Desaulneirs DE, Cherry JA, Fritz P (1981) Origin, age and movement of pore water in argillaceous Quaternary deposits at four sites in Southwestern Ontario. J Hydrol 50: 231-257

Dettman DL, Smith AJ, Rea DK, Moore TC Jr., Lohmann KC (1995) Glacial meltwater in Lake Huron during early postglacial time as inferred from single-valve analysis of oxygen isotopes in ostracodes. Quat Res 43: 297-310

deVernal A, Hilliare-Marcel C, Bilodeau G (1996) Reduced meltwater outflow from the Laurentide ice margin during the Younger Dryas. Nature 381: 774–777

Dobson DM, Moore TC Jr., Rea DK (1995) The sedimentation history of Lake Huron and Georgian Bay: results from analysis of seismic reflection profiles. J Paleolimnol 13: 231-249

Dorale JA, González LA, Reagan MK, Pickett DA, Murrell MT, Baker RG (1992) A high-resolution record of Holocene climate change in speleothem calcite from Coldwater cave, Northeast Iowa. Science 258: 1626-1630

Ebbesen H, Hald M (2004) Unstable Younger Dryas climate in the northeast North Atlantic. Geology 32: 673-676

Edwards TWD, Wolfe BB, MacDonald GM (1996) Influence of changing atmospheric circulation on precipitation $\delta^{18}O$ – temperature relations in Canada during the Holocene. Quat Res 46: 211-218

Eschman DF, Karrow PF (1985) Huron basin glacial lakes: a review. In: Karrow PF, Calkin PE (eds) Quaternary Evolution of the Great Lakes. Geol Assoc Canada Spec Paper 30, pp 79-93

Farrand WR, Drexler CW (1985) Lake Wisconsinan and Holocene history of the Lake Superior basin. In: Karrow PF, Calkin PE (eds) Quaternary Evolution of the Great Lakes. Geol Assoc Canada Spec Paper 30, pp 17-32

Finamore PF (1985) Glacial Lake Algonquin and the Fenelon Falls outlet. In: Karrow PF, Calkin PE (eds) Quaternary Evolution of the Great Lakes. Geol Assoc Canada Spec Paper 30, pp 125-132

Fisher TG (2003) Chronology of glacial Lake Agassiz meltwater routed to the Gulf of Mexico. Quat Res 59: 271-276

Fisher TG (2007) Abandonment chronology of glacial Lake Agassiz's Northwestern outlet. Palaeogeogr Palaeoclimatol Palaeoecol 246: 31-44

Fisher TG, Smith DG (1994) Glacial Lake Agassiz: its northwest maximum extent and outlet in Saskatchewan (Emerson phase). Quat Sci Rev 13: 845-858

Fisher TG, Smith DG, Andrews JT (2002) Preboreal oscillation caused by a glacial Lake Agassiz flood. Quat Sci Rev 21: 873-878

Fisher TG, Weyer KA, Boudreau AM, Martin-Hayden JM, Krantz DE, Breckenridge A (2010) Constraining Holocene lake levels and coastal dune activity in the Lake Michigan basin. J Paleolimnol DOI 10.1007/s10933-010-9460-2

Fisher TG, Yansa CH, Lowell TV, Lepper K, Hajdas I, Ashworth A (2008) The chronology, climate and confusion of the Moorhead Phase of glacial Lake Agassiz: new results from the Ojata Beach, North Dakota, USA. Quat Sci Rev 27: 1124-1135

Flesche Kleiven H, Kissel C, Laj C, Ninnemann US, Richter TO, Cortijo E (2008) Reduced North Atlantic Deep Water coeval with the Glacial Lake Agassiz freshwater outburst. Science 319: 60-64

Forester RM, Colman SM, Reynolds RL, Keigwin LD (1994) Lake Michigan's late Quaternary limnological and climate history from ostracode, oxygen isotope, and magnetic susceptibility. J Great Lakes Res 20: 93-107

Friedman I, O'Neil JR (1977) Compilation of stable isotope fractionation factors of geochemical interest. In: Fleischer M (ed) Data of Geochemistry. USGS, Washington, pp KK1-KK12

Godsey HS, Moore TC Jr, Rea DK, Shane LCK (1999) Post-Younger Dryas seasonality in the North American midcontinent region as recorded in Lake Huron varved sediments. Can J Earth Sci 36: 533-547

Gonfiantini R (1986) Environmental isotopes in lake studies. In: Fritz P, Fontes JC (eds) Handbook of Environmental Isotope Geochemistry: The Terrestrial Environment, v. 1A. Elsevier, Amsterdam, pp 113-168

Grootes PM, Stuiver M, White JWC, Johnsen S, Jouzel J (1993) Comparison of oxygen isotope records from the GISP2 and GRIP Greenland ice cores. Nature 366: 552-554

Guiot J, Harrison SP, Prentice IC (1993) Reconstruction of Holocene precipitation patterns in Europe using pollen and lake-level data: Quat Res 40: 139-149

Hansel AK, Mickelson DM (1988) A reevaluation of the timing and causes of high lake phases in the Michigan Basin. Quat Res 29: 113-128

Hansel AK, Mickelson DM, Schneider AF, Larsen CE (1985) Late Wisconsinan and Holocene history of the lake Michigan basin. In: Karrow PF, Calkin PE (eds) Quaternary Evolution of the Great Lakes. Geol Assoc Canada Spec Paper 30, pp 40-53

Hladyniuk R, Longstaffe FJ (2011) A stable Carbon-isotope record of biogenic carbonate from Lake Ontario since >12.3 ka BP. Programs and Abstracts of the 54th Conference on Great Lake Research, pp 102

Holmes JA, Chivas AR (2002) Ostracod shell chemistry – Overview. In: Holmes JA, Chivas AR (eds) The Ostracoda: Applications in Quaternary Research. AGU Monogr 131, pp 185-204

Hough JL (1958) Geology of the Great Lakes. University Illinois Press, Urbana, Illinois

Hughen KA, Overpeck JT, Peterson LC, Trumbore, S (1996) Rapid climate changes in the tropical Atlantic region during the last deglaciation. Nature 380: 51-54

Jouzel J, Alley RB, Cuffey KM, Dansgaard W, Grootes PM, Hoffman G, Johnson SJ, Koster RD, Peel D, Shuman CA, Stievenard M, Stuiver M, White JC (1997) Validity of the temperature reconstruction from water isotopes in ice cores. J

Geophys Res 102: 471-487

Karrow PF, Dreimanis A, Barnett PJ (2000) A proposed diachronic revision of Late Quaternary time-stratigraphic classification in the eastern and northern Great Lakes area. Quat Res 5: 49-87

Keigwin LD, Jones GA (1995) The marine record of deglaciation from the continental margin off Nova Scotia. Paleoceanography 10: 973-985

Kerr-Lawson LJ, Karrow PF, Edwards TWD, Mackie GL (1992) A paleoenvironmental study of the molluscs from the Don Formation (Sangamonian?) Don Valley Brickyard, Toronto, Ontario. Can J Earth Sci 29: 2406-2417

Kesling RV (1951) The morphology of ostracod molt stages. Illinois Biol Monogr 21, pp 1-126

Kolak JJ, Long DT, Matty JM, Larson GJ, Sibley DF, Councell TB (1999) Ground-water, large-lake interactions in Saginaw Bay, Lake Huron: A geochemical and isotopic approach. Geol Soc Am Bull 111: 177-188

Krishnamurthy RV, Syrup K, Baskaran M, Long A (1995) Late glacial climate record of Midwestern USA from the hydrogen isotope record of lake organic matter. Science 269: 1565-1567

Kutzbach JE, Webb TI (1993) Conceptual basis for understanding Late-Quaternary climates. In: Wright HEJ, Kutzbach JE, Webb TI, Ruddiman WF, Street-Perrott FA, Bartlein PJ (eds) Global Climates Since the Last Glacial Maximum. Univ Of Minnesota Press, Minneapolis, pp 5-11

Larsen CE (1985) Lake level, uplift and outlet incision, the Nipissing and Algoma Great Lakes. In: Karrow PF, Calkin PE (eds) Quaternary Evolution of the Great Lakes. Geol Assoc Canada Spec Paper 30, pp 63-77

Larson G, Schaetzl R (2001) Origin and Evolution of the Great Lakes. J Great Lakes Res 27: 518-546

Last WM, Teller JT, Forester RM (1994) Paleohydrology and paleochemistry of Lake Manitoba, Canada: the isotope and ostracode records. J Paleolimnol 12: 269-282

Leng MJ, Marshall JD (2004) Palaeoclimate interpretation of stable isotope data from lake sediment archives. Quat Sci Rev 23: 811-831

Leverington DW, Mann JD, Teller JT (2000) Changes in the bathymetry and volume of glacial Lake Agassiz between 11,000 and 9,300 ^{14}C yr BP. Quat Res 54: 174-181

Levesque AJ, Cwynar LC, Walker IR (1997) Exceptionally steep north-south gradients in lake temperatures during the last deglaciation. Nature 385: 423-426

Lewis CFM, Anderson TW (1989) Oscillations of levels and cool phases of the Laurentian Great Lakes caused by inflows from glacial Lakes Agassiz and Barlow-Ojibway. J Paleolimnol 2: 99-14

Lewis CFM, Anderson TW (1992) Stable isotope (O and C) and pollen trends in eastern Lake Erie, evidence for a locally-induced climatic reversal of Younger Dryas age in the Great Lakes basin. Clim Dynam 6: 241-250

Lewis CFM, Blasco SM, Gareau PL (2005) Glacio-isostatic adjustment of the Laurentian Great Lakes basin: using the empirical record of strandline deformation for reconstruction of early Holocene paleo-lakes and discovery of a hydrologically closed phase. Géog Phys et Quat 59: 171-193

Lewis CFM, Heil Jr CW, Hubeny JB, King JW, Moore Jr TC, Rea DK (2007) The Stanley unconformity in Lake Huron basin: evidence for a climate-driven closed lowstand about 7900 ^{14}C ka BP, with similar implications for the Chippewa lowstand in Lake Michigan basin. J Paleolimnol 37: 435-452

Lewis CFM, Karrow PF, Blasco SM, McCarthy FMG, King JW, Moore Jr TC, Rea DK (2008) Evolution of lakes in the Huron basin: Deglaciation to present. Aquat Ecosyst Health Manage 11: 127-136

Lewis CFM, Moore Jr TC, Rea DK, Dettman DL, Smith AM, Mayer LA (1994) Lakes of the Huron basin: their record of runoff from the Laurentide Ice Sheet. Quat Sci Rev 13: 891-922

Lovan NA, Krishnamurthy RV (2011) Inferring paleotemperature from the D/H ratio of lacustrine organic matter. Quat Internat 229: 38-46

Lowell TV, Fisher TG, Comer GC, Hajdas I, Waterson N, Glover K, Loope HM, Schaefer JM, Rinterknecht VR, Broecker W, Denton GH Teller JT (2005) Testing the Lake Agassiz meltwater trigger for the Younger Dryas. EOS 86: 365-372

Lowell TV, Fisher TG, Hadjas I, Glover K, Loope HM, Henry T (2009) Radiocarbon deglaciation chronology of the Thunder Bay, Ontario area and implications for ice sheet retreat patterns. Quat Sci Rev 28: 1597-1607

Macdonald RM, Longstaffe FJ (2008) The Late Quaternary oxygen-isotope composition of southern Lake Huron. Aquat Ecosyst Health Manage 11: 137-143

McConnaughey T (1989a) ^{13}C and ^{18}O isotopic disequilibrium in biological carbonates: I Patterns. Geochim Cosmochim Acta 53: 151-162

McConnaughey T (1989b) ^{13}C and ^{18}O isotopic disequilibrium in biological carbonates: II In vitro simulation of kinetic isotope effects. Geochim Cosmochim Acta 53: 163-171

McIntosh JC, Walter LM (2006) Paleowaters in Silurian-Devonian carbonate aquifers: Geochemical evolution of groundwater in the Great Lakes region sine the Lake Pleistocene. Geochim Cosmochim Acta 70: 2454-2479

McKenzie SM (2010) Late Pleistocene to mid-Holocene climate variability in Ireland: Evidence from Ostracode Geochemistry. Ph.D. thesis, University of Saskatchewan, Saskatoon, pp 57

Moore TC Jr, Rea DK, Mayer LA, Lewis CFM, Dobson DM (1994) Seismic stratigraphy of Lake Huron - Georgian Bay and postglacial lake history. Can J Earth Sci 31: 1606-1617

Moore TC Jr, Walker JCG, Rea DK, Lewis CFM, Shane LCK, Smith AJ (2000) Younger Dryas interval and outflow from the Laurentide ice sheet. Paleoceanography 15: 4-18

Murton JB, Bateman MD, Dallimore SR, Teller JT, Zhirong Yang (2010) Identification of Younger Dryas outburst flood path from Lake Agassiz to the Arctic Ocean. Nature 464: 740-743

North Greenland Ice Core Project members (2004) High-resolution record of Northern Hemisphere climate extending into the last interglacial period. Nature 431: 147-151

Obbink EA, Carlson AE, Klinkhammer GP (2010) Eastern North American freshwater discharge during the Bølling-Allerød warm periods. Geology 38: 171-174

Odegaard C, Rea DK, Moore TC (2003) Stratigraphy of the mid-Holocene black bands in Lakes Michigan and Huron: Evidence for possible basin-wide anoxia. J Paleolimnol 29: 221-234

O'Neil JR, Clayton RN, Mayeda TK (1969) Oxygen isotope fractionation of divalent metal carbonates. J Chem Phys 30: 5547-5558

Peltier WR (2007) Rapid climate change and Arctic Ocean freshening. Geology 35: 1147-1148

Rahmstorf S (2006) Thermohaline Ocean Circulation. In: Elias SA (ed) Encyclopedia of Quaternary Sciences. Elsevier, Amsterdam, pp 1-10

Rasmussen SO, Andersen KK, Svensson AM, Steffensen JP, Vinther BM, Clausen HB, Siggaard-Andersen ML, Johnsen SJ, Larsen LB, Dahl-Jensen D, Bigler M, Röthlisberger R, Fischer H, Goto-Azuma K, Hansson ME, Ruth U (2006) A new Greenland ice core chronology for the last glacial termination. J Geophys Res 111: D06102, DOI 10.1029/2005JD006079

Rea DK, Moore TC Jr, Lewis CFM, Mayer LA, Dettman DL, Smith AL, Dobson DM (1994a) Stratigraphy and paleolimnologic record of lower Holocene sediments in northern Lake Huron and Georgian Bay. Can J Earth Sci 31: 1586-1605

Rea DK, Moore TC Jr, Anderson TW, Lewis CFM, Dobson DM, Dettman DL, Smith AJ, Mayer LA, (1994b) Great Lakes paleohydrology: complex interplay of glacial meltwater, lake levels and sill depths. Geology 22: 1059-1062

Remenda VH, Cherry JA, Edwards TWD (1994) Isotopic composition of old ground water from Lake Agassiz: implications for late Pleistocene climate. Science 226: 1975-1978

Rensenn H, Seppä H, Heiri O, Roche DM, Goosse H, Fichefet T (2009) The spatial and temporal complexity of the Holocene thermal maximum. Nature Geosci 2: 411-414

Rodrigues CG, Vilks G (1994) The impact of glacial lake runoff on the Goldthwait and Champlain seas: the relationship between glacial Lake Agassiz and the Younger Dryas. Quat Sci Rev 13: 923-944

Romanek CS, Grossman EL, Morse JW (1992) Carbon isotopic fractionation in synthetic aragonite and calcite: Effects of temperature and precipitation rate. Geochim Cosmochim Acta 56: 419-430

Rooth C (1982) Hydrology and ocean circulation. Prog Oceanogr 11: 131-149

Rosenfeld A (1982) The secretion process of the ostracod carapace. In: Bate RH, Robinson E, Sheppard LM (eds) Fossil and Recent Ostracods. Ellis Harwood, London, pp 12–24

Rozanski K, Araguas L, Gonfiantini R (1993) Isotopic patterns in modern global precipitation. In: Swart PK, McKenzie J, Lohmann KC, Savin S (eds) Climate Change in Continental Isotopic Records. AGU Monogr 78, pp 1-36

Safarudin, Moore Jr TC (1999) The history and architecture of lacustrine depositional systems in the northern Lake Michigan basin. J Paleolimnol 22: 475-496

Schneider AF, Need EA (1985) Lake Milwaukee: An "early" proglacial lake in the Lake Michigan Basin. In: Karrow PF, Calkin PE (eds) Quaternary Evolution of the Great Lakes. Geol Assoc Canada Spec Paper 30, pp 55-62

Shuman B, Bartlein P, Logar N, Newby P, Webb III T (2002) Parallel climate and vegetation responses to the early Holocene collapse of the Laurentide Ice Sheet. Quat Sci Rev 21: 1793-1805

Shuman B, Plank C (2011) Orbital, ice sheet, and possible solar controls on Holocene moisture trends in the North Atlantic drainage basin. Geology 39: 151-154

Sima A, Paul A, Schulz M, Oerlemans J (2006) Modeling the oxygen-isotopic composition of the North American Ice Sheet and its effect on the isotopic composition of the ocean during the last glacial cycle. Geophys Res Lett 33: L15706, DOI 10.1029/2006GL026923

Smith DG, Fisher TG (1993) Glacial Lake Agassiz - the northwestern outlet and paleoflood. Geology 21: 9-12

Stuiver M, Grootes PM, Braziunas TF (1995) The GISP2 $\delta^{18}O$ climate record of the past 16,500 years and the role of sun, ocean, and volcanoes. Quat Res 44: 341-354

Teller JT (1985) Glacial Lake Agassiz and its influence on the Great Lakes. In: Karrow PF, Calkin PE (eds) Quaternary Evolution of the Great Lakes. Geol Assoc Canada Spec Paper 30, pp 1-12

Teller JT, Thorleifson LH (1983) The Lake Agassiz-Lake Superior connection. In: Teller JT, Clayton L (eds) Glacial Lake Agassiz. Geol Assoc Canada Spec Paper 26, pp 261-290

Teller JT, Leverington DW, Mann JD (2002) Freshwater outbursts to the oceans from glacial Lake Agassiz and their role in climate change during the last deglaciation. Quat Sci Rev 21: 879-887

Teller JT, Boyd M, Yang ZR, Kor PSG, Fard AM (2005) Alternative routing of Lake Agassiz overflow during the Younger Dryas: new dates, paleotopography, and a re-evaluation. Quat Sci Rev 24: 1890-1905

Teller JT, Leverington DW (2004) Glacial Lake Agassiz: A 5000 yr history of change and its relationship to the $\delta^{18}O$ record of Greenland. Geol Soc Am Bull 116: 729-742

Tevesz MJS, Spongberg AL, Fuller JA (1998) Stable carbon and oxygen isotope records of central Lake Erie sediments. J Paleolimnol 20: 295-305

Turpen JB, Angell RW (1971) Aspects of molting and calcification in the ostracod *Heterocypris*. Biol Bull 140: 331-338

von Grafenstein U, Erlenkeuser H, Brauer A, Jouzel J, Johnsen SJ (1999) A mid-European decadal isotope-climate record from 15 500 to 5000 years B.P. Science 284: 1654-1657

Williams JW, Shuman B, Bartlein PJ, Diffenbaugh NS, Webb T III (2010) Rapid, time-transgressive, and variable responses to early Holocene midcontinental drying in North America. Geology 38: 135-138

Webb T III, Bartlein PJ, Harrison SP, Anderson KH (1993) Vegetation, lake level, and climate change in eastern North America. In: Wright HE Jr, Kutzbach JE, Webb III T, Ruddiman WF, Street-Perrott FA, Bartlein PJ (eds) Global Climates Since the Last Glacial Maximum. University of Minnesota Press, Minneapolis, pp 415-467

Wold RJ, Paull RA, Wolosin CA, Friedel RJ (1981) Geology of central Lake Michigan. Am Assoc Petr Geol 65: 1621-1632

Xia J, Ito E, Engstrom DR (1997) Geochemistry of ostracode calcite: Part 1. An experimental determination of oxygen isotope fractionation. Geochim Cosmochim Acta 61: 377-382

Yu S, Colman SM, Lowell TV, Milne GA, Fisher TG, Breckenridge A, Boyd M, Teller JT (2010) Freshwater outburst from Lake Superior as a trigger for the cold event 9300 years ago. Science 328: 1261-1266

Yu Z (2000) Ecosystem response to Lateglacial and early Holocene climate oscillations in the Great Lakes region of North America. Quat Sci Rev 19: 1723-1747

Yu Z, Eicher U (1998) Abrupt climate oscillations during the last deglaciation in central North America. Science 282: 2235-2238

Yu Z, Eicher U (2001) Three amphi-Atlantic century-scale cold events during the

Bølling-Allerød warm period. Géog Phys et Quat 55: 171-179

Yu Z, McAndrews JH, Eicher U (1997) Middle Holocene dry climate caused by change in atmospheric circulation patterns: Evidence from lake levels and stable isotopes. Geology 25: 251-254

Zolitzschka B, Brauer A, Negendank JFW, Stockhausen H, Lang A (2000) Annually dated Late Weichselian continental paleoclimate record from the Eifel, Germany. Geology 28: 783-786

CHAPTER 2

Oxygen- and Carbon-Isotope Fractionations between Modern Lake Huron Biogenic Carbonates and Lake Huron Water

2.1 INTRODUCTION

This study reports the oxygen- and carbon-isotope compositions of modern ostracode, bivalve and gastropod shells from Lake Huron. The oxygen isotopic data are used to evaluate the oxygen-isotope fractionation between the shells of these species and the Lake Huron water in which they lived. Many of these species are represented in fossil assemblages from Great Lake sediment cores. Hence, knowledge of the shell-water oxygen-isotope fractionation factors ($\alpha_{\text{carbonate-water}}$) for these species is required to calculate paleo-lakewater compositions. We test the assumption of von Grafenstein et al. (1999) that oxygen-isotope vital effects during calcite shell formation are constant for all species of an ostracode genus by analyzing five different Candoninae species, all of which are present in the Great Lakes fossil record. We also assess whether other shelly organisms (bivalves and gastropods) present in sediment cores from the Great Lakes form their shells in oxygen-isotope equilibrium with lake water. The carbon-isotope compositions of the shells from these modern specimens are used to examine aspects of the carbon cycle in Lake Huron.

Many studies have used the oxygen-isotope composition of ostracodes and molluscs from Great Lake sediment cores to deduce lakewater composition during and since glacial times – principally as a means of tracking the flow of glacial meltwater (Colman et al. 1990, 1994a, 1994b; Lewis and Anderson 1992; Forester et al. 1994; Last et al. 1994; Lewis et al. 1994; Rea et al. 1994a, 1994b; Dettman et al. 1995; Tevesz et al. 1998; Godsey et al. 1999; Moore et al. 2000; Macdonald and Longstaffe 2008; Breckenridge and Johnson 2009; Hyodo and Longstaffe 2011). Large volumes of water originating from Lake Agassiz and passing through the Great Lakes have been implicated in major global climate changes. In particular, cold, fresh water flows originating from melting continental ice sheets have been linked to a disruption in global ocean currents (Rooth 1982; Broecker et al. 1988, 1989; Peltier 2007).

The calcitic valves of ostracodes and aragonitic shells of bivalves (clams) and gastropods (snails) are excellent proxies for lakewater oxygen-isotope composition, which in turn carries information on the isotopic composition of regional precipitation, precipitation:evaporation ratios, water temperature and average air temperature (Holmes and Chivas 2002). Beyond their isotopic compositions, variations in the species assemblages of ostracodes and bivalves from Great Lake sediment cores are also useful markers for environmental or climatic changes and fluctuations in lake level (Colman et al. 1990; Forester et al. 1994; Macdonald and Longstaffe 2007; Chapter 3, this thesis).

2.1.1. Controls on the isotopic compositions of biogenic carbonates

The carbon- and oxygen-isotope compositions of biogenic carbonates generally record local environmental conditions at the time of shell formation. Under equilibrium conditions, the carbonate oxygen-isotope composition ($\delta^{18}O_{shell}$) is controlled by water composition ($\delta^{18}O_{lakewater}$) and temperature. Within lacustrine environments, the effects of temperature on the $\delta^{18}O_{shell}$ values are commonly masked by large temporal variations in $\delta^{18}O_{lakewater}$ values (Holmes and Chivas 2002; Leng and Marshall 2004). For example, the isotopic composition of species living below the thermoclime, where temperatures are normally between 1-4°C and do not fluctuate much (Dettman et al. 1995), is largely controlled by the isotopic composition of the water in which they live (e.g., the ostracode *Candona subtriangulata*). The effect of temperature on variation in $\delta^{18}O_{shell}$ values can largely be minimized if the species forms its shell only over a very narrow temperature range.

Not all aquatic organisms precipitate their calcium carbonate shells in isotopic equilibrium with water. These differences are generally attributed to vital effects, which are commonly classified as either kinetic (affecting both $\delta^{13}C$ and $\delta^{18}O$ values) or metabolic (affecting only $\delta^{13}C$ values) (McConnaughey 1989a, 1989b). The $\delta^{18}O_{shell}$

values of most biogenic carbonates precipitated out of isotopic equilibrium with host water are more negative than predicted for equilibrium. Ostracodes and some bivalves, however, are typically enriched in ^{18}O by ~1-2 ‰ relative to equilibrium conditions (McConnaughey 1989a, 1989b; von Grafenstein et al. 1999; Xia et al. 1997; Wetterich et al. 2008; Decrouy et al. 2011b). Barnacles, foraminifera, limpets and marine snails have also been found to have higher δ^{18}O values than expected for equilibrium precipitation (Fenger et al. 2007). The vital effect is commonly considered to be genus-specific; i.e., its size and sign is believed to be the same for all species of the ostracode genus *Candona*. Vital effects exhibited by ostracodes are also commonly considered to be constant over a range of temperatures and for all instars of a species (von Grafenstein et al. 1999; Decrouy et al. 2011b).

The δ^{13}C values of biogenic carbonates are largely controlled by the carbon-isotope composition of dissolved inorganic carbonate (DIC). The carbon-isotope composition of DIC, in turn, is controlled by a number of biological (e.g., photosynthesis, respiration, decay of organic matter) and abiotic processes (e.g., carbonate dissolution, exchange with atmospheric CO_2) (Kerr-Lawson et al. 1992; Leng and Marshall 2004). The δ^{13}C values of inorganic calcite and aragonite precipitated from dissolved HCO_3^- are largely temperature-independent at low temperatures (10-40 °C), and are enriched in ^{13}C by ~1‰ or ~2.7‰, respectively, over their DIC source (Romanek et al. 1992; Holmes and Chivas 2002; Keatings et al. 2002).

The spatial distribution of ostracodes species is mainly controlled by water temperature, the composition of major dissolved ions (solutes) and their concentration (total dissolved solids, TDS; Forester et al. 1994). As a result of individual species tolerances to these physical and chemical variables, different species of ostracodes and molluscs inhabiting the Great Lakes consistently occupy similar habitats/environments. Some of these species have narrow optimum-growth temperature ranges. Ostracodes – a mainstay for paleoenvironment reconstruction of the Great Lakes – grow incrementally by molting in stages known as instars. This process usually occurs eight to nine times during an ostracode's life (Kesling 1951; Xia et al. 1997; Boomer 2002). Ostracode valves are composed of low-Mg calcite. Each newly calcified carapace (two valves attached by a hinge) uses ions obtained directly from the water (e.g., HCO_3^-, Ca^{2+}), rather than the previous instar or the biomass of the ostracode itself (Turpen and Angell 1971). Since the whole calcification process takes only hours to a few days (Boomer 2002; Holmes and Chivas 2002), the $\delta^{18}O_{shell}$ values of individual valves provide a record of the oxygen-isotope composition of lakewater for that brief period of time.

Unlike ostracodes, which produce new calcitic valves after each molt, bivalves and gastropods accumulate aragonite shelly material continuously as they grow. Bivalve shell growth is not constant throughout the year. Shell growth is rapid during the spring, during which time a band of transparent carbonate is formed. This carbonate is consolidated during the rest of the warm season (von Grafenstein et al. 1999). The shell of a bivalve is secreted by the mantle (a thin organ lining the inside of the shell) and consists of two layers: the outer organic (conchiolin) layer called the periostracum, and the inner aragonitic layer (Mackie 2007). Growth lines, the concentric striations on the surface of bivalve shells, form during periods of slow to no growth (e.g., usually over the winter months; Goewert et al. 2007). The shelly material formed between growth lines can offer high-resolution – as great as daily – records of environmental conditions during the period of rapid growth (Schöne 2008).

Gastropod shells contain both calcareous (aragonite, as is the case for this study, or calcite) and organic (conchiolin) layers. The shells grow as new material, both mineral and organic, is secreted by the outer edge of the mantle and added to the lips of the aperture (aka, the shell opening; Ruppert et al. 2004). Calcium and other ions required for shell formation are obtained directly from the organisms' environment, through the gills, or in a few cases from digestion (Wilbur and Saleuddin 1983). Carbonate used to form the shell is extracted from the mantle CO_2-bicarbonate pool, which itself is drawn from either the surrounding environment or from metabolic carbon (Shanahan et al. 2005). Studies of aquatic molluscs have shown that metabolic carbon can account for up to 6 – 10 % of the total carbon utilized during shell growth (McConnaughey et al. 1997; Lorrain et al. 2004; Gillikin et al. 2006; McConnaughey and Gillikin 2008) and that this amount can increase as the organism ages (Goewert et al. 2007). Gastropod shell growth is discontinuous; growth lines, as for bivalves, indicate hiatuses between periods of growth. For most gastropods, shell growth rate declines with age (Ruppert et al. 2004).

2.1.2. Previous oxygen isotopic calibrations for Lake Huron ostracodes

Two earlier reports have assumed ostracode valve formation occurs in oxygen isotopic equilibrium with Lake Huron water (Rea et al. 1994a; Dettman et al. 1995). Rea et al. (1994a) measured the δ^{18}O values of Lake Huron (-7 ‰ SMOW) and ostracodes and bivalves (-3.5 to -4.0 ‰, PDB) from surface sediment grab samples collected from below the thermocline. They concluded -3.5 ‰ to be the expected separation between biogenic carbonates and lake water (on their respective reference scales) at ~4.5 °C, and that there was no discernable oxygen-isotope vital effect for Lake Huron's ostracodes and bivalves. This offset was then applied in this and subsequent studies to calculate paleowater δ^{18}O values for Lake Huron (Rea et al. 1994a, 1994b; Moore et al. 2000).

Dettman et al. (1995) measured the oxygen-isotope compositions of ostracodes, bivalves and water from Lake Huron and calculated a $\alpha_{\text{carbonate-water}}$ of 1.0358 for their most ^{18}O-rich *C. subtriangulata* specimen (i.e., the ostracode whose carapace formed at the lowest temperature) and Lake Huron water. They assumed that ostracodes precipitated their valves under equilibrium or near-equilibrium conditions. Dettman et al. (1995) also applied this fractionation factor to the other *Candona* species (*Candona rawsoni*) present in their sample. Fractionation factors were not determined for *Cytherissa lacustris* or bivalves (*Pisidium* genus) although isotopic data were reported for modern samples of both.

Dettman et al. (1995) obtained an average of -6.9 ‰ for water collected from various depths at three stations in northwestern Lake Huron, which was used in the calculation of α. Subsequent studies, however, have shown that although Lake Huron is very homogeneous in its oxygen isotopic composition, a few distinct localities have δ^{18}O values consistently higher or lower than average (Macdonald and Longstaffe 2004, 2007).

These areas include northwestern Lake Huron where Lake Michigan, with an average $\delta^{18}O$ value of -5.9 ‰, flows into Lake Huron (Macdonald and Longstaffe 2007; Macdonald et al. 2007).

Most recently, Macdonald and Longstaffe (2008) calculated the oxygen-isotope composition of Lake Huron paleowater by combining the oxygen-isotope low-Mg calcite–water geothermometer of Friedman and O'Neil (1977) with the oxygen-isotope vital effect of +2.2 ‰ measured for *C. subtriangulata* by von Grafenstein et al. (1999). This approach could be used best for *C. subtriangulata* because, unlike most Great Lake ostracode species, its growth-tolerance temperature range is well-known (mean water temperature ~4-5 °C, range 3-19 °C; Delorme 1978, 1991, 2001; Colman et al. 1990; Dettman et al. 1995). The result is an isotopic separation between *C. subtriangulata* $\delta^{18}O$ (VPDB) values and calculated paleowater $\delta^{18}O$ (VSMOW) values of ~ -5 ‰, rather than the value of ~ -3.5 ‰ employed in earlier studies.

2.2 MATERIALS AND METHODS

Water was sampled throughout Lake Huron and Georgian Bay by staff and crew of the *CCGS Limnos or CCGS Griffon* during various spring, summer and fall cruises over the period 2004-2007. Samples were collected at various depths, ranging from 1 to 192 m (bottom-minus-2 m). The water samples were placed in 15 or 30 ml HDPE Nalgene bottles with no headspace, sealed with parafilm to prevent evaporation and leakage, and kept refrigerated prior to isotopic analysis. Results for samples collected from 2004-2006 (n = 201) were summarized by Macdonald and Longstaffe (2004, 2007). Results for samples collected in 2007 (n = 183) have not been reported previously.

Four box cores were collected from Lake Huron in June 2007, while onboard the *CCGS Griffon* (Fig. 2.1). Sediment from the upper 5-10 cm of the box core was sieved and material >125 μm was retained. This fraction contained organic materials (seeds, pollen, a few insect pieces) and a few bivalves and ostracodes. At the time of collection, some of the ostracodes were alive for their soft parts were very well preserved. Box core

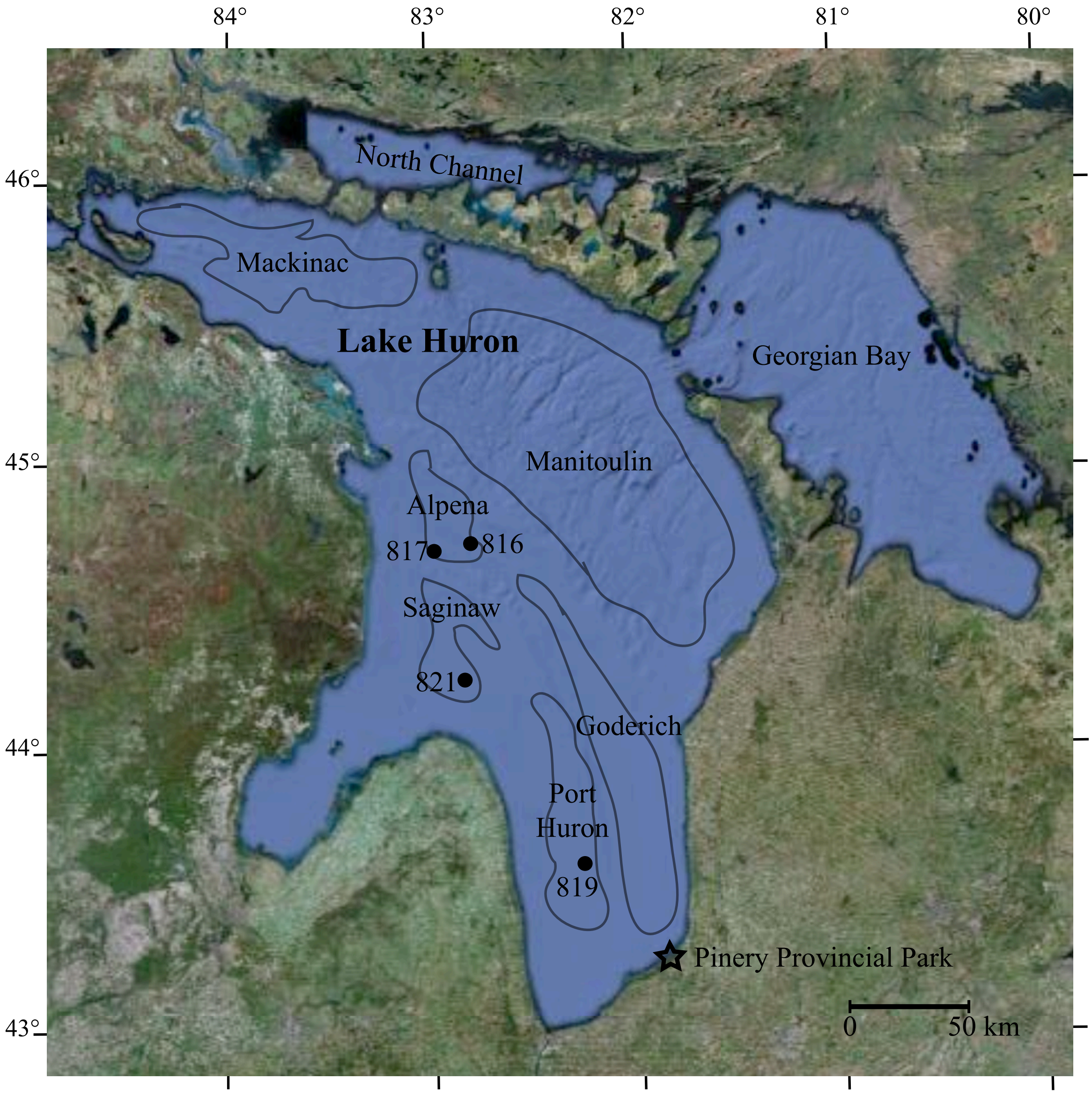

Figure 2.1. Map of the Huron Basin showing sub-basins, box core sites and the location of Pinery Provincial Park. Coordinates of the box cores are: core #816–44° 47' 01" N and 82° 45' 47" W; core #817–44° 41' 35" N and 82° 52' 57" W; core #819–43° 31' 41" N and 82° 14' 17" W; core #821–44° 25' 21" N and 82° 44' 59" W.

#816 yielded many bivalves (*Pisidium* sp.) and one carapace each of *C. subtriangulata* and *Candona crogmaniana*; box core #819 yielded bivalves (*Pisidium* sp.) and one carapace of *C. subtriangulata*, and box cores #817 and #821 did not contain any biogenic carbonates.

Modern ostracode, bivalve and gastropod samples were also collected in October 2007 and June, August, September and October 2008 from strand line deposits at Beach #9, Pinery Provincial Park, which is located on the southeastern shore of Lake Huron (Fig. 2.2). The October 2007 sample was largely composed of gastropods (mainly *Valvata* species) but also contained significant numbers of bivalves (*Pisidium* species) and ostracodes (*C. lacustris*, *C. subtriangulata, C. rawsoni* and *C. crogmaniana*). The June 2008 sample was dominated by zebra mussels, but also contained a few gastropods (*Valvata* species), bivalves (*Pisidium* species) and one *C. rawsoni* valve. We did not analyze the zebra mussels, as they are recent invaders to the Great Lakes and not present in the sedimentary record of interest to us. The August 2008 sample contained large numbers of gastropods (*Valvata* species and a few others*)* and bivalves (*Pisidium* and *Sphaerium* species) but no ostracodes. The September 2008 sample was largely composed of gastropods but also contained *C. crogmaniana*, *C. rawsoni*, *Fabaeformiscandona caudata, Candona acuta*, and *C. lacustris*. The October 2008 sample contained many species of gastropods (mainly *Valvata species)* and bivalves (*Pisidium* and *Sphaerium* species) and a few ostracode species (*C. rawsoni* and *C. lacustris*). Colman et al. (1990) recovered many of the same species of gastropods from a southern Lake Michigan core (*Valvata sincera, V. tricarinata, Marstonia decepta, Amnicola limosa, Probythinella lacustris* and *Stagnicola emarginata*). Taxonomic information for all ostracode and mollusc species is provided in Appendix A and ecological information is summarized in Appendix B. Photographs of all ostracode species as well as unidentified *Pisidium* clams are provided in Appendix C.

All oxygen- and carbon-isotope results are reported in the standard δ-notation:

$$\delta^{18}O \text{ or } \delta^{13}C = [(R_{sample}/R_{standard}) - 1] \text{ (permil, or ‰)} \qquad (1)$$

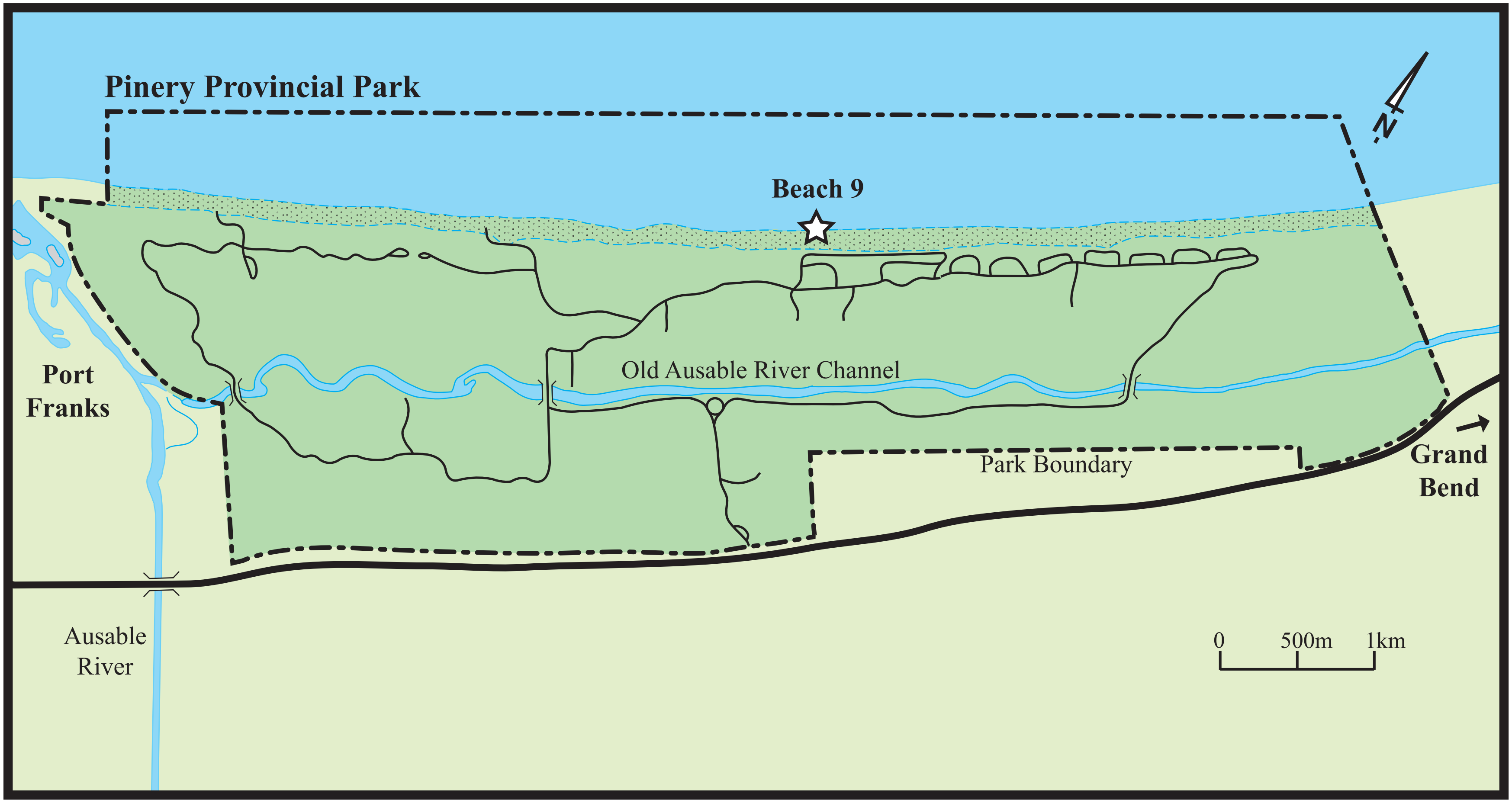

Figure 2.2. Map of Pinery Provincial Park, located at 43° 15’ 36” N and 81° 49’ 40” W on the south-eastern shores of Lake Huron (Fig. 2.1). Modern biogenic carbonates were sampled from Beach 9.

where R_{sample} and $R_{standard}$ are the ratios of $^{18}O/^{16}O$ (or $^{13}C/^{12}C$) in the sample and standard, respectively (Coplen 2011). Carbonate $\delta^{18}O$ and $\delta^{13}C$ values are reported relative to VPDB and water $\delta^{18}O$ values are reported relative to VSMOW (Coplen 1996).

The $\delta^{18}O$ values of water samples were determined on one ml samples by equilibration with CO_2 (Epstein and Mayeda 1953) for ~20 hours at 30 °C and analyzed in continuous flow mode using a GasBench II device attached to a ThermoFinnigan™ Delta^{Plus} XL® stable isotope ratio mass spectrometer. Four laboratory standards (HEAVEN, EDT, MID, LSD), calibrated to VSMOW and SLAP, were measured with each set of samples. HEAVEN and LSD were used to provide a calibration curve, and EDT and LSD were used to assess accuracy. Over the course of the study, a value of –7.3 ± 0.1 ‰ (1σ; n = 113) was obtained for EDT, which compares well with its accepted value of –7.3 ‰, and a value of –13.1 ± 0.1 ‰ (1σ; n = 38) was obtained for MID, which compares well with its accepted value of –13.1 ‰. The standard deviation (1σ) for replicate analysis of unknown samples was ± 0.1 ‰ (n = 80).

Beach samples were dry-sieved and gastropods, bivalves and ostracode valves picked from the sieved fractions and identified. Box core samples were wet-sieved using tap water, and bivalves and ostracodes picked from the sieved fractions, once they were air-dried. Prior to isotopic analyses, most ostracode valves were cleaned in a solution of 1 part distilled water to 2 parts 5 % bleach (sodium hypochlorite) solution for a few hours, or until mud and/or skeletal remains were dislodged from the valves. Some gastropods with sand grains lodged in their shells were treated in an ultrasonication bath for ~30 seconds or less – until the grains were dislodged. As most ostracodes were found as complete carapaces, both valves were used for one isotopic analysis. When individual valves were found, two to four were combined to obtain sufficient material for analysis. Small mollusc shells were analyzed whole; larger shells were fragmented, and representative fractions selected for analysis.

The biogenic carbonates were reacted with orthophosphoric acid at 90 °C using a Micromass MultiPrep device coupled to a VG Optima mass spectrometer. Four laboratory standards (NBS-19, NBS-18, SUPRAPUR and WS-1), calibrated to VPDB and VSMOW, were measured with each set of samples. NBS-19 and NBS-18 were used to provide a calibration curve for oxygen-isotope compositions on the VSMOW scale, and NBS-19 and SUPRAPUR were used to provide a calibration curve for carbon-isotope compositions on the VPDB scale. WS-1 was used to assess accuracy of both the oxygen- and carbon-isotope measurements. SUPRAPUR was also used to assess the accuracy of the oxygen-isotope measurements, and NBS-18 to assess the accuracy of the carbon-isotope measurements. Over the course of the study, WS-1 had a δ^{13}C value of 0.7 ± 0.3 ‰ (1σ; n = 8) and a δ^{18}O value of 26.2 ± 0.1 ‰ (1σ; n = 8), which compares well with its expected values of 0.7 and 26.2 ‰, respectively. Additionally, a δ^{13}C value of –5.0 ± 0.1 ‰ (1σ; n = 17) was obtained for NBS-18, which compares well with its defined δ^{13}C value of –5.0 ‰, and a δ^{18}O value of 13.2 ± 0.1 ‰ (1σ; n = 17) was obtained for SUPRAPUR, which compares well with its accepted δ^{18}O value of 13.2 ‰. Oxygen-isotope results, as needed, were converted from VSMOW to VPDB using the expression of Coplen et al. (1983):

$$\delta^{18}\mathrm{O}_{\mathrm{VPDB}} = 0.97002 * \delta^{18}\mathrm{O}_{\mathrm{VSMOW}} - 29.98 \qquad (2)$$

The oxygen isotopic fractionation factor between carbonate and water is calculated as:

$$\alpha_{\mathrm{carbonate\text{-}water}} = (1000 + \delta^{18}\mathrm{O}_{\mathrm{carbonate}})/(1000 + \delta^{18}\mathrm{O}_{\mathrm{water}}). \qquad (3)$$

Both δ-values used in equation (3) are measured relative to the VSMOW scale.

In the discussions that follow concerning equilibrium precipitation of inorganic carbonate, we have employed the following oxygen- and carbon-isotope geothermometers or enrichment factors:

(a) O'Neil et al. (1969) as revised by Friedman and O'Neil (1977) – which describes oxygen-isotope fractionation between low-Mg calcite and water (relative to VSMOW):

$$1000 \ln(\alpha) = 2.78 * 10^6/T^2 \text{ (K)} - 2.89, \tag{4}$$

(b) Böhm et al. (2000) – which describes oxygen-isotope fractionation between aragonite and water:

$$1000 \ln(\alpha) = 18.45 * 10^3/T \text{ (K)} – 32.54, \tag{5}$$

(c) Romanek et al. (1992) – which describes the enrichment of ^{13}C in calcite formed under equilibrium over that of the source bicarbonate (HCO_3^-):

$$\varepsilon_{\text{calcite – HCO3}^-} = 1.0 \pm 0.2 \text{ ‰} \tag{6}$$

and,

(d) Romanek et al. (1992) – which describes the enrichment of ^{13}C in aragonite formed under equilibrium over that of the source bicarbonate (HCO_3^-):

$$\varepsilon_{\text{aragonite – HCO3}^-} = 2.7 \pm 0.6 \text{ ‰} \tag{7}$$

We acknowledge that equations 6 and 7 were calibrated for 10–40 °C, and that lower temperatures are characteristic of deeper waters in Lake Huron.

2.3 RESULTS

The 384 Lake Huron water samples range in $\delta^{18}O$ values from -9.0 to -6.4 ‰, averaging -7.4 ‰ ($1\sigma = 0.4$ ‰) (Macdonald and Longstaffe 2004, 2007; this study). There is no significant difference in the oxygen isotopic results obtained for surface water (1 m) versus deeper water (bottom-minus-2 m) samples.

The oxygen- and carbon-isotope compositions of the ostracodes, bivalves and gastropods are listed in Tables 2.1, 2.2 and 2.3, respectively. Overall, the $\delta^{18}O$ and $\delta^{13}C$ values of the six ostracode species (two genera) range from -6.9 to -1.3 ‰ and -5.2 to 2.6 ‰, respectively (Fig. 2.3). *Candona rawsoni* (n = 8) shows the widest range in $\delta^{18}O$ values, -6.9 to -1.3 ‰, and the highest $\delta^{13}C$ values, 0.0 to 2.6 ‰. Such variation in $\delta^{18}O$ values has been observed previously in the Great Lakes by Dettman et al. (1995) for *C. lacustris* valves and attributed to contamination from that animal's fleshy remains. However, such organic material is unlikely to liberate significant quantities of CO_2 during reaction with orthophosphoric acid. Variations in near-shore water temperature and/or composition, perhaps of an ephemeral or seasonal nature, are more likely explanations. Otherwise – and in part because of sample size – individual species show smaller ranges in $\delta^{18}O$ and $\delta^{13}C$ values: *C. subtriangulata* (n = 3), -3.0 to -2.1 ‰ and -2.8 to 0.4 ‰; *C. crogmaniana* (n = 7), -5.3 to -4.0 ‰ and -5.2 to -1.7 ‰; *F. caudata* (n = 2), -5.6 to -5.2 ‰ and -2.9 to -1.4 ‰; *C. acuta* (n = 2), -3.7 ‰ and -1.1 to 0.0 ‰, and *C. lacustris* (n = 7), -6.7 to -5.4 and -3.3 to -1.4 ‰.

The calculated average oxygen-isotope fractionation factors between the ostracode valves and Lake Huron water ($\alpha_{\text{carbonate-water}}$) are listed in Table 2.1: *C. subtriangulata*, 1.0359±0.0006 (1σ) – similar to the value of 1.0358 reported by Dettman et al. (1995); *C. crogmaniana*, 1.0338±0.0006; *C. rawsoni*, 1.0341±0.0022 – higher than the values of 1.0322 and 1.0305 reported by Xia et al. (1997) for *C. rawsoni* cultured at 15 and 25 °C; *F. caudata*, 1.0330±0.0005; *C. lacustris*, 1.0323±0.0007; and *C. acuta,* 1.0347±0.0004.

The oxygen- and carbon-isotope compositions of the nine bivalve species (two genera) range from -7.6 to -1.4 ‰ and -8.0 to 0.7 ‰, respectively (Table 2.2; Fig. 2.4). We did not identify the box core *Pisidium* clams (n = 8) at the species level. Previous studies of *Pisidium* clams in Lake Huron (*P. conventus*, *P.* cf. *casertanum*; Dettman et al. 1995) and Lake Michigan (*P. conventus, P. ferrugineum, P. lacustris*, *P. nitidum*; Colman et al. 1990) have shown their growth environments, tolerances and isotopic behaviour to be similar. The clams from the box core have significantly higher $\delta^{18}O$ values (-4.3 to -

Table 2.1. Oxygen-and carbon-isotope results for the Lake Huron ostracodes. Calculated carbonate-water[1] α-values and growth temperatures are also listed.

Species	**Sample Location**	**δ^{18}O (VSMOW)**	**δ^{18}O (VPDB)[2]**	**δ^{13}C (VPDB)**	**calculated O-isotope $\alpha_{carbonate\text{-}water}$-value**	**average $\alpha_{carbonate\text{-}water}$-value for species**	**O-isotope vital effect[3] (‰)**	**calculated growth temperature (°C)**	**species average growth temperature (°C)**
Candona subtriangulata	Box Core 816	27.8	-3.0	-2.8	1.0355	1.0359	+2.2	7	5
	Box Core 819	28.2	-2.6	0.4	1.0359			5	
	Beach Oct 2007	28.7	-2.1	-1.5	1.0364			3	
Candona crogmaniana	Box Core 816	25.8	-5.0	-4.4	1.0334	1.0338	+2.2	15	13
	Beach Oct 2007	26.1	-4.6	-2.6	1.0338			13	
	Beach Oct 2007	26.7	-4.1	-2.2	1.0343			11	
	Beach Oct 2007	26.8	-4.0	-1.7	1.0345			11	
	Beach Oct 2007	25.4	-5.3	-5.2	1.0331			16	
	Beach Oct 2007	26.0	-4.7	-2.9	1.0337			14	
	Beach Sept 2008	26.3	-4.5	-2.1	1.0339			13	
Candona rawsoni	Beach Oct 2007	28.5	-2.4	0.6	1.0361	1.0341	+2.2	4	13
	Beach Oct 2007	24.5	-6.2	0.4	1.0322			20	
	Beach Oct 2007	28.6	-2.2	0.7	1.0363			4	
	Beach Oct 2007	25.9	-4.9	2.6	1.0336			14	
	Beach Oct 2007	23.8	-6.9	0.3	1.0314			24	
	Beach June 2008	29.6	-1.3	0.0	1.0373			0	
	Beach Oct 2008	24.8	-5.9	2.2	1.0325			19	
	Beach Oct 2008	25.6	-5.1	1.2	1.0333			15	
Fabaeformiscandona caudata	Beach Sept 2008	25.1	-5.6	-2.9	1.0328	1.0330	+2.2	18	17
	Beach Sept 2008	25.5	-5.2	-1.4	1.0332			16	
Candona acuta	Beach Sept 2008	27.1	-3.7	0.0	1.0347	1.0347	+2.2	10	10
	Beach Sept 2008	27.1	-3.7	-1.1	1.0348			9	
Cytherissa lacustris	Beach Oct 2007	25.3	-5.5	-1.7	1.0329	1.0323	+1.2	13	15
	Beach Oct 2007	25.4	-5.4	-3.3	1.0330			12	
	Beach Oct 2007	24.1	-6.6	-2.0	1.0318			17	
	Beach Oct 2007	24.2	-6.5	-2.9	1.0318			17	
	Beach Oct 2007	24.6	-6.1	-3.0	1.0323			15	
	Beach Oct 2007	24.0	-6.7	-1.4	1.0316			18	
	Beach Oct 2007	25.0	-5.8	-2.0	1.0326			14	

[1] A δ^{18}O value of -7.4 ‰ for Lake Huron has been used in these calculations.

[2] calculated using equation (2)

[3] von Grafenstein et al. (1999)

Table 2.2. Oxygen-and carbon-isotope results for the Lake Huron bivalves. Calculated carbonate-water[1] α-values and growth temperatures are also listed.

Species	**Sample Location**	**$\delta^{18}O$ (VSMOW)**	**$\delta^{18}O$ (VPDB)[2]**	**$\delta^{13}C$ (VPDB)**	**calculated O-isotope $\alpha_{carbonate\text{-}water}$-value**	**average $\alpha_{carbonate\text{-}water}$-value for species**	**calculated growth temperature (°C)** (v.e. correction of -0.8 ‰ / no v.e. correction)	**average growth temperature (°C)** (v.e. correction of -0.8 ‰ / no v.e. correction)
unidentified *Pisidium* sp.	Box Core 816	27.9	-2.9	-0.6	1.0356	1.0352	3 / 0	5 / 2
	Box Core 816	26.5	-4.3	-0.4	1.0342		9 / 6	
	Box Core 816	29.5	-1.4	0.7	1.0371		-3 / -6	
	Box Core 816	27.2	-3.6	-0.1	1.0349		6 / 3	
	Box Core 816	28.5	-2.3	0.1	1.0362		1 / -2	
	Box Core 816	26.8	-4.0	-4.1	1.0344		8 / 5	
	Box Core 819	27.2	-3.6	-1.1	1.0349		6 / 3	
	Box Core 819	27.0	-3.8	-1.9	1.0347		-7 / 4	
Pisidium casertanum	Beach Aug 2008	24.5	-6.2	-3.4	1.0321	1.0315	18 / 14	all beach *Pisidium* clams
	Beach Aug 2008	23.9	-6.8	-2.4	1.0315		21 / 17	21 / 17
	Beach Aug 2008	23.6	-7.1	-1.1	1.0312		22 / 18	
	Beach Aug 2008	24.0	-6.7	-3.4	1.0316		20 / 17	
	Beach Aug 2008	23.8	-6.9	-2.9	1.0314		21 / 18	
	Beach Aug 2008	23.6	-7.1	-3.1	1.0313		22 / 18	
Pisidium compressum	Beach June 2008	23.5	-7.2	-3.0	1.0312	1.0316	22 / 19	
	Beach June 2008	23.7	-7.0	-1.8	1.0314		22 / 18	
	Beach Aug 2008	23.8	-6.9	-0.7	1.0314		21 / 17	
	Beach Aug 2008	24.8	-5.9	-2.6	1.0324		17 / 13	
	Beach Aug 2008	23.9	-6.8	-1.8	1.0315		21 / 17	
	Beach Aug 2008	24.3	-6.4	-3.1	1.0320		19 / 15	
Pisidium nitidum	Beach Aug 2008	23.4	-7.3	-2.1	1.0310	1.0311	23 / 19	
	Beach Aug 2008	23.6	-7.1	-1.9	1.0312		22 / 18	
Pisidium amnicum	Beach Oct 2008	23.5	-7.2	-1.4	1.0311	1.0311	23 / 19	
	Beach Oct 2008	23.5	-7.2	-0.5	1.0311		23 / 19	
	Beach Oct 2008	23.3	-7.3	0.2	1.0310		23 / 19	
Pisidium fallax	Beach Oct 2008	24.4	-6.3	-1.9	1.0321	1.0321	18 / 15	
Pisidium ventricosum	Beach Oct 2008	23.7	-7.0	-1.1	1.0313	1.0313	22 / 18	
Sphaerium striatinum	Beach Aug 2008	25.4	-5.3	-2.2	1.0331	1.0315	14 / 10	all *Sphaerium* clams
	Beach Aug 2008	23.5	-7.2	-1.4	1.0311		23 / 19	21 / 17
	Beach Aug 2008	23.5	-7.1	-0.8	1.0312		22 / 19	
	Beach Aug 2008	23.5	-7.2	-0.7	1.0311		23 / 19	
	Beach Oct 2008	23.4	-7.3	-5.3	1.0310		23 / 19	
Sphaerium rhomboideum	Beach Aug 2008	24.9	-5.9	-1.7	1.0325	1.0316	16 / 13	
	Beach Oct 2008	23.5	-7.2	0.5	1.0312		22 / 19	
	Beach Oct 2008	23.3	-7.4	0.2	1.0309		24 / 20	
	Beach Oct 2008	24.1	-6.6	-1.9	1.0317		20 / 16	
Sphaerium simile	Beach Aug 2008	23.8	-6.9	-1.2	1.0315	1.0311	21 / 17	
	Beach Aug 2008	23.0	-7.6	-1.2	1.0307		25 / 21	
	Beach Aug 2008	23.5	-7.2	-1.9	1.0312		22 / 19	
	Beach Oct 2008	23.4	-7.3	-8.0	1.0310		23 / 19	

[1] A $\delta^{18}O$ value of -7.4 ‰ for Lake Huron has been used in these calculations.

[2] calculated using equation (2)

Table 2.3. Oxygen-and carbon-isotope results for the Lake Huron gastropods. Calculated carbonate-water[1] α-values and growth temperatures are also listed.

Species	**Sample Location**	**$\delta^{18}O$ (VSMOW)**	**$\delta^{18}O$ (VPDB)[2]**	**$\delta^{13}C$ (VPDB)**	**calculated O-isotope $\alpha_{carbonate-water}$-value**	**average $\alpha_{carbonate-water}$-value for species**	**calculated growth temperature (°C)**	**average growth temperature (°C)**
Valvata perdepressa	Beach Oct 2007	23.7	-7.0	-1.5	1.0313	1.0316	18	gill-breathing gastropods
	Beach Oct 2007	23.8	-6.9	-1.6	1.0314		17	16
	Beach Oct 2007	23.2	-7.4	-1.5	1.0309		20	
	Beach June 2008	24.9	-5.8	0.3	1.0326		13	
	Beach June 2008	23.6	-7.0	1.9	1.0313		18	
	Beach Aug 2008	24.0	-6.7	1.1	1.0316		17	
	Beach Aug 2008	24.3	-6.4	-2.9	1.0320		15	
Valvata tricarinata	Beach Oct 2007	24.4	-6.3	-2.9	1.0321	1.0324	15	
	Beach Oct 2007	25.4	-5.4	-2.2	1.0330		11	
	Beach Oct 2007	24.8	-5.9	-3.5	1.0325		13	
	Beach Oct 2007	25.4	-5.4	-1.9	1.0330		11	
	Beach Aug 2008	24.0	-6.7	-3.4	1.0316		17	
	Beach Aug 2008	24.6	-6.1	-1.2	1.0322		14	
Valvata sincera	Beach Oct 2007	23.7	-7.0	-1.4	1.0314	1.0317	18	
	Beach Oct 2007	23.9	-6.8	-0.3	1.0315		17	
	Beach Oct 2007	24.3	-6.4	-2.0	1.0319		15	
	Beach Aug 2008	24.9	-5.8	-2.6	1.0325		13	
	Beach Aug 2008	24.0	-6.7	0.2	1.0316		17	
	Beach Aug 2008	23.8	-6.9	-0.8	1.0314		18	
Valvata piscinalis	Beach Aug 2008	23.2	-7.4	0.0	1.0309	1.0320	20	
	Beach Aug 2008	25.6	-5.2	0.3	1.0332		10	
Amnicola limosa	Beach Oct 2007	23.9	-6.8	-1.7	1.0315	1.0318	17	
	Beach Oct 2007	23.8	-6.9	-2.0	1.0314		18	
	Beach Oct 2007	23.8	-6.9	-2.7	1.0315		17	
	Beach Oct 2007	25.0	-5.7	-2.3	1.0327		12	
	Beach Aug 2008	24.1	-6.6	-2.2	1.0317		16	
Marstonia decepta	Beach Oct 2007	25.0	-5.8	-0.8	1.0326	1.0319	12	
	Beach Oct 2007	23.4	-7.3	0.1	1.0310		19	
	Beach Oct 2007	25.5	-5.3	-1.8	1.0331		10	
	Beach Oct 2007	23.9	-6.8	-1.1	1.0316		17	
	Beach Aug 2008	23.6	-7.1	-3.1	1.0313		18	
Probythinella lacustris	Beach Aug 2008	24.3	-6.4	-3.0	1.0320	1.0314	15	
	Beach Aug 2008	23.4	-7.3	-1.8	1.0310		19	
	Beach Aug 2008	23.7	-7.0	-1.7	1.0313		18	
Stagnicola elodes	Beach Oct 2007	25.9	-4.9	-1.5	1.0335	1.0334	9	lung-breathing gastropods
	Beach Oct 2007	25.5	-5.2	-2.0	1.0332		10	9

[1] A $\delta^{18}O$ value of -7.4 ‰ for Lake Huron has been used in these calculations.

[2] calculated using equation (2)

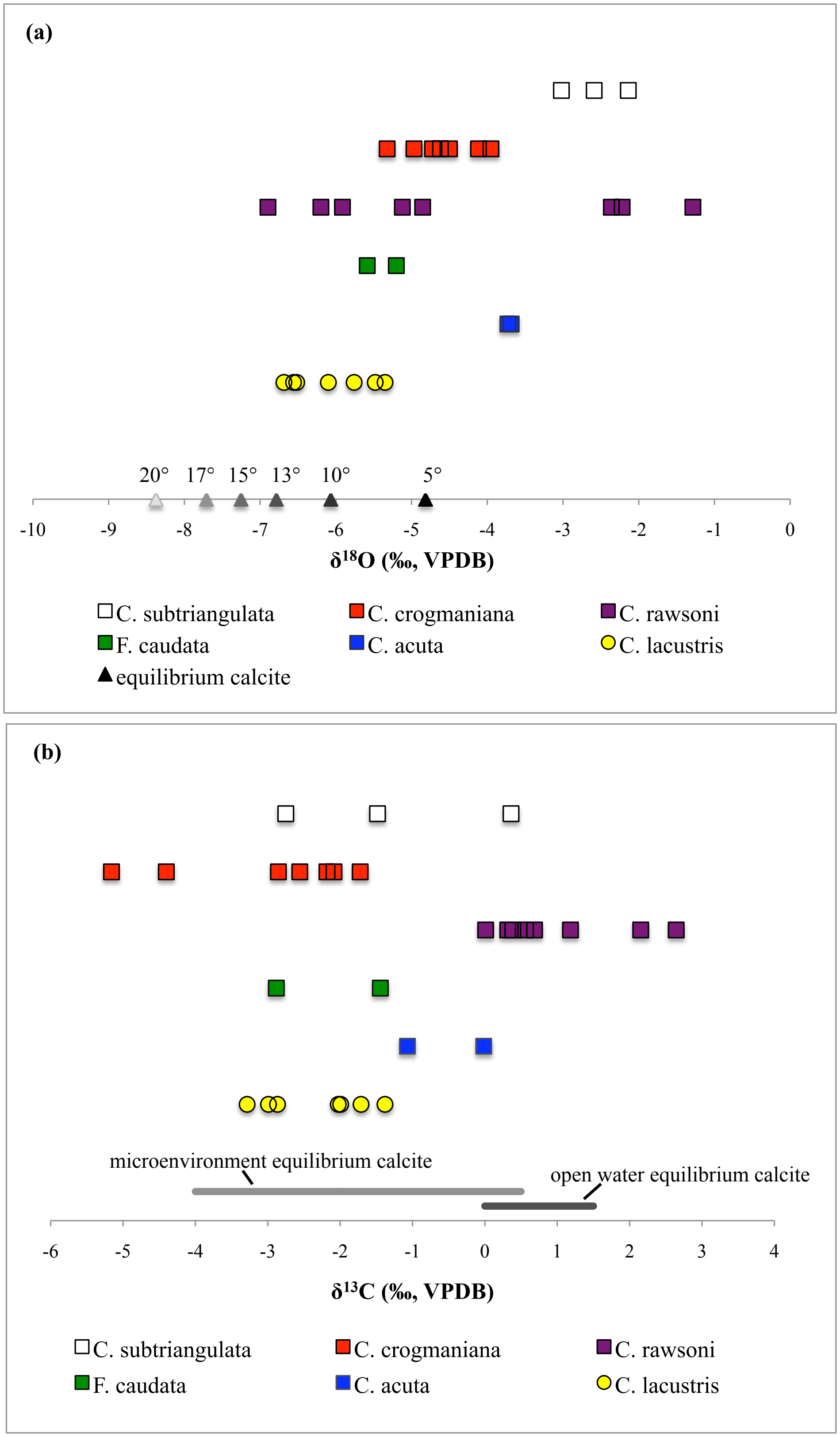

Figure 2.3. Oxygen- (a) and carbon- (b) isotope compositions of Lake Huron ostracodes. Predicted values for calcite formed under equilibrium conditions are also indicated.

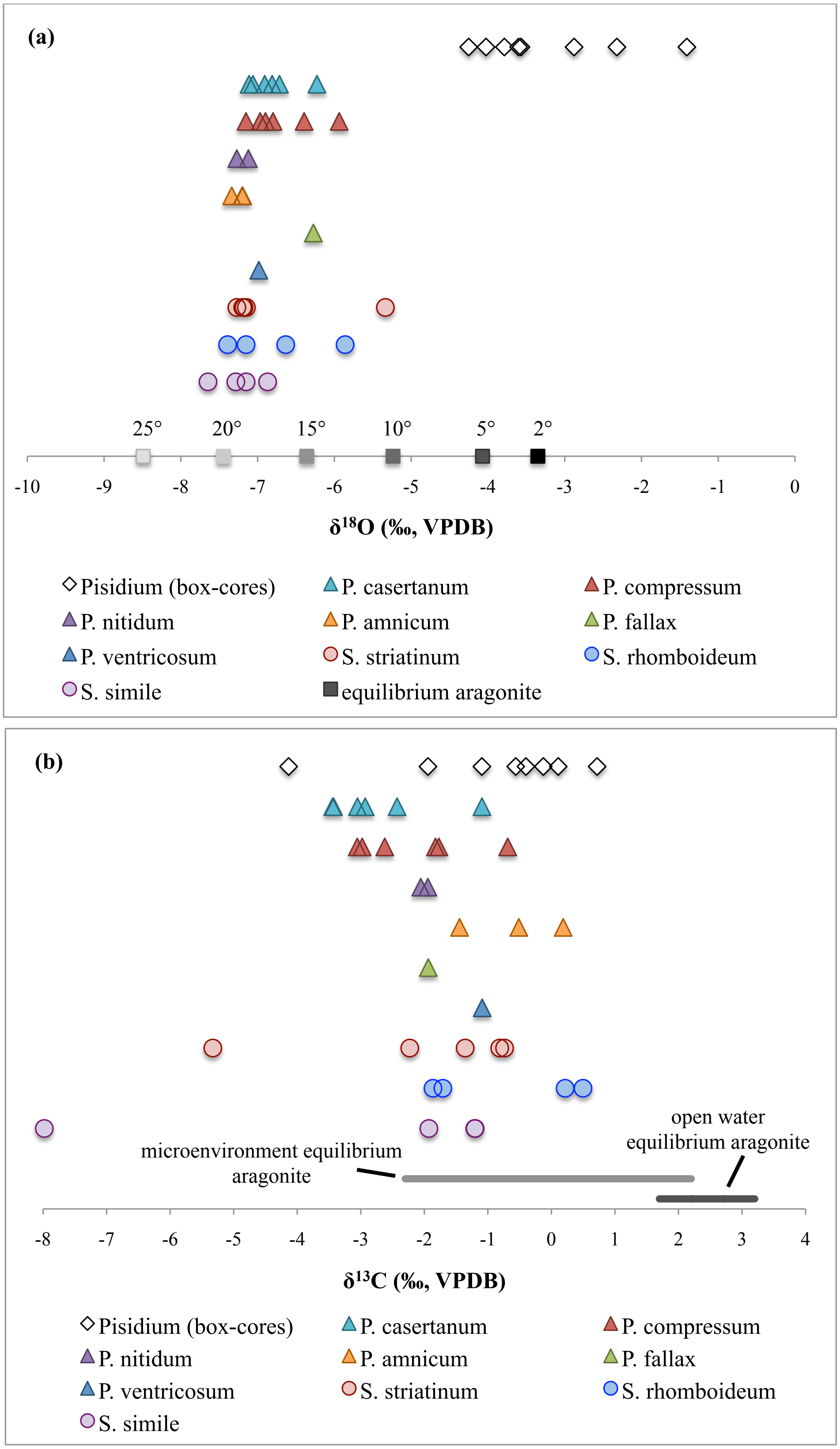

Figure 2.4. Oxygen- (a) and carbon- (b) isotope compositions of Lake Huron bivalves. Predicted values for aragonite formed under equilibrium conditions are also indicated.

1.4 ‰) than those collected from the beach (-7.6 to -5.3 ‰), but the range of δ^{13}C values is similar for both suites. Ranges of δ^{18}O and δ^{13}C values for individual species of *Pisidium* are: *P. casertanum* (n = 6), -7.1 to -6.2 ‰ and -3.4 to -1.1‰; *P. compressum* (n = 6), -7.2 to -5.9 ‰ and -3.1 to -0.7 ‰; *P. nitidum* (n = 2), -7.3 to -7.1 ‰ and -2.1 to -1.9 ‰; *P. amnicum* (n = 3), -7.3 to -7.2 ‰ and -1.4 to 0.2 ‰; *P. fallax* (n = 1), -6.3 and -1.9 ‰, and *P. ventricosum* (n = 1), -7.0 and -1.1 ‰. Bivalves of the *Sphaerium* genus have very similar δ^{18}O values to *Pisidium* clams, but a few *Sphaerium* individuals have significantly lower δ^{13}C values (Table 2.2, Fig. 2.4): *S. striatinum* (n = 5), -7.3 to -5.3 ‰ and -5.3 to -0.7 ‰; *S. rhomboideum* (n = 4), -7.4 to -5.9 ‰ and -1.9 to 0.5 ‰, and *S. simile* (n = 4), -7.6 to -6.9 ‰ and -8.0 to -1.2 ‰.

The calculated average oxygen-isotope values of $\alpha_{\text{carbonate-water}}$ for the bivalve shells are listed in Table 2.2: undifferentiated *Pisidium* clams from the box cores, 1.0352±0.0011; and from the beach deposits, *Pisidium casertanum*, 1.0315±0.0005; *P. compressum*, 1.0316±0.0006; *P. nitidum*, 1.0311±0.0004; *P. amnicum*, 1.0311±0.0004; *P. fallax,* 1.0321; *P. ventricosum,* 1.0313; *Sphaerium striatinum*, 1.0315±0.0010; *S. rhomboideum*, 1.0316±0.0008, and *S. simile*, 1.0311±0.0005. In particular for juvenile *Pisidium* clams, the close similarity in $\alpha_{\text{carbonate-water}}$ values within the same environment is helpful. These species can be difficult to distinguish from each other if their hinge teeth have been abraded during depositional processes (G. Mackie, pers. communication).

The eight gastropod species (five genera) exhibit a similar range of δ^{18}O (-7.4 to -4.9 ‰) and δ^{13}C values (-3.5 to 1.9 ‰) values as the ostracodes and bivalves (Table 2.3). The ranges of δ^{18}O and δ^{13}C values for individual species are illustrated in Figure 2.5: *Valvata perdepressa* (n = 7), -7.4 to -5.8 ‰ and -2.9 to 1.9 ‰; *V. tricarinata* (n = 6), -6.7 to -5.4 ‰ and -3.5 to -1.2 ‰; *V. sincera* (n = 6), -7.0 to -5.8 ‰ and -2.6 to 0.2 ‰; *V. piscinalis* (n = 2), -7.4 to -5.2 ‰ and 0.0 to 0.3 ‰; *Amnicola limosa* shells (n = 5), -6.9 to -5.7 ‰ and -2.7 to -1.7 ‰; *Marstonia decepta* (n = 5), -7.3 to -5.3 ‰ and -3.1 to 0.1 ‰; *Probythinella lacustris* (n = 3), -7.3 to -6.4 ‰ and -3.0 to -1.7 ‰, and *Stagnicola elodes* (n = 2), -5.2 to -4.9 ‰ and -2.0 to -1.5 ‰.

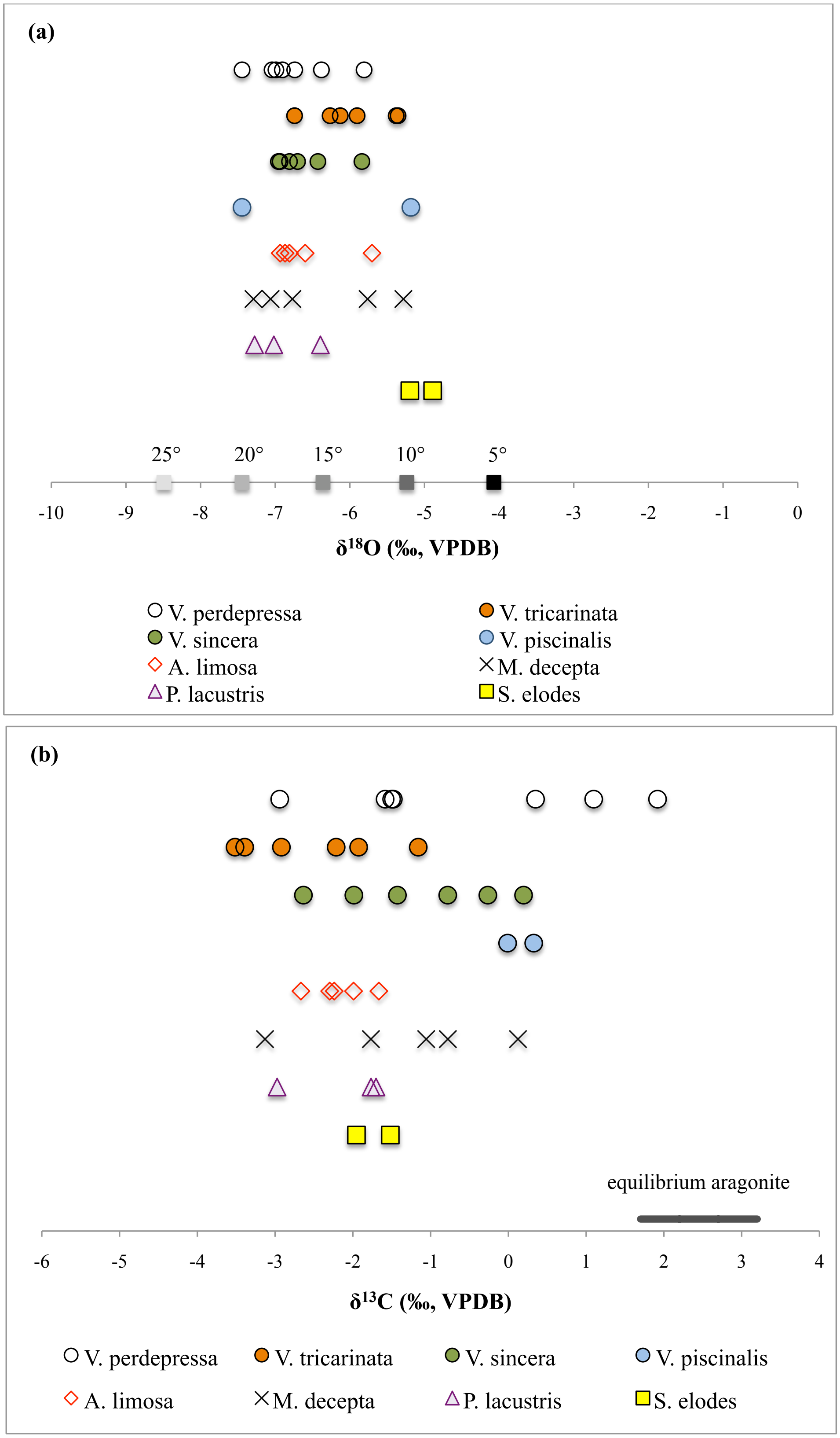

Figure 2.5. Oxygen- (a) and carbon- (b) isotope compositions of Lake Huron gastropods. Predicted values for aragonite formed under equilibrium conditions are also indicated.

The calculated average oxygen-isotope values of $\alpha_{carbonate-water}$ for the gastropod shells are listed in Table 2.3: *Valvata perdepressa*, 1.0316±0.0007; *V. tricarinata*, 1.0324±0.0007; *V. sincera*, 1.0317±0.0006; *V. piscinalis*, 1.0320±0.0017; *Amnicola limosa,* 1.0318±0.0007; *Marstonia decepta,* 1.0319±0.0010*; Probythinella lacustris*, 1.0314±0.0006, and *Stagnicola elodes*, 1.0334±0.0005.

2.4 DISCUSSION

2.4.1 Oxygen-isotope composition of Lake Huron ostracodes

The various *Candona* species examined in this study have noticeably different oxygen-isotope compositions (Fig. 2.3a, Table 2.1). Because these species live in the same body of water, whose isotopic composition is known to be largely constant and homogeneous, the differences in δ- and α-values must arise from differences in water temperature, vital effects or some combination of both. von Grafenstein et al. (1999) showed that all European members of the sub-family Candoninae exhibit the same vital effect (+2.2 ± 0.15 ‰), which is similar to the ~ +2.1 ‰ offset between calcite formed at equilibrium at 4-5 °C ($\delta^{18}O_{equilibrium\ calcite}$ = -4.6 to -4.8 ‰ VPDB) and the *C. subtriangulata* specimens analyzed here (average $\delta^{18}O$ value -2.6 ‰). This result gives us confidence that North American Candoninae exhibit the same vital effect as European members of this sub-family (von Grafenstein 2002). Decrouy et al. (2011b) reported a similar – albeit slightly higher – vital effect of ~3 ‰ for the Candoninae.

Xia et al. (1997) reported that valves of *C. rawsoni* cultured at 15 and 25 °C were enriched in ^{18}O by 0.8 – 1.0 ‰ (i.e., exhibited a vital effect) over inorganic calcite precipitated at equilibrium. However, this vital effect value was calculated using the calcite-water geothermometer of O'Neil et al. (1969), which is slightly different from the revised version employed here (Friedman and O'Neil 1977; equation 4). When fractionation factors for equilibrium calcite precipitated at 15 and 25 °C are calculated using equation 4 and compared to the measured *C. rawsoni* values of Xia et al. (1997), vital effect values of 1.2 – 1.6 ‰ are obtained. This enrichment in ^{18}O is slightly lower than the 2.2 ‰ vital effect measured by von Grafenstein et al. (1999).

By correcting the measured oxygen-isotope compositions of *Candona* species for the vital effect (von Grafenstein's value of +2.2 ‰ value is used here), and then applying equation 4, we have calculated the average growth temperature of the *Candona* species sampled from Lake Huron during this study. The average growth temperature calculated for *C. subtriangulata*, 5 °C (Table 2.1), is virtually identical to that reported for this species' mean habitat temperature (~4-5 °C, Delorme 1978, 1991, 2001; Colman et al. 1990; Dettman et al. 1995). Water at this temperature is present year-round below the thermocline of the lakes, and is consistent with the box core collection sites of two of the three *C. subtriangulata* individuals. The one carapace collected from the Pinery beach has a similar oxygen-isotope composition to the two individuals collected from the box core. This one sample may have been reworked, resulting in its redeposition at the shallower- and warmer-water beach site.

All other ostracode species analyzed from Lake Huron have higher average growth temperatures (Table 2.1). Both *C. crogmaniana* and *C. rawsoni* have average growth temperatures of 13 °C, consistent with higher water temperatures expected at the Pinery Beach collection site for the majority of these species' carapaces, relative to a deeper-water site. The lone deeper-water carapace of *C. crogmaniana* may have been transported to the box-core site. *Candona rawsoni* is known to prefer still warmer water temperatures and has been thought to be scarce in the modern Great Lakes (Colman et al. 1990). The occurrence of numerous individuals at the Pinery beach suggests that it may be more common – at least in some Great Lakes – than previously reported. Xia et al. (1997) found that *C. rawsoni* has an optimum growth molting and calcification temperature of 25 °C and becomes stressed at (and below) 15 °C. Delorme (1991, 2001) likewise found this species to live at an average temperature of 17.5 °C. The wide range of $\delta^{18}O$ values exhibited by *C. rawsoni* in this study may suggest that this species is tolerant to a wide range of temperatures or environments, or may suggest that the calculated average growth temperature of 13 °C underestimates this species' optimum growth temperature. Additionally, *C. rawsoni* may be more sensitive to physiological changes during carapace precipitation (e.g. pH at the calcification site), which could affect valve precipitation and thus oxygen-isotope compositions.

The highest growth temperatures were calculated for *F. caudata* (17 °C) and *C. lacustris* (15 °C). These temperatures are both 5 °C higher than previously reported for their mean water temperatures (12 and 10 °C, respectively; Delorme 1991, 2001). *Fabaeformiscandona caudata* had been considered to live in relatively deep-water sites (Delorme 1970a); hence, its occurrence in the Pinery beach sample conceivably could indicate redeposition from a deeper and cooler site. That said, all individuals of *C. lacustris* were also found in the Pinery beach sample, which suggests that Lake Huron is supporting healthy populations of *C. lacustris*, regardless of whether or not redeposition is a significant phenomenon. A contrasting situation is provided by *C. acuta*, for which we have determined a mean water temperature of 10 °C for our beach sample. *Candona acuta* is known to live in shallow regions of Lake Michigan (Colman et al. 1990), and its previously reported mean water temperature is ~18 °C (Delorme 1991, 2001).

We conclude that much of the difference in δ- and α-values among the various species reflects valve formation at different water temperatures – consistent with their known ecological preferences (Appendix B). These variations in apparent temperature of valve formation are not unexpected. The temperature of the water from which a living ostracode is collected does not necessarily reflect the optimum growth temperature for these species. In many cases, ostracodes (and other shelly organisms) will molt only when water temperatures fall within their optimum range (Boomer 2002; Schöne et al. 2006). We suggest that the temperatures calculated here for each ostracode species represents their calcification temperature more accurately than the temperatures at which these species are most commonly collected.

2.4.2 Oxygen-isotope composition of Lake Huron bivalves

There have been several previous efforts to identify whether freshwater bivalves precipitate aragonite shells in oxygen-isotope equilibrium with host waters (e.g., Grossman and Ku 1986; Patterson et al. 1993; Böhm et al. 2000). The choice of oxygen-isotope geothermometer used to predict equilibrium $\delta^{18}O$ values is central to this discussion. Vital effects may already be embedded into geothermometers calibrated using biologically produced aragonite. A comparison of common aragonite geothermometers shows that for a given water temperature within the range of 5 to 25 °C, $\delta^{18}O_{aragonite}$ values calculated using Grossman and Ku (1986) and Böhm et al. (2000) differ by up to 0.16 ‰. The aragonite-water oxygen-isotope geothermometer of Patterson et al. (1993), which was modeled after freshwater fish ootoliths, predicts $\delta^{18}O_{aragonite}$ values as much as 0.74 ‰ lower (for precipitation at 25 °C). We have chosen to use the aragonite-water geothermometer of Böhm et al. (2000) (equation 5), as it includes cold-water mollusks in addition to foraminifera and sponges in its calibration, all of which are presumed to precipitate their skeletons in oxygen-isotope equilibrium.

Numerous studies have suggested that a wide variety of bivalve species precipitate from water at oxygen isotopic equilibrium (Dettman and Lohmann 1993; Dettman 1994; Tevesz et al. 1996; Dettman et al. 1999; Wurster and Patterson 2001; Goewert et al. 2007; Andrus and Whatley Rich 2008). However, von Grafenstein et al. (1999) reported an oxygen-isotope vital effect of +0.86 ‰ for clams of the *Pisidium* genus, which was determined by comparing measured values for *Pisidium* shells (aragonite) with values calculated using the calcite-water geothermometer of Friedman and O'Neil (1977; equation 4). Inorganically produced aragonite, however, is enriched in ^{18}O by 0.6 ± 0.3 ‰ relative to calcite crystallized at 25° C under the same conditions (Tarutani et al. 1969). Recalculation of von Grafenstein et al.'s results using the aragonite-water geothermometer of Böhm et al. (2000) over the reported range of water temperatures (6 – 15 °C) indicates that the clams are only depleted of ^{18}O by ~ 0.1 ‰ relative to equilibrium conditions. Such a difference is not significant within the analytical error of most carbonate measurements.

The significantly higher $\delta^{18}O$ values of the box-core *Pisidum* clams reflect their lower temperature of shell formation relative to those collected from the Pinery beach

(Fig. 2.4a; Table 2.2). We suspect that these deep-water bivalves from the box cores included *P. conventus,* and/or *P. ferrugineum*. *Pisidium conventus* is known to prefer living at great depths and cold water in large lakes (Clarke, 1981) and *P. ferrugineum* is common in all the Great Lakes at waters depths of ~10 m (Kerr-Lawson et al. 1992). Although further work is required to identify the species of clams in this and other deep-water portions of Lake Huron, we nonetheless anticipate that if clams of the *Pisidium* genus do in fact exhibit a vital effect, this value would be applicable to all species. When equation 5 and the temperature (5 °C) calculated for *C. subtriangulata* from the box cores is applied to these clams, an aragonite shell $\delta^{18}O$ value of -4.0 ‰ (VPDB) is predicted, which lies near the lower end of the measured range of oxygen-isotope compositions for these specimens (Fig. 2.4a). The average shell $\delta^{18}O$ value, by comparison, is 0.8 ‰ higher (-3.2 ‰ VPDB), which for an average growth temperature of 5 °C would imply a vital effect correction of -0.8 ‰. Without such a correction, an average growth temperature of 2±4 °C is obtained. Dettman et al. (1995) noted that water present below the thermocline in Lake Huron may remain as cold as 1 °C during much of the year.

All six *Pisidium* clam species collected from the Pinery beach have similar $\delta^{18}O$ values (Fig. 2.4a), suggesting shell formation under very similar conditions. All of these species are known to inhabit shallow waters (Clarke 1981; Kerr-Lawson et al. 1992). The average oxygen-isotope $\alpha_{\text{carbonate-water}}$ for these beach *Pisidium* clams is 1.0315±0.0007, which suggests an average shell formation temperature of 17±3 °C in the absence of any vital effect. The average growing temperature is higher, 21±3 °C, if a vital effect of -0.8 ‰ is incorporated into the calculation. Individuals of the *Sphaerium* genus exhibit only a slightly larger range in $\delta^{18}O$ values than the *Pisidium* clams, and a virtually identical average value of $\alpha_{\text{carbonate-water}}$, 1.0314±0.0005.

All of these bivalves grow continuously throughout the year, so long as physiological tolerances of the species are not exceeded (von Grafenstein et al. 1999, Schöne 2008). Wurster and Patterson (2001) have shown that growth below 12 °C is unlikely in *S. simile*, as also has been reported for other Great Lake clam species (Dettman 1994; Dettman et al. 1999; Goewert et al. 2007). Maximum water temperatures at Pinery Provincial Park can reach ~ 23 °C during the summer months (NOAA's GLERL website). All of the Pinery beach bivalves have oxygen-isotope compositions that fall within – or at least close to – this temperature range (10-21 °C), assuming formation in isotopic equilibrium with average Lake Huron water (Fig. 2.4a). If a vital effect of -0.8 ‰ is presumed, this range shifts upwards to 14-25 °C. Bivalve shell formation within both temperature ranges is feasible; hence, these results do not answer the question of whether or not these species precipitate their shells in oxygen isotopic equilibrium.

Evidence for a vital effect exists for some other bivalve genera. Wurster and Patterson (2001) found that $\delta^{18}O$ values obtained for *Sphaerium simile* clams correlated well with the geothermometer of Patterson et al. (1993). However, this geothermometer likely underestimates equilibrium oxygen-isotope compositions by ~0.6 ‰, suggesting that the oxygen isotopic composition of this species of clam is actually lower than expected for equilibrium by ~ 0.6 ‰. Similarly, Tevesz et al. (1996) reported $\delta^{18}O$ values for *S. striatinum* clams that were 0.5 ‰ lower than expected for equilibrium during the period of shell formation. Fastovsky et al. (1993) reported that the $\delta^{18}O$ values of certain unionid clam shells were as much as 1-3 ‰ lower than expected for equilibrium, though Dettman et al. (1999) suggested several analytical reasons (e.g., sampling pretreatment and coarse sampling resolution) why the magnitude of this effect may have been overestimated. The similar vital effect value calculated here (-0.8 ‰) is in close agreement with previously reported values and adds to this discussion but – alas – does not resolve it.

2.4.3. Oxygen-isotope composition of Lake Huron gastropods

Previous studies demonstrated that the aragonitic shells of several gastropod species form in isotopic equilibrium with water (Fritz and Poplawski 1974; Leng et al. 1999; White et al. 1999; Abell and Hoelzmann 2000). However, these studies also highlighted that whether the gastropods are gill or lung breathers exerts strong control on their oxygen isotopic compositions. For several species of snails from springs in southern Nevada, Shanahan et al. (2005) found the aragonite shell $\delta^{18}O$ values of gill-breathing gastropods

(Prosobranchia) were predicted accurately by the geothermometer of Böhm et al. (2000), whereas the $\delta^{18}O$ values of lung-breathing gastropods (Pulmonata) were significantly higher than predicted. They determined that some of the isotopic differences observed among species likely resulted from growth at different water temperatures during different times of the year.

The seven species of gill-breathing gastropods collected from the Pinery beach exhibit a small range of $\delta^{18}O$ values (Fig. 2.5a), which is suggestive of shell formation under similar environmental conditions over a similar range of temperatures. Assuming that these gastropods do not exhibit a vital effect, the results indicate growth between 10 and 20 °C, which is very similar to the 10-21 °C growth range estimated for Pinery beach bivalves (Fig. 2.5a). A similar range, 10-39 °C, was reported by Herschler (1998) for genera of the Hydrobiidae family (of which *A. limosa*, *M. decepta* and *P. lacustris* are members), although this range extends much higher than water temperatures at the Pinery. In short, the $\delta^{18}O$ values of the gill-breathing gastropods lie within the range expected for equilibrium precipitation of aragonite, although non-equilibrium effects cannot be ruled out.

Similar to Shanahan et al.'s (2005) observations, the two specimens of a lung-breathing gastropod (*S. elodes*) analyzed in this study have $\delta^{18}O$ values at the highest end of the range obtained for all gastropod samples (Fig. 2.5a). Such compositions – at equilibrium – would require shell formation at 9-10 °C from Lake Huron water. Given the growth temperatures determined for the other Pinery beach gastropods and bivalves, it is possible that *S. elodes* – and perhaps other lung-breathing gastropods – exhibits an ^{18}O-enrichment that results from vital effects during shell formation. If *S. elodes* forms its shell at 16 °C, the average growth temperature of the gill-breathing gastropods, a vital effect correction of -1.5 ‰ is required. Alternatively, the higher $\delta^{18}O$ values of *S. elodes* may suggest that lung-breathing gastropods occasionally emerge from the water, with the higher-than-expected $\delta^{18}O$ values reflecting shell formation from water affected by significant evaporation (Shanahan et al. 2005). Further investigations of the oxygen-isotopic compositions of gill- versus lung-breathing gastropods are required to identify the cause(s) of their disparate compositions.

2.4.4. Carbon-isotope compositions of Lake Huron ostracodes, bivalves and gastropods

We have used equations 6 and 7 and the $\delta^{13}C_{DIC}$ values (-1.0 to 0.5 ‰ for HCO_3^-) reported by Dettman et al. (1995) for Lake Huron to calculate the $\delta^{13}C$ values of calcite or aragonite expected for equilibrium precipitation in Lake Huron. Similar $\delta^{13}C_{DIC}$ values (-1.0 to 1.4 ‰) have been measured for Lake Ontario (Hodell et al. 1998) and are significantly higher than the $\delta^{13}C_{DIC}$ values of tributaries within the Great Lakes Basin, which can be as low as -13.9‰ (Yang et al. 1996; Dettman et al. 1999; Heidenheim 2004). Lakewater from just offshore of the Pinery beach has $\delta^{13}C_{DIC}$ values that vary from -3.5 ‰ in the winter to -7 ‰ in the summer (B. Schilman, pers. comm.). However, these compositions reflect significant anthropogenic and terrestrial inputs to the immediate nearshore environment and are not representative of Lake Huron water as a whole. Lakewater $\delta^{13}C_{DIC}$ values are close to equilibrium with atmospheric CO_2, which had a value of ~ -7.7 ‰ in 1991 (Dettman et al. 1995) (and has decreased to a modern value of ~ -8 ‰ (Bowling et al. 2008)) likely because the longer residence time of lakes compared to rivers facilitate isotopic equilibration between the atmosphere and carbonate species in the water (Yang et al. 1996). Another contributor to the DIC of Lake Huron is dissolution of Paleozoic carbonates ($\delta^{13}C$ values = -1 to 4 ‰, Lohmann and Walker 1989), which surround much of the Lake Huron Basin.

There have been several efforts to identify whether ostracodes form their valves in carbon-isotope equilibrium with lakewater DIC. Some species appear to precipitate valves out of equilibrium, having $\delta^{13}C$ values higher or lower than expected, whereas others, including the Candoninae, apparently form at equilibrium (von Grafenstein et al. 1999; Keatings et al. 2002; Decrouy et al. 2011b). An important factor for assessing equilibrium valve formation is measurement of the actual DIC source utilized by the ostracodes. In particular, some ostracodes, including the Candoninae and *C. lacustris*, are infaunal species, and so may not be in contact with open Lake Huron water. The predicted carbon-isotope compositions of calcite formed at equilibrium from open Lake Huron water range from 0 to 1.5 ‰. These values are significantly higher than ostracode valves measured here (Fig. 2.3b) except for *C. rawsoni* and one individual each of *C. subtriangulata* and *C. acuta*. This discrepancy between the $\delta^{13}C$ values of predicted calcite and measured ostracodes suggests that lakewater-DIC is not utilized by most of these species. Alternatively, Decrouy et al. (2011b) showed that porewater $\delta^{13}C_{DIC}$ values from 0 to 3 cm below the sediment-water interface in Lake Geneva had $\delta^{13}C$ values 1 – 4 ‰ lower than lakewater-DIC because of contributions from decaying organic matter, with the lowest values occurring at the greatest depths. If the same scenario is true for Lake Huron, $\delta^{13}C_{DIC}$ values within the microenvironments inhabited by ostracodes would range from -5 to -0.5 ‰, and equilibrium calcite forming from this source would have $\delta^{13}C$ values between -4 and 0.5 ‰ (Fig. 2.3b). The majority of measured ostracode valves fall within this predicted range of compositions, suggesting that a microenvironment correction of 1 to 4 ‰ for fossil ostracodes may be necessary to interpret changes in the $\delta^{13}C_{DIC}$ composition of lakewater.

Similarly, most species of *Pisidium* clams are infaunal and although they live close to the sediment surface (Meier-Brook 1969; Lopez and Holopainen 1987; Mackie 2007), they may not be in direct contact with lakewater-DIC. *Sphaerium* clams, on the other hand, are not infaunal (Mackie 2007); hence the putative effects of lower $\delta^{13}C_{DIC}$ values within an organism's microenvironment are less likely to be important. The predicted range of carbon-isotope compositions for aragonite formed at equilibrium from open Lake Huron water is 1.7 to 3.2 ‰. Clams utilizing open lakewater-DIC should have $\delta^{13}C$ values within this range; however, none of the clams measured here have values this high (Fig. 2.4b). Alternatively, if clams living below the sediment surface utilize porewater-DIC with values 1 – 4 ‰ lower than lakewater-DIC, their shells should range in composition from -2.3 to 2.2 ‰. The majority of measured shells fall within this range (n = 28), although some individuals (n = 11) have $\delta^{13}C$ values that are lower still (Fig. 2.4b). Two specimens had particularly low $\delta^{13}C$ values – *S. striatinum* (-5.3 ‰) and *S. simile* (-8.0‰). These shells may have formed in the very nearshore environment or near the mouth of a tributary, both of which have $\delta^{13}C_{DIC}$ values lower than open Lake Huron. Apart from these two individuals, the carbon-isotope compositions of the *Pisidium* and *Sphaerium* clams both fall within the range from -4.1 to 0.7 ‰. Although it is possible that the *Pisidium* and *Sphaerium* clams draw upon different DIC sources, the fact that there is no distinct offset between their carbon-isotope compositions may suggest that these two genera both utilize open lakewater-DIC but modify its composition.

Gastropods are not infaunal, and as such the effects of microenvironments and lower $\delta^{13}C_{DIC}$ are not considered here. The equilibrium $\delta^{13}C$ values calculated for Lake Huron aragonite, ranging from 1.7 to 3.2 ‰, are significantly higher than the $\delta^{13}C$ values measured gastropod shells, of which only one sample of the gill-breathing *V. perdepressa* has a $\delta^{13}C$ value as high as the expected range for equilibrium precipitation from Lake Huron (Fig. 2.5b). McConnaughey et al. (1997) reported that gill-breathing snails normally have shells with $\delta^{13}C$ values close to that of DIC, whereas the shells of lung-breathing snails contain higher amounts of metabolic carbon, which results in lower $\delta^{13}C$ values. Such a difference, however, is not apparent for the two samples of *S. elodes* analyzed here. The range is -3.5 to 1.9 ‰, similar but slightly higher than the carbon-isotope range of the bivalves.

2.4.5. Non-equilibrium fractionation in Lake Huron biogenic carbonates

Figure 2.6 summarizes the extent of deviation of Lake Huron ostracodes, bivalves and gastropods from the carbon- and oxygen-isotope compositions predicted for equilibrium formation from average Lake Huron water over expected temperature ranges (ostracodes; 2-20 °C, 2-25 °C for bivalves, and 5-25 °C for gastropods). As introduced earlier, these differences are generally attributed to vital effects (kinetic, metabolic) – a range of processes that can modify the isotopic compositions of the carbonate-secreting fluid and thus the biogenic hard tissues (Schöne 2008).

Kinetic fractionations are usually larger in magnitude than those ascribed to metabolic effects and are typically caused by discrimination against the heavier isotopes

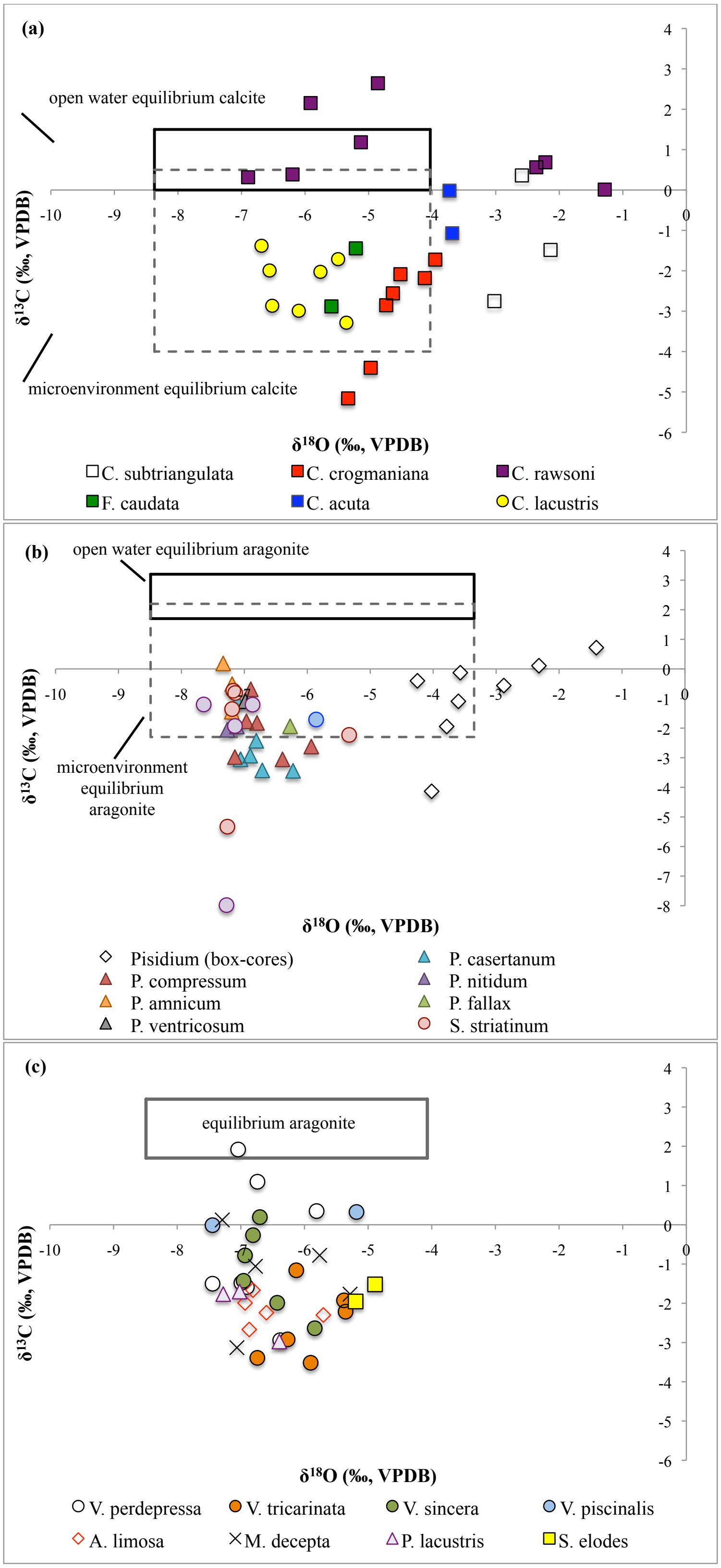

Figure 2.6. Carbon- versus oxygen-isotope compositions for Lake Huron ostracodes (a), bivalves (b), and gastropods (c) The boxes indicate the range in carbon- and oxygen-isotope compositions predicted for equilibrium fractionation. The temperature range used for ostracodes is 2-20 °C, for bivalves is 2-25 °C, and for gastropods is 5-25 °C.

of both O and C during CO_2 hydration and hydroxylation (McConnaughey 1989b). These reactions result in biogenic carbonate $\delta^{18}O$ and $\delta^{13}C$ values that are lower than expected for equilibrium. When biogenic carbonates precipitate faster than the hydroxylation of carbon dioxide ($CO_2 + OH^- \Rightarrow HCO_3^-$), preferential hydroxylation of $^{12}C^{16}O_2$ leads to lower $\delta^{13}C$ and $\delta^{18}O$ values in the resulting carbonate relative to equilibrium (McConnaughey 1989a, 1989b; Ziveri et al. 2003). The availability of the enzyme carbonic anhydrase, which speeds the conversion of CO_2 to HCO_3^- and facilitates oxygen isotopic exchange, is likely key to this process. If carbonic anhydrase is present in sufficient quantities at the site of mineralization in an organism, kinetic isotopic fractionation, at least for oxygen isotopes, is eliminated (Weiner and Dove 2003).

Molluscs in general typically do not exhibit kinetic effects (McConnaughey and Gillikin 2008), which is consistent with the absence of significant covariation between $\delta^{18}O$ and $\delta^{13}C$ values for the Lake Huron bivalves and gastropods examined here (R values of 0.13 and 0.16, respectively), except perhaps for the undifferentiated *Pisidium* samples collected from the box cores (R value of 0.63). Such covariation is also not readily apparent among the ostracode species (R value for all species combined is 0.21), and in that case – and perhaps also for the box-core clams – the tendency is towards ^{18}O-enrichment rather than ^{18}O-depletion. Ziveri et al. (2003) suggested that kinetic fractionation could not produce carbonates enriched in ^{13}C and/or ^{18}O relative to equilibrium conditions.

There is general agreement that ^{18}O-enrichment relative to equilibrium cannot be explained by common models (McConnaughey et al. 1989a; von Grafenstein et al. 1999; Shanahan et al. 2005; Fenger et al. 2007). Other approaches focus on the intermediate reservoir (extracellular calcifying fluids, ECF, the fluid between the mantle and the shell) where many organisms temporarily store the ions used for shell formation (McConnaughey 1989b; Weiner and Dove 2003; Fenger et al. 2007). The membrane of this reservoir regulates the pH and pCO_2 of the fluid, and hence the precipitated biomineral (Weiner and Dove, 2003). It has been suggested that, if the ECF is enriched in ^{18}O relative to the surrounding environment, rapid fluid transport, together with rapid shell precipitation, might prevent equilibrium with the host environment and could result in a higher-than-equilibrium $\delta^{18}O$ value (von Grafenstein et al. 1999). However, recent comparisons of ostracodes with different calcification rates suggest that the rate of valve formation is not a factor in isotopic fractionation (Decrouy et al. 2011b).

Small changes in pH on the microenvironment scale or within the ECF may be involved in non-equilibrium oxygen-isotope compositions of biogenic carbonates. The relative abundances of CO_3^{2-} and HCO_3^- are controlled by pH, both within the host environment and the organism (Zeebe 1999; Adkins et al. 2003; Ziveri et al. 2003). At low temperatures, CO_2 and related DIC species are much more enriched in ^{18}O than coexisting water (e.g., at 19 °C, enrichments relative to coexisting H_2O are CO_3^{2-}, 18 ‰; HCO_3^-, 34 ‰, and CO_2, 42 ‰). At high pH CO_3^{2-} is the dominant DIC species whereas at intermediate pH, HCO_3^- is dominant; thus it follows that shell formation at higher pH results in carbonates with relatively lower $\delta^{18}O$ values (Zeebe 1999). This reasoning has been used to explain oxygen-isotope compositions of deep-sea corals that are lower than predicted for equilibrium (Adkins et al. 2003). Adkins et al. (2003) suggest that a biologically induced pH gradient may develop in the ECF, allowing the $\delta^{18}O$ values of DIC species to affect the $\delta^{18}O$ value of the precipitated shell. This in turns suggests that the DIC pool does not re-equilibrate with H_2O, which is a much larger O-bearing reservoir. In the case of ostracodes (and perhaps the box core clams), however, the precipitated carbonate valves (shells) are enriched in ^{18}O relative to carbonate precipitated at equilibrium. If pH caused this isotopic enrichment, it would require the ECF to have a lower pH than the external environment (modern Lake Huron has a pH of 8.2 and the HCO_3^- ion is the major source of DIC (Dettman et al. 1995)). Previous work indicates that the pH at the site of calcite precipitation in ostracodes is indeed relatively low (≤ 7; Keating et al. 2002), which would favour utilization of ^{18}O-enriched $CO_{2(aq)}$ ion during valve formation (Zeebe 1999; Decrouy et al. 2011b).

Metabolic effects provide the simplest explanation for the ^{13}C-depletion characteristic of the Lake Huron bivalves and gastropods (Fig. 2.6). Metabolic effects are brought on by changes in the ^{13}C content of the DIC reservoir caused by photosynthesis and respiration; photosynthesis raises the $\delta^{13}C$ value of this reservoir, and respiration lowers its $\delta^{13}C$ value (McConnaughey 1989a, 1989b; Auclair et al. 2003). In non-photosynthesizing organisms, such as molluscs, metabolic carbon is derived from the diet (Michener and Shell 1994). Most *Pisidium* and *Sphaerium* clams are filter feeders, and as such consume particulate organic matter such as photosynthetic algae or bacteria, and aquatic plants (Mackie 2007). The gastropods likely have similar diets. The majority of organic matter deposited in sediments of the Great Lakes is algal in origin, and typically has $\delta^{13}C$ values of ~ -30 to -25‰ (Meyers and Ishiwatari 1993; Hodell and Schelske 1998; Meyers 2003). Hence, even small additions of metabolic carbon from the diets of these organisms would significantly lower the $\delta^{13}C$ value of their internal DIC reservoirs. Generally, the DIC pool within lakes is stratified, with higher $\delta^{13}C$ values at the surface caused by primary productivity and lower $\delta^{13}C$ values at depth resulting from the accumulation and oxidation of low-^{13}C organic matter (Dettman et al. 1995; Leng and Marshall 2004; Decrouy et al. 2011a). Dettman et al. (1995) showed that within Lake Huron, $\delta^{13}C_{DIC}$ values are relatively low at ~ -1 ‰ below a water depth of ~60 m versus a value of 0.5 ‰ at the surface. These low $\delta^{13}C$ values are not reflected by the box-core *Pisidium* clams, which generally have higher $\delta^{13}C$ values than those collected from the Pinery beach. We speculate that this might suggest lower metabolic rates and less incorporation of metabolic carbon at these lower temperatures.

2.5 CONCLUSIONS

The valves of modern ostracodes collected from Lake Huron exhibit the same positive vital effect (+2.2 %) reported for European Candoninae by von Grafenstein et al. (1999). Average (or optimum) growth temperatures for these ostracodes, as calculated from the isotopic data, range from 5 °C for *Candona subtriangulata* to 17 °C for *Fabaeformiscandona caudata*. The calculated temperature of shell formation for *C. subtriangulata* matches well with the previously reported mean temperature for this species' habitat. Calculated temperatures for *C. rawsoni* and *C. acuta*, by comparison, are lower (13 *vs.* 17.5 °C & 10 *vs.* 18 °C) and those for *F. caudata* and *Cytherissa* *lacustris* are higher (17 *vs.* 12 °C & 15 *vs.* 10 °C) than generally reported for environments in which these species typically live.

The lung-breathing gastropod *S. elodes* also exhibits apparent ^{18}O-enrichment relative to equilibrium compositions. The higher $\delta^{18}O$ values may indicate a vital effect, but it may also be a consequence of evaporation during intervals of emergence from the lake. The shells of all other modern Lake Huron bivalves and gastropods have oxygen-isotope compositions indicating formation at equilibrium from average Lake Huron water. Hence, these species are suitable proxies for water oxygen-isotope compositions in paleolimnological studies of the Great Lakes Basin, and the fractionation factors reported here can be used to calculate the $\delta^{18}O$ value of paleolakewater present at the time of valve (or shell) formation.

The $\delta^{13}C$ values of the modern ostracodes – save for *C. rawsoni* – likely form in carbon-isotope equilibrium with DIC present in their interstitial microenvironment, which is likely a few permil lower than open lakewater-DIC. As a result, a "microenvironment" correction may be required to interpret carbon-isotope records provided by ostracodes in sediment cores. Modern bivalves and gastropods have $\delta^{13}C$ values lower than expected for shell formation under equilibrium conditions. These compositions most likely reflect some contribution of metabolically produced carbon during shell formation. To interpret the carbon-isotope records provided by these molluscs, a "metabolic" correction may be needed. Even though carbon-isotope corrections may be necessary for these organisms, relative changes in $\delta^{13}C_{DIC}$ should still be evident in lake core records, allowing for inferences to be made regarding changes in DIC source(s) and/or rates of productivity.

2.6 REFERENCES

Adkins JF, Boyle EA, Curry WB, Lutringer A (2003) Stable isotopes in deep-sea corals and a new mechanisms for "vital effects". Geochim Cosmochim Acta 67: 1129-1143

Abell PI, Hoelzmann P (2000) Holocene palaeoclimates in northwestern Sudan: stable isotope studies on molluscs. Glob Planet Change 26: 1-12

Andrus CFT, Whatley Rich K (2008) A preliminary assessment of oxygen isotope fractionation and growth increment periodicity in the estuarine clam *Rangia cuneata.* Geo-Mar Lett 28: 301-308

Auclair A-C, Joachimski MM, Lecuyer C (2003) Deciphering kinetic, metabolic and environmental controls on stable isotope fractionations between seawater and the shell of *Terebratalia transversa* (Brachiopoda). Chem Geol 202: 59-78

Böhm F, Joachimski MM, Dullo W-C, Eisenhauer A, Lehner H, Reitner J, Worheid G (2000) Oxygen isotope fractionation in marine aragonite of coralline sponges. Geochim Cosmochim Acta 64: 1695-1703

Boomer I (2002) Environmental applications of marine and freshwater ostracoda. In: Haslett SK (ed) Quaternary Environmental Micropalaeontology. Arnold, London. pp 115-138

Bowling DR, Pataki DE, Randerson JT (2008) Carbon isotopes in terrestrial ecosystem pools and CO_2 fluxes. New Phytologist 178: 24-40

Breckenridge A, Johnson TC (2009) Paleohydrology of the upper Laurentian Great Lakes from the late glacial to early Holocene. Quat Res 71: 397-408

Broecker WS, Anree M, Wolfli W, Oeschger H, Bonani G, Kennett J, Peteet D (1988) The chronology of the last deglaciation: Implications to the cause of the Younger Dryas event. Paleoceanography 3: 1-19

Broecker WS, Kennett JP, Flower BP, Teller JT, Trumbore S, Bonani G, Wolfli W (1989) Routing of meltwater from the Laurentide Ice Sheet during the Younger Dryas cold episode. Nature 341: 318-321

Buckley SB (1975) Study of post-Pleistocene ostracode distribution in the soft sediments of southern Lake Michigan. Ph.D. thesis, University of Illinois, Urbana, Illinois

Clarke AH (1979) Gastropods as indicators of trophic lake stages. Nautilus 94: 138-142

Clarke AH (1981) The Freshwater Molluscs of Canada. National Museums of Canada, Ottawa

Colman SM, Keigwin LD, Forester RM (1994a) Two episodes of meltwater influx from glacial Lake Agassiz into the Lake Michigan basin and their climatic contrasts. Geology 22: 73-92

Colman SM, Jones GA, Forester RM, Foster DS (1990) Holocene paleoclimatic evidence and sedimentation rates from a core in southwestern Lake Michigan. J Paleolimnol 19: 285-296

Colman SM, Forester RM, Reynolds RL, Sweetkind DS, King JW, Gangemi P, Jones GA, Keigwin LD, Foster DS (1994b) Lake-Level History of Lake Michigan for the Past 12,000 Years: The Records from Deep Lacustrine Sediments. J Great Lakes Res 20: 73-92

Coplen TB (1996) New guidelines for reporting stable hydrogen, carbon, and oxygen isotope-ratio data. Geochim Cosmochim Acta 60: 3359-3360

Coplen TC (2011) Guidelines and recommended terms for expression of stable-isotope ratio and gas-ratio measurement results. Rapid Commun Mass Spectrom 25: 2538-2560

Coplen TB, Kendall C, Hopple J (1983) Comparison of stable isotope reference samples. Nature 302: 236-238

Decrouy L, Vennemann TW, Ariztegui D (2011a) Controls on ostracod valve geochemistry, Part 1: Variations of environmental parameters in ostracod (micro-) habitats. Geochim Cosmochim Acta 75: 7364-7359

Decrouy L, Vennemann TW, Ariztegui D (2011b) Controls on ostracod valve geochemistry: Part 2. Carbon and oxygen isotope compositions. Geochim Cosmochim Acta 75: 7380-7399

Delorme LD (1970a) Freshwater ostracodes of Canada, part III; Family Candonidae. Can J Zoo 48: 1099-1127

Delorme LC (1970b) Freshwater ostracodes of Canada, part IV; Families Ilyocyprididae, Notodromadidae, Darwinulidae, Cytherideidae and Entocytheridae. Can J Zoo 48: 1251-1259

Delorme LD (1978) Distribution of freshwater ostracodes in Lake Erie. J Great Lakes Res 4: 216-220

Delorme LD (1989) Methods in Quaternary Ecology 7 - Freshwater ostracodes. Geosci Canada 16: 85-90

Delorme LD (1991) Ostracoda. In: Thorp JH, Covich AP (eds) Ecology and classification of North American freshwater invertebrates. Academic Press, New York, pp 691-722

Delorme LD (2001) Ostracoda. In: Thorp JH, Covich AP (eds) Ecology and classification of North American freshwater invertebrates, second edition. Academic Press, New York, pp 811-848

Dettman DL (1994) Stable isotope studies of freshwater bivalves (Unionidae) and ostracodes (Podocopida): Implications for late Cretaceous / Paleogene and early Holocene paleoclimatology and paleo-hydrology of North America. Ph.D. thesis, University of Michigan, Ann Arbor, Michigan

Dettman DL, Lohmann KC (1993) Seasonal change in Paleogene surface water δ^{18}O: freshwater bivalves of western North America. In: Swart P, Lohmann KC, McKenzie J, Savin S (eds) Climate Change in Continental Isotopic Records. AGU Monogr 78, pp 153-163

Dettman DL, Reische AK, Lohmann KC (1999) Controls on the stable isotope composition of seasonal growth bands in aragonitic fresh-water bivalves (unionidae). Geochim Cosmochim Acta 63: 1049-1057

Dettman DL, Smith AJ, Rea DK, Moore TC Jr., Lohmann KC (1995) Glacial Meltwater in Lake Huron during early postglacial time as inferred from single-valve analysis of oxygen isotopes in ostracodes. Quat Res 43: 297-310

Epstein S, Mayeda T (1953) Variation of ^{18}O content of waters from natural sources. Geochim Cosmochim Acta 4: 213-224

Fastovsky DE, Arthur ME, Strater NH, Foss A (1993) Freshwater bivalves (Unionidae), disequilibrium isotopic fractionation and temperatures. Palaios 8: 602-608.

Fenger T, Surge D, Schöne B, Milner N (2007) Sclerochronology and geochemical variation in limpet shells (*Patella vulgata*): A new archive to reconstruct coastal sea surface temperature. Geochem Geophys Geosyst 8: 7001, doi:10.1029/2006GC001488

Forester RM, Colman SM, Reynolds RL, Keigwin LD (1994) Lake Michigan's Late Quaternary limnological and climate history from ostracode, oxygen isotope, and magnetic susceptibility. J Great Lakes Res 20: 93-107

Friedman I, O'Neil JR (1977) Compilation of stable isotope fractionation factors of geochemical interest. In: Fleischer M (ed) Data of Geochemistry. USGS, Washington, pp KK1-KK12

Fritz P, Poplawski S (1974) 18O and 13C in the shells of freshwater molluscs and their environments. Earth Planet Sci Lett 24: 91-98

Gillikin DP, Lorrain A, Bouillon S, Willenz P, Dehairs F (2006) Stable carbon isotope composition of *Mytilus edulis* shells: relation to metabolism, salinity, $\delta^{13}C_{DIC}$, and phytoplankton. Org Geochem 37: 1371-1382

Grigorovich IA, Mills EL, Richards CB, Breneman D, Ciborowski JJH (2005) European valve snail *Valvata piscinalis* (Müller) in the Laurentian Great Lakes Basin. J Great Lakes Res 31: 135-143

Grossman EL, Ku TL (1986) Oxygen and carbon isotope fractionation is biogenic aragonite: temperature effects. Chem Geol 59: 59-74

Goewert A, Surge D, Carpenter SJ, Downing J (2007) Oxygen and carbon isotope ratios of *Lampsilis cardium* (Unionidae) from two streams in agricultural watersheds of Iowa, USA. Palaeogeogr Palaeoclimatol Palaeoecol 252: 637-648

Heidenheim JA (2004) The stable isotope systematics of modern snails from Pinery Provincial Park, Ontario, Canada. M.Sc. thesis, The University of Western Ontario, London

Herschler R (1998) A systematic review of the Hydrobiid snails (Gastropoda: Rissooidea) of the Great Basin, Western United States. Part 1. Genus *Pyrgulopsis*. The Veliger 41: 1-132

Holmes JA, Chivas AR (2002) Ostracod shell chemistry – Overview. In: Holmes JA, Chivas AR (eds) The Ostracoda: Applications in Quaternary Research. AGU Monograph 131: 185-204

Hodell DA, Schelske CL, Fahnenstiel GL, Robbins LL (1998) Biologically induced calcite and its isotopic composition in Lake Ontario. Limnol Oceanogr 43: 187-199

Hodell SA, Schelske CL (1998) Production, sedimentation, and isotopic composition of organic matter in Lake Ontario. Limnol Oceanogr 43: 200-214

Hyodo A, Longstaffe FJ (2011) Variations in the oxygen-isotope composition of ancient Lake Superior between 10,600 and 8,800 cal BP. J Paleolimnol, DOI 10.1007/s10933-011-9552-7

Keatings KW, Heaton THE, Holmes JA (2002) Carbon and oxygen isotope fractionation in non-marine ostracods: Results from a ‘natural culture’ environment. Geochim Cosmochim Acta 66: 1701-1711

Kerr-Lawson LJ, Karrow PF, Edwards TWD, Mackie GL (1992) A paleoenvironmental study of the molluscs from the Don Formation (Sangamonian?) Don Valley Brickyard, Toronto, Ontario. Can J Earth Sci 29: 2406-2417

Kesling RV (1951) The morphology of ostracod molt stages. Illinois Biol Monogr 21: 1-126

Last WM, Teller JT, Forester RM (1994) Paleohydrology and paleochemistry of Lake Manitoba, Canada: the isotope and ostracode records. J Paleolimnol 12: 269-282

Leng MJ, Marshall JD (2004) Palaeoclimate interpretation of stable isotope data from lake sediment archives. Quat Sci Rev 23: 811-831

Leng MJ, Lamb AL, Lamb HF, Telford RJ (1999) Palaeoclimatic implications of isotopic data from modern and early Holocene shells of the freshwater snail *Melanoides tuberculata*, from lakes in the Ethiopian rift valley. J Paleolimnol 21: 97-106

Lewis CFM, Anderson TW (1989) Oscillations of levels and cool phases of the Laurentian Great Lakes caused by inflows from glacial Lakes Agassiz and Barlow-Ojibway. J Paleolimnol 2: 99-146

Lohmann KC, Walker JCG (1989) The δ^{18}O record of Phanerozoic abiotic marine calcite cements. Geophys Res Lett 16: 319-322.

Lopez GR, Holopainen IJ (1987) Interstitial suspension-feeding by *Pisidium* spp. (Pisidiidae: Bivalvia): a new guild in the lentic benthos? Am Malacol Bull 5: 21-30

Lorrain A, Paulet Y-V, Chauvaud L, Dunbar R, Mucciarone D, Fontugne M (2004) δ^{13}C variation in scallop shells: increasing metabolic carbon contribution with body size. Geochim Cosmochim Acta 68: 3509-3519

Mackie GL (2007) Biology of Freshwater Corbiculid and Sphaeriid Clams of North America. Ohio Biological Survey, Columbus, Ohio

Mackie GL, White DS, Zdeba TW (1980) A guide to freshwater mollusks of the Laurentian Great Lakes with special emphasis on the genus *Pisidium*. US EPA, Research and Development Report EPA-600/3-80-068

Macdonald RA, Longstaffe FJ (2004) The oxygen and hydrogen isotope composition of Lake Huron. EOS Trans 85: PP43A-0621

Macdonald RA, Longstaffe FJ (2007) The oxygen and hydrogen isotope compositions of the Great Lakes. Programs and Abstracts of the 50th Conference on Great Lake Research pp 117-118

Macdonald RM, Longstaffe FJ (2008) The Late Quaternary oxygen-isotope composition of southern Lake Huron. Aquat Ecosyst Health Manage 11: 137–143

Macdonald RA, Longstaffe FJ, Crowe AS (2007) The Late Quaternary oxygen isotope composition of Lake Michigan. EOS Trans 88: PP13B-1283

McConnaughey T (1989a) ^{13}C and ^{18}O isotopic disequilibrium in biological carbonates: I Patterns. Geochim Cosmochim Acta 53: 151-162

McConnaughey T (1989b) ^{13}C and ^{18}O isotopic disequilibrium in biological carbonates: II In vitro simulation of kinetic isotope effects. Geochim Cosmochim Acta 53: 163-171

McConnaughey TA, Gillikin DP (2008) Carbon isotopes in mollusk shell carbonates. Geo-Mar Lett 28: 287-299

McConnaughey TA, Burdett J, Whelan JF, Paull CK (1997) Carbon isotopes in biological carbonates: Respiration and photosynthesis. Geochim Cosmochim Acta 61: 611-622

Meier-Brook C (1969) Substrate relations in some Pisidium species (Eulamellibranchiata: Sphaeriidae). Malacologia 9: 121-125

Meyers PA (2003) Applications of organic geochemistry of paleolimnological reconstructions: a summary of examples from the Laurentian Great Lakes. Org Geochem 34: 261-289

Meyers PA, Ishiwatari R (1993) Lacustrine organic geochemistry - an overview of indicators of organic matter sources and diagenesis in lake-sediments. Org Geochem 20: 867-900

Michener RH, Shell DM (1994) Stable isotope ratios as tracers in marine aquatic food webs. In: Lajtha K, Michener RJ (eds) Stable Isotopes in Ecology and Environmental Studies. Blackwell Scientific Publications, Oxford, pp 138-157

Moore TC Jr, Walker JCG, Rea DK, Lewis CFM, Shane LCK, Smith AJ (2000) Younger Dryas interval and outflow from the Laurentide ice sheet. Paleoceanography 15: 4-18

O'Neil JR, Clayton RN, Mayeda TK (1969) Oxygen isotope fractionation in divalent metal carbonates. J Chem Phys 51: 5547-5558

Patterson WP, Smith GR, Lohmann KC (1993) Continental paleothermometry and seasonality using the isotopic composition of aragonitic otoliths of freshwater fishes. In: Swart PK, McKenzie J, Lohmann KC, Savin S (eds) Climate Change in Continental Isotopic Records. AGU Monogr 78, pp 191-202

Peltier WR (2007) Rapid climate change and Arctic Ocean freshening. Geology 35: 1147–1148

Rea DK, Moore TC Jr, Lewis CFM, Mayer LA, Dettman DL, Smith AJ, and Dobson DM (1994a) Stratigraphy and paleolimnologic record of lower Holocene sediments in northern Lake Huron and Georgian Bay. Can J Earth Sci 31: 1586-1605

Rea DK, Moore TC Jr, Anderson TW, Lewis CFM, Dobson DM, Dettman DL, Smith AJ, Mayer LA (1994b) Great Lakes paleohydrology: complex interplay of glacial meltwater, lake levels and sill depths. Geology 22: 1059-1062

Romanek CS, Grossman EL, Morse JW (1992) Carbon isotopic fractionation in synthetic aragonite and calcite: Effects of temperature and precipitation rate. Geochim Cosmochim Acta 56: 419-430

Rooth C (1982) Hydrology and ocean circulation. Progress in Oceanography 11: 131-149

Ruppert EE, Fox RS, Barnes RD (2004) Invertebrate Zoology – A Functional Evolutionary Approach, 7th Edition. Brooks/Cole-Thomson Learning, Belmont, California

Schöne BR (2008) The curse of physiology – challenges and opportunities in the interpretation of geochemical data from mollusk shells. Geo-Mar Lett 28: 269-285

Schöne BR, Rodland DL, Fiebig J, Oschmann W, Goodwin D, Flessa KW, Dettman D (2006). Reliability of multitaxon, multiproxy reconstructions of environmental conditions from accretionary biogenic skeletons. J Geology 114: 267-285

Shanahan TM, Pigati JS, Dettman DL, Quade J (2005) Isotopic variability in the aragonite shells of freshwater gastropods living in springs with nearly constant temperature and isotopic composition. Geochim Cosmochim Acta 69: 3949-3966

Tarutani T, Clayton RN, Mayeda TK (1969) The effect of polymorphism and magnesium substitution on oxygen isotope fractionation between calcium carbonate and water. Geochim Cosmochim Acta 33: 987-996

Tevesz MJS, Barrera E, Schwlgien SF (1996) Seasonal variation in oxygen isotope composition of two freshwater bivalves: *Sphaerium striatinum* and *Anodonta grandis*. J Great Lakes Res 22: 906-916

Tevesz MJS, Spongberg AL, Fuller JA (1998) Stable carbon and oxygen isotope records of central Lake Erie sediments. J Paleolimnol 20: 295-305

Turpen JB, Angell RW (1971) Aspects of molting and calcification in the ostracod *Heterocypris*. Biol Bull 140: 331-338

von Grafenstein U (2002) Oxygen-isotope studies of ostracods from deep lakes. In: Holmes JA, Chivas AR (eds) The Ostracoda: Applications in Quaternary Research. AGU Monogr 131, pp 249-266

von Grafenstein U, Erlernkeuser H, Trimborn P (1999) Oxygen and carbon isotopes in modern fresh-water ostracode valves: assessing vital offsets and autecological effects of interest for palaeoclimate studies. Palaeogeogr Palaeoclimatol Palaeoecol 148: 133-152

Weiner S, Dove PM (2003) An overview of biomineralization processes and the problem of the vital effect. In: Dove PM, DeYoreo JJ, Weiner S (eds) Biomineralization. Reviews in Mineralogy & Geochemistry 54. Am Min Soc, Washington, pp 1-29

Wetterich S, Schirrmeister L, Meyer H, Viehber FA, Mackensen A (2008) Arctic freshwater ostracods from modern periglacial environments in the Lena River Delta (Siberian Arctic, Russia): geochemical applications for palaeoenvironmental reconstructions. J Paleolimnol 39: 427-449

White WMP, Dennis PF, Atkinson TC (1999) Experimental calibration and field investigation of the oxygen isotopic fractionation between biogenic aragonite and water. Rapid Commun Mass Spec 13: 1242-1247

Wilbur KM, Saleuddin ASM (1983) Shell formation. In: Wilbur KM, Saleuddin ASM (eds) Physiology Vol 4. Academic Press, New York, pp 235-287

Wurster CM, Patterson WP (2001) Seasonal variation in stable oxygen and carbon isotope values recovered from modern lacustrine freshwater molluscs: Paleoclimatological implications for sub-weekly temperature records. J Paleolimnol 26: 205-218

Xia J, Ito E, Engstrom DR (1997) Geochemistry of ostracode calcite: Part 1. An experimental determination of oxygen isotope fractionation. Geochim Cosmochim Acta 61: 377-382

Yang C, Telmer K, Veizer J (1996) Chemical dynamics of the “St. Lawrence” riverine system: δD_{H2O}, $\delta^{18}O_{H2O}$, $\delta^{13}C_{DIC}$, $\delta^{34}S_{sulfate}$, and dissolved $^{87}Sr/^{86}Sr$. Geochim Cosmochim Acta 60: 851-866

Zeebe RE (1999) An explanation of the effect of seawater carbonate concentration on foraminiferal oxygen isotopes. Geochim Cosmochim Acta 63: 2001-2007

Ziveri P, Stoll H, Probert I, Klaas C, Geisen M, Ganssen G, Young J (2003) Stable isotope “vital effects” in coccolith calcite. Earth Planet Sci Lett 210: 137-149

CHAPTER 3

Late Pleistocene and Holocene History and Oxygen and Carbon Isotopic Evolution of Lake Michigan

3.1 INTRODUCTION

Here we describe the oxygen- and stable carbon-isotope results for ostracodes and clams present in three sediment cores from the Michigan Basin (Fig. 3.1). These proxies provide lakewater records that span the late Pleistocene to mid Holocene, and potentially include the oldest samples yet recovered from Lake Michigan. We explore the differences among the stable isotopic compositions of shallower- and deep-water ostracodes and clams to evaluate whether ancient Lake Michigan was stratified in isotopic composition at various times during the Pleistocene.

Sediment cores from the Great Lakes contain information about water sources (including glacial meltwater inflows), sediment sources and accumulation rates, and climate fluctuations within the Great Lakes Basin since deglaciation began at ~15.5 ka [18,800 cal] BP. Large, rapid inputs of freshwater to the North Atlantic and/or Arctic regions have been implicated in disrupting North Atlantic deep water (NADW) formation and the associated major ocean current that regulates climate in much of the Northern Hemisphere (Broecker et al. 1989; Barber et al. 1999; Peltier 2007). Numerous studies have proposed that the delivery of such freshwater – originating from glacial Lake Agassiz and/or directly from the Laurentide Ice Sheet (LIS) – to the North Atlantic and/or the Arctic Oceans initiated some of the most rapid climate changes in the late Pleistocene and Holocene, including the Younger Dryas cold period (11.0 – 10.0 ka [12,900 – 11,500 cal] BP), an unnamed event at ~8.3 ka [9,300 cal] BP and the '8.2 ka [calendar] event' (~7.7 ka [8,450 cal] BP; Rooth 1982; Alley et al. 1997; Broecker et al. 1989; Clark et al. 2001; Fisher et al. 2002; Teller et al. 2002; Teller and Leverington 2004; Rasmussen et al. 2006; Daley et al. 2009; Murton et al. 2010; Yu et al. 2010).

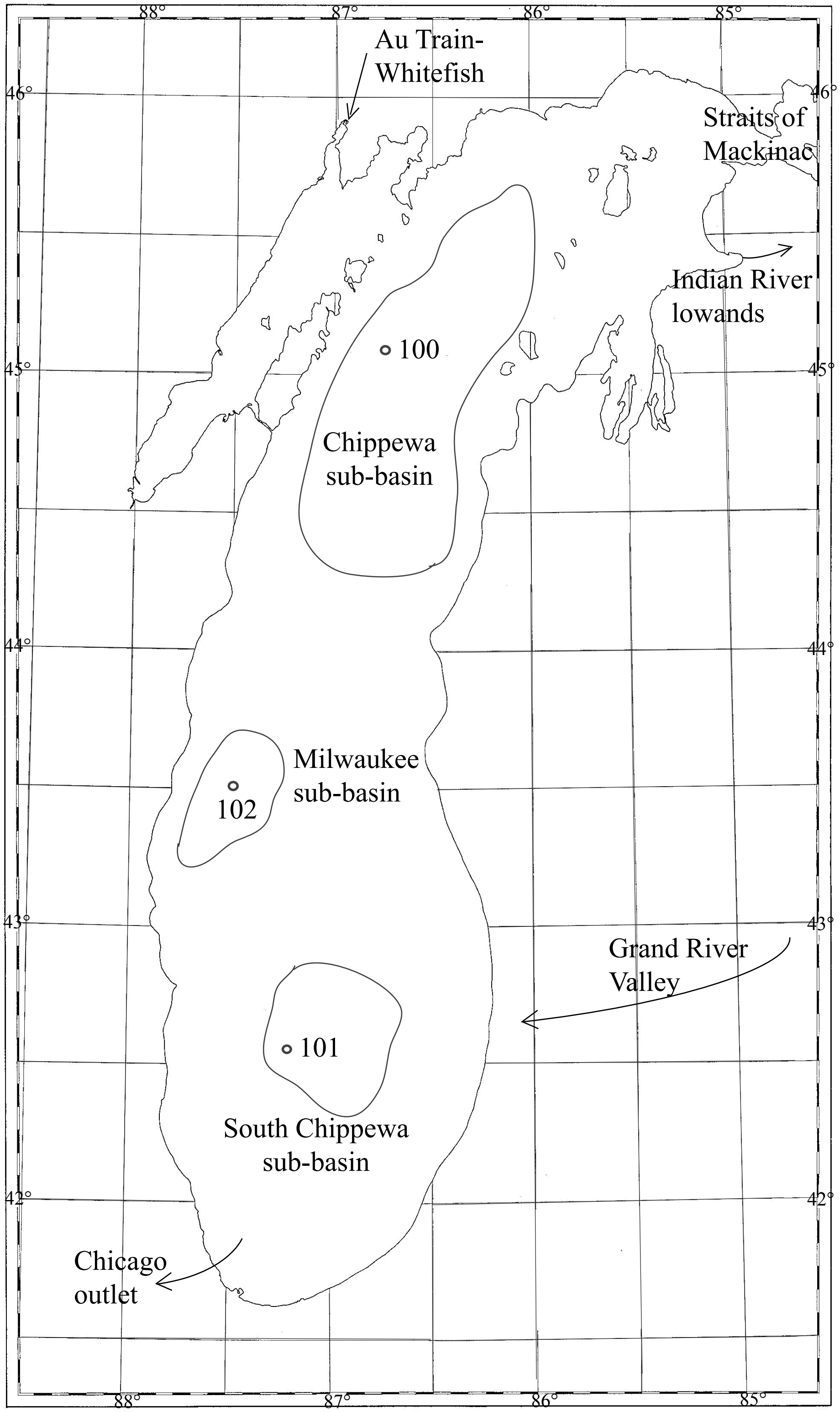

Figure 3.1. Map showing locations of sediment cores (core 101 - 42°33’53” N 87°13’54” W, water depth 134 m; core 102 - 43°30’59” N 87°28’05” W, water depth 140 m; core 100 - 45°07’00” N 86°42’33” W, water depth 164 m) as well as major inlets and outlets.

Peltier (2007) suggested that such influxes of freshwater to either the Arctic or North Atlantic Oceans would have been equally capable of disrupting ocean circulation patterns. As such, the focus on identifying the various pathways of Lake Agassiz floods, which has been the subject of many debates, has expanded beyond the Great Lakes Basin. It is well-documented that prior to its Moorhead phase (before ~11 ka [12,900 cal] BP), Lake Agassiz drained south through the Mississippi River and into the Gulf of Mexico (Teller and Thorleifson 1983; Fisher 2003, 2007; Teller and Leverington 2004). A common theory has been that continued retreat of the LIS opened eastward outlets at ~11 ka [12,900 cal] BP, allowing for drainage through the Great Lakes Basin and onto the North Atlantic Ocean (Teller 1985; Broecker et al. 1989; Lewis and Anderson 1989; Lewis et al. 1994; Teller and Leverington 2004). This has recently been called into question by new evidence of a large flood from the Agassiz Basin through the Mackenzie River Valley between ~11.1 – 10.8 ka [13,000 – 12,800 cal] BP (Teller et al. 2005; Murton et al. 2010). Lake Agassiz most likely drained through its NW outlet to the Arctic Ocean around 11.1 ka [13,000 cal] BP for a few hundred years (Murton et al. 2010) and then was rerouted through its eastern outlet into the Great Lakes Basin.

The Marquette glacial advance at ~10 ka [11,500 cal] BP redirected drainage from the Agassiz Basin through its NW outlet until ~9.6 ka [11,000 cal] BP (Fisher 2003, 2007; Couch and Eyles 2008; Murton et al. 2010), after which it drained south to the Gulf of Mexico until ~9.4 ka [10,650 cal] BP (Fisher 2003). At this time, overflow from Lake Agassiz was redirected again eastwards to the Great Lakes Basin, resulting at times in large, catastrophic floods (Teller 1985; Colman et al. 1994a; Lewis et al. 1994; Teller et al. 2002; Fisher 2003; Breckenridge and Johnson 2009; Breckenridge et al. 2010). Previously investigated sediment cores from the Great Lakes Basin have provided a record of relative rates and timing of various water sources; however, not all records from the various lake basins are in agreement. It appears that some Agassiz-sourced floods were major events in certain basins while contemporaneous records from adjacent basins suggest these floods had little to no impact. Additional examination of Great Lakes Basin cores, together with well-established chronologies, are necessary to fully uncover the history of the Great Lakes Basin since the end of the last glacial period.

Two major influxes of water, the A1 and A2 events, which likely originated from Lake Agassiz, are recorded in Lake Michigan sediments. The A1 event, which deposited a distinctive, typically massive, grey silty clay known as the Wilmette Bed, is thought to have occurred during the first half of Lake Agassiz's Moorhead phase between 11.0 and 10.5 ka [12,900 – 12,600 cal] BP, shortly after the opening of its eastern outlet (Colman et al. 1994b, 1994c; Teller and Thorleifson 1983; Teller and Leverington 2004; Teller et al. 2005), near the beginning of the Younger Dryas. Previous descriptions of the Wilmette Bed describe sharp contacts with overlying and underlying red clay, an absence of organic matter and very few ostracodes (Colman et al. 1994a, 1994b, 1994c). The approximate age of the Wilmette Bed is based upon its relative position above the Two Rivers Till (deposited until 11.1 ka [13,000 cal] BP) and below the Chippewa unconformity, which has been dated at ~10.3 ka [12,100 cal] BP (Hansel et al. 1985; Colman et al. 1994a, 1994c). Colman et al. (1994c) narrowed the timing for deposition of the Wilmette Bed to ~10.6 ka [12,700 cal] BP, and recent examinations of the Lake Agassiz water level report a rapid (months to a century) drop of ~110 m at 10.9 – 10.8 ka [12,900 – 12,800 cal] BP (Leverington et al. 2000; Fisher 2003; Teller and Leverington 2004; Teller et al. 2005). This timing correlates well with the rerouting of Agassiz outflow from its northwest outlet to eastward flow through the Great Lakes Basin (Murton et al. 2010). The presence of low-^{18}O waters in the Erie Basin between 11 – 10.5 ka [12,900 – 12,600 cal] BP is also attributed to this flooding (Lewis and Anderson 1992). Maximum lake levels in the Michigan Basin during the A1 event, however, are presently unknown.

Records of the A2 event(s) suggest two pulses of flooding during Lake Agassiz's Nipigon phase (9.5 – 8.2 ka [10,700 – 9,100 cal] BP; Teller and Thorleifson 1983; Teller and Leverington 2004; Teller et al. 2005). The A2 event is associated with a bed of grey clay (Colman et al. 1994a), and a decrease of ~6 ‰ in the oxygen-isotope composition of lake water (Colman et al. 1990, 1994a). Colman et al. (1994a) originally dated the two pulses of the A2 event at 8.9 and 8.6 ka [10,000 and 9,550 cal] BP. Lewis et al. (2005) placed the timing of two Mattawa highstands in the Huron Basin, also believed to be the result of Lake Agassiz outflows, at 8.7 and 8.1 ka [9,700 and 9,000 cal] BP. Breckenridge and Johnson (2009) re-evaluated lacustrine records from the Michigan and Huron Basins, and placed the two A2 pulses at 8.4 – 8.2 ka [9,450 – 9,100 cal] BP. This timing coincides with the '9,300 cal BP event', which has been linked to substantial lowering of ancient Lake Superior and major Northern Hemispheric climate cooling (Fleitmann et al. 2008; Yu et al. 2010).

The Lake Michigan sediment record also records a third influx of low-^{18}O waters between 9.6 – 9.4 ka [11,000 – 10,600 cal] BP (Breckenridge and Johnson 2009). Eastward overflow of Lake Agassiz at the beginning of its Nipigon phase is believed to have been the source of this water (Teller and Thorleifson 1983; Teller and Leveringon 2004; Teller et al. 2005).

The recognition of large outflows from Lake Agassiz using lacustrine records from the Great Lakes is complicated by uncertainty over the oxygen-isotope composition of Lake Agassiz. Lake Agassiz is commonly assumed to have contained glacial meltwater with very low δ^{18}O values (~ -30 ‰; Dansgaard and Tauber 1969; Fairbanks 1989; Sima et al. 2006). However, co-existing benthic and pelagic proxies suggest that the surface and bottom waters had distinctly different oxygen-isotope compositions for much of Lake Agassiz's history (Buhay and Betcher 1998; Birks et al. 2007; Remenda et al. 1994; Last et al. 1994). Birks et al. (2007), for example, suggested that by Lake Agassiz's Nipigon phase, precipitation – which is enriched in ^{18}O relative to glacial meltwater – had become an important source for the Agassiz Basin. Increased evaporation during climatic warming is thought to have further enriched Lake Agassiz's surface waters in ^{18}O, producing a difference of up to 18 ‰ between surface and bottom waters (Lewis et al. 1994; Buhay and Betcher 1998; Birks et al. 2007).

The variable but low δ^{18}O values reported for ancient Lake Superior at least until ~7.95 ka [8,800 cal] BP also provide a possible source of low-^{18}O water for downstream Great Lakes during this time (Mae and Longstaffe 2007; Mae et al. 2007; Breckenridge and Johnson 2009; Hyodo 2010; Yu et al. 2010; Hyodo and Longstaffe 2011b).

However, the ancient lower Great Lakes at times had significantly higher $\delta^{18}O$ values than expected for inflow originating from glacial meltwater-dominated ancient Lake Superior. One explanation for the discrepancy is that outflow from Lake Superior was diverted northwards or passed only through Georgian Bay during the times of elevated $\delta^{18}O$ values in the lower ancient Great Lakes (Mae and Longstaffe 2007; Mae et al. 2007; Breckenridge and Johnson 2009, Hyodo 2010; Hyodo and Longstaffe 2011b). Another possibility is that Lake Superior was stratified in isotopic composition during these times and that only the upper layer of ^{18}O-enriched waters flowed into the Michigan and Huron Basins. To date, however, evidence is sparse for such stratification in Lake Superior, or indeed for any of the ancient Great Lakes during any part of the late Pleistocene or Holocene.

3.1.1 Late Pleistocene and Holocene history of the Michigan Basin

The first water body known from the Michigan Basin – glacial Lake Milwaukee – developed against the northward retreating ice sheet between 15.5 – 15 ka [18,800 – 18,500 cal] BP. During the Cary advance (15 – 13.5 ka [18,500 – 16,050 cal] BP), the high-level Lake Chicago was formed, which existed until the Kirkfield phase of Lake Algonquin (~11.1 ka [13,000 cal] BP (Schneider and Need 1985; Hansel et al. 1985). Lake Chicago, along with other early proglacial lakes in the Great Lakes Basin, was dominantly fed by glacial meltwater (Hansel et al. 1985). Glacial activity in the Michigan Basin during this portion of the late Pleistocene was quite dynamic; the Lake Michigan Lobe of the ice sheet was thin and unstable and probably advanced and retreated very rapidly (Clark 1994; Clark et al. 1994; Colman et al. 1994b). The period from ~15 – 11 ka [18,500 – 12,900 cal] BP is characterized by three major glacial re-advances into the Michigan Basin: the Cary advance from ~15 – 13.5 ka [18,500 – 16,050 cal] BP, the Port Huron advance from 13 – 12.2 ka [15,300 – 14,050 cal] BP, and the Two Rivers advance from 11.8 – 11.1 ka [13,700 – 13,000 cal] BP (Hansel et al. 1985; Hansel and Mickelson 1988; Colman et al. 1994c; Lewis et al. 1994). These re-advances blocked the northern connection to the Huron Basin via the Straits of Mackinac and/or the Indian River lowlands (Fig. 3.1) and generally resulted in high lake levels. During the Cary and Port

Huron advances, water from the Huron and Erie Basins drained westwards into Lake Chicago via the Grand Valley. At times when the ice sheet blocked its northern outlets, drainage from the Michigan Basin was south through the outlet at Chicago (Fig. 3.1; Hansel et al. 1985; Hansel and Mickelson 1988).

During the periods of glacial retreat (Cary-Port Huron interstade from 13.5 – 13 ka [16,050 – 15,300 cal] BP; Two Creeks interstade from 12.2 – 11.8 ka [14,050 – 13,700 cal] BP), the ice sheet was situated to the north of the connections between the Michigan and Huron Basins, which resulted in significantly lower water levels in the Michigan Basin (Hansel et al. 1985; Hansel and Mickelson 1988; Colman et al. 1994b, 1994c). Glacial retreat from the Huron Basin opened the Fenelon Falls outlet shortly before 12 ka [13,900 cal] BP, commencing drainage through the Simcoe Basin and leading to the low-level Kirkfield phase of Lake Algonquin (Eschman and Karrow 1985; Finamore 1985; Lewis et al. 1994). The Kirkfield phase within the Michigan Basin was temporarily interrupted by the Two Rivers advance but resumed by ~11.1 ka [13,000 cal] BP, once the ice retreated north of the Straits of Mackinac and allowed confluence of the Michigan and Huron Basins (Hansel et al. 1985; Safarudin and Moore 1999). The extremely high water levels of the Main Lake Algonquin phase in the Huron, Michigan and Superior Basins ensued (~11 – 10.3 ka [13,000 – 12,100 cal] BP), which then fell rather abruptly once the retreating LIS opened the North Bay outlet at ~10.3 ka [12,100 cal] BP (Larsen 1987; Lewis and Anderson 1989; Lewis et al. 1994; Colman et al. 1994b). The rapid rise of Main Lake Algonquin is thought to have coincided with major outpourings from Lake Agassiz, which was connected to the Great Lakes Basin at ~10.9 ka [12,900 cal] BP (Lewis and Anderson 1989; Moore et al. 2000; Leverington et al. 2000; Fisher 2003; Teller and Leverington 2004; Teller et al. 2005; Murton et al. 2010).

The history of ancient Lake Michigan following Main Lake Algonquin until the Nipissing transgression (~10.3 – 5 ka [12,100 – 5,700 cal] BP) has long been described as a prolonged period of low lake levels known as Lake Chippewa (Hansel et al. 1985, Hansel and Mickelson 1988; Colman et al. 1990, 1994a, 1994b, 1994c; Forrester et al. 1994; Breckenridge and Johnson 2009). Safarudin and Moore (1999) identified major lowstand stages during this time – as indicated by coarse-grained horizons – which were correlated to lowstands in the Huron Basin. Lewis et al. (2005, 2007) proposed that lake level phases within the Michigan Basin were, for the most part, identical to phases within the Huron Basin, reflecting their connection via the Indian River lowland and Straits of Mackinac during much of their histories (Fig. 3.1). As such, Lewis et al. (2005, 2007) suggest that the Michigan Basin experienced three pronounced low-level phases during the Holocene, referred to as the Chippewa lowstands, which were interspersed by highstands resulting from influxes of upstream Lake Agassiz waters (Lewis and Anderson 1989; Lewis et al. 2007, 2008).

Records of the isotopic composition of the Michigan and Huron Basins during the Pleistocene are quite sparse. Holocene records of the oxygen-isotope composition of Lakes Michigan and Huron are much more complete, although they generally do not correlate well with each other. For example, influxes of water from Lake Agassiz into the Michigan Basin during the A2 event are commonly associated with the main Mattawa highstands at ~8.4 – 8.2 ka [9,450 – 9,100 cal] BP in the Huron Basin (Lewis and Anderson 1989; Lewis et al. 1994, 2005; Breckenridge and Johnson 2009) but this relationship is not clearly described in most studies. Likewise, although there is some agreement that the Mattawa highstands in Huron Basin were caused by flooding events from Lake Agassiz, most researchers have associated these phases with relatively high-^{18}O waters (Rea et al. 1994a, 1994b; Moore et al. 1994, 2000; Dettman et al. 1995; Macdonald and Longstaffe 2008). In contrast, it is generally assumed that overflow from the Lake Agassiz basin should be characterized by low-^{18}O waters. A significant effort at resolving these uncertainties was made by Breckenridge and Johnson (2009). Here, we endeavour to further clarify the relationships between major events in these neighbouring basins.

3.2 MATERIALS AND METHODS

Three piston cores were collected from Lake Michigan in 2006: core 100 from the Chippewa sub-basin, core 101 from the South Chippewa sub-basin and core 102 from the

Milwaukee sub-basin (Fig. 3.1). Following lengthwise splitting, one half of the core was digitally imaged using a GEOTEK® multi-sensor core logger at the Graduate School of Oceanography, University of Rhode Island. The other half was sub-sampled at 10 cm intervals for isolation of biogenic carbonate for oxygen and carbon isotopic analysis and organic matter for radiocarbon dating. These samples were weighed and wet-sieved using 1 mm, 500, 250 and 125 μm mesh-sizes. Biogenic carbonates and large fragments of organic matter were picked from the dried sieve-fractions using a camel hair or tweezers. Generally, up to 1 m of sediment is lost between the sediment-water interface and the top of the recovered material during piston coring. The sediment depths reported here are recorded from the top of the recovered sediment.

Five species of ostracodes (*Candona subtriangulata*, *Candona rawsoni*, *Candona crogmaniana*, *Cytherissa lacustris* and *Limnocythere friabilis*) and three species of bivalves from the *Pisidium* (Pea Clam) genus (*P. casertanum*, *P. nitidum* and *P. ferrugineum*) were identified in samples from all three cores. The individual species of ostracodes were counted and analyzed separately, whereas the various *Pisidium* clam species were not differentiated for purposes of counting or isotopic analysis. *Limnocythere friabilis* was not analyzed because of its extremely small size (<0.75 mm in length) and the inherent difficulties involved in cleaning its relatively thin valves.

Most sediment adhering to the ostracode valves and bivalve shells was removed during wet sieving. The few samples that retained some sediment were soaked overnight at room temperature in a 2.5 % solution of sodium hypochlorite (bleach), which facilitated removal of the remaining adherents. When available, adult ostracode valves were selected for analysis over younger instars. Valves or shells that appeared to be damaged were not analyzed. Two to four ostracode valves were normally required for isotopic analysis. For *Pisidium* samples, individual shells were fragmented and/or powdered to obtain sufficiently small aliquots.

The oxygen- and carbon-isotope compositions of the biogenic carbonates were obtained by reaction with orthophosphoric acid at 90 °C using a Micromass MultiPrep device coupled to a VG Optima dual-inlet, stable isotope ratio mass-spectrometer. All oxygen- and carbon-isotope results are reported in the standard δ-notation:

$$\delta^{18}\mathrm{O} \text{ or } \delta^{13}\mathrm{C} = [(R_{\mathrm{sample}}/R_{\mathrm{standard}}) - 1] \text{ (permil, or ‰)} \qquad (1)$$

where R_{sample} and R_{standard} are the ratios of $^{18}\mathrm{O}/^{16}\mathrm{O}$ (or $^{13}\mathrm{C}/^{12}\mathrm{C}$) in the sample and standard, respectively. Carbonate and calculated paleo-lakewater $\delta^{18}\mathrm{O}$ values are reported relative to VSMOW and carbonate $\delta^{13}\mathrm{C}$ values are reported relative to VPDB, as calibrated using defined values for NBS-19 (Coplen 1996). Internal standards WS-1 and Suprapur (both calcite), as well as NBS-18, were used to evaluate the accuracy and precision of the analyses. Over the course of this study, WS-1 had a $\delta^{18}\mathrm{O}$ value of 26.1 ± 0.1 ‰ (1σ; n = 22) and a $\delta^{13}\mathrm{C}$ value of 0.7 ± 0.1 ‰ (1σ; n = 20), which compares well with its accepted values of 26.2 and 0.7 ‰, respectively. A $\delta^{18}\mathrm{O}$ value of 13.2 ± 0.1 ‰ (1σ; n = 61) was obtained for Suprapur, which compares well with its accepted $\delta^{18}\mathrm{O}$ value of 13.2 ‰. A $\delta^{13}\mathrm{C}$ value of –5.0 ± 0.1 ‰ (1σ; n = 63) was obtained for NBS-18, which compares well with its accepted value of –5.0 ‰.

Radiocarbon dates were obtained for two samples of bivalves (mixed *Pisidium* clams; South Chippewa and Milwaukee sub-basin cores), one sample of ostracodes (*C. subtriangulata*, *C. rawsoni* and *C. crogmaniana*; Chippewa sub-basin core) and a large wood fragment (Milwaukee sub-basin core). All dates were obtained using accelerator mass spectrometry (AMS) at the NSF-Arizona AMS Facility, The University of Arizona.

3.3 RESULTS

3.3.1 Radiocarbon dates

Radiocarbon dates obtained for these cores are listed in Table 3.1. A hard-water effect correction of 250 years was applied to dates for the Lake Michigan biogenic carbonates (Rea and Colman 1995; Moore et al. 1998). Calibrated dates (in square

Table 3.1 Radiocarbon dates obtained for the Lake Michigan cores

Core	Sample Interval (m)	Lab No.	Material	$\delta^{13}C$ (‰, VPBD)	^{14}C Date (year BP)	HWE Correction[1]	Accepted Date	Calibrated Date[2] (cal year BP)	Range[3] (cal year BP)
South Chippewa (101)	0.6 - 0.7	AA83993	mixed *Pisidium* clams	1.0	7583 ± 45	-250	7333	8170	8300 - 8017
Milwaukee (102)	1.89 (in situ)	AA83994	large wood fragment	-25.3	8011 ± 48		8011	8990	9017 - 8659
Milwaukee (102)	3.2 - 3.3	AA83995	mixed *Pisidium* clams	-0.8	9972 ± 50	-250	9722	11 185	11 242 - 10 871
Chippewa (100)	1.4 - 1.5	AA83992	mixed ostracode species	-1.7	7391 ± 89	-250	7141	7965	8168 - 7792

[1] hard-water effect correction is from Rea and Colman (1995) and Moore et al. (1998)

[2] radiocarbon dates were converted to calibrated dates using INTCAL04 (Reimer et al. 2004)

[3] ranges on calibrated dates were calculated using OxCal 4.1

brackets following radiocarbon dates) were obtained using INTCAL04 (Reimer et al. 2004).

3.3.2 Core descriptions

Lithostratigraphic units observed in cores 100, 101 and 102 (Fig. 3.2) are described here following the approach of Colman et al. (1994c), who informally modified the more formal stratigraphy of Hough (1955) and Lineback et al. (1979). A significant portion of Michigan Basin late Pleistocene and early to mid Holocene history is represented in these sediments (Fig. 3.2).

South Chippewa sub-basin – Core 101

Figure 3.3. illustrates the stratigraphy of the South Chippewa sub-basin, as identified in seismic-reflection, by Colman et al. (1994c). Sediments from the base of core 101 (16.6 m) to ~12.8 m consist of massive grey mud to sand (Munsell Soil Colour Chart values 10YR 4/1, 10YR 5/1, 10YR 5/2, 2.5Y 5/2) interpreted to be the Equality Formation (Fig. 3.4; Wickham et al. 1978; Lineback et al. 1979). This unit contains abundant pink, grey and beige clay clasts up to ~0.5 cm in diameter and infrequent pebbles up to 3 cm in diameter. Paleozoic fossil fragments (e.g. corals, crinoids) are common, likely reworked from the terrain surrounding much of the lower Great Lakes Basin. Few ostracode valves were found in this unit. The sediments between ~12.8 – ~10.8 m undergo a gradual transition from the grey muds and sands of the Equality Formation to the redder muds of the Lower unit of the Lake Michigan Formation (henceforth the 'Lower unit'). This transitional interval is likely represented by the Equality Formation outwash on Figure 3.3. The Equality Formation, a unit comprising relatively coarse, grey, sublacustrine outwash, and the Lower unit were interpreted by Colman et al. (1994c) to represent different lateral facies in a proglacial lacustrine environment.

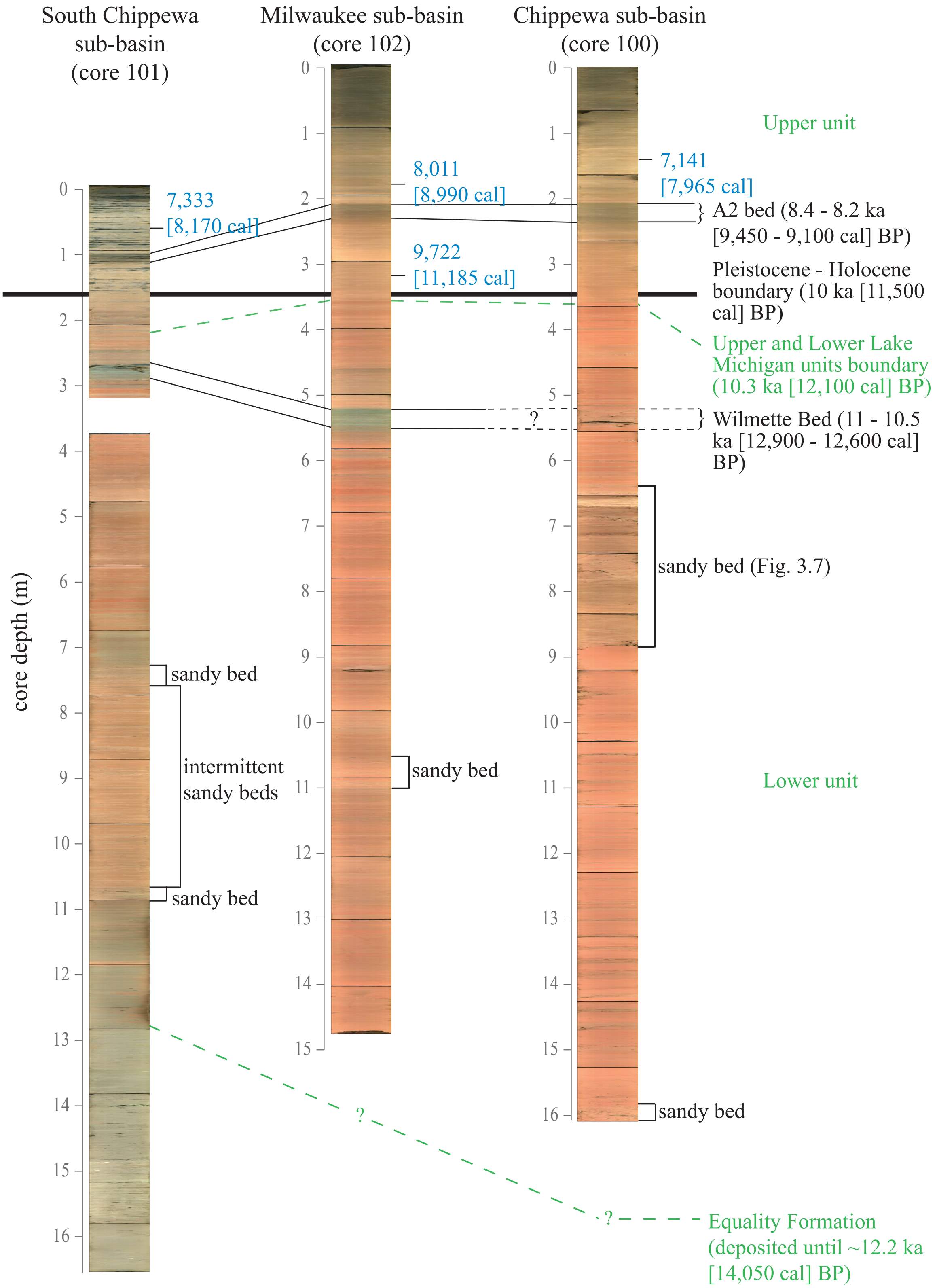

Figure 3.2. Images of the Lake Michigan Basin sediment cores. The cores are hung at a datum of 10 ^{14}C ka [11,500 cal] BP (thick black line), the Pleistocene-Holocene boundary. The main sedimentary units (in green), key lithostratigraphic features, and radiocarbon dates (in blue) are also indicated.

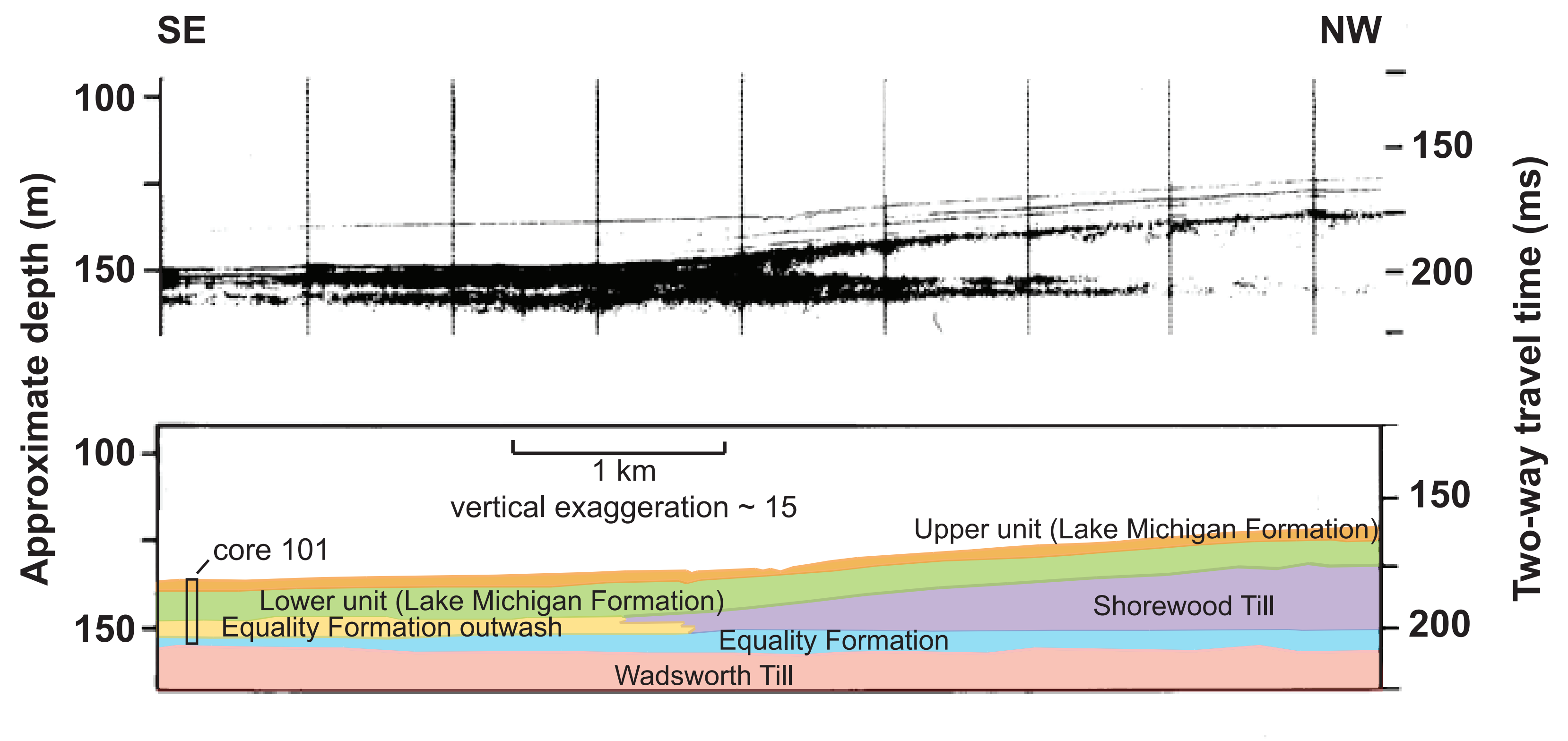

Figure 3.3. Seismic-reflection profile (3.5 kHz) showing the sedimentary sequence of the South Chippewa sub-basin approximately 15 km north of the site of core 101. The Shorewood Till was deposited during the Port Huron glacial advance at 13 - 12.2 ka [15,300 - 14,050 cal] BP. This till does not extend as far south as the site of core 101. The approximate position of core 101 within this sequence is shown. Modified after Colman et al. (1994c).

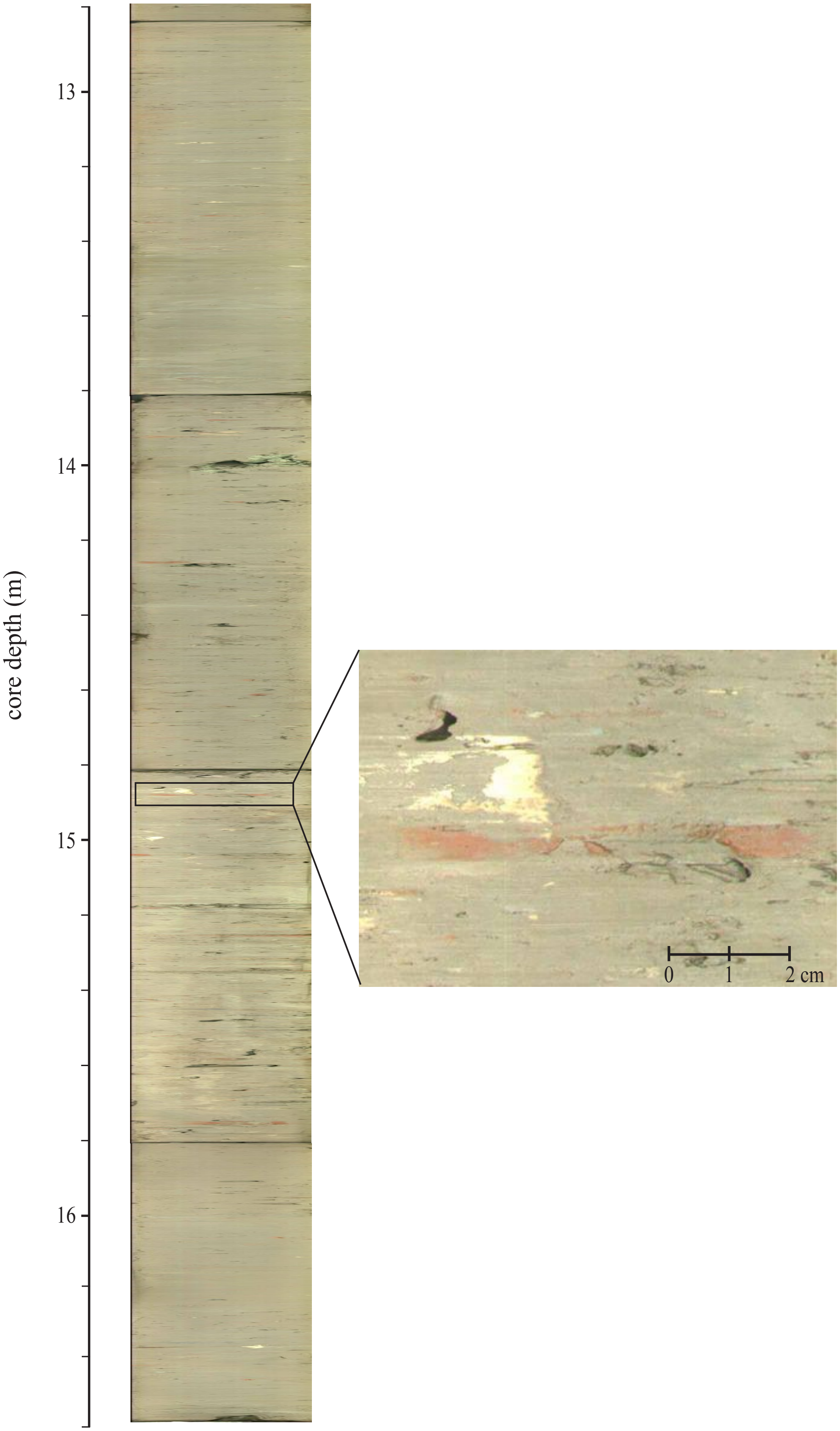

Figure 3.4. Images of the South Chippewa sub-basin (core 101) showing the Equality Formation from ~16.6 - 12.8 m (stretched horizontally ~5 times). The interval at ~14.85 m has been enlarged to show the clay clasts in detail.

Sediments from ~12.8 – ~2.2 m represent the Lower unit, which is characterized by reddish brown glaciolacustrine clays (5YR 4/3, 5YR 4/4, 5YR 5/4). This unit was deposited in association with the red tills (the Shorewood, Manitowoc and Two Rivers tills) that line much of the Michigan Basin but at a greater distance from the glacial front (Colman et al. 1994c). Deposition of the Lower unit within the South Chippewa sub-basin likely began following retreat of the Port Huron glacier at ~12.2 ka [14,050 cal] BP (Colman et al. 1994b, 1994c). The Lower unit is for the most part massive, although intermittent sandy intervals do occur. These brown sandy beds (7.5YR 5/3; usually ~1-2 cm thick) are common from 10.9 – 7.3 m, with particularly thick sandy units found from 7.6 – 7.3 m and 10.9 – 10.7 m. These two thicker sandy intervals contain sparse pebbles up to 1-2 cm in size. The Wilmette Bed, characterized as a distinctive grey (5Y 5/1) silty-clay unit (Colman et al. 1994a), is apparent in this core towards the top of the Lower unit from 2.73 – 2.59 m (Fig. 3.5). The upper ~8 cm of the Wilmette Bed exhibits black banding/mottling, likely indicating iron-sulfide minerals in the sediment and suggestive of reducing conditions within the sediment column (Colman et al. 1994c; Odegaard et al. 2003). The transition from the red muds of the Lower unit into the grey Wilmette Bed occurs over 9 cm (from 2.82 – 2.73 m). By comparison, the upper boundary between the Wilmette Bed and the overlying Lower unit is very sharp. Colman et al. (1994a) provided a similar description of the Wilmette Bed, although they noted sharp contacts with the surrounding red sediments at both the bottom and top of the bed.

The boundary between the Lower and Upper units of the Lake Michigan Formation is typically marked by the Chippewa unconformity (10.3 ka [12,100 cal] BP) in relatively shallow water and by a transitional colour change from red to grey-brown in deeper water (Colman et al. 1994c). This boundary is not particularly distinct in core 101 but occurs between 2.23 – 2.18 m. The Upper unit of the Lake Michigan Formation (henceforth the ‘Upper unit’) is composed of brown (10YR 5/3) to greyish-brown (10YR 5/2, 2.5Y 5/2) glaciolacustrine clays. Black iron-sulfide streaking is common in the Upper unit (Colman et al. 1994c) and is pronounced in the upper 1.5 m of core 101. These iron-sulfide bands disappear quickly following their exposure to air as they become oxidized (Colman et al. 1994c; Odegaard et al. 2003). A greyish-brown silty clay (10YR

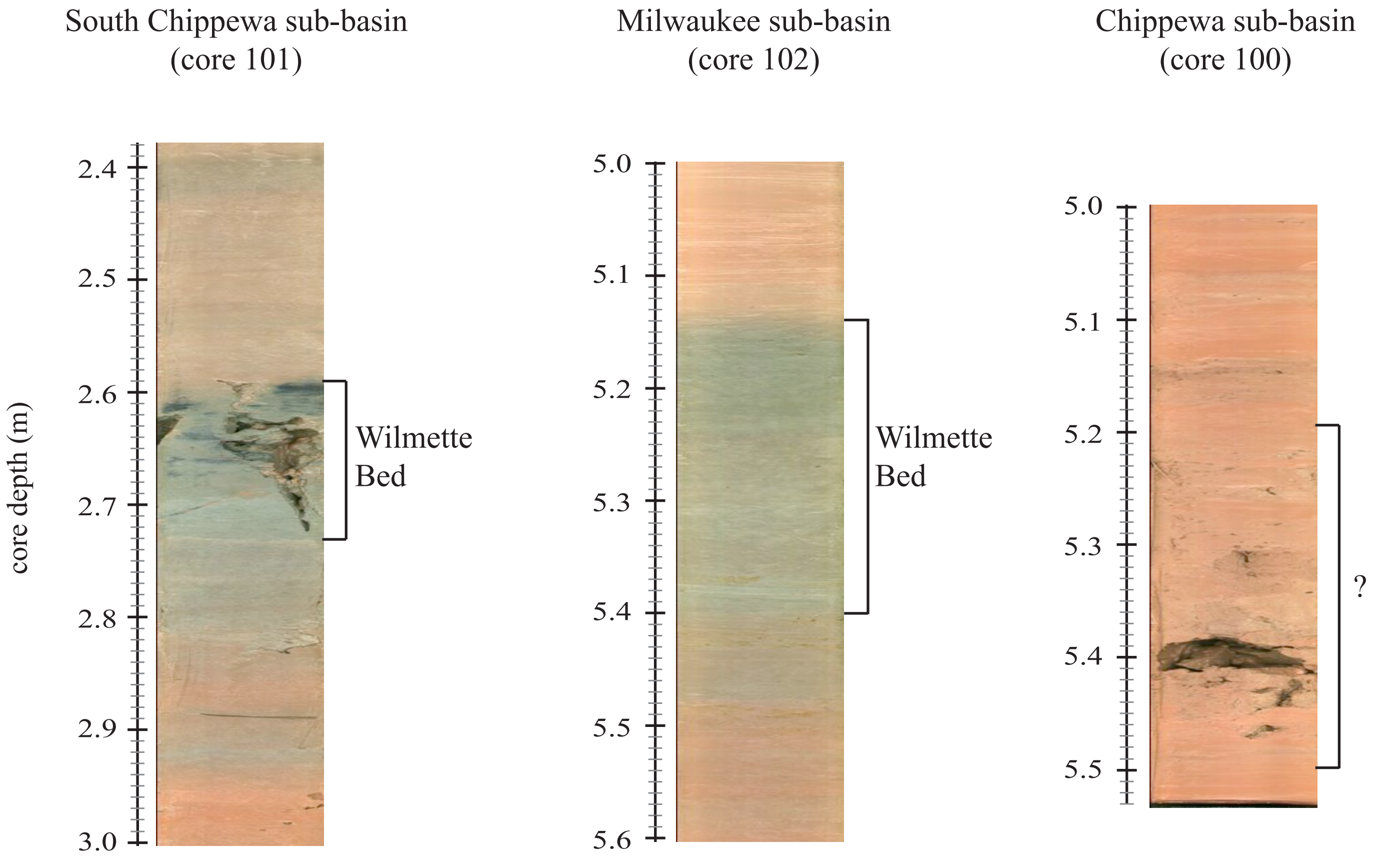

Figure 3.5. Images of the Wilmette Bed in the South Chippewa and Milwaukee sub-basin cores deposited by the initial flood of Lake Agassiz water through the Great Lakes Basin at ~10.9 – 10.8 ka [12,900 – 12,800 cal] BP. The disturbed and silty bed in the Chippewa sub-basin core may also be associated with the Wilmette flooding event. The core images are stretched horizontally ~2 times to show detail.

4/2, 10YR 5/2), which we have identified as the A2 Bed, is present between ~1.1 – 0.96 m (Fig. 3.6). Its lower boundary (the transition from the Upper unit into the A2 bed) occurs over ~5 cm while the upper boundary (from the A2 Bed back into Upper unit sediments) is sharp.

Milwaukee sub-basin – Core 102

The sediments of core 102 consist entirely of a thick sequence of Lake Michigan Formation (Fig. 3.2). Massive reddish-brown muds (5YR 4/4, 5YR 5/3, 5YR 5/4) characteristic of the Lower unit are present from the core bottom at 14.73 m to ~3.5 m. Within this interval, a sandy unit containing grey to beige clay clasts is present from ~11.0 – 10.6 m and thin (usually < 1 cm) intermittent sandy brown beds (7.5YR 4/3, 7.5YR 5/3) are found throughout. A unit identified as the Wilmette Bed, marked by a distinctive dark-grey to grey clay-rich bed (5Y 4/1, 5Y 5/1), is present between 5.40 – 5.14 m (Fig. 3.5). The lower boundary of the Wilmette Bed is transitional, as observed in core 101; a general darkening and greying of the sediment occurs over ~7 cm. The upper boundary of the Wilmette Bed and the overlying Lower unit is sharp. Black banding or mottling were not observed in the Wilmette Bed in core 102.

The boundary between the Lower and Upper units in the Milwaukee sub-basin core is more distinctive than in the South Chippewa sub-basin. The Upper unit (3.5 – 0 m) exhibits shades of dark greyish brown (10YR 4/2), greyish brown (10YR 5/2) and brown (10YR 5/3) and is more massive with substantially less black iron-sulfide banding than in core 101. Vivianite grains are present in the upper ~1 m of the core. A dark greyish-brown interval (10YR 4/2), identified as the A2 Bed, is present within the Upper unit from 2.26 – 2.06 m (Fig. 3.6). As also exhibited by the Wilmette Bed in this core, the A2 Bed has a gradual lower boundary and a sharp upper boundary with sediments of the Upper unit.

Chippewa sub-basin – Core 100

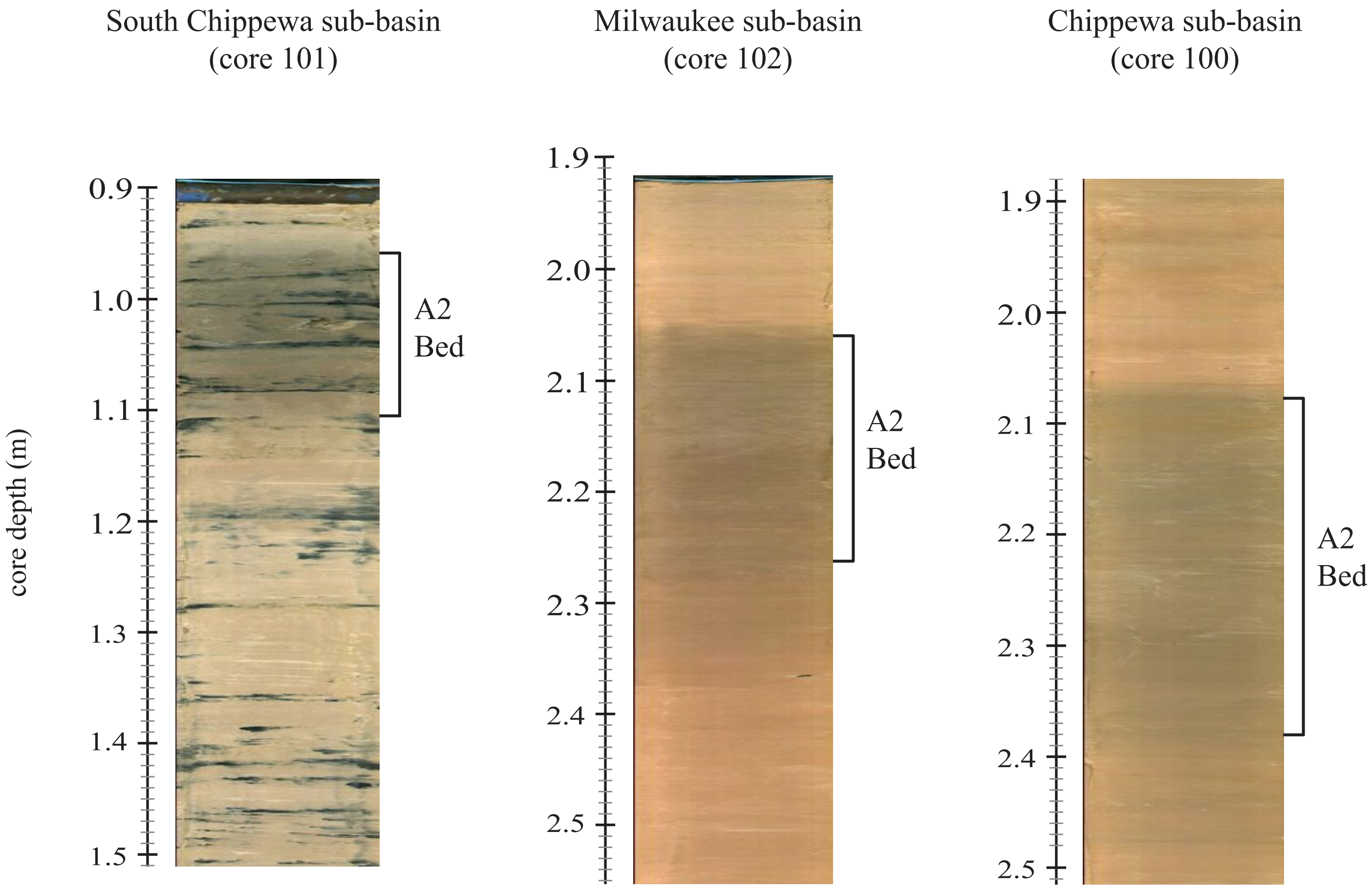

Figure 3.6. Images of the A2 Bed deposited between 8.4 - 8.2 ka [9,450 - 9,100 cal] BP by a two-pulsed flood originating from Lake Agassiz. Core images are stretched horizontally ~2 times to show detail.

The entire ~16 m length of core 100 consists of sediments from the Lake Michigan Formation (Fig. 3.2). The reddish-brown Lower unit (5YR 5/3, 5YR 5/4) is present from the bottom of the core (16.02 m) to 3.6 m. Sandy beds, generally brown (7.5YR 4/3 7.5YR 5/3) to light brown (7.5YR 6/3) and a few cm thick, are common throughout the Lower unit; thicker sandy beds are also present within the bottom ~30 cm of the core as well as a between ~8.8 – 6.5 m (Fig. 3.7). The sandy beds may indicate closer proximity to the glacial terminus at the time of deposition. It is also possible that these units are gravity flows from shallower regions of the lake.

A somewhat disturbed silty brown bed (7.5YR 5/3), which occurs from 5.50 – 5.19 m, may be associated with the Wilmette flooding event (Fig. 3.5). However, this bed does not contain the distinctive grey clay that normally characterizes the Wilmette Bed. Nevertheless, its location at a depth similar to the Wilmette Bed in the Milwaukee sub-basin core (which exhibits overall good correlation with the Chippewa sub-basin core; Fig. 3.2), and its presence towards the top of biostratigraphic interval 1 (discussed below), lend support to this bed's association with the Wilmette flooding event. The bed's browner and coarser-grained nature may reflect a more proximal location to the Agassiz and Superior Basins, and more generally, the sources of flood waters.

The brown (7.5YR 5/3, 10YR 5/3) to greyish-brown (10YR 5/2, 2.5Y 5/2) Upper unit is present from 3.6 m to the top of the core. Black banding appeared within the upper portions (beginning at ~0.8 m) of the Upper unit, but it was much fainter and sparser than in the other two cores. A dark greyish-brown bed (10YR 4/2, 10YR 5/2) present from 2.38 – 2.08 m is identified as the A2 Bed (Fig. 3.6). This bed has a gradual lower boundary and a sharp upper boundary with the Upper unit, as also observed in the other cores.

3.3.3. Biostratigraphy

Figures 3.8-3.10 summarize the distribution of ostracodes and clams in the three cores (data are listed in Appendix D). All three cores are dominated by *C. subtriangulata*

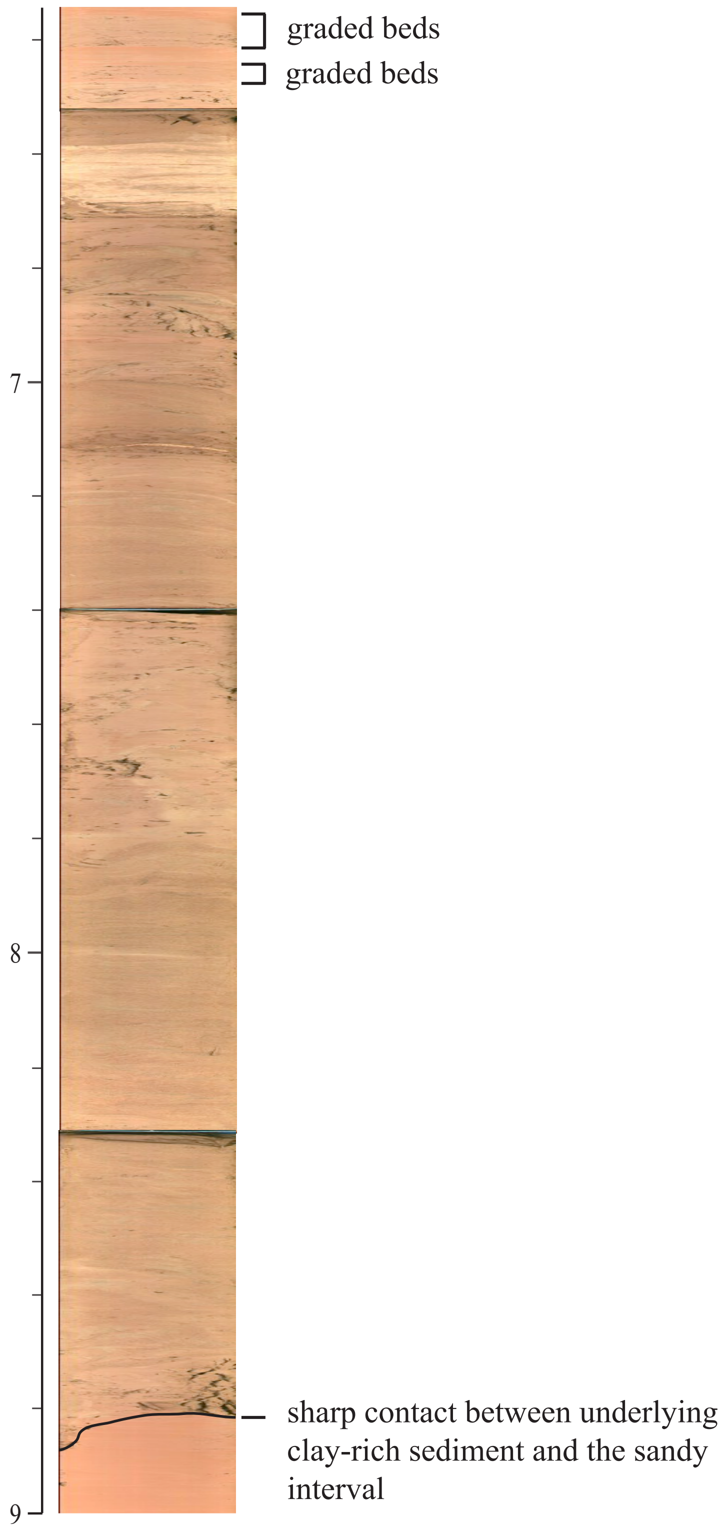

Figure 3.7. Thick sandy interval in the Chippewa sub-basin core from ~8.8 - 6.5 m. Much of this sandy interval is massive with little to no discernable structures. Core images are stretched ~3 times horizontally to show detail.

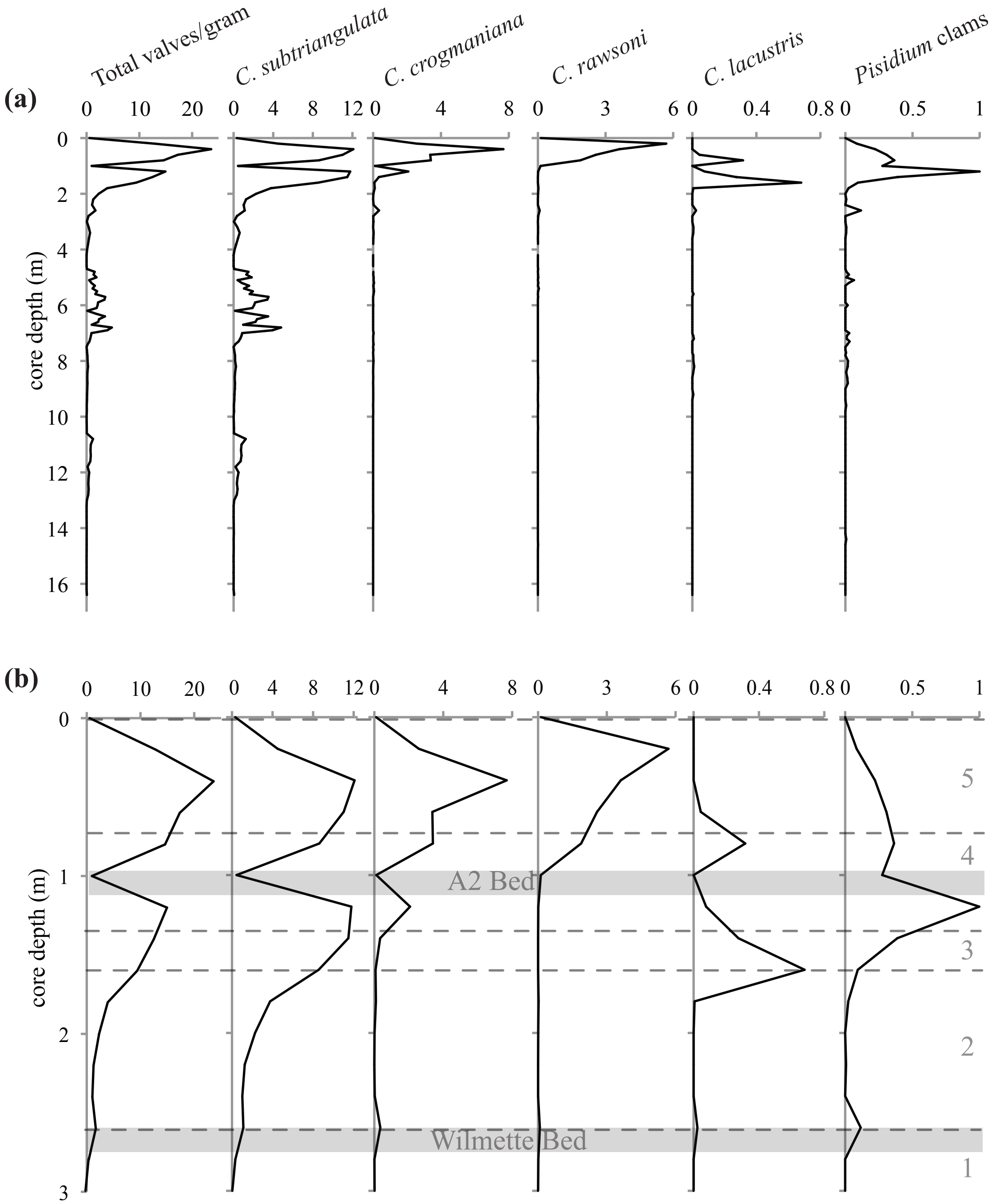

Figure 3.8. Ostracode and *Pisidium* clam valve concentrations (in valves per gram of sediment) for the entire South Chippewa sub-basin core (a) and the uppermost 3 m (b). Biostratigraphic intervals, as defined by Colman et al. (1990) and Forester et al. (1994), are indicated by grey numbers and dashed lines. Two key sedimentary features, the Wilmette and A2 Beds, are indicated by the grey shaded regions.

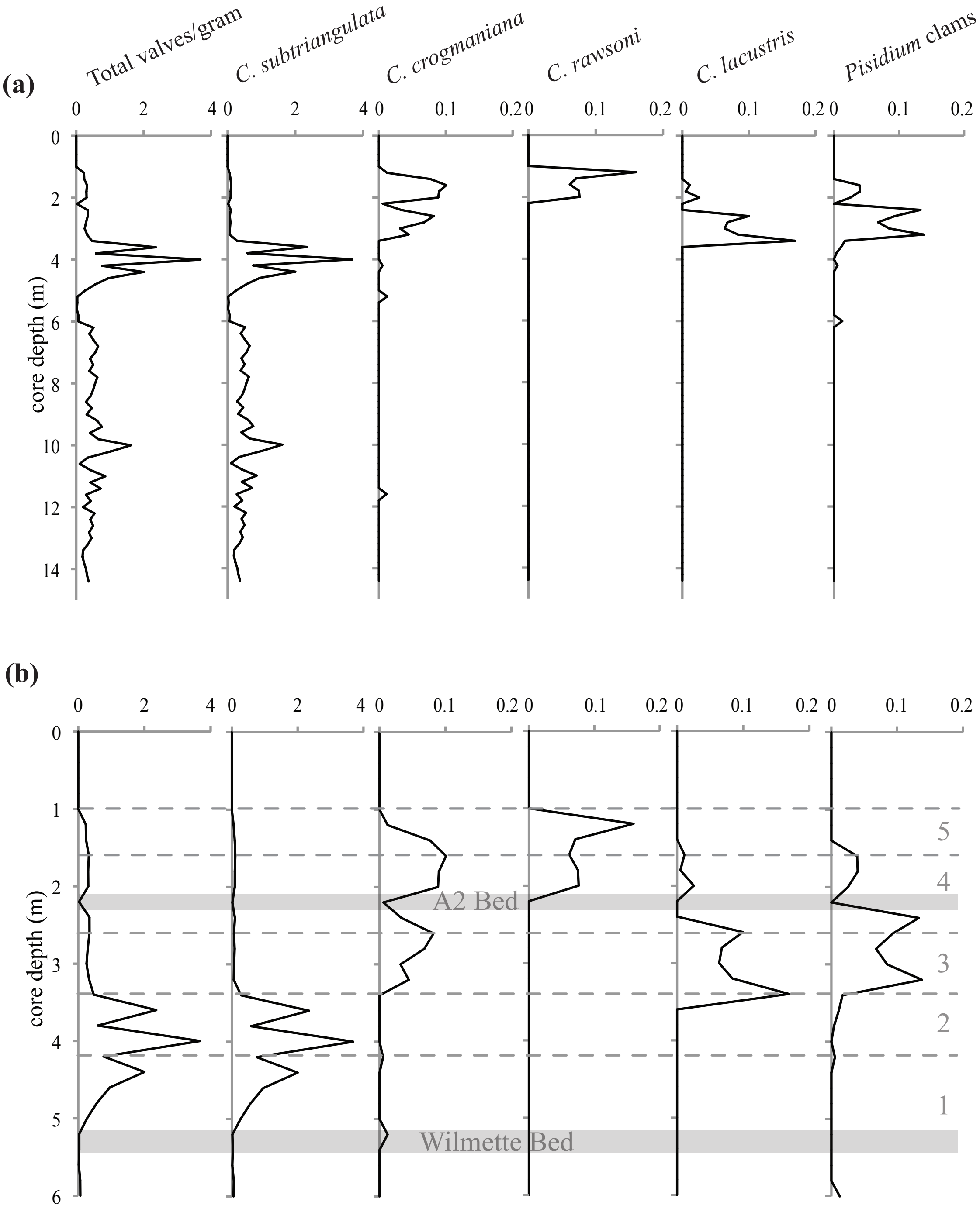

Figure 3.9. Ostracode and *Pisidium* clam valve concentrations (in valves per gram of sediment) for the entire Milwaukee sub-basin core (a) and the uppermost 6 m (b). Biostratigraphic intervals, as defined by Colman et al. (1990) and Forester et al. (1994), are indicated by grey numbers and dashed lines. Two key sedimentary features, the Wilmette and A2 Beds, are indicated by the grey shaded regions.

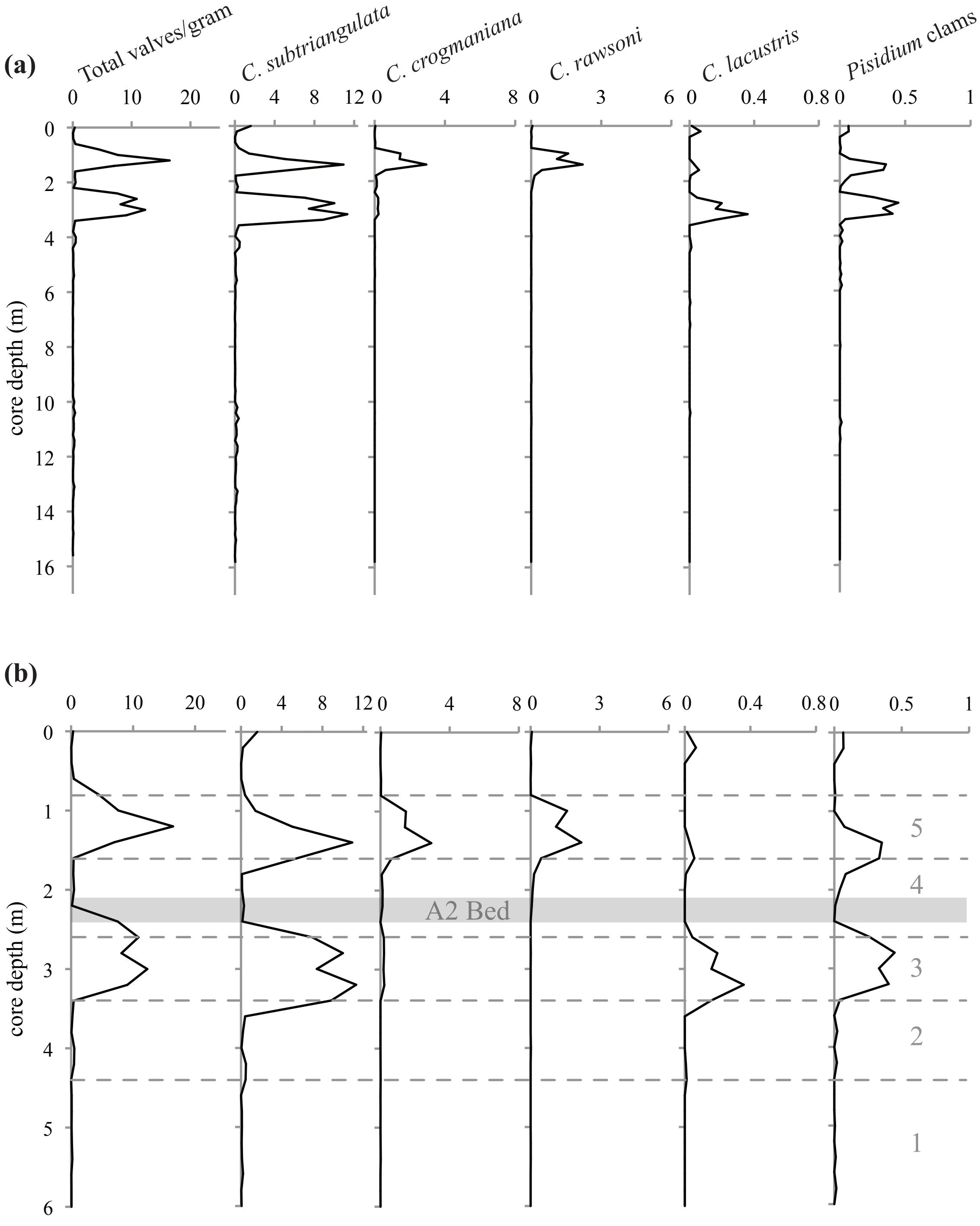

Figure 3.10. Ostracode and *Pisidium* clam valve concentrations (in valves per gram of sediment) for the entire Chippewa sub-basin core (a) and the uppermost 6 m (b). Biostratigraphic intervals, as defined by Colman et al. (1990) and Forester et al. (1994), are indicated by grey numbers and dashed lines. The A2 Bed is indicated by the grey shaded region.

(a deep-water ostracode species). Shallower-water species become more common towards the top of each core. There is much variation in the number of valves per gram of sediment (v/g) among the three sub-basins. The South Chippewa sub-basin core contains the most biogenic carbonate, with a maximum of 23.6 v/g at 0.4 m (Fig. 3.8). The Milwaukee sub-basin core contains the least biogenic carbonate, with a maximum of 3.7 v/g at a depth of 4.0 m (Fig. 3.9). The Chippewa sub-basin core contains an intermediate amount of biogenic carbonate, with a maximum of 16.5 v/g at 1.4 m (Fig. 3.10).

3.3.4 Oxygen- and carbon-isotope compositions

The oxygen-isotope compositions of paleolakewater ($\delta^{18}O_{lakewater}$) and the carbon-isotope compositions ($\delta^{13}C$) of the biogenic carbonates are illustrated in Figures 3.11 and 3.12, respectively, for each of the cores (the data are listed in Appendix E). Paleolakewater compositions were calculated using the oxygen-isotope compositions of the ostracode and clam species and the valve/shell-water oxygen-isotope fractionation factors measured for each species in modern Lake Huron, as reported in Chapter 2 (*C. subtriangulata* – 1.0359; *C. crogmaniana* – 1.0338; *C. rawsoni* – 1.0341; *C. lacustris* – 1.0323; *Pisidium* clams – 1.0315). The usefulness of employing a fractionation factor specific to individual species is that for most ostracode species, the average growth temperature is unknown and thus must be estimated. In many cases, ostracodes (and other shelly organisms) will molt only when water temperatures fall within their optimum range (Boomer 2002; Schöne et al. 2006), so it is crucial to accurately estimate water temperature. By calibrating the oxygen-isotope fractionation between modern Lake Huron water and modern ostracode species collected from Lake Huron, we determined that the average (preferred) growth temperatures of these four ostracode species range from 5 °C (*C. subtriangulata*) to 15 °C (*C. lacustris*).

The $\delta^{18}O_{lakewater}$ values obtained for *C. subtriangulata* are consistently lower than obtained for the other shallower-water species, with the differences in isotopic composition being particularly pronounced below ~2-3 m depth in each core (Fig. 3.11).

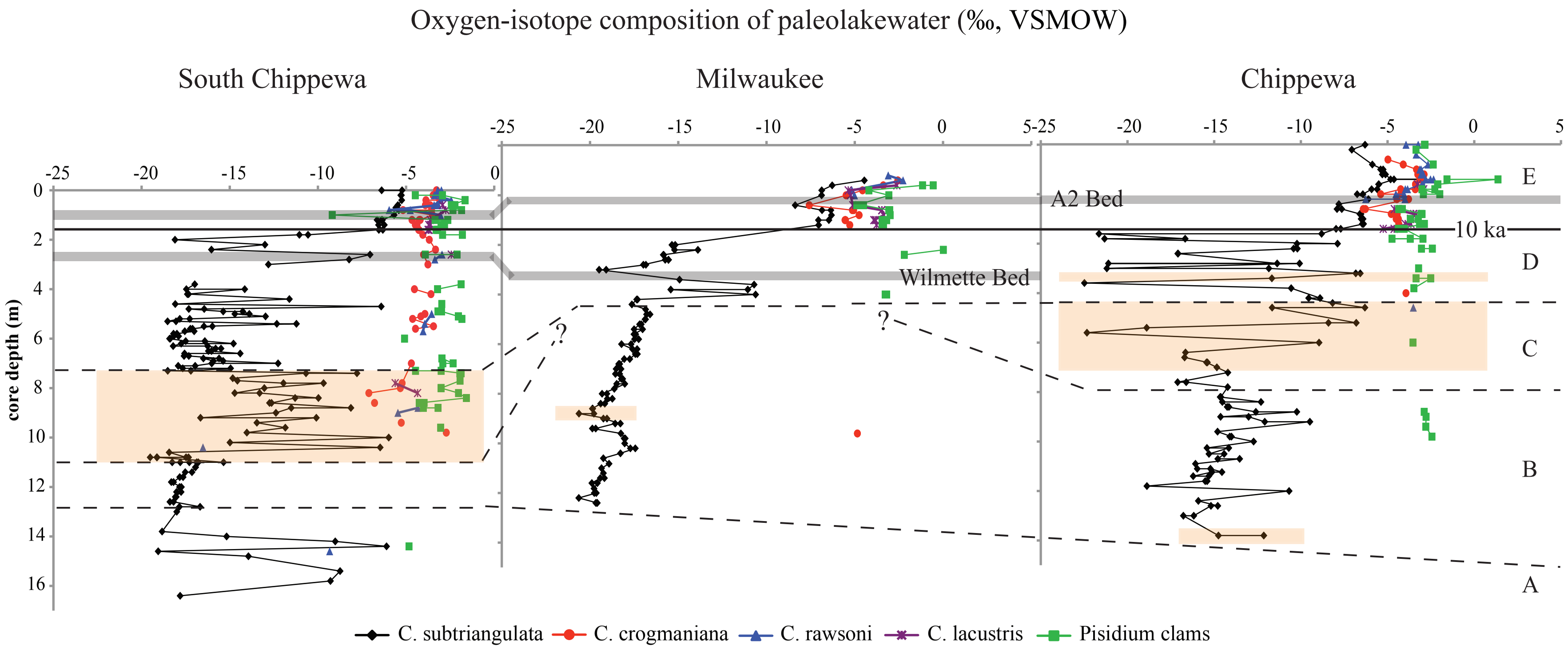

Figure 3.11. Oxygen-isotope composition of paleolakewater as calculated using biogenic carbonates from the South Chippewa, Milwaukee and Chippewa sub-basin cores, respectively. The graphs are hung at a datum of 10 ka [11,500 cal] BP, the Pleistocene-Holocene boundary (solid black line). The lower grey shaded line indicates the position of the Wilmette Bed (A1 event) and the upper grey shaded line indicates the position of the A2 event. The orange shaded regions indicate sandy intervals. The boundaries of the informal Isotope Zones A-E described in the text are shown by the black dashed lines.

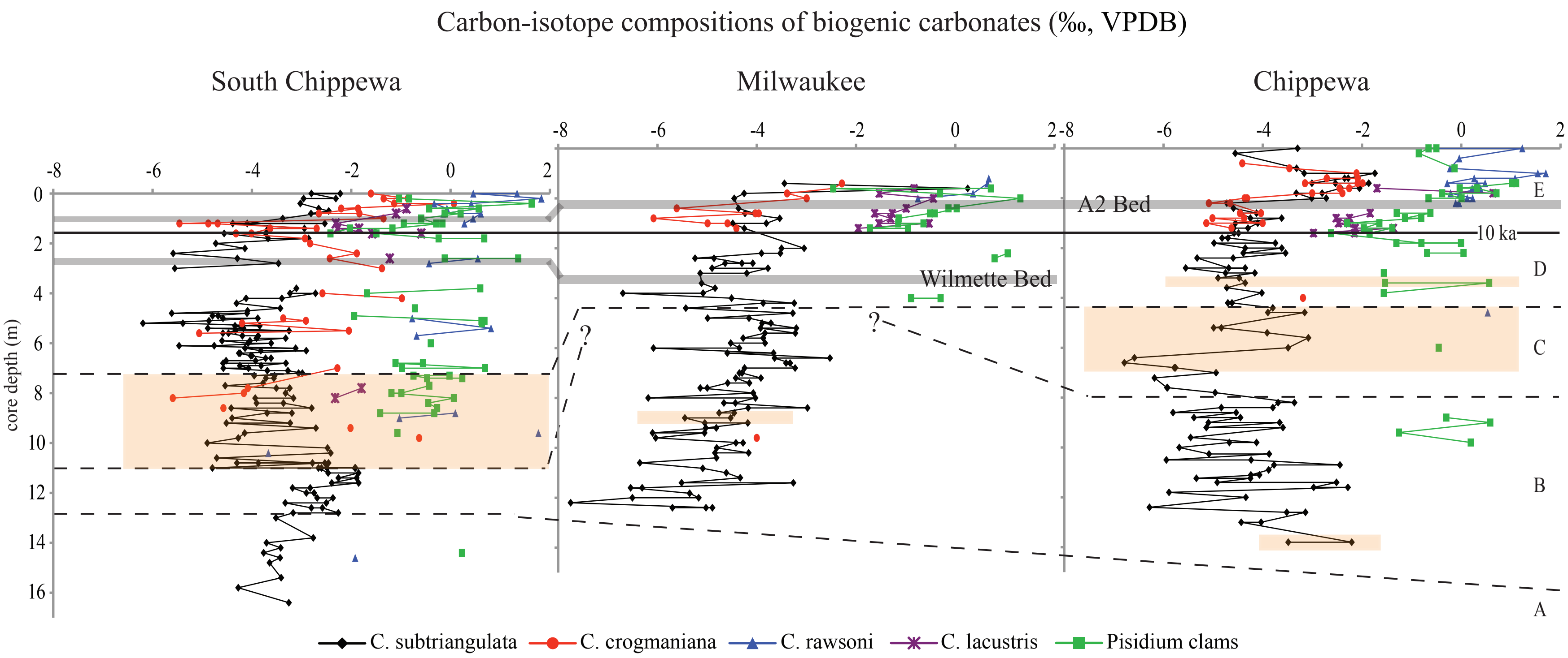

Figure 3.12. Carbon-isotope compositions of ostracode and clam fossils from the South Chippewa, Milwaukee and Chippewa sub-basins, respectively. The graphs are hung at a datum of 10 ka [11,500 cal] BP, the Pleistocene-Holocene boundary (solid black line). The lower grey shaded line indicates the position of the Wilmette Bed (A1 event) and the upper grey shaded line indicates the position of the A2 event. The orange shaded regions indicate sandy intervals. The boundaries of the informal Isotope Zones A-E described in the text are shown by the black dashed lines.

In the South Chippewa and Chippewa sub-basin cores, the $\delta^{18}O_{lakewater}$ values calculated for *C. subtriangulata* show great variability over short depth intervals, whereas in the Milwaukee sub-basin core, such fluctuations are much more limited (Fig. 3.11).

In the South Chippewa sub-basin core, $\delta^{18}O$ values of *C. subtriangulata* valves range from -19.5 to -5.2 ‰, and there is a clear difference in valve compositions above and below a depth of 1.6 m. Below this depth, values range from -19.5 to -6.0 ‰. Above this depth, $\delta^{18}O$ values range from -6.6 to -5.2 ‰ and match closely with those of shallower-water species in this core: *C. crogmaniana*, -7.1 to -2.7 ‰; *C. rawsoni*, -16.5 to -2.4 ‰; *C. lacustris*, -5.6 to -2.4 ‰, and *Pisidum* clams, -9.2 to -1.6 ‰. The lowermost two samples of *C. rawsoni* (14.6 and 10.4 m) have unusually low $\delta^{18}O$ values (-9.3 and -16.5 ‰, respectively). At shallower depths (9.6 – 0 m), values are much higher (-6.0 to -2.4 ‰), similar to samples from the Milwaukee and Chippewa sub-basin cores.

In the Milwaukee sub-basin core, $\delta^{18}O$ values of *C. subtriangulata* valves range from -20.6 to -10.6 ‰ below 3.4 m, and from -8.4 to -4.5 ‰ above 3.4 m. The higher $\delta^{18}O$ values of *C. subtriangulata* valves are much closer to those of the shallower-water species: *Candona crogmaniana*, -7.6 to -2.6 ‰; *C. rawsoni*, -5.2 to -2.3 ‰; *C. lacustris* -5.4 to -2.6 ‰, and *Pisidum* clam shells, -4.9 to 0 ‰.

In the Chippewa sub-basin core, $\delta^{18}O$ values of *C. subtriangulata* valves also exhibit such differences: below 3.4 m, -22.5 to -6.3 ‰, and above 3.4 m, -8.0 to -3.1 ‰. The $\delta^{18}O$ values of the latter group are more similar to the shallower-water species: *Candona crogmaniana*, -5.2 to -2.9 ‰; *C. rawsoni,* -6.3 to -2.3 ‰; *C. lacustris*, -6.4 to -2.9 ‰, and *Pisidum* clam shells, -4.7 to +1.4 ‰.

The valves and shells of ostracode and clam species exhibit narrow ranges in $\delta^{13}C$ values, with *C. crogmaniana* and *C. subtriangulata* being most depleted of ^{13}C (Fig. 3.12). In the South Chippewa sub-basin core, *C. subtriangulata* valves have $\delta^{13}C$ values between -6.2 and -1.9 ‰. Below 1.6 m, the full range of $\delta^{13}C$ values is observed. Above 1.6 m, the $\delta^{13}C$ values vary between -4.6 and -2.2 ‰. The other species exhibit the following ranges in $\delta^{13}C$ values: *Candona crogmaniana*, -5.6 to +0.1 ‰; *C. rawsoni,* -3.7 to +1.8 ‰; *C. lacustris*, -2.3 to -0.6 ‰, and *Pisidium*, -2.4 to +1.6 ‰. In the Milwaukee sub-basin core, *C. subtriangulata* valves below 3.4 m have $\delta^{13}C$ values ranging from -7.7 to -2.5 ‰, and above 3.4 m, -4.5 to +0.2 ‰. The $\delta^{13}C$ values of the other species are: *Candona crogmaniana*, -6.1 to -2.3 ‰; *C. rawsoni*, -0.8 to +0.7 ‰; *C. lacustris*, -2.0 to -0.4 ‰, and *Pisidium*, -2.5 to +1.3 ‰. In the Chippewa sub-basin core, *C. subtriangulata* valves below a depth of 3.4 m have $\delta^{13}C$ values ranging from -6.8 to -2.2 ‰. Above 3.4 m, *C. subtriangulata* valves range in value from -4.7 to -1.7 ‰. The $\delta^{13}C$ values of the other species are: *Candona crogmaniana*, -3.0 to +0.6 ‰; *C. rawsoni*, -0.7 to +1.7 ‰; *C. lacustris,* -5.1 to -2.0 ‰, and *Pisidium*, -2.6 to +1.1 ‰.

The linear coefficient (r-value) between $\delta^{13}C$ and $\delta^{18}O$ values of all *C. subtriangulata* samples from late Pleistocene sediments is 0.070 (Fig. 3.13a). This r-value suggests that lakewater oxygen- and carbon-isotope (DIC) compositions were influenced by independent factors at this time. For samples from early to mid Holocene sediments, the r-value for all *C. subtriangulata* samples is 0.609 (Fig. 3.13b), suggesting that lakewater oxygen- and carbon-isotope (DIC) compositions were influenced by similar factors.

3.4 DISCUSSION

3.4.1 Age of the sediments

Radiocarbon dates

Radiocarbon dates obtained for organic material from Great Lakes sediments are often problematic. First, dates for organic matter can be too old by up to thousands of years because of inclusion of terrestrial detritus that is significantly older than the enclosing sediments (Nambudiri et al. 1980; Brown et al. 1989; Colman et al. 1990). To evaluate this possibility for the wood fragment obtained from core 102 at 1.9 m, we compared its date with that obtained for clam shells at 3.2 m. The difference of ~1700

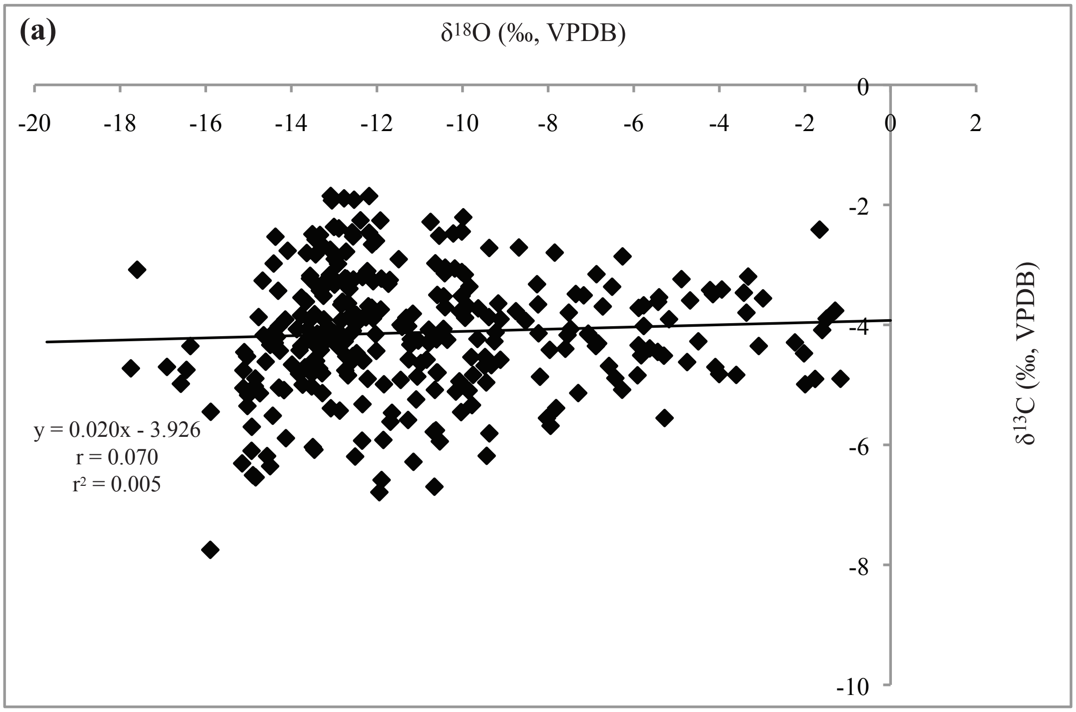

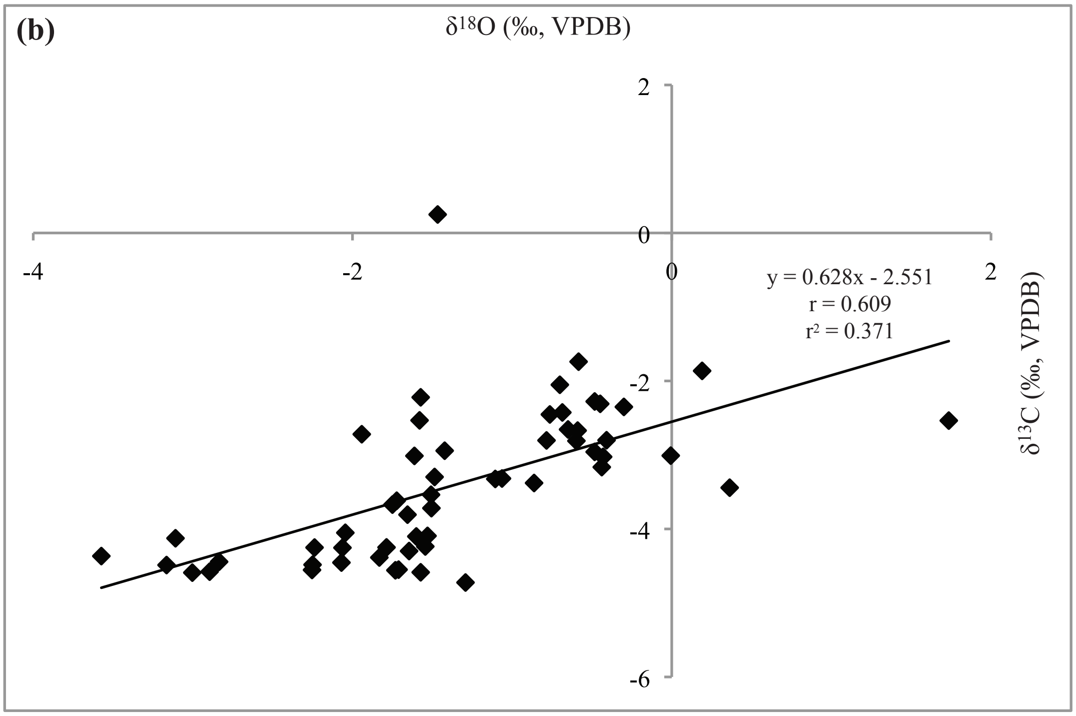

Figure 3.13. Statistical correlation between the carbon- and oxygen-isotope compositions of *C. subtriangulata* valves from the three Michigan Basin cores during the late Pleistocene (a) and the early to mid Holocene (b).

years between the two dates represents an average sedimentation rate of 0.8 mm/yr. This value lies midway within the range of sedimentation rates (0.3 mm/yr to 1.5 mm/yr) reported for this time period in Lake Michigan by Rea et al. (1980) and Colman et al. (1990), thus increasing our confidence in this date. Second, dates for biogenic carbonates can be erroneously old. Radioactively inert carbon from old carbonate rocks within the lake's catchment basin can be added to a lake's dissolved bicarbonate reservoir, which is used by organisms to form their shells (Rea and Colman 1995; Moore et al. 1998). This hard-water effect (HWE) can cause dates to be hundreds of years older than the true age of the material. Bivalves collected from Lake Michigan in the early- to mid-1900s were used to calculate a HWE value of ~250 years for this basin (Rea and Colman 1995; Moore et al. 1998). This amount was subtracted from radiocarbon dates obtained for bivalves and ostracodes from Lake Michigan (Table 3.1).

Biostratigraphy

Colman et al. (1990) and Forester et al. (1994) used the ostracode assemblages of four cores collected from in and around the South Chippewa sub-basin to define five biostratigraphic intervals, which provide a detailed record of lake conditions from ~11 to 6 ka [12,900 to 6,850 cal] BP. In their scheme, Interval 1 was deposited until 10.5 ka [12,600 cal] BP and consisted largely of *C. subtriangulata* valves, a species typical of deep- and cold-water environments (Delorme 1978, 2001; Dettman et al. 1995). Other shallower-water species were limited to only a few shells throughout the sedimentary sequence. All three cores examined in the present study are dominated by *C. subtriangulata*, and it is virtually the only species present in the lowermost 70-80 % of each core (Figs. 3.8-3.10). Its overwhelming dominance suggests that ancient Lake Michigan was cold and had a very low concentration of total dissolved solids (TDS) at this time (Delorme 2001), consistent with glacial meltwater. Interval 1 is present at the following depths: South Chippewa sub-basin, core bottom at 16.6 m to 2.6 m; Milwaukee sub-basin, core bottom at ~14.7 m to 4.2 m, and Chippewa sub-basin, core bottom at ~16.0 m to ~ 4.4 m.

Interval 2 (10.5 – 10.0 ka [12,600 – 11,500 Cal] BP) of Colman et al. (1990) and Forester et al. (1994) is characterized by the appearance of *L. friabilis* (present, but not counted in this study) and other shallower-water species (e.g., *Pisidium* clams, *C. rawsoni*) (Figs. 3.5-3.7). The appearance of shallower-water species can be explained by the decrease in lake level (to ~80 m below present level) during the Chippewa lowstand (10.3 ka [12,100 cal] BP (Forester et al. 1994; Colman et al. 1994c; Lewis et al. 2007). Colman et al. (1990) estimated that shallower-water temperatures ranged from 10 to 14 °C and varied seasonally during this time. Interval 2 occurs at depths of 2.6 – 1.6 m in the South Chippewa sub-basin core, 4.2 – 3.4 m in the Milwaukee sub-basin core, and ~4.4 – 3.4 m in the Chippewa sub-basin core.

Interval 3 (10.0 – 9.3 ka [11,500 – 10,500 cal] BP) of Colman et al. (1990) and Forester et al. (1994) is distinguished by the appearance of *C. lacustris* and the disappearance of *L. friabilis*. Interval 3 occurs at depths of 1.6 – 1.3 m in the South Chippewa sub-basin core, 3.4 – 2.6 m in the Milwaukee sub-basin core, and 3.4 – 2.6 in the Chippewa sub-basin core (Figs. 3.8-3.10). The biostratigraphic records observed for this interval are somewhat different among the three cores examined here. In the South Chippewa and Chippewa sub-basins, the populations of *C. subtriangulata*, *C. lacustris* and *Pisidium* clams increase at the onset of this interval. The increase in both shallower-water species and *C. subtriangulata* suggests that epilimnion waters experienced an increase in both TDS and temperature, whereas the hypolimnion waters remained dilute and cold. However, in the Milwaukee sub-basin, the populations of *C. crogmaniana*, *C. lacustris* and *Pisidium* clams increase whereas the population of *C. subtriangulata* decreases sharply (Fig. 3.9). This behaviour suggests that TDS and temperature also increased in the hypolimnion and that there was more thorough mixing between epilimnion and hypolimnion waters in this sub-basin.

Interval 4 (9.3 – 7.9 ka [10,500 – 8,650 cal] BP) of Colman et al. (1990) and Forester et al. (1994) is characterized by a decrease in *C. lacustris* and an increase in other shallower-water ostracode species, including *C. crogmaniana*, *C. rawsoni* and *L. friabilis*. Interval 4 is present from 1.3 – 0.7 m in the South Chippewa sub-basin core, from 2.6 – 1.6 m in the Milwaukee sub-basin core, and from 2.6 – 1.6 m in the Chippewa sub-basin core. A brief but substantial decline in the populations of all ostracode and clam species has been previously reported within this interval and attributed to the influx of Lake Agassiz waters during the A2 flood at 8.4 – 8.2 ka [9,400 – 9,100 cal] BP (Colman et al. 1990, 1994a, 1994c; Miller et al. 2000; Breckenridge and Johnson 2009). This event is observed within all three cores examined here (Figs. 3.8-3.10). Such a population crash is consistent with an influx of cold and dilute waters, which shallower and warmer water species in particular would not have been able to tolerate.

Interval 5 (7.9 – 6.0 ka [8,650 – 6,850 cal] BP) of Colman et al. (1990) and Forester et al. (1994) is defined by an increase in *C. crogmaniana* and *C. rawsoni*, and a gradual decrease in *C. subtriangulata*. Similar features were observed in the three cores examined in this study (Interval 5 is present from 0.7 m to the top of the South Chippewa sub-basin core, from 1.6 – 1.0 m in the Milwaukee sub-basin core, and from 1.6 – 0.8 m in the Chippewa sub-basin core; Figs. 3.8-3.10). Interval 5 is similar to Interval 3 in that the deep- and cold-water species *C. subtriangulata* and the shallower-water species are present in high numbers in the South Chippewa and Chippewa sub-basins, whereas only the shallower-water species are plentiful in the Milwaukee sub-basin. The increase in shallower-water species in all cores is consistent with the drop in lake level that caused Lake Michigan to become a closed basin lake from ~7.9 – 7.0 ka [8,700 – 7,800 cal] BP (Lewis et al. 2005, 2007; Forester et al. 1994).

Forester et al. (1994) suggested that TDS rose substantially during the time period represented by this interval, which coincides with the Holocene Hypsithermal warm and dry period (~8.0 – 4.0 ka [9,000 – 4,400 cal] BP). Lake conditions during this time were probably warm in shallower, near-shore regions of the lake and may have remained cold in deeper regions. Sedimentation rates decreased during this time (Colman et al. 1994c), which commonly leads to dissolution and hence poor preservation of biogenic carbonates. Instead, observations in this study show that populations of ostracodes increased, in some cases to their highest concentrations of valves per gram of sediment within the cores examined here (Figs. 3.8-3.10). Such preservation likely occurred because the lakewater was saturated in calcium carbonate during this time of increased TDS (Colman et al. 1994c; Forester et al. 1994).

By the end of Interval 5, biogenic carbonates are poorly represented in the sediment. This change likely reflects low sedimentation rates and a lowering of lakewater TDS as the lake level rose and shell dissolution increased (Colman et al. 1990; Colman et al. 1994c, Forester et al. 1994). For example, sedimentation rates within the South Chippewa sub-basin decreased five-fold from ~0.3 mm/year at 10 – 5 ka [11,500 – 5,700 cal] BP to ~0.06 mm/year at ~5 ka [5,700 cal] BP, coincident with the peak of the Nipissing transgression (Lewis and Anderson 1989; Colman et al. 1990). Only a few valves occur above 1.0 m and 0.8 m (the upper boundary of Interval 5) in the Milwaukee and Chippewa sub-basin cores, respectively. The upper boundary of Interval 5 occurs at the top of the South Chippewa sub-basin core.

Age model

Figure 3.14 illustrates age models for each of the three Michigan Basin cores using the radiocarbon dates, ages inferred from the biostratigraphy of each core, and previously determined dates for key sedimentary features, such as the Wilmette Bed, the Chippewa unconformity and the A2 event. Using this model, average sedimentation rates for the early Holocene (10 – 6 ka [11,500 – 6,850 cal] BP) are: South Chippewa sub-basin (core 101): 0.4 mm/yr; Milwaukee sub-basin (core 102), 0.6 mm/yr; and Chippewa sub-basin (core 100), 0.65 mm/yr.

3.4.2 The oxygen-isotope history of Ancient Lake Michigan

The late Pleistocene

The oxygen isotopic results for the cores from the South Chippewa, Milwaukee and Chippewa sub-basins can be subdivided into five main zones, A – E (Fig. 3.11). Isotope Zone A is present only within the bottom few metres of the South Chippewa sub-

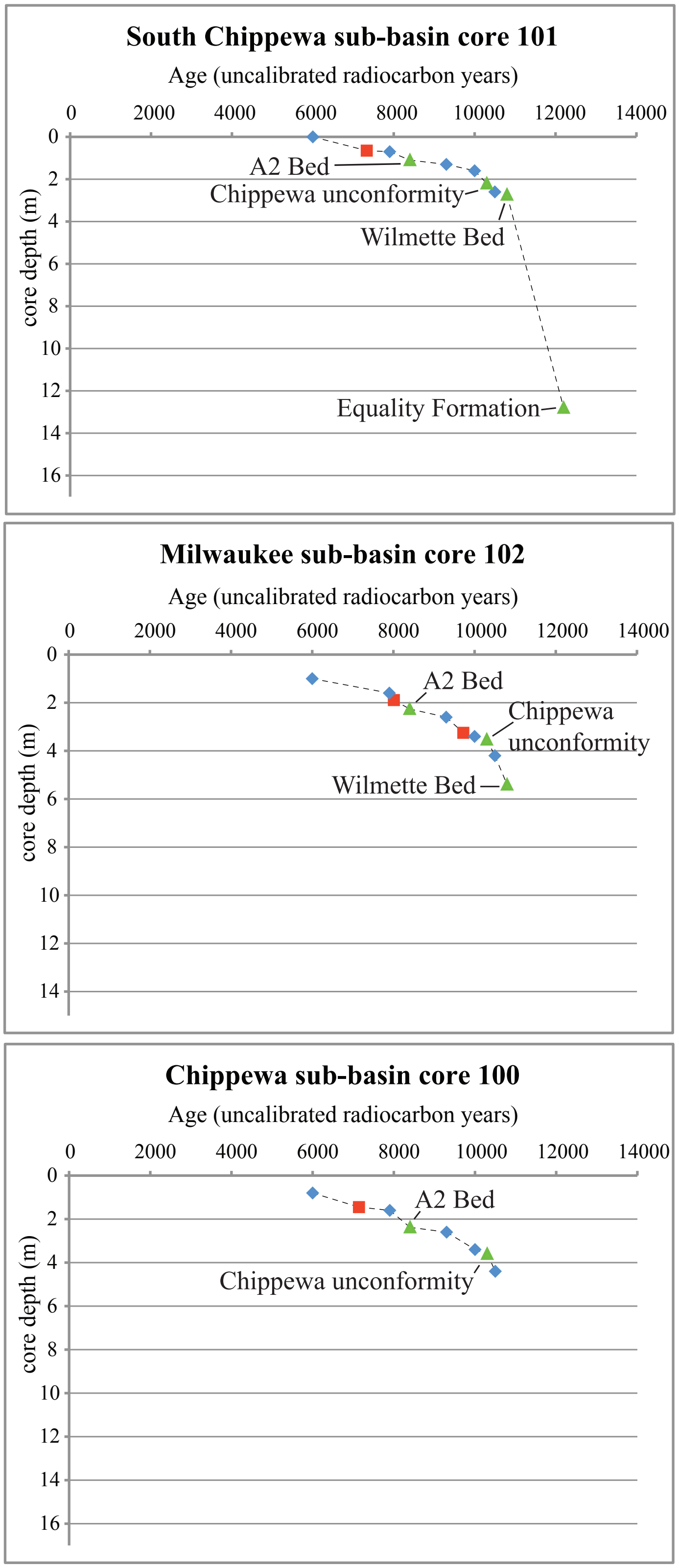

Figure 3.14. Age models for the Lake Michigan cores. Radiocarbon dates are denoted by red squares, inferred biostratigraphic dates by blue diamonds, and dates of key sedimentary features by green triangles.

basin core, and comprises the sediments of the Equality Formation. Colman et al. (1994b, 1994c) suggest that these sediments were deposited near the glacial terminus during periods of glacial readvancement into the Michigan Basin. It is likely that the Port Huron advance (13 – 12.2 ka [15,300 – 14,050 cal] BP), the last advance to extend as far south as the South Chippewa sub-basin (Hansel et al. 1985; Hansel and Mickelson 1988; Colman et al. 1994b), is responsible for this unit.

A wide and oscillating range of water $\delta^{18}O$ values, from -19.1 to -6.1 ‰, is evident from the compositions of *C. subtriangulata* recovered from these sediments (Fig. 3.11). In addition, one sample each of *C. rawsoni* and *Pisidium* clams yield water $\delta^{18}O$ values of -9.3 and -4.8 ‰, respectively, and correspond to times when *C. subtriangulata* was also enriched in ^{18}O relative to most samples of this species. Several factors may have contributed to these variations. First, water inputs from the Huron and Erie Basins via the Grand River Valley (Fig. 3.1) are known to have been intermittent and occasionally to involve immense floods during this time (Hansel et al. 1985; Kehew 1993). The earliest records available for these basins indicate lakewater with $\delta^{18}O$ values of ~ -18 to -16 ‰ at ~12.2 ka [14,000 cal] BP (Lewis and Anderson, 1992; Lewis et al. 1994; Rea et al. 1994a; Moore et al. 2000). Second, proximity to the Michigan Lobe of the LIS would have continuously released low-^{18}O meltwater directly into the Michigan Basin until its final retreat following the Two Rivers glaciation at ~11.1 ka [13,000 cal] BP (Hansel et al. 1985; Colman et al. 1994b, 1994c). If the ice sheet advanced and retreated over short time periods, as proposed by Clark et al. (1994) and Clark (1994), the relative proportions of low-^{18}O glacial meltwater versus more ^{18}O-rich local/regional precipitation and runoff could have varied substantially over short time periods. Third, oscillations in the oxygen-isotope record of water may have recorded mixing events between bottom- and surface-waters with different isotope compositions (see below).

Isotope Zone B is present within the red glacial-lacustrine clays of the Lower unit in all three sediment cores (Fig. 3.11). Compared to Isotope Zone A, Zone B is characterized by much less variable lakewater $\delta^{18}O$ values that generally range from ~ -20 to -15 ‰, although higher values (up to ~ -10 ‰) are recorded in the Chippewa sub-basin. Representatives of shallower-water ostracodes and clams are rare and, with the exception of a lone sample of *C. rawsoni* at 10.4 m in the South Chippewa sub-basin core, yield water $\delta^{18}O$ values that are significantly higher than obtained for *C. subtriangulata*. These results are suggestive of a consistent supply of glacial meltwater during a period of ice sheet retreat, likely the Two Creeks interstade (12.2 – 11.8 ka [14,050 – 13,700 cal] BP). The gradually increasing $\delta^{18}O$ values toward the top of Isotope Zone B may indicate a dwindling supply of glacial meltwater relative to more local precipitation and runoff.

Isotope Zone C is present in the South Chippewa and Chippewa sub-basin cores within the Lower unit. This interval contains much sandier sediment than other portions of the cores (Fig. 3.7). Lakewater oxygen-isotope compositions calculated from *C. subtriangulata* from the South Chippewa sub-basin range from -19.5 to -6 ‰ and mostly fall between -15 to -10 ‰. Shallower-water species yield higher lakewater compositions; the overall range is -7.1 to -1.6 ‰ but most $\delta^{18}O$ values lie between -5 and -2 ‰. Lakewater oxygen-isotope compositions calculated from *C. subtriangulata* in the Chippewa sub-basin core exhibit large oscillations with an overall range of -22.3 to -6.3 ‰. Shallower-water species are uncommon in this core; one sample each of *C. rawsoni* and *Pisidium* clams yields lakewater values of -3.5 ‰ (Fig. 3.11). The Milwaukee sub-basin core does not contain this thick sandy unit.

We propose that Zone C was deposited during a period of glacial advancement into the Michigan Basin, specifically the Two Rivers advance from 11.8 – 11.1 ka [13,700 – 13,000 cal] BP, which extended as far as the southernmost edge of the Chippewa sub-basin. The ~2 m thick sandy interval may be the result of under-ice meltwater streaming or may have been caused by gravity flows triggered by the nearby ice lobe (e.g. Evanson et al. 1977). We do not consider the thick sandy interval to be associated with the Whitefish Fan, a thick sandy deltaic deposit located ~20 km north of core 100 in the Chippewa sub-basin. This fan was deposited from ~10 – 9.5 ka [11,500 – 10,700 cal] BP as a result of connection to the Superior Basin via the Au Train-Whitefish Channel (Fig. 3.1) after lake levels dropped following the opening of the North Bay outlet at 10.3 ka [12,100 cal] BP (Safarudin and Moore 1999; Kincare and Larson 2009). The sandy interval in Chippewa sub-basin core 100 is located within the Lower unit of the Lake Michigan Formation (Fig. 3.2), ~3 m below the boundary between the Upper and Lower units, which marks the onset of decreasing lake levels just prior to the deposition of the Whitefish Fan.

Within the South Chippewa sub-basin, the ~3.5 m-thick sandy interval consists of intermittent sandy beds, and is under- and overlain by slightly thicker sandy beds (~20 – 30 cm). These sandy beds may be the result of sediment destabilization in shallow regions of the lake and redeposition of coarser material in deeper regions by gravity flows (Lister et al. 1988). Alternatively, these intermittent sandy beds may represent coarser-grained material delivered by ice-rafting. These types of sandy sedimentary deposits may be characteristic of times when glacial lobes were present within the Michigan Basin. We are unsure why this zone does not appear in the Milwaukee sub-basin core.

The wide range in lakewater oxygen-isotope compositions that characterize Zone C may indicate widely fluctuating amounts of glacial meltwater released into the basin, consistent with multiple rapid advances and retreats of the Michigan Lobe, as proposed by Clark et al. (1994) and Clark (1994). Alternatively, it may reflect reworking of previously deposited biogenic carbonates from shallower regions of the lake. That said, all efforts were made to avoid specimens that displayed physical evidence for post-depositional transport.

Isotope Zone D is present within all three cores; it includes the uppermost portion of the Lower unit as well as a small portion of the Upper unit below the Pleistocene-Holocene boundary. Lakewater $\delta^{18}O$ values, as calculated using *C. subtriangulata*, generally range from ~ -18 to -10 ‰ in the lower portion of Zone D, decreasing slightly to as low as -22 ‰ in its upper portion. We propose that the lower portion of Isotope Zone D correlates to the Kirkfield phase of Lake Algonquin (11.1 – 11.0 ka [13,000 – 12,900 cal] BP), which evolved into Main Lake Algonquin (11.0 – 10.3 ka [12,900 – 12,100 cal] BP) and then was followed by a period of low lake levels, known as the Early

Chippewa lowstand, at 10.3 ka [12,100 cal] BP (Larsen 1987; Colman et al. 1994c; Lewis et al. 2005, 2007). The shift to lower $\delta^{18}O$ values during Main Lake Algonquin is suggestive of increasing glacial meltwater contribution, yet direct inputs of meltwater into the Michigan Basin are generally considered to have ended by 11.1 ka [13,000 cal] BP following the end of the Two Rivers advance (Hansel et al. 1985; Colman et al. 1994b). This decrease may instead reflect increased connectivity to the Superior and Agassiz Basins, which both contained water with very low oxygen-isotope compositions at this time (Last et al. 1994; Remenda et al. 1994; Birks et al. 2007; Breckenridge and Johnson 2009; Hyodo and Longstaffe 2011b).

The Wilmette Bed has been identified towards the top of the Lower unit at 2.73 – 2.59 m in the South Chippewa sub-basin and 5.14 – 5.40 m in the Milwaukee sub-basin. Unlike previous sediment cores retrieved from the Michigan Basin (e.g., Forester et al. 1994; Colman et al. 1994c), these samples of the Wilmette Bed contained sufficient ostracode valves for analysis, although the populations were very low (Figs. 3.8-3.10). Wilmette Bed lakewater calculated from *C. subtriangulata* had $\delta^{18}O$ values of -7.0 ‰ in the South Chippewa sub-basin and -14.9 ‰ in the Milwaukee sub-basin. Ostracodes from units immediately overlying the Wilmette Bed lived in water with much lower $\delta^{18}O$ values, between -19 and -18 ‰ (Fig. 3.11). The range in water composition inferred using ostracodes from the Wilmette Bed likely reflects mixing of water masses from just before and during the flooding event; data for immediately overlying fauna are probably more characteristic of the floodwaters themselves.

Shallower-water species are present throughout Isotope Zone D although in very low populations (Figs. 3.8-3.10). The oxygen-isotope compositions of lakewater calculated using these samples range from -5.2 to 0.0 ‰ and cluster at ~ -3 ‰. The $\delta^{18}O$ values of the shallower-water species are significantly higher than those obtained for *C. subtriangulata*, which records the composition of the deepest regions of lakes.

The wide oscillations in oxygen isotopic composition of *C. subtriangulata* in Isotope Zone D, together with the sparse but persistent presence of shallower-water ostracode and clam species with much higher $\delta^{18}O$ values (Fig. 3.11), may indicate the presence of, and intermittent mixing between, stratified waters with different isotopic compositions during this period of ancient Lake Michigan's history. Birks et al. (2007) proposed a stratified water model for Lake Agassiz to explain ^{18}O-enrichment of surface water proxies relative to bottom water proxies. According to this model, colder and denser low-^{18}O meltwater from the LIS accumulated at the bottom of Lake Agassiz while more ^{18}O-rich and warmer precipitation and surface runoff pooled at and near its surface. Birks et al. (2007) showed that during its Moorhead phase (~11 – 10 ka [12,900 – 11,500 cal] BP), Lake Agassiz surface waters were enriched in ^{18}O by ~7 ‰ relative to bottom waters. By its Nipigon phase (9.5 – 8.2 ka [10,700 – 9,100 cal] BP), precipitation contributions and climate-induced evaporation had enriched Lake Agassiz's surface waters in ^{18}O by as much as 18 ‰ over its bottom waters (Lewis et al. 1994; Buhay and Betcher 1998; Birks et al. 2007).

Birks et al. (2007) suggested that the difference in oxygen-isotope compositions between precipitation-rich surface waters and underlying glacial meltwater occurred seasonally, and was enhanced by summer-season evaporative ^{18}O-enrichment. We predict, however, that the putative role of seasonal evaporative-enrichment was relatively small in Lake Michigan, given that the modern Great Lakes show only small differences of this nature (<2 ‰; Patterson et al. 1993; Macdonald and Longstaffe 2007). Normal seasonal mixing in the modern Great Lakes system occurs when lakewater passes through 4 °C (temperature of maximum density). Seasonal mixing between the upper and lower portions of the water column may have been inhibited if glacial meltwater, ponding in the deeper regions of the Michigan Basin, contained a high amount suspended solids. If so, stratification may have persisted for years at a time. The $\delta^{18}O$ results for the shallower-water species suggest that surface waters, and hence precipitation and runoff inputs, had relatively constant compositions throughout Isotope Zone D. The extreme variability in the $\delta^{18}O_{lakewater}$ values recorded by *C. subtriangulata*, by comparison, suggests a more complex structure for the underlying water, whose composition varied with the fraction of glacial meltwater present, the isotopic composition of that meltwater, and the degree of mixing with surface waters during transport or following arrival in the Michigan Basin.

Early to mid Holocene

Isotope Zone E, which occurs exclusively within the Upper unit of the Lake Michigan Formation, spans the Holocene history of the Michigan Basin (Fig. 3.11). Within Isotope Zone E, all shelly fauna analyzed have $\delta^{18}O_{lakewater}$ values of ~ -8 to -0 ‰, and the difference between the oxygen isotopic compositions of deep- versus shallower-water species is much smaller than in Isotope Zones B, C and D (Fig. 3.11). These results indicate that the water supply to the Michigan Basin changed dramatically at the onset of the Holocene. In particular, eastward drainage of Lake Agassiz through the Great Lakes Basin was blocked by the Marquette advance in the Superior Basin at ~10 ka [11,500 cal] BP, which diverted Lake Agassiz's overflow to the Mackenzie River via its northwestern outlet (Smith and Fisher 1993; Fisher and Smith 1994; Fisher et al. 2002; Fisher 2003; Teller and Leverington 2004; Lowell et al. 2005; Couch and Eyles 2008; Murton et al. 2010).

The relatively ^{18}O-rich composition of lakewater in the Michigan Basin at this time suggests little to no connection with the Superior Basin, which was characterized by lakewater with a low $\delta^{18}O$ value of nearly -25 ‰ during the early Holocene (Breckenridge and Johnson 2009; Hyodo 2010; Hyodo and Longstaffe 2011b). However, an outlet from Lake Duluth in the western Superior Basin via the Au Train-Whitefish Channel (Fig. 3.1) is believed to have opened briefly (for a few hundred years) following Main Lake Algonquin at ~10 ka [11,500 cal] BP (Safarudin and Moore 1999). Although it is possible that the biogenic carbonate record extracted from our cores does not capture this fairly short interval, previously studied cores from the Michigan Basin also do not clearly indicate an early Holocene interval dominated by low-^{18}O water. It may be that water in the Superior Basin at this time was isotopically stratified (as per the model of Birks et al. 2007; Breckenridge and Johnson 2009) but presently there is no evidence to support this conjecture. Further work is needed to firmly establish the timing of connection between the western Superior Basin and the northern Michigan Basin, which led to development of the Whitefish Fan.

Some variation in $\delta^{18}O_{lakewater}$ values does occur during this interval of Holocene time. During the A2 event (8.4 – 8.2 ka [9,450 – 9,100 cal] BP; Colman et al. 1994a; Breckenridge et al. 2009), for example, a decrease of ~ 2 to 3 ‰ is exhibited by most species, and clams from the South Chippewa sub-basin show decrease of ~6 ‰ (Fig. 3.11). This change in isotopic composition is accompanied by significant decline in the populations of ostracodes and clams in the A2 Bed at ~1.0 m in the South Chippewa sub-basin, ~2.1 m in the Milwaukee sub-basin and ~2.2 m in the Chippewa sub-basin (Figs. 3.8-3.10).

Setting aside the excursion to lower compositions during the A2 event, the $\delta^{18}O_{lakewater}$ values calculated here for the early to mid Holocene sediments are, on average, somewhat higher than measured for modern Lake Michigan, which has an average $\delta^{18}O$ value of -5.9 ‰ (Macdonald and Longstaffe 2007; Macdonald et al. 2007). This difference likely reflects more ^{18}O-rich regional precipitation plus enhanced evaporation during the Holocene Hypsithermal warm period (~8 – 4 ka [9,000 – 4,400 cal] BP. During this time, central North America was drier than at present and summer temperatures were up to 4 °C higher (Dorale et al. 1992; Kutzbach and Webb 1993; Krishnamurthy et al. 1995; Dean et al. 1996; Edwards et al. 1996; Yu et al. 1997; Lovan and Krishnamurthy 2011). Precipitation would consequently have had higher $\delta^{18}O$ values. Precipitation in southwestern Ontario during the Hypsithermal, for example, had $\delta^{18}O$ values of ~ -8 ‰, the highest average composition of the last 12 ka (Edwards et al. 1996). Additionally, outflow from Lake Agassiz-Ojibway was diverted from the Great Lakes Basin through the Ottawa and St. Lawrence River valleys at ~8.1 ka [9,000 cal] BP (Teller and Leverington 2004; Lewis et al. 2007). The combined result of this reduction in water supply and dry climate was hydrologically closed lake phases within the Michigan, Huron and Georgian Bay Basins from 7.9 to 7.5 ka [8,650 – 8,350 cal] BP (Lewis et al. 2005, 2007). Increased evaporative water loss during the warmer and drier climate at this time further contributed to the lowering of lake levels (Lewis et al. 2007; Forester et al. 1994).

The small but consistent difference between the oxygen-isotope compositions of deep- and shallower-water species throughout the Holocene record of these cores remains unexplained. It may indicate a small but systematic (~2-3 ‰) difference between the surface and bottom waters within the basin at that time. Ostracodes typically molt during the spring to fall (Delorme 2001; von Grafenstein 1999). If molting occurs after development of the thermocline, precipitation and runoff may accumulate in the surface waters with little chance of mixing with the bottom waters. That said, such behaviour is not evident in the study of modern ostracode (and mollusc) species from Lake Huron (Chapter 2, this thesis).

A decrease in $\delta^{18}O_{lakewater}$ values to as low as -7.1 ‰ is present towards the top of the oxygen-isotope records of both the South Chippewa and Chippewa sub-basin cores, and is exhibited by both *C. subtriangulata* and the shallower-water species (Fig. 3.11). Even lower lakewater values (~ -10 ‰) have previously been documented for a core from the Chippewa sub-basin at approximately 6.5 ka [7,425 cal] BP (Moore et al. 2000; Odegaard et al. 2003). Such compositions are anomalous within the Hypsithermal period, given that both temperatures and precipitation $\delta^{18}O$ values were likely higher than at present. This low-^{18}O excursion also occurred long after both meltwater originating from the ice sheet and Lake Agassiz outflow were diverted northwards away from the Great Lakes Basin at ~8.1 ka [9,000 cal] BP (Teller and Leverington 2004; Lewis et al. 2007), and long after the breakup of the Laurentide Ice Sheet over Hudson Bay and the final outburst flood from Lake Agassiz-Ojibway at ~7.7 ka [~8,450 cal] BP (Barber et al. 1999; Ellison et al. 2006; Daley et al. 2009). One explanation for the particularly low $\delta^{18}O$ values reported by Moore et al. (2003) and Odegaard et al. (2003) is that these ostracodes were reworked from older sediments during the rising lake levels of the Nipissing phase of the Great Lakes (~7 – 3 ka [~7,800 – 3,200 cal] BP). For the ostracodes examined in the present study, there was no physical evidence of reworking. The $\delta^{18}O_{lakewater}$ values of ~ -7.1 ‰ are only ~1 ‰ lower than modern Lake Michigan and may simply reflect regional climate fluctuations.

Early to mid Holocene oxygen-isotope records from the Great Lakes Basin

The magnitude of $\delta^{18}O_{lakewater}$ fluctuations during the early to mid Holocene is more subdued in the samples studied here than previously reported for Michigan Basin cores, and all samples show less variation in oxygen isotopic composition than Huron Basin cores for the same time period (Fig. 3.15). From 10 – 9.3 ka [11,500 – 10,500 cal] BP, Lake Michigan $\delta^{18}O_{lakewater}$ values described here fluctuate between -7 and -6 ‰. Previous studies suggest that, shortly after 9.7 ka [11,200 cal] BP, lakewater oxygen-isotope compositions in the Michigan Basin were lower than -10 ‰ (Fig. 3.15) (Breckenridge and Johnson 2009; Colman et al. 1990; Colman et al. 1994a, 1994b, 1994c; Forester et al. 1994). Such compositions were attributed to the initial Holocene influx of Lake Agassiz waters at ~9.6 – 9.4 ka [~11,100 – 10,600 cal] BP (Breckenridge and Johnson 2009; Breckenridge et al. 2010). This earlier work also indicates that Michigan Basin $\delta^{18}O_{lakewater}$ values gradually increased to ~ -7 ‰ by ~ 9.0 ka [10,200 cal] BP, before sharply decreasing to ~ -12 ‰ from ~8.4 – 8.2 ka [9,450 – 9,100 cal] BP during A2 event flooding (Colman et al. 1990; Colman et al. 1994a, 1994b; Forester et al. 1994; Moore et al. 2000; Odegaard et al. 2003; Breckenridge and Johnson 2009). The present study records higher $\delta^{18}O_{lakewater}$ values (~ -9 ‰) during the A2 event. The lower variability and generally higher $\delta^{18}O_{lakewater}$ values observed for this time interval in the present study may be a consequence of the relatively compact Holocene record in our cores (1.6 m thick in the South Chippewa sub-basin; 3.4 m thick in both the Milwaukee and Chippewa sub-basins), given the coarse sampling resolution that we employed (every second 10 cm-thick sediment package was analyzed for its biogenic carbonates).

Differences between the isotopic compositions of water in the Huron versus the Michigan Basins may be explained by the overall hydrology of the Great Lakes system. Generally, outflow from the Superior Basin entered the Huron Basin before backflooding into the Michigan Basin via the Straits of Mackinac. This low-^{18}O water would presumably have been diluted by water already present in the Huron Basin (e.g. accumulated precipitation and runoff), resulting in water with relatively higher $\delta^{18}O$ values entering the Michigan Basin. Very high-resolution Holocene records of lake levels and $\delta^{18}O_{lakewater}$ values from the Huron Basin record a minimum of three major

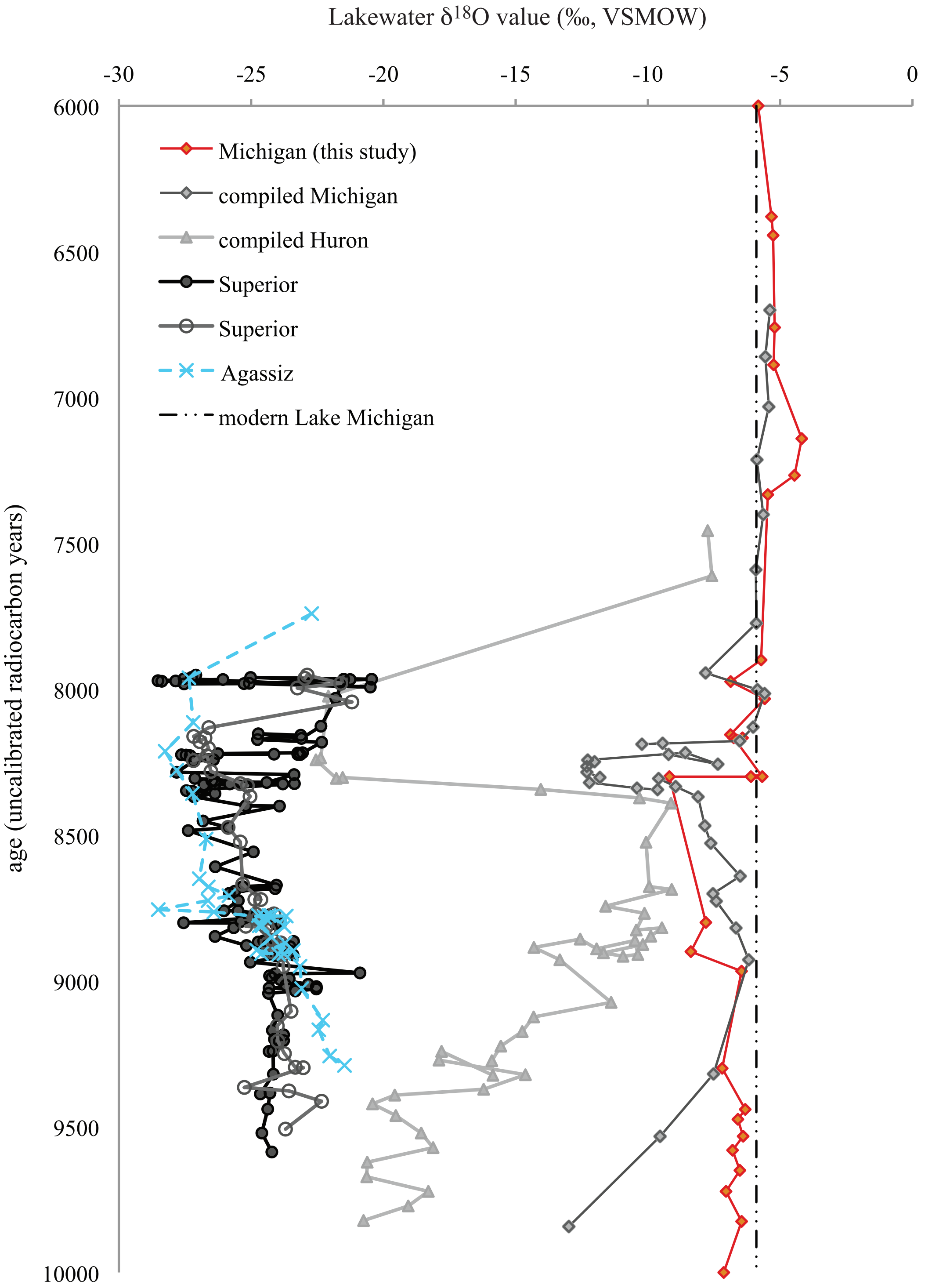

Figure 3.15. Oxygen-isotope compositions of the Great Lakes during the early to mid Holocene, from 10 - 6 ka [11,500 - 6,850 cal] BP. "Compiled" Michigan data are from Colman et al. (1994a, 1994c) and Forester et al. (1994). "Compiled" Huron data are from Rea et al. (1994) and Moore et al. (2000). Records from these two lakes were recalibrated by Breckenridge and Johnson (2009). Superior records are from Hyodo and Longstaffe (2011b; filled circles) and Breckenridge and Johnson (2009; open circles). Lake Agassiz data are from Lewis et al. (2003) and were presented in Breckenridge and Johnson (2009). Data for modern Lake Michigan water are from Macdonald and Longstaffe (2007).

influxes of low-^{18}O waters between ~10 – 7.5 ka [11,500 – 8,350 cal] BP), which were most pronounced at ~9.5 and 8.4 – 8.2 ka [10,700 and 9,450 – 9,100 cal] BP (Lewis et al. 1994; Rea et al. 1994a, 1994b; Dettman et al. 1995; Odegaard et al. 2003; Macdonald and Longstaffe 2008; Breckenridge and Johnson 2009; Breckenridge et al. 2010). The sediments from the Michigan Basin seem not to contain this finely detailed record of low-^{18}O events.

The oxygen-isotope records for ostracodes from Lakes Agassiz and Superior show that these lakes had low δ^{18}O values throughout the early to mid Holocene (Fig. 3.15). However, such compositions are not always reflected in downstream lakes (e.g. Lakes Huron and Michigan), even when overflow is believed to have occurred. Lake Agassiz is known to have drained eastwards to the Great Lakes (via the Lake Nipigon Basin) during its Nipigon phase from 9.5 – 8.2 ka [10,700 – 9,100 cal] BP (Teller and Thorleifson 1983; Leverington and Teller 2003; Breckenridge 2007; Breckenridge and Johnson 2009; Breckenridge et al. 2010). Outflow from the Agassiz Basin was often in the form of catastrophic floods with up to 8,000 km^3 of water released within only a few years (Leverington and Teller 2003). Consistent with this behaviour, low oxygen-isotope compositions of ostracodes in the Superior Basin, as well as a continuous record of varves, indicates that the Superior Basin received a continuous supply of Lake Agassiz outflow and/or meltwater during those periods when its lakewater oxygen-isotope compositions do not match up with those reported for the Huron and Michigan Basins (i.e. ~9.2 – 8.4 ka [10,400 – 9,450 cal] BP) (Breckenridge et al. 2010; Hyodo 2010; Hyodo and Longstaffe 2011b; Breckenridge and Johnson 2009).

One hypothesis explaining the discrepancies between oxygen-isotope records of the different basins is that low-^{18}O waters from the Superior Basin flowed through the North Channel into Georgian Bay and then departed via the North Bay outlet, thus bypassing the central Huron Basin and the Michigan Basin (Dettman et al. 1995; Lewis et al. 1994; Rea et al. 1994b). A second explanation invokes the stratified lake model of Birks et al. (2007), in which water flowing into the downstream basins was composed of relatively ^{18}O-enriched hypolimnion waters. A third possibility is that outflow from the

Superior Basin was diverted northeastwards to Lake Ojibway sometime between 9.2 – 8.8 ka [10,400 – 9,900 cal] BP after an ice dam was breached until either isostatic rebound or a glacial re-advancement once again redirected water southwards to the Huron and Michigan Basins (Breckenridge and Johnson 2009; Breckenridge et al. 2010; Hyodo and Longstaffe 2011b). This latter idea is consistent with evidence for a massive influx of water (A2 event in the Michigan Basin; main Mattawa highstand in the Huron Basin) when flow returned at ~8.4 ka [9,450 cal] BP. In the Michigan Basin, this event is marked by a decrease in δ^{18}O values of up to ~6 ‰ and Huron Basin records show a decrease of ~ 12 ‰ (Fig. 3.15) (Breckenridge and Johnson 2009; Lewis et al. 1994; Rea et al. 1994a, 1994b; Dettman et al. 1995). The ultimate source of the A2/main Mattawa floodwaters was likely both the Agassiz (Leverington and Teller 2003; Teller and Leverington 2004) and Superior (Yu et al. 2010) Basins.

3.4.3. The carbon-isotope history of Ancient Lake Michigan

Valves of *C. subtriangulata* and *C. crogmaniana* have the lowest δ^{13}C values (-7.7 to 0.2 ‰ and -6.1 to 0.1 ‰, respectively) in all three Michigan Basin cores (Fig. 3.9). The δ^{13}C values for the shallower-water species, *C. rawsoni*, *C. lacustris* and *Pisidium* clams (-3.7 to 1.8 ‰) overlap considerably, and are consistently higher by ~3 to 4 ‰ than results for *C. subtriangulata*.

In general, the δ^{13}C value of dissolved inorganic carbonate (DIC) dominates the composition of biogenic carbonates with some contributions from metabolic carbon (i.e., diet), and/or carbon cycling in microenvironments created by these organisms (Tanaka et al. 1986; Dettman et al. 1995, 2005; von Grafenstein et al. 1999; Holmes and Chivas 2002; Leng and Marshall 2004; Decrouy et al. 2011a, 2011b). The δ^{13}C values of DIC are influenced by exchange with atmospheric CO_2, the amount and composition of allochthanous carbonate in the lake, and the extent of organic decay in the sediments (Meyers 2003; Leng and Marshall 2004; Hyodo and Longstaffe 2011a). In productive freshwater lakes, photosynthesis is responsible for most of the fractionation within the carbon cycle. Photosynthesis (by primary producers such as photosynthetic algae and bacteria) enriches the aquatic organic matter in ^{12}C and causes DIC to become enriched in ^{13}C (Lister 1988; Farquhar et al. 1989; Hollander and McKenzie 1991; Leng and Marshall 2004). For example, the dominant species of DIC in modern Lake Huron is bicarbonate, HCO^{3-}, which has been shown to have $\delta^{13}C$ values of -1 to 0.5 ‰ (Dettman et al. 1995). The lower values in this range occur at greater depths, and are attributed to increased contribution of carbon from oxidation of organic matter relative to atmospheric carbon dioxide and/or dissolution of Paleozoic carbonate minerals (Dettman et al. 1995; Decrouy et al. 2011a). Additionally, higher DIC $\delta^{13}C$ values in shallower water may reflect preferential consumption of ^{12}C-rich DIC by photosynthesizing organisms. These processes may explain at least some of the observed ~3 to 4 ‰ difference between deep- and shallower-water species of ancient Lake Michigan.

Modern ostracodes and clams from Lake Huron, with the exception of *C. rawsoni*, have lower $\delta^{13}C$ values than expected for precipitation at equilibrium using open lakewater-DIC as the carbon source (Chapter 2, this thesis). For ostracodes, this difference is attributed to DIC sourced from their microenvironment, which is likely ~1-4 ‰ lower than lakewater-DIC (Decrouy et al. 2011b). For clams, this difference is attributed to incorporation of metabolic carbon. Although corrections could be applied to the carbon-isotope compositions of the ostracodes and clams to calculate the composition of lakewater-DIC, relative changes in $\delta^{13}C_{DIC}$ values are still provided by these organisms, allowing for inferences to be made regarding changes in productivity and/or DIC source(s).

In their studies of Lake Huron sediments, Rea et al. (1994b) and Lewis et al. (1994) found that excursions to lower ostracode valve $\delta^{13}C$ values generally coincided with low $\delta^{18}O$ values, and suggested that the lower carbon isotopic compositions arose from sudden input of dissolved organic material (e.g. soil organic carbon) carried to the lake by glacial meltwater. In the Lake Michigan cores studied here, glacial meltwater was present in significant quantities only during the late Pleistocene (Fig. 3.11), but there is little correlation between $\delta^{13}C$ and $\delta^{18}O$ values of *C. subtriangulata* valves (Fig. 3.13a). A stronger correlation exists between $\delta^{13}C$ and $\delta^{18}O$ values for *C. subtriangulata* valves during the early to mid Holocene (Fig. 3.13b), and both values are generally higher than in the late Pleistocene. The higher $\delta^{18}O_{lakewater}$ values indicate decreased meltwater input and increased contributions of precipitation/runoff during Holocene warming (Fig. 3.11). The higher $\delta^{13}C_{DIC}$ values likely reflect related processes. As Hyodo and Longstaffe (2011a) suggested for the Superior Basin, primary productivity in the Michigan Basin likely increased during the Holocene warming, facilitated by increased nutrient input from the watershed as glacial meltwater input came to an end.

The finer structure of the $\delta^{13}C$ values of biogenic carbonate from the Michigan Basin cores (Fig. 3.12) warrants further discussion. The carbon-isotope compositions of *C. subtriangulata* within Isotope Zone A oscillate between -4 and -3 ‰, gradually increasing into Zone B (Fig. 3.12). Within Zone B, $\delta^{13}C$ values of *C. subtriangulata* in the South Chippewa and Milwaukee sub-basins increase from ~ -3 to -2 ‰, and from ~ -6 to -4 ‰, respectively, towards the top of the zone. In the Chippewa sub-basin, the $\delta^{13}C$ values generally fluctuate between -6 to -4 ‰ after an initial decrease from as high as -2 ‰ (Fig. 3.12). Oxygen-isotope compositions of biogenic carbonates in Isotope Zone B show minimal variation (oscillations of <4 ‰ in the South Chippewa and Milwaukee sub-basins, up to ~9 ‰ in the Chippewa sub-basin; Fig. 3.11). This is interpreted to represent the steady supply of meltwater to the Michigan Basin during the Two Creeks retreat (12.2 – 11.8 ka [14,050 – 13,700 cal] BP). In the two more southerly sub-basins, the increase in $\delta^{13}C$ values may indicate increasing primary productivity through time. Closer proximity to the continuous supply of meltwater into the northern end of the Michigan Basin may have suppressed primary productivity there by supplying large amounts of rock flour, which would have drastically minimized light penetration (Rhee and Gotham 1981; Diehl 2002).

Isotope Zone C is interpreted to include the final (Two Rivers) glacial advance (11.8 – 11.1 ka [13,700 – 13,000 cal] BP) into the Michigan Basin. In the South Chippewa sub-basin, the $\delta^{13}C$ values of *C. subtriangulata* range from -4.9 to -2.5 ‰ and are overlapped by *C. crogmaniana* (-5.6 to -0.6 ‰). The shallower-water species are commonly enriched in ^{13}C relative to *C. subtriangulata* by ~3 to 4 ‰ (Fig. 3.12). A decrease in *C. subtriangulata* $\delta^{13}C$ values (by ~2-3 ‰) at the start of this zone may indicate a decrease in primary productivity. In the Chippewa sub-basin, there are more pronounced fluctuations in *C. subtriangulata* $\delta^{13}C$ values: lower portion, -6.8 to -5.0 ‰; upper portion, -5.0 to -3.1 ‰. The higher $\delta^{13}C$ values occur within thick sandy intervals and may indicate greater incorporation of DIC derived from allochthonous Paleozoic carbonate ($\delta^{13}C$ = -1 to 4 ‰; Lohmann and Walker 1989).

Within the lower portions of Zone D (corresponding to the Kirkfield phase, 11.1 – 11.0 ka [13,000 – 12,900 cal] BP), the $\delta^{13}C$ values of *C. subtriangulata* decrease by as much as ~2 to 3 ‰ (Fig. 3.12). Within the upper portions of Zone D (corresponding to Lake Algonquin, 11.0 – 10.3 ka [12,900 – 12,100 cal] BP), the $\delta^{13}C$ values of *C. subtriangulata* then increase by ~1 ‰. There is no clear association between ostracode valve $\delta^{13}C$ values and the occurrence of the Wilmette Bed. In the South Chippewa sub-basin, *C. subtriangulata* $\delta^{13}C$ values decrease by ~2 ‰ in the sediments immediately overlying the Wilmette Bed. In the Milwaukee sub-basin, *C. subtriangulata* $\delta^{13}C$ values increase by ~1.5 ‰ immediately above the Wilmette Bed before decreasing again by the same amount (Fig. 3.12). Hyodo and Longstaffe (2011a) found that $\delta^{13}C$ values of ostracode valves from Lake Superior sediments varied by up to 5 ‰ during times when the basin was strongly influenced by glacial meltwater, and determined that this variation reflected changing DIC sources.

In Isotope Zone E, the carbon isotopic compositions of biogenic carbonates within the early Holocene (from 10 ka [11,500 cal] BP until the A2 event at 8.4 – 8.2 ka [9,450 – 9,100 cal] BP) are similar to those measured for the latest Pleistocene (Zones A – D). The $\delta^{13}C$ values for *C. subtriangulata* and *C. crogmaniana* in all three cores are ~ -4 ‰, whereas shallower-water species are higher by ~3 to 4 ‰ (Fig. 3.12). Following the A2 event, which marks the final surge of low-^{18}O waters into the Michigan Basin, the $\delta^{13}C$ values of all species increase by as much as ~4 ‰ (Fig. 3.12). Conditions in the Michigan Basin changed considerably following the A2 event. Hydrological closure, resulting both from diversion of Lake Agassiz-Ojibway outflow elsewhere and an increasingly warm and dry climate, occurred from 7.9 – 7.5 ka [8,650 – 8,350 cal] BP.

Increasing biogenic carbonate $\delta^{13}C$ values above the A2 Bed most likely reflect increased primary productivity, which is also indicated by the high populations of ostracodes and clams in Isotope Zone E (Figs. 3.8-3.10). The high ostracode and clam populations also suggest that salinity and/or alkalinity did not increase to intolerably high levels during this period of no outflow from the Michigan Basin.

A decrease in biogenic carbonate $\delta^{13}C$ values, accompanied by slightly lower $\delta^{18}O$ values, occurs in the uppermost samples within the South Chippewa and Chippewa sub-basins. This change may reflect a climatic fluctuation in the region, which produced lower primary productivity. The number of ostracode valves and clam shells contained in these sediments was quite low (Figs. 3.8 and 3.10), which may also suggest an overall decrease in productivity within the lake.

3.4.4 Ancient flooding in the Upper Great Lakes

Lacustrine records spanning the late Pleistocene to mid Holocene from Lakes Superior, Huron and Michigan collectively indicate four major flooding events, which likely originated from Lake Agassiz. Oxygen-isotope compositions together with intervals of thick varves within Lake Superior sediments – interpreted as records of large flooding events – suggest that the Superior Basin was inundated with waters derived from Lake Agassiz (and/or the LIS) from ~9.4 – 8.1 ka [10,600 – 9,000] BP and again at ~8 ka [8850 cal] BP (Breckenridge et al. 2004; Breckenridge 2007; Breckenridge and Johnson 2009; Hyodo 2010; Hyodo and Longstaffe 2011b, 2011c). Sediments from Lake Huron contain evidence for three floods – the Mattawa highstands – at 9.5 ka [10,700 cal] BP, 8.4 ka [9,450 cal] BP and ~8.2 ka [9,100 cal] BP (Lewis et al. 1994; Rea et al. 1994a, 1994b; Dettman et al. 1995; Moore et al. 2000; Lewis et al. 2005; Macdonald and Longstaffe 2008). The Michigan Basin sediment record reveals three flooding events, the A1 event (11.0 – 10.5 ka [12,900 – 12,600 cal] BP, an unnamed flood at ~9.5 ka [10,700 cal] BP, and the A2 event at 8.4 – 8.2 ka [9,450 – 9,100 cal] BP (Colman et al. 1990, 1994a, 1994c; Miller et al. 2000; Breckenridge and Johnson 2009; Fisher et al. 2010). The earliest of these floods, the A1 event, has only been documented in the Michigan

Basin. The Superior and Huron Basins should also have been affected by this flood but sufficiently old sediment records that could contain evidence of this event have not yet been obtained.

A new naming system for these floods would do much to clarify and reinforce the linked histories of these lake basins. Such an undertaking, however, would first require much better resolution for the timing of short-duration flooding events, particularly those that occurred during Lake Agassiz's Nipigon phase from 9.5 – 8.2 ka [10,700 – 9,100 cal] BP.

3.5 CONCLUSIONS

The oxygen-isotope results for deep-water ostracodes (*C. subtriangulata)* versus shallower-water species of ostracodes and clams from late Pleistocene portions of three sediment cores from Lake Michigan suggest that it was stratified in isotopic composition (~ -15 versus ~ -3 ‰) at least during its Lake Algonquin phase (11 – 10.3 ka [12,900 – 12,100 cal] BP). Such stratification has been previously reported for Lake Agassiz (Birks et al. 2007). This study presents the first evidence for such a process during Pleistocene times within the Great Lakes Basin.

The oxygen isotopic results for *C. subtriangulata* indicate a more-or-less continuous supply of low-^{18}O glacial meltwater to the Michigan Basin during most of the late Pleistocene intervals sampled here (~13 – 10 ka [15,300 – 11,500 cal] BP). The oxygen-isotope results for the shallower-water ostracodes and clams provide a measure of the δ^{18}O value of regional precipitation and surface runoff, and hence more local climatic conditions. Large oscillations in the Pleistocene $\delta^{18}O_{lakewater}$ values, as calculated using *C. subtriangulata*, are commonly observed, particularly in the South Chippewa and Chippewa sub-basins of the Michigan Basin. These rapid changes are indicative of a dynamic system, involving some combination of mixing between ^{18}O-poor bottom water and ^{18}O-rich surface water, intermittent inflows of water from the Huron and Erie basins, and/or rapid advances and retreats of the Michigan Lobe of the LIS.

The $\delta^{18}O_{lakewater}$ values, as calculated using *C. subtriangulata*, increased substantially at the onset of the Holocene from ~ -15 to ~ -7 ‰. These compositions are slightly lower than the range calculated for the shallower-water ostracodes and clams (~ -5 to -1 ‰). Such compositions are reflective of a warmer and drier climate throughout much of the mid Holocene. A return to slightly lower $\delta^{18}O_{lakewater}$ values in the youngest Holocene sediments recovered from the Chippewa Basin likely represents a shift toward cooler regional temperatures at that time.

Two distinctive sedimentary units identified within the cores, the Wilmette and A2 Beds, can be correlated to major flooding events originating from Lake Agassiz. The Wilmette Bed was deposited by the A1 flood, likely at ~10.9 – 10.8 ka [12,900 – 12,800 cal] BP, as Agassiz outflow was rerouted from the northwest outlet eastwards towards the Great Lakes Basin (Teller et al. 2005; Murton et al. 2010). Biogenic carbonates from sediment immediately overlying the Wilmette Bed in the South Chippewa and Milwaukee sub-basin cores are probably most characteristic of the oxygen-isotope composition of the floodwaters, and indicate that $\delta^{18}O_{lakewater}$ values decreased to nearly -20 ‰ at this time.

The A2 bed was deposited at ~8.4 – 8.2 ka [9,450 – 9,100 cal] BP, possibly as the Huron and Michigan Basins began to receive outflow from the Superior Basin after it had been temporarily diverted northwards (Breckenridge et al. 2010; Breckenridge and Johnson 2009). As this time, $\delta^{18}O_{lakewater}$ values in the Huron Basin decrease by ~12 ‰, whereas $\delta^{18}O_{lakewater}$ values in the Michigan Basin decrease by ~6 ‰ (and only ~2-3 ‰ in the cores examined here). This is likely an effect of the low-^{18}O waters spilling more directly into the Huron Basin through the St. Mary's River while the Michigan Basin instead received backflooded waters through the Straits of Mackinac, which would have mixed with lakewater already present in the Huron Basin.

These two major flooding events, the A1 and A2, correlate with two major global cooling events, the Younger Dryas (11-10 ka [12,900 – 11,500 cal] BP) and the unnamed ~8.3 ka [9,300 cal] BP event. Both are marked by distinctive sedimentary units within the cores examined here and are associated with low-^{18}O waters. This observation supports the hypothesized linkage made previously between movement of large volumes of meltwater through the Great Lakes Basin and the effect of such waters on ocean circulation patterns and global climate (Peltier 2007; Fleitmann et al. 2008; Daley et al. 2009; Yu et al. 2010).

During the latest Pleistocene, carbon-isotope compositions of biogenic carbonates suggest that the Michigan Basin lakewater was oligotrophic (i.e., primary productivity rates were low; Fig. 3.12). Carbon-isotope compositions during this time were likely influenced by addition of DIC derived from Paleozoic carbonates, including detritus carried from great distances by glacial and glacial-fluvial transport processes, including meltwater floods, and perhaps also by small fluctuations in primary productivity. During the Holocene, particularly after the A2 flood, productivity within the lake increased, resulting in higher biogenic carbonate δ^{13}C values than earlier in the Basin's history.

3.6 REFERENCES

Alley RB, Shuman CA, Meese DA, Gow AJ, Taylor KC, Cuffey KM, Fitzpatrick JJ, Grootes PM, Zielinski GA, Ram M (1997) Visual-stratigraphic dating of the GISP2 ice core: Basis, reproducibility, and application. J Geophys Res 102: 26367–26381

Barber DC, Dyke A, Hillaire-Marcel C, Jennings AE, Andrews JT, Kerwin MW, Bilodeau G, McNeely R, Southon J, Morehead MD, Gagnon J-M (1999) Forcing of the cold event of 8,200 years ago by catastrophic drainage of Laurentide lakes. Nature 400: 344-348

Birks SJ, Edwards TWD, Remenda VH (2007) Isotopic evolution of Glacial Lake Agassiz: New insights from cellulose and porewater isotopic archives. Palaeogeogr Palaeoclimatol Palaeoecol 246: 8-22

Boomer I (2002) Environmental applications of marine and freshwater ostracoda. In Haslett SK (ed) Quaternary Environmental Micropalaeontology. Arnold, London. pp 115-138

Breckenridge A (2007) The Lake Superior varve stratigraphy and implications for eastern Lake Agassiz outflow from 10,700 to 8,900 cal ybp (9.5–8.0 ^{14}C ka). Palaeogeogr Palaeoclimatol Palaeoecol 246: 45-61

Breckenridge A, Johnson TC (2009) Paleohydrology of the upper Laurentian Great Lakes from the late glacial to early Holocene. Quat Res 71: 397-408

Breckenridge A, Johnson TC, Beske-Diehl S, Mothersill JS (2004) The timing of regional late glacial events and postglacial sedimentation rates from Lake Superior. Quat Sci Rev 23: 2355-2367

Breckenridge A, Lowell TV, Fisher TG, Yu S (2010) A late Lake Minong transgression in the Lake Superior basin as documented by sediments from Fenton Lake, Ontario. J Paleolimnol DOI 10.1007/s10933-101-9447-z

Broecker WS, Kennett J, Flower B, Teller JT, Trumbore S, Bonani G, Wolfli W (1989) Routing of meltwater from the Laurentide Ice Sheet during the Younger Dryas cold episode. Nature 341: 318-321

Brown TA, Nelson DE, Mathewes RW, Vogel JS, Southon JR (1989) Radiocarbon dating of pollen by accelerator mass spectrometry. Quat Res 32: 205-212

Buhay WM, Betcher RN (1998) Paleohydrologic implications of ^{18}O-enriched Lake Agassiz water. J Paleolimnol 19: 285-296

Clark JA, Hendriks M, Timmermans TJ, Struck C, Hilverda KJ (1994) Glacial isostatic deformation of the Great Lakes region. Geol Soc Am Bull 106: 19-30

Clark PU (1994) Unstable behavior of the Laurentide Ice Sheet over deforming sediments and its implications for climate change. Quat Res 41: 19-25

Clark PU, Marshall SJ, Clarke GKC, Hostetler SW, Licciardi JM, Teller JT (2001) Freshwater forcing of abrupt climate change during the last glaciation. Science 293: 283-287

Colman SM, Keigwin LD, Forester RM (1994a) Two episodes of meltwater influx from glacial Lake Agassiz into the Lake Michigan basin and their climatic contrasts. Geology 22: 547-550

Colman SM, Jones GA, Forester RM, Foster DS (1990) Holocene paleoclimate evidence and sedimentation rates from a core in southwestern Lake Michigan. J Paleolimnol 4: 269-284

Colman SM, Clark JA, Clayton L, Hansel AK, Larsen CE (1994b) Deglaciation, lake levels, and meltwater discharge in the Lake Michigan basin. Quat Sci Rev 13: 879-890

Colman SM, Forester RM, Reynolds RL, Sweetkind DS, King JW, Gangemi P, Jones GA, Keigwin LD, Foster DS (1994c) Lake-level history of Lake Michigan for the past 12,000 years: the record from deep lacustrine sediments. J Great Lakes Res 20: 73-92

Coplen TB (1996) New guidelines for reporting stable hydrogen, carbon, and oxygen isotope-ratio data. Geochim Cosmochim Acta 17: 3359-3360

Couch AG, Eyles N (2008) Sedimentary record of glacial Lake Mackenzie, Northwest Territories, Canada: Implications for Arctic freshwater forcing. Palaeogeogr Palaeoclimatol Palaeoecol 268: 26-38

Daley TJ, Street-Perrott FA, Loader NJ, Barber KE, Hughes PDM, Fisher EH, Marshall JD (2009) Terrestrial climate signal of the “8200 yr B.P. cold event” in the Labrador Sea region. Geology 37: 831-834

Dansgaard W, Tauber H (1969) Glacier oxygen-18 content and Pleistocene ocean temperature. Science 166: 499-502

Dean WE, Ahlbrandt TS, Anderson RY, Bradbury JP (1996) Regional aridity in North America during the middle Holocene. The Holocene 6: 145-155

Decrouy L, Vennemann TW, Ariztegui D (2011a) Controls on ostracod valve geochemistry, Part 1: Variations of environmental parameters in ostracod (micro-) habitats. Geochim Cosmochim Acta 75: 7364-7359

Decrouy L, Vennemann TW, Ariztegui D (2011b) Controls on ostracod valve geochemistry: Part 2. Carbon and oxygen isotope compositions. Geochim Cosmochim Acta 75: 7380-7399

Delorme LD (1978) Distribution of freshwater ostracodes in Lake Erie. J Great Lakes Res 4: 216-220

Delorme LD (2001) Ostracoda. In: Thorp JH, Covich AP (eds) Ecology and classification of North American freshwater invertebrates, second edition. Academic Press, New York, pp 811-848

Dettman DL, Palacios-Fest MR, Nkotagu HH, Cohen AS (2005) Paleolimnological investigations of anthropogenic environmental change in Lake Tanganyika: VII. Carbonate isotope geochemistry as a record of riverine runoff. J Paleolimnol 34: 93-105

Dettman DL, Smith AJ, Rea DK, Moore TC Jr., Lohmann KC (1995) Glacial meltwater in Lake Huron during early postglacial time as inferred from single-valve analysis of oxygen isotopes in ostracodes. Quat Res 43: 297-310

Diehl S (2002) Phytoplankton, light and nutrients in a gradient of mixing depths: Theory. Ecology 83: 386-398

Dorale JA, González LA, Reagan MK, Pickett DA, Murrell MT, Baker RG (1992) A high-resolution record of Holocene climate change in speleothem calcite from Coldwater cave, Northeast Iowa. Science 258: 1626-1630

Edwards TWD, Wolfe BB, MacDonald GM (1996) Influence of changing atmospheric circulation on precipitation $\delta^{18}O$ – temperature relations in Canada during the Holocene. Quat Res 46: 211-218

Ellison CRW, Chapman MR, Hall IR (2006) Surface and deep ocean interactions during the cold climate event 8200 years ago. Science 312: 1929-1932

Eschman DF, Karrow PF (1985) Huron basin glacial lakes: a review. In: Karrow PF, Calkin PE (eds) Quaternary Evolution of the Great Lakes. Geol Assoc Canada Spec Paper 30, pp 79-93

Evanson EB, Dreimanis A, Newsome JW (1977) Subaquatic flow tills: a new interpretation for the genesis of some laminated till deposits. Boreas 6: 115-133

Fairbanks RG (1989) A 17,000-year glacio-eustatic sea level record: influence of glacial melting rates on the Younger Dryas event and deep-ocean circulation. Nature 342: 637-642

Farquhar GD, Ehleringer JR, Hubick KT (1989) Carbon isotope discrimination and photosynthesis. Annu Rev Plant Physiol Plant Mol Biol 40: 503-537

Finamore PF (1985) Glacial Lake Algonquin and the Fenelon Falls outlet. In: Karrow PF, Calkin PE (eds) Quaternary Evolution of the Great Lakes. Geol Assoc Canada Spec Paper 30, pp 125-132

Fisher TG (2003) Chronology of glacial Lake Agassiz meltwater routed to the Gulf of Mexico. Quat Res 59: 271-276

Fisher TG (2007) Abandonment chronology of glacial Lake Agassiz's Northwestern outlet. Palaeogeogr Palaeoclimatol Palaeoecol 246: 31-44

Fisher TG, Smith DG (1994) Glacial Lake Agassiz: its northwest maximum extent and outlet in Saskatchewan (Emerson phase). Quat Sci Rev 13: 845-858

Fisher TG, Smith DG, Andrews JT (2002) Preboreal oscillation caused by a glacial Lake Agassiz flood. Quat Sci Rev 21: 873-878

Fisher TG, Weyer KA, Boudreau AM, Martin-Hayden JM, Krantz DE, Breckenridge A

(2010) Constraining Holocene lake levels and coastal dune activity in the Lake Michigan basin. J Paleolimnol DOI 10.1007/s10933-010-9460-2

Fleitmann D, Mudelsee M, Burns SJ, Bradley RS, Kramers J, Matter A (2008) Evidence for a widespread climatic anomaly at around 9.2 ka before present. Paleoceanography 23, PA1102 1029/2007PA001519

Forester RM, Colman SM, Reynolds RL, Keigwin LD (1994) Lake Michigan's late Quaternary limnological and climate history from ostracode, oxygen isotope, and magnetic susceptibility. J Great Lakes Res 20: 93-107

Hansel AK, Mickelson DM (1988) A reevaluation of the timing and causes of high lake phases in the Michigan Basin. Quat Res 29: 113-128

Hansel AK, Mickelson DM, Schneider AF, Larsen CE (1985) Late Wisconsinan and Holocene history of the lake Michigan basin. In: Karrow PF, Calkin PE (eds) Quaternary Evolution of the Great Lakes. Geol Assoc Canada Spec Paper 30, pp 39-53

Hodell SA, Schelske CL (1998) Production, sedimentation, and isotopic composition of organic matter in Lake Ontario. Limnol Oceanogr 43: 200-214

Hollander DJ, McKenzie JA (1991) CO_2 control on carbon-isotope fractionation during aqueous photosynthesis; a paleo-pCO_2 barometer. Geology 19: 929-932

Holmes JA, Chivas AR (2002) Ostracod shell chemistry – Overview. In: Holmes JA, Chivas AR (eds) The Ostracoda: Applications in Quaternary Research. AGU Monogr 131, pp 185-204

Hough JL (1955) Lake Chippewa, a low stage of Lake Michigan indicated by bottom sediments. Geol Soc Am Bull 66: 957-968

Hyodo A (2010) The Holocene paleolimnology of Lake Superior. Ph.D. thesis. The University of Western Ontario, London, pp 330

Hyodo A, Longstaffe FJ (2011a) The paleoproducivity of ancient Lake Superior. Quat Sci Rev 30: 2988-3000

Hyodo A, Longstaffe FJ (2011b) Variations in the oxygen-isotope composition of ancient Lake Superior between 10,600 and 8,800 cal BP. J Paleolimnol, DOI 10.1007/s10933-011-9552-7

Hyodo A, Longstaffe FJ (2011c) The Chronostratigraphy of Holocene sediments from four Lake Superior sub-basins. Can J Earth Sci 48: 1581-1599

Kehew AE (1993) Glacial-lake outburst erosion of the Grand Valley, Michigan, and impacts on glacial lakes in the Lake Michigan Basin. Quat Res 39: 36-44

Kincare KA, Larson GJ (2009) Geologic evolution of the Great Lakes. In: Schaetzl RJ, Darden JT, Brandt D (eds) Michigan Geography and Geology. Pearson Custom Publishers, Boston, MI, pp 174-190

Krishnamurthy RV, Syrup K, Baskaran M, Long A (1995) Late glacial climate record of Midwestern USA from the hydrogen isotope record of lake organic matter. Science 269: 1565-1567

Kutzbach JE, Webb TI (1993) Conceptual basis for understanding Late-Quaternary climates. In: Wright HEJ, Kutzbach JE, Webb TI, Ruddiman WF, Street-Perrott FA, Bartlein PJ (eds) Global Climates Since the Last Glacial Maximum. University of Minnesota Press, Minneapolis, MN, pp 5-11

Larsen CE (1987) Geological history of glacial Lake Alogonquin and the upper Great Lakes. USGS Bull 1801: 1-36

Last WM, Teller JT, Forester RM (1994) Paleohydrology and paleochemistry of Lake Manitoba, Canada: the isotope and ostracode records. J Paleolimnol 12: 269-282

Leng MJ, Marshall JD (2004) Palaeoclimate interpretation of stable isotope data from lake sediment archives. Quat Sci Rev 23: 811-831

Leverington D, Teller J (2003) Paleotopographic reconstructions of the eastern outlets of glacial Lake Agassiz. Can J Earth Sci 40: 1259-1278

Leverington DW, Mann JD, Teller JT (2000) Changes in the bathymetry and volume of glacial Lake Agassiz between 11,000 and 9,300 ^{14}C yr BP. Quat Res 54: 174-181

Lewis CFM, Anderson TW (1989) Oscillations of levels and cool phases of the Laurentian Great Lakes caused by inflows from glacial Lakes Agassiz and Barlow-Ojibway. J Paleolimnol 2: 99-146

Lewis CFM, Anderson TW (1992) Stable isotope (O and C) and pollen trends in eastern Lake Erie, evidence for a locally-induced climatic reversal of Younger Dryas age in the Great Lakes basin. Clim Dynam 6: 241-250

Lewis CFM, Blasco SM, Gareau PL (2005) Glacio-isostatic adjustment of the Laurentian Great Lakes basin: using the empirical record of strandline deformation for reconstruction of early Holocene paleo-lakes and discovery of a hydrologically closed phase. Géog Phys et Quat 59: 171-193

Lewis CFM, Forbes DL, Todd BJ, Thorleifson LH, Matile GLD (2003) Were the oxygen isotopic compositions of Lake Agassiz outflows more enriched than previously thought? Can Quat Assoc/Can Geomorph Res Group, Halifax, Canada, Abstr pp A65

Lewis CFM, Heil CW Jr, Hubeny JB, King JW, Moore TC Jr, Rea DK (2007) The Stanley unconformity in Lake Huron basin: evidence for a climate-driven closed lowstand about 7900 ^{14}C BP, with similar implications for the Chippewa lowstand in Lake Michigan basin. J Paleolimnol 37: 435-452

Lewis CFM, Moore TC Jr, Rea DK, Dettman DL, Smith AM, Mayer LA (1994) Lakes of the Huron basin: their record of runoff from the Laurentide Ice Sheet. Quat Sci Rev 13: 891-922

Lewis CFM, Karrow PF, Blasco SM, McCarthy FMG, King JW, Moore TC Jr, Rea DK (2008) Evolution of lakes in the Huron basin: Deglaciation to present. Aquat Ecosyst Health Manage 11: 127-136

Lineback JA, Dell CI, Gross DI (1979) Glacial and postglacial sediments in Lake Superior and Michigan. Geol Soc Am Bull 90: 781-791

Lister GS (1988) Stable isotopes from lacustrine ostracoda as tracers for continental palaeoenvironments. In: DeDeckker P, Colin JP, Peypouquet J-P (eds) Ostracoda in the Earth Sciences, Elsevier, Amsterdam, pp 201-218

Lohmann KC, Walker JCG (1989) The δ^{18}O record of Phanerozoic abiotic marine calcite cements. Geophys Res Lett 16: 319-322.

Lovan NA, Krishnamurthy RV (2011) Inferring paleotemperature from the D/H ratio of lacustrine organic matter. Quat International 229: 38-46

Lowell TV, Fisher TG, Comer GC, Hajdas I, Waterson N, Glover K, Loope HM, Schaefer JM, Rinterknecht VR, Broecker W, Denton GH Teller JT (2005) Testing the Lake Agassiz meltwater trigger for the Younger Dryas. EOS 86: 365-372

Macdonald RA, Longstaffe FJ (2007) The oxygen and hydrogen isotope compositions of the Great Lakes. Programs and Abstracts of the 50th Conference on Great Lake Research, pp 117-118

Macdonald RM, Longstaffe FJ (2008) The Late Quaternary oxygen-isotope composition of southern Lake Huron. Aquat Ecosyst Health Manage 11: 137-143

Macdonald RA, Longstaffe FJ, Crowe AS (2007) The Late Quaternary oxygen isotope composition of Lake Michigan. EOS Trans AGU 88: PP13B-1283

Mae A, Longstaffe, FJ (2007) Oxygen isotope studies of ostracodes from the Duluth Basin, Lake Superior, and the variation in lake water composition since the Late Pleistocene. Programs and Abstracts of the 50th Conference on Great Lake Research, pp 119

Mae A, Longstaffe FJ, Crowe AS (2007) Variations in the oxygen-isotope composition of Holocene Lake water based on ostracodes from Lake Superior. EOS Trans AGU 88: PP13B-1282

Meyers PA (2003) Application of organic geochemistry to paleolimnological reconstructions: a summary of examples from the Laurentian Great Lakes. Org Geochem 34: 261-289

Meyers PA, Ishiwatari R (1993) Lacustrine organic geochemistry - an overview of indicators of organic matter sources and diagenesis in lake-sediments. Org Geochem 20: 867-900

Miller BB, Tevesz MJS, Pranschke FA (2000) An early Holocene oxygen isotope record from the Olson buried forest bed, southern Lake Michigan. J Paleolimnol 24: 271-276

Moore TC Jr, Rea DK, Godsey H (1998) Regional variation in modern radiocarbon ages and the hard-water effects in Lakes Michigan and Huron. J Paleolimnol 20: 347-351

Moore TC Jr., Rea DK, Mayer LA, Lewis CFM, Dobson DM (1994) Seismic stratigraphy of Lake Huron - Georgian Bay and postglacial lake history. Can J Earth Sci 31: 1606-1617

Moore TC Jr, Walker JCG, Rea DK, Lewis CFM, Shane LCK, Smith AJ (2000) Younger Dryas interval and outflow from the Laurentide ice sheet. Paleoceanography 15: 4-18

Munsell Color (2000) Munsell Soil Color Charts, Year 2000 Revised Washable Edition. GretagMacbeth, New Windsor, NY

Murton JB, Bateman MD, Dallimore SR, Teller JT, Zhirong Yang (2010) Identification of Younger Dryas outburst flood path from Lake Agassiz to the Arctic Ocean. Nature 464: 740-743

Nambudiri EVM, Teller JT, Last WM (1980) Pre-Quaternary microfossils – A guide to errors in radiocarbon dating. Geology 8: 123-126

Odegaard C, Rea DK, Moore TC (2003) Stratigraphy of the mid-Holocene black bands in Lakes Michigan and Huron: Evidence for possible basin-wide anoxia. J Paleolimnol 29: 221-234

Palacios-Fest MR, Cohen AS, Ruiz J, Blank B (1993) Comparative paleoclimatic interpretations from nonmarine ostracodes using faunal assemblages, trace elements shell chemistry and stable isotope data. In: Swart PK, McKenzie J, Lohmann KC, Savin S (eds) Climate Change in Continental Isotopic Records. AGU Monogr 78, pp 179-190

Patterson WP, Smith GR, Lohmann KC (1993) Continental paleothermometry and seasonality using the isotopic composition of aragonitic otoliths of freshwater fishes. In: Swart PK, McKenzie J, Lohmann KC, Savin S (eds) Climate Change in Continental Isotopic Records. AGU Monogr 78, pp 191-202

Peltier WR (2007) Rapid climate change and Arctic Ocean freshening. Geology 35: 1147-1148

Rasmussen SO, Andersen KK, Svensson AM, Steffensen JP, Vinther BM, Clausen HB, Siggaard-Andersen ML, Johnsen SJ, Larsen LB, Dahl-Jensen D, Bigler M, Röthlisberger R, Fischer H, Goto-Azuma K, Hansson ME, Ruth U (2006) A new Greenland ice core chronology for the last glacial termination. J Geophys Res 111, D06102, doi:10.1029/2005JD006079

Rea DK, Colman SM (1995) Radiocarbon ages of pre-bomb clams and the hard-water effect in Lakes Michigan and Huron. J Paleolimnol 14: 88-91

Rea DK, Bourbonniere RA, Meyers PA (1980) Southern Lake Michigan sediments: changes in accumulation rate, mineralogy, and organic content. J Great Lakes Res 6: 321-330

Rea DK, Moore TC Jr, Lewis CFM, Mayer LA, Dettman DL, Smith AL, Dobson DM (1994a) Stratigraphy and paleolimnologic record of lower Holocene sediments in northern Lake Huron and Georgian Bay. Can J Earth Sci 31: 1586-1605

Rea DK, Moore TC Jr, Anderson TW, Lewis CFM, Dobson DM, Dettman DL, Smith AJ, Mayer LA, (1994b) Great Lakes paleohydrology: complex interplay of glacial meltwater, lake levels and sill depths. Geology 22: 1059-1062

Reimer PJ, Baillie MGL, Bard E, Bayliss A, Beck JW, Bertrand CJH, Blackwell PG, Buck CE, Burr GS, Cutler KB, Damon PE, Edwards RL, Fairbanks RG, Friedrich M, Guilderson TP, Hogg AG, Hughen KA, Kromer B, McCormac G, Manning S, Ramsey CB, Reimer RW, Remmele S, Southon JR, Stuiver M, Talamo S, Taylor FW, van der Plicht J, Weyhenmeyer CE (2004) INTCAL04 Terrestrial radiocarbon age calibration. Radiocarbon 46: 1029-1058

Remenda VH, Cherry JA, Edwards TWD (1994) Isotopic composition of old ground water from Lake Agassiz: implications for late Pleistocene climate. Science 226: 1975-1978

Rhee GY, Gotham IJ (1981) The effect of environmental factors on phytoplankton growth - light and the interactions of light with nitrate limitation. Limnol Oceanogr 26: 649-659

Rooth C (1982) Hydrology and ocean circulation. Prog Oceanogr 11: 131-149

Safarudin, Moore Jr TC (1999) The history and architecture of lacustrine depositional systems in the northern Lake Michigan basin. J Paleolimnol 22: 475-496

Schneider AF, Need EA (1985) Lake Milwaukee: An "early" proglacial lake in the Lake Michigan Basin. In: Karrow PF, Calkin PE (eds) Quaternary Evolution of the Great Lakes. Geol Assoc of Canada Spec Paper 30, pp 55-62

Schöne BR, Rodland DL, Fiebig J, Oschmann W, Goodwin D, Flessa KW, Dettman D (2006) Reliability of multitaxon, multiproxy reconstructions of environmental conditions from accretionary biogenic skeletons. J Geology 114: 267-285

Sima A, Paul A, Schulz M, Oerlemans J (2006) Modeling the oxygen-isotopic composition of the North American Ice Sheet and its effect on the isotopic composition of the ocean during the last glacial cycle. Geophys Res Lett 33:

L15706, doi 10.1029/2006GL026923

Smith DG, Fisher TG (1993) Glacial Lake Agassiz - the northwestern outlet and paleoflood. Geology 21: 9-12

Tanaka N, Monaghan MC, Rye DM (1986) Contribution of metabolic carbon to mollusc and barnacle shell carbonate. Nature 320: 520-523

Teller JT (1985) Glacial Lake Agassiz and its influence on the Great Lakes. In: Karrow PF, Calkin PE (eds) Quaternary Evolution of the Great Lakes. Geol Assoc of Canada Spec Paper 30, pp 1-12

Teller JT, Leverington DW (2004) Glacial Lake Agassiz: A 5000 yr history of change and its relationship to the $\delta^{18}O$ record of Greenland. Geol Soc Am Bull 116: 729-742

Teller JT, Thorleifson LH (1983) The Lake Agassiz-Lake Superior connection. In: Teller JT, Clayton L (eds) Glacial Lake Agassiz. Geol Assoc of Canada Spec Paper 26, pp 261-290

Teller JT, Leverington DW, Mann JD (2002) Freshwater outbursts to the oceans from glacial Lake Agassiz and their role in climate change during the last deglaciation. Quat Sci Rev 21: 879-887

Teller JT, Boyd M, Yang ZR, Kor PSG, Fard AM (2005) Alternative routing of Lake Agassiz overflow during the Younger Dryas: new dates, paleotopography, and a re-evaluation. Quat Sci Rev 24: 1890-1905

von Grafenstein U, Erlernkeuser H, Trimborn P (1999) Oxygen and carbon isotopes in modern fresh-water ostracode valves: assessing vital offsets and autecological effects of interest for palaeoclimate studies. Palaeogeogr Palaeoclimatol Palaeoecol 148: 133-152

Wickham JT, Gross DL, Thomas RL (1978) Late Quaternary sediments of Lake Michigan. Illinois State Geol Survey Environ Geol Note 84: 26

Yu S, Colman SM, Lowell TV, Milne GA, Fisher TG, Breckenridge A, Boyd M, Teller JT (2010) Freshwater outburst from Lake Superior as a trigger for the cold event 9300 years ago. Science 328: 1261-1266

Yu Z, McAndrews JH, Eicher U (1997) Middle Holocene dry climate caused by change in atmospheric circulation patterns: Evidence from lake levels and stable isotopes. Geology 25: 251-254

CHAPTER 4

Late Pleistocene and Holocene History and Oxygen and Carbon Isotopic Evolution of Lake Huron

4.1 INTRODUCTION

This study examines the history of Lake Huron, as recorded in the sediments of cores collected from the Goderich and Manitoulin sub-basins (cores 594, 146 and 596, respectively, Fig. 4.1). In particular, we describe the oxygen- and carbon-isotope compositions of ostracodes and clams, which can serve as proxies for lakewater composition, for much of the Holocene in these eastern and southeastern portions of the Huron Basin. There are few previous studies of these portions of the Huron Basin. The cores examined here provide new opportunities to examine the timing and pathways of glacial meltwater floods originating from Lake Agassiz and the possible correlation of these floods with such events in the Michigan Basin.

Rapid influxes of glacial meltwater to both the Arctic and North Atlantic Oceans have been associated with dampening or halting formation of the North Atlantic deep water (NADW) current, which plays a major role in regulating climate in the Northern Hemisphere (Rooth 1982; Broecker et al. 1989; Alley et al. 1997; Barber et al. 1999; Peltier 2007). Lake Agassiz has been identified as the most likely source of such freshwater floods, and massive drops in Agassiz lake level have been associated with major climate events during the late Pleistocene and Holocene, including the Younger Dryas (11.0 – 10.0 ka [12,900 – 11,500 cal] BP), an unnamed event at ~8.3 ka [9300 cal] BP and the '8.2 ka [calendar] event' (~7.7 ka [8,450 cal] BP; Rooth 1982; Alley et al. 1997; Broecker et al. 1989; Clark et al. 2001; Fisher et al. 2002; Teller et al. 2002; Teller and Leverington 2004; Rasmussen et al. 2006; Daley et al. 2009; Murton et al. 2010; Yu et al. 2010).

Figure 4.1. Map of the Huron Basin showing sub-basins and core locations (core 594 - 43°48'02" N 82°06'57" W, water depth 88.5 m; core 146-1 - 44°14'55" N 82°15'16" W, core 146-2 - 44°14'42" N 82°15'48" W, water depth 92.4 m; core 596 - 44°41'13" N 81°54'42" W, water depth 120 m). Major inlets and outlets are also shown.

Prior to its Moorhead phase (before ~11.1 ka [13,000 cal] BP), drainage of Lake Agassiz was directed south to the Gulf of Mexico via the Mississippi River (Teller and Thorleifson 1983; Fisher 2003, 2007; Teller and Leverington 2004). The Younger Dryas (YD) event (11.0 – 10.0 ka [12,900 – 11,500 cal] BP) was originally thought to have been triggered by a large flood through the Great Lakes Basin (Rooth 1982; Teller 1985; Broecker et al. 1989; Lewis and Anderson 1989; Lewis et al. 1994; Teller and Leverington 2004). Newer evidence points to a flood through the Mackenzie River Valley and onto the Arctic Ocean between ~11.1 – 10.8 ka [13,000 – 12,800 cal] BP as the cause of this event (Murton et al. 2010; Teller et al. 2005). By approximately 10.8 ka [12,800 ca] BP, Agassiz outflow was again directed eastwards through the Great Lakes Basin, which potentially resulted in a large flood (the A1 event) responsible for the Wilmette Bed in the Michigan Basin (Chapter 3; Colman et al. 1994a, 1994c; Teller and Leverington 2004). Outflow from Lake Agassiz during its Emerson phase (9.9 – 9.5 ka [11,300 – 10,700 cal] BP for the most part passed through its northwest outlet and onto the Arctic Ocean via the MacKenzie River Valley (Smith and Fisher 1993; Fisher and Smith 1994; Fisher et al. 2002; Fisher 2003, 2007; Teller and Leverington 2004; Lowell et al. 2005; Couch and Eyles 2008; Murton et al. 2010), although flow may have intermittently been directed south to the Gulf of Mexico (Fisher 2003; Boyd 2007). Lake Agassiz drained eastwards through the Great Lakes Basin during its Nipigon phase (9.5 – 8.2 ka [10,700 – 9,100 cal] BP) (Teller and Thorleifson 1983; Teller 1985; Lewis and Anderson 1989; Colman et al. 1994a; Lewis et al. 1994; Teller et al. 2002, 2005; Fisher 2003; Teller and Leverington 20046). The pathway of this water may have been temporarily diverted away from the Huron Basin through an outlet on the NE shore of the Superior Basin between ~8.9 – 8.4 ka (Breckenridge and Johnson 2009; Breckenridge et al. 2010). Sediment cores from Lake Huron in particular are well positioned to provide detailed information about water sources, including meltwater movement, during the early Holocene as the Huron Basin often served as a main conduit for water from upstream Lakes Agassiz and Superior to the St. Lawrence River and the Atlantic Ocean.

4.1.1 Late Pleistocene and Holocene history of the Huron Basin

Early in the history of the Great Lakes Basin, lake levels fluctuated – often over short time periods – as the ice sheet oscillated, as inlets and outlets changed, and as isostatic rebound differentially uplifted and tilted the basins. The initial lake phases within the Huron Basin were present by ~15.5 ka [18,800 cal] BP, but sedimentary records of these early phases were largely erased by the Port Bruce (15 – 13.8 ka [18,500 – 16,400 cal] BP) and Port Huron advances (13 – 12.2 ka [15,300 – 14,050 cal] BP; Lewis et al. 1994). The final advance into the Huron Basin, the Greatlakean advance at 11.8 – 11.1 ka [13,700 – 13,000 cal] BP, extended over the Mackinac sub-basin and the North Channel (Eschman and Karrow 1985; Lewis et al. 1994). The history of the Huron Basin during the late Pleistocene is not as well constrained as for the Michigan Basin, as very few sediment cores spanning this interval have been recovered.

High water levels characterized the Huron, Michigan and southern Superior Basins during Main Lake Algonquin (~11-10.3 ka [12,900 – 12,100 cal] BP), but fell rather abruptly once the retreating Laurentide Ice Sheet opened the North Bay outlet at ~10.3 ka [12,100 cal] BP (Fig. 1; Hansel et al. 1985; Eschman and Karrow 1985; Larsen 1987; Lewis and Anderson 1989; Lewis et al. 1994). Over the following ~2,500 years, water in the Huron Basin alternated between high levels (referred to as the Mattawa highstands) and low levels (the Stanley lowstands). The Mattawa highstand phases were relatively short in duration (~few hundred years) and originated mainly from glacial Lake Agassiz outflow, possibly with the addition of meltwater sourced directly from the Laurentide Ice Sheet or backflooding of Lake Barlow-Ojibway outflow along the Ottawa River Valley (Lewis and Anderson 1989; Lewis et al. 1994, 2005, 2007; Rea et al. 1994a, 1994b; Breckenridge 2007).

Sediment records from the Huron Basin indicate three large Mattawa flooding events (Lewis and Anderson 1989; Lewis et al. 1994, 2005, 2007, 2008a; Rea et al. 1994a, 1994b; Moore et al. 1994, 2000; Dettman et al. 1995; Godsey et al. 1999; Macdonald and Longstaffe 2008; Breckenridge and Johnson 2009). The designation of “early” “main” or “late” in reference to Mattawa highstands or Stanley lowstands is largely omitted in more recent studies (Breckenridge and Johnson 2009; Breckenridge et al. 2010; Fisher et al. 2010; Brooks and Medioli 2010; Brooks et al. 2010). For clarity and ease of discussion, the Mattawa highstands are herein referred to as Mattawa I, II and III. Mattawa I occurred between 9.6 – 9.4 ka [11,100 – 10,600 cal] BP. Mattawa III occurred at ~8.2 ka [9,100 cal] BP (Lewis and Anderson 1989; Lewis et al. 1994, 2005, 2007, 2008a; Rea et al. 1994a, 1994b; Breckenridge and Johnson 2009). There is uncertainty over the timing of Mattawa II as radiocarbon dates between 9 – 8 ka [10,000 – 9,000 cal] BP on Huron Basin sediments are generally unreliable (Breckenridge and Johnson 2009). Lake level chronology following Lewis et al. (2005) suggests that Mattawa II occurred at ~8.7 ka [9,650 cal] BP. Breckenridge and Johnson (2009) correlated Huron sediment records to the better-dated Michigan records, and placed the Mattawa II flood at 8.4 ka [9,450 cal] BP. Breckenridge and Johnson (2009) refer to the Mattawa II and III as a 'two-pulsed' flooding event that occurred from 8.4 – 8.2 ka [9,450 – 9,100 cal] BP. These two floods in the Huron Basin correlate to the A2 event in the Michigan Basin (Colman et al. 1994a) and are associated with a large drop in water levels in the Superior Basin as well as a major cooling episode in the Northern Hemisphere (Fleitmann et al. 2008; Breckenridge et al. 2010; Yu et al. 2010). Here we use the date of 8.4 ka for the Mattawa II flood because of its agreement with the histories of adjacent lake basins.

In the absence of large influxes of water from upstream Lakes Agassiz and/or Superior, the Stanley lowstands dominated much of the early Holocene history of the Huron Basin. These lowstands were first identified as sedimentary intervals of coarser grain size within sediment cores (Rea et al. 1994a) and as intervals showing erosional truncation in seismic reflection profiles (Moore et al. 1994). New evidence for closed basin conditions at ~8.5 ka [9,500 cal] BP (Brooks et al. 2010; Brooks and Medioli 2010), in addition to the well-documented closed basin from ~7.9 – 7.5 ka [8,650 – 8,350 cal] BP (Lewis et al. 2005, 2007, 2008b), suggest that the lowstand phases may have been linked to the dry climatic conditions affecting much of the early to mid Holocene (Dorale et al. 1992; Kutzbach and Webb 1993; Krishnamurthy et al. 1995; Dean et al. 1996; Edwards et al. 1996; Yu et al. 1997; Brooks et al. 2010; Lovan and Krishnamurthy 2011).

The Laurentide Ice Sheet retreated over Hudson Bay at ~8.1 ka [9,000 cal] BP, causing Lakes Agassiz and Ojibway to merge in the Hudson Bay lowlands (Bajc et al. 1997; Barber et al. 1999) and diverting outflow away from the Great Lakes and into the Ottawa River Valley (Lewis and Anderson 1989; Lewis et al. 1994; Teller and Leverington 2004). The Mattawa-Stanley phase of the Huron Basin ended as the North Bay outlet was uplifted, causing lake levels to rise gradually during the Nipissing transgression. This transgression peaked at ~ 5 ka [5,700 cal] BP when the outlet shifted from North Bay to Port Huron (Thompson and Baedke 1997; Lewis et al. 2007). Erosion of the Port Huron outlet caused abandonment of Lake Michigan's Chicago outlet at ~ 3.8 ka [4,200 cal] BP; Michigan lakewater has since drained through the Straits of Mackinac into Lake Huron (Eschman and Karrow 1985; Hansel et al. 1985; Larson et al. 1985). Continued erosion of the Port Huron outlet has caused Lakes Michigan and Huron to drop to their current levels of 176 m asl (The Great Lakes Environmental Atlas 1995).

Earlier studies of the isotopic composition of biogenic carbonates from the Huron Basin suggested that low-^{18}O values characterized Stanley lowstands and high-^{18}O waters, Mattawa highstands (Lewis et al. 1994; Rea et al. 1994a, 1994b; Dettman et al. 1995; Godsey et al. 1999; Moore et al. 2000; Odegaard et al. 2003; Macdonald and Longstaffe 2008). In contrast, Lewis and Anderson (1989) proposed that large inflows from upstream Lake Agassiz would substantially raise lake levels and lower the oxygen-isotope compositions of the lakewater. The explanation provided by Rea et al. (1994a) for this puzzling association of lowstand phases and low $\delta^{18}O_{lakewater}$ values was that a more or less consistent flow of meltwater entered the Huron Basin, which was most noticeable when other sources of water (e.g. large, upstream Agassiz floods) were not present. During highstand phases, lakewater was impounded within the basin by high or constricted outlets, which allowed the more ^{18}O-rich precipitation and runoff to accumulate. Evaporation would have further enriched lakewater in ^{18}O during high lake phases, which are characterized by longer water residence times (Rea et al. 1994a). Conversely, lowstand phases are believed to have had relatively short residence times, which prevented precipitation and runoff from accumulating.

The chronologies on which Rea et al.'s (1994a) findings were based were overly reliant on radiocarbon dates, many of which have since been found not to reflect depositional ages. More recent studies in the Huron Basin correlate periods of low-^{18}O values to the Mattawa highstands, which likely originated from Lake Agassiz, as per the original model of Lewis and Anderson (1989) (Lewis et al. 2005, 2007, 2008a; Breckenridge and Johnson 2009; Breckenridge et al 2010; Brooks et al. 2010; Brooks and Medioli 2010).

The association of low lake levels and low $\delta^{18}O_{lakewater}$ values, following the model of Rea et al. (1994a), has not been previously applied to the history of the Michigan Basin; large influxes of low-^{18}O waters have always been attributed to Lake Agassiz and/or direct contributions from the ice sheet (Colman et al. 1990, 1994a, 1994b, 1994c; Forester et al. 1994; Breckenridge and Johnson 2009; Chapter 3, this thesis). That said, identifying the downstream flow paths of Lake Agassiz waters is complicated by conflicting results for the oxygen-isotope composition of its waters. A comparison of benthic versus pelagic proxies for Lake Agassiz's $\delta^{18}O_{lakewater}$ values suggest that surface waters may have been enriched by up to 18 ‰ over bottom waters as a result of the accumulation of precipitation and runoff, as well as additional enrichment via evaporation (Last et al. 1994; Remenda et al. 1994; Buhay and Betcher 1998; Birks et al. 2007). Nonetheless, most researchers generally assume that Lake Agassiz waters present in downstream basins can be identified by their low δ^{18}O values.

4.2 MATERIALS AND METHODS

Three piston cores were collected during two separate coring cruises on Lake Huron (Fig. 4.1); core 146 is comprised of two cores collected within 17 m of each other, and was collected in 2003 from the Goderich sub-basin. The first core retrieved at this site (core 146-1, 15 m in length) had a crack in its liner, so a second shorter core (core 146-2, nearly 12 m in length) was retrieved. The combined sediments from these two cores make up core 146; the first, cracked core (146-1) accounts for sediments from a depth of 12.14 to 14.8 m, and the shorter intact core (146-2) accounts for sediments from a depth of 11.88 m to the top of the sediment (core depth 0 m). There is a 26 cm gap in the sediments between the two cores. Core 594 (~15 m in length), also retrieved from the Goderich sub-basin, and core 596 (~12 m in length) from the Manitoulin sub-basin, were collected in 2004. The cores were collected by the *CCGS Limnos* and are permanently stored at The University of Western Ontario.

The cores were cut open longitudinally and biogenic carbonates were sampled from 20 cm-long segments. Most sediment adhering to ostracode valves was removed during wet sieving, but the few samples retaining some mud were treated overnight in a solution of equal parts bleach (5 % sodium hypochlorite) and distilled water. Adult valves were preferentially selected for analysis. Two to four ostracode valves were normally required, depending on their weight. *Pisidium* shells were fragmented and/or powdered to obtain the correct amount of carbonate required for analysis. The oxygen- and carbon-isotope compositions of the biogenic carbonates were obtained by reaction with orthophosphoric acid at 90 °C, using a Micromass MultiPrep device coupled to a VG Optima mass spectrometer. All results are reported in the standard δ-notation:

$$\delta^{18}O \text{ or } \delta^{13}C = [(R_{sample}/R_{standard}) - 1] \text{ (permil, or ‰)} \qquad (1)$$

where R_{sample} and $R_{standard}$ are the ratios of $^{18}O/^{16}O$ (or $^{13}C/^{12}C$) in the sample and standard, respectively. Carbonate and calculated paleo-lakewater $\delta^{18}O$ values are reported relative to VSMOW and carbonate $\delta^{13}C$ values are reported relative to VPDB, as calibrated using defined values for NBS-19 (Coplen 1996). The $\delta^{18}O$ and $\delta^{13}C$ values were reproducible to better than ±0.2 ‰. Accuracy was evaluated using internal calcite standards, WS-1 and Suprapur, calibrated against NBS-19 and verified versus NBS-18. WS-1 had an average $\delta^{18}O$ value of 26.2 ± 0.1 ‰ (1σ; n = 34) and an average $\delta^{13}C$ value of 0.74 ± 0.1 ‰ (1σ; n = 32), which compares well with its accepted values of 26.2 and 0.76 ‰, respectively. Suprapur had an average $\delta^{18}O$ value of 13.2 ± 0.1 ‰ (1σ; n = 108), which compares well with its accepted value of 13.3 ‰. NBS-18 had an average $\delta^{13}C$ value of 7.2 ± 0.2 ‰ (1σ; n = 110), which compares well with its accepted value of 7.2 ‰.

Biogenic carbonates and large pieces of organic matter were picked from the dried sediment using camel hairs or tweezers. Five species of ostracodes (*Candona subtriangulata*, *Candona rawsoni*, *Candona crogmaniana*, *Cytherissa lacustris* and *Limnocythere friabilis*) and bivalves from the *Pisidium* (Pea Clam) genus were identified from cores 594 and 146. Only *C. subtriangulata* was found in core 596. The isotopic compositions of the various ostracode species were measured separately because the various species have different (and specific) optimum growth temperatures and live in slightly different environments. *Limnocythere friabilis* valves were not analyzed. The oxygen-isotope compositions of paleolakewater were calculated from the measured valve/shell values using the fractionation factors measured for each species in modern Lake Huron (Chapter 2, this thesis).

Sediment colour was classified using Munsell colour codes (Munsell Colour 2000). Digital images of the core sections were obtained using a GEOTEK® multi-sensor core logger at the Graduate School of Oceanography, University of Rhode Island. X-ray diffraction patterns were obtained for bulk sediment samples and blue-black mineral grains isolated from core 594. Bulk sediment samples were dried at room temperature, powdered with a stainless steel mortar and pestle, and backpacked into Al sample holders to ensure random orientation of the sediment grains. Grains of the blue-black mineral were crushed, dispersed in a small amount of distilled water, pipetted onto glass slides and allowed to dry at room temperature. All samples were analyzed in the Department of Earth Sciences, The University of Western Ontario, using a Rigaku RU-200BVH rotating anode X-ray diffractometer equipped with Co K-alpha radiation. The samples were scanned from 2° to 82° 2θ, using a step size of 0.02° 2θ and a scan rate of 10° 2θ/min. The relative abundances of individual minerals present within the bulk sediment samples were determined using the background-subtracted peak height of the most intense, characteristic diffractions of each phase. A form factor of x1 was applied to the most intense diffraction height of most phases, but form factors of x2 were used for kaolinite and chlorite, and x4 for illite. Accuracy of mineral abundance estimates is within 5 %.

Radiocarbon dates were obtained for five samples of organic matter (twigs, seeds and insect fragments) and three bivalve samples (mixed *Pisidium* clams) from eight intervals within core 594. No datable material was found in either core 146 or 596. All ages were determined using accelerator mass spectrometry (AMS) at the NSF-Arizona AMS Facility, The University of Arizona.

Dr. Thane Anderson, Geological Survey of Canada, Ottawa, conducted pollen grain analyses of 22 samples from core 594 and 16 samples from core 596. Pollen was isolated from the sediment samples using hydrochloric and hydrofluoric acids followed by acetolysis. The pollen residues were then mounted in Hoyers medium and 200-250 tree, shrub and herb pollen, excluding aquatics, counted from each sample to derive a pollen sum. Samples with low pollen concentrations were sieved using a 10 µm mesh sieve to reduce the fine clay fraction and concentrate the pollen grains. A pollen sum of 200 could not be obtained for the basal two samples of core 596 because pollen was extremely scarce. The pollen data was entered into a TILIA spreadsheet and pollen figures were prepared using the TILIA graphing program. Ages were assigned to the pollen stratigraphies by correlation with similar radiocarbon-dated pollen stratigraphies known for nearby terrestrial sites, such as Manitoulin Island (Anderson 2002; Anderson and Lewis 2002), Western Lake Huron (Lewis and Anderson 1989), Twiss Marl Pond (Southwestern Ontario; Yu 2000), 18 Mile River (near Lake Nipissing; Karrow et al. 1975) and Lake Sixteen (Eastern Michigan; Futyma and Miller 1986).

4.3 RESULTS

4.3.1 Images

Core images are provided in Figure 4.2 and are annotated with radiocarbon dates, pollen ages and key sedimentary features. Unfortunately, these cores were opened up to two years before images could be obtained and a few sections of the cores had dried out while in refrigerated storage. Additionally, a few intervals from core 594 are missing

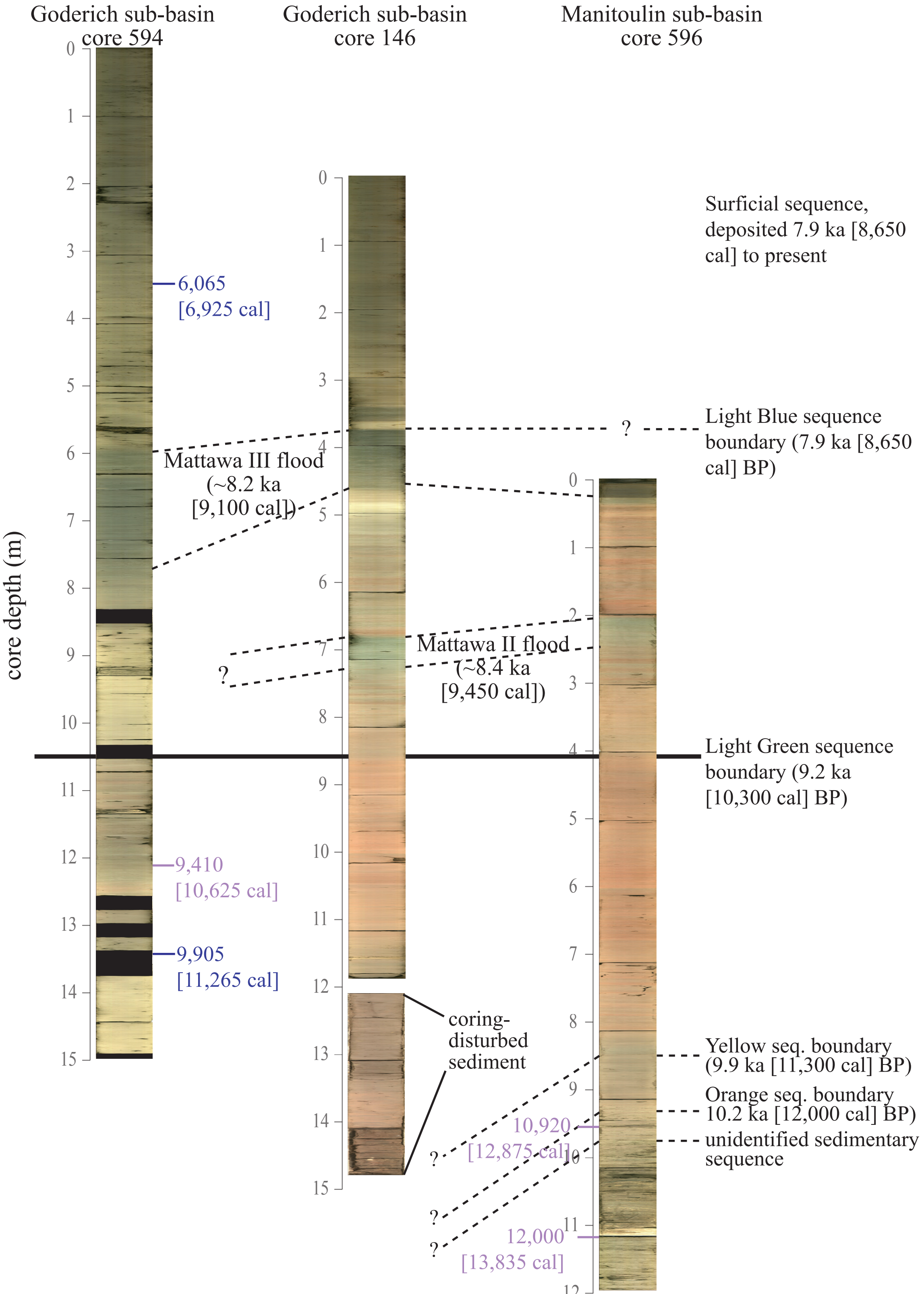

Figure 4.2. Images of the Huron Basin sediment cores. The cores are hung at a datum of ~9.2 ^{14}C ka [10,300 cal] BP (thick black line), the Light Green sequence boundary. Sedimentary sequences were identified following Moore et al. (1994), Rea et al. (1994a) and Godsey et al. (1999). Blacked out regions in core 594 represent sediment that was used for radiocarbon analyses. Applicable radiocarbon (blue) and pollen (purple) ages, sedimentary sequences and key sedimentary features are shown where appropriate.

from the photographic record because extra sediment was needed for radiocarbon analyses.

4.3.2 Core descriptions

In general, the stratigraphic sequence of glacial and postglacial sediments in all of the Great Lakes is similar. Bedrock in most regions of the lakes is covered by till deposited by the LIS. As the early lakes formed against the retreating ice sheet, glaciolacustrine sediments, very fine-grained, often reddish in colour and occasionally varved, were deposited on top of the tills (Rea et al. 1981). Lowstand phases during the early to mid Holocene resulted in erosion of exposed glaciolacustrine clays, deposition of shallow-water sediments around the new low-level shorelines, and continued deposition of fine-grained sediments in the deepest portions of the basins. Postglacial muds, fine grained, grey and often containing thin (~mm-thick) black bands of iron-sulfides, have been deposited more or less continuously since the mid Holocene and lie overtop of these earlier deposits (Rea et al. 1981).

Previous descriptions of the sedimentary units within the Huron Basin are based on relatively short piston cores and acoustic profiles of the sediments obtained from northern Lake Huron and Georgian Bay (Lewis et al. 1994; Moore et al. 1994; Rea et al. 1994a; Dobson et al. 1995). Fluctuating lake levels through time have exerted strong control on the grain-size distributions of sediments within the Great Lakes, with coarser sediments deposited during lowstand phases appearing as reflective boundaries in acoustic profiles (Thomas et al. 1973; Colman et al. 1994b; Moore et al. 1994; Lewis et al. 1994). Seven prominent reflection horizons marking lowstands within the Huron and Michigan Basins were identified and mapped, with the resulting sedimentary sequences being named after the colour arbitrarily assigned to their upper reflective (coarse-grained) boundary (Moore et al. 1994; Rea et al. 1994a; Dobson et al. 1995); e.g. the Yellow sequence comprises sediments deposited above the Orange reflector and below the Yellow reflector. Cores from more southerly locations in the Huron Basin are examined in this study, and are described below.

These previous studies largely sampled and described sedimentary sequences deposited during the Holocene. Sediments deposited in the Huron Basin during the late Pleistocene were not described in these studies; although these units were identified in the seismic reflection profiles (Moore et al. 1994; Dobson et al. 1995) they were not sampled by piston coring. Below we describe some late Pleistocene sediments, but are unable to assign them to a sedimentary sequence.

Goderich sub-basin core 594

A short sequence of sediments, ~25 cm, was extruded from the bottom of the core liner as it was brought onto the boat deck immediately upon its retrieval. This may have occurred as a result of gas expansion within the sediment, and/or over-pressurization of the sediment. Over-pressurization may occur either because of over-penetration of the core liner into the sediment, or because extra material was added to the core liner as it was pulled from the sediment column, i.e., collection of a repeated interval (CFM Lewis, pers. comm.). The ~25 cm-long portion of extruded material was collected in a plastic zip-lock bag after it had expanded out of the core liner. A radiocarbon date measured on a sample of plant fragments collected from this parcel of sediment implies that this interval is a repeated section. Sediment and biogenic carbonates from this interval are not considered further.

Sediments from the bottom of the core at 15 m to a depth of ~10.5 m are characterized by mm-scale tricolour banding (grey layer – Munsell Soil Colour Chart value 5Y 5/1; reddish layer – 10YR 5/2; darker layer – 5Y 5/2), which is often faint and occurs within overall greyish brown (2.5Y 5/2, 10YR 5/2) clay-rich sediment (Fig. 4.2). Some simple red (10YR 5/2) and grey (2.5Y 5/2) banding also occurs within this unit. Based largely on the presence of the distinctive tricolour banding, this interval is interpreted as the Light Green sequence, which was deposited from 9.9 to 9.2 ka [11,300 – 10,300 cal] BP (Lewis et al. 2007; Moore et al. 1994; Rea et al. 1994a; Godsey et al. 1999).

Sediments from a depth of ~10.5 to ~8.7 m exhibit faint banding (1-2 mm) in shades of grey (5Y 5/1), olive grey (5Y 5/2) and greyish brown (2.5Y 5/2). From ~8.7 – 7.75 m, the sediment is a fairly homogeneous greyish-brown colour (2.5Y 5/2, 5Y 5/1). A thick, dark-grey bed (5Y 4/1 from ~7.75 – 6.0 m; Fig 4.2) occurs at the top of this interval. This bed is associated with an overall increase in grain size from ~8.2 – 6.0 m and a decrease in the number of ostracode and clams. Charophyte stem encrustations (gyrogonites) as well as vivianite grains are numerous within this section. Sediments from ~10.5 – 6.0 m are interpreted as the Light Blue sequence, which was deposited from 9.2 – 7.9 ka [10,300 – 8,650 cal] BP (Lewis et al. 2007; Moore et al. 1994; Rea et al. 1994a; Godsey et al. 1999). Sediments of the Light Blue sequence are less red that those of the underlying Light Green sequence.

Sediments from ~6.0 m to the top of the core are very clay-rich and gradually darken from grey (5Y 5/1) at ~6.0 m to very dark grey (5Y 3/1) and dark olive grey (5Y 3/2) at the top of this interval. These sediments exhibit prominent black iron-sulfide banding (Fig. 4.3a). Vivianite grains are particularly plentiful from 3.6 – 1.6 m. Based on the massive grey nature of the sediments as well as the characteristic black banding, this interval is interpreted as the Surface sequence, which has been deposited since ~7.9 ka [8,650 cal] BP (Moore et al. 1994; Rea et al. 1994a; Lewis et al. 2005, 2007; Odegaard et al. 2003).

The sediments of core 594 exhibit more black iron-sulfide banding than has been previously reported for cores from the Huron Basin. This banding was faint and intermittent from the bottom of the core to 13.4 m and was absent from 13.4 – 10.5 m. Banding was sparse from 10.5 to 6.0 m and then became very prominent to the top of the core (Fig. 4.3a). The banding is not easily apparent in the core images (Fig. 4.2), likely because of iron-sulfide oxidation between the time of core opening and imaging.

Goderich sub-basin core 146

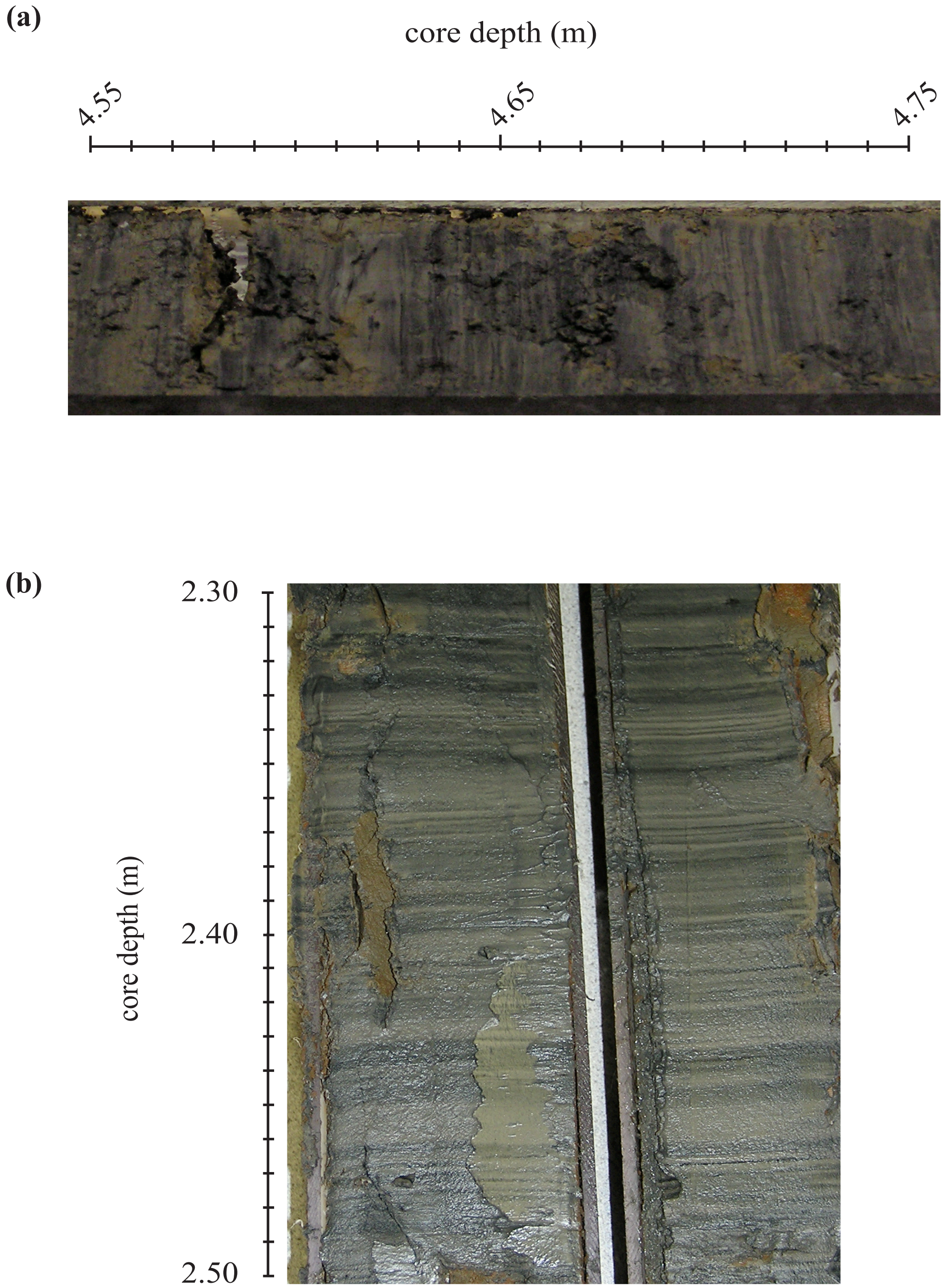

Figure 4.3. Photographs of the Surface sedimentary sequence within cores 594 (a) and 146 (b). The black bands of iron-sulfide minerals oxidized and disappeared shortly after exposure to air.

Sediment from ~14.8 – 12.14 m, which is composed entirely of sediments from core 146-1 (the longer core from this site that was partially split during its collection) is red to dark brown, very sandy, and contained red to beige clay clasts as well as relatively low numbers of ostracodes. Many Paleozoic fossil fragments, similar to those observed in the Equality Formation from the South Chippewa sub-basin core (core 101, Chapter 3, this thesis), were present in this interval. A few (~5) pronounced red-grey couplets, possibly varves, occur at depths of ~13.0 m, 12.75 m and at the top of this interval at 12.14 m. The remainder of sediment within this interval is massive with few structures, and may be disturbed. Vertical streaks, perhaps vertically stretched beds, were found within this interval, especially within the lowermost ~1 m (Fig. 4.4). Vertical streaking is often an artifact of coring and suggests that this sediment was drawn into the piston corer during its retrieval and likely does not accurately represent deposits from this depth interval. Accordingly, this interval of core 146 is excluded from further discussion.

Sediments from the bottom of core 146-2 at 11.88 m to a depth of 8.6 m exhibit tricolour banding (grey layer – 7.5YR 5/2; reddish layer – 5YR 5/3, 7.5YR 5/3; darker layer – 10YR 5/2), characteristic of the Light Green sequence (deposited 9.9 – 9.2 ka [11,300 – 10,300 cal] BP) (Lewis et al. 2007; Moore et al. 1994; Rea et al. 1994a; Godsey et al. 1999). This tricolour banding is most noticeable from ~11.3 – 10.5 m (Fig. 4.2).

Sediments from 8.6 – 3.8 m are overall more grey in colour (10YR 5/2, 2.5Y 5/2) than the underlying Light Green sequence, which makes the frequent cm-scale bands of red sediment (7.5YR 5/2) more distinctly visible. A thick, sandy interval occurs from ~8.4 – 6.8 m, and within it, a thick grey (5Y 5/1) clay bed is present between 7.2 – 6.8 m. This grey clay initially exhibited pronounced black iron-sulfide streaking. The grey clay occurs directly above a pronounced sequence of red-grey bands and has a sharp boundary with overlying red-grey banded sediments, which continue to ~5.2 m. The interval from 5.1 – ~3.6 m contains abundant shallow-water indicators, such as sand, seeds and charophyte gyrogonites. A thick dark grey (5Y 4/1) bed occurs from 4.6 – 3.8 m. This bed contained a relatively low amount of biogenic carbonates and it originally showed intermittent black banding. This interval of greyer sediments from 8.6 – 3.8 m is

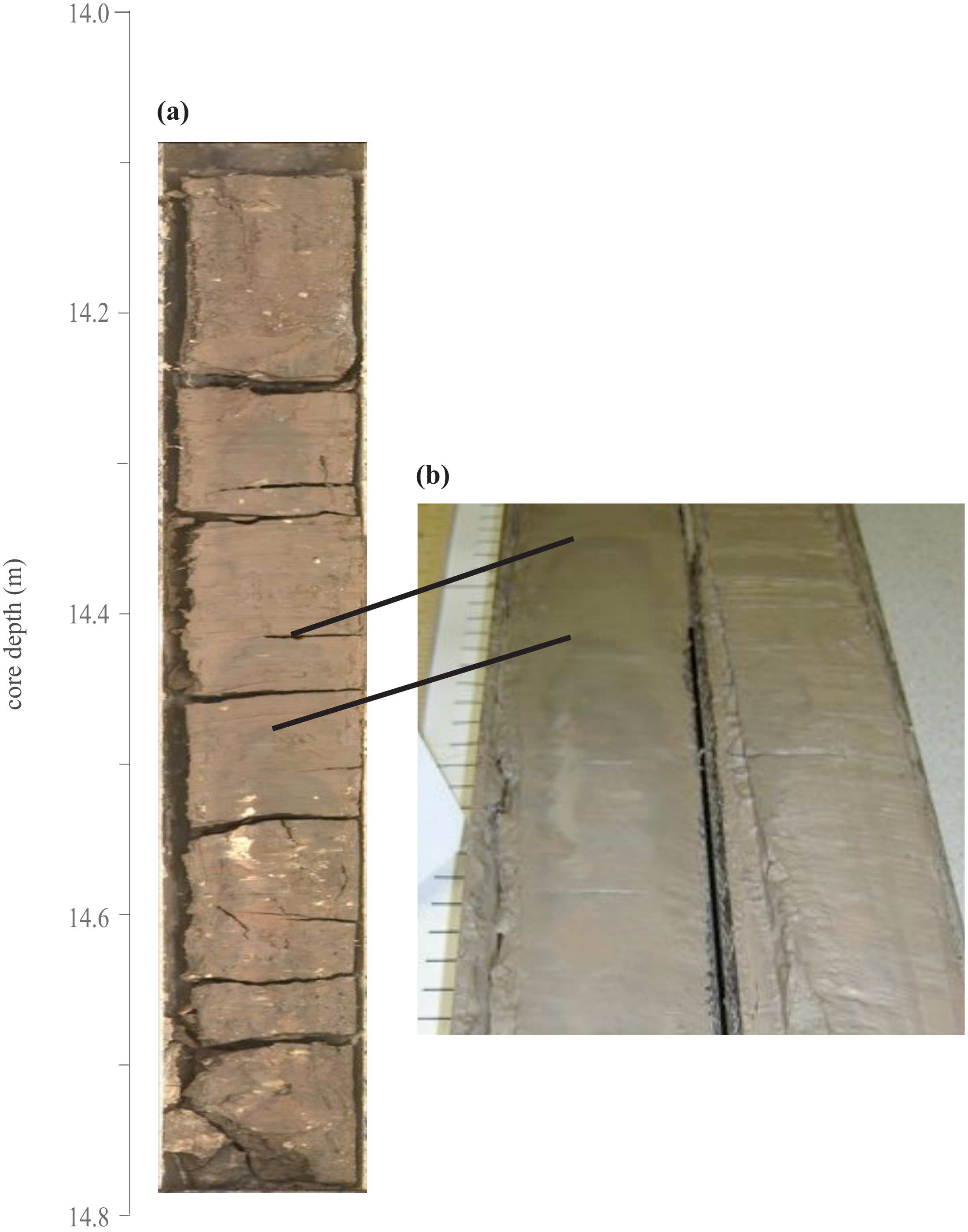

Figure 4.4. Lowermost section of the Goderich sub-basin core 146-1 illustrating the disturbed nature of the sediments, and in particular, vertical streaking within the sediment. Such vertical streaking is often an artifact of coring and suggests that this sediment was drawn into the bottom of the piston corer during its collection. The sediment had largely dried out by the time the core image (a) was taken (the core image is stretched horizontally ~1.5 times to show detail). The photograph (b) was taken when the sediment was still fresh, immediately after the core liner was opened. Note the many red and beige clay clasts present in the sediment.

interpreted to be the Light Blue sequence (9.2 – 7.9 ka [10,300 – 8,650 cal] BP (Lewis et al. 2007; Moore et al. 1994; Rea et al. 1994a; Odegaard et al. 2003). Three samples of clams in this core at ~6.6, 6.2 and 5.8 m are likely reworked. Clam shells in these intervals were very rare, showed minor signs of abrasion and their oxygen-isotope compositions differed significantly from those of the ostracode *C. subtriangulata*, which was present in greater quantities.

Sediment in core 146 from 3.8 m to the top of the core is dark grey (2.5Y 4/1) to greyish brown (2.5Y 5/2) and exhibited pronounced black iron-sulfide banding (Fig. 4.3b). From 3.0 – 1.6 m, macroscopic organic matter in the sediments increased in abundance, with seeds and charophyte gyrogonites being quite common. Vivianite grains were common between 2.4 – 1.6 m. Based on the distinctive black banding and the massive grey nature of the sediments, this uppermost sedimentary interval is interpreted as the Surface sequence, which has been deposited since 7.9 ka [8,650 cal] BP (Moore et al. 1994; Rea et al. 1994a; Lewis et al. 2005, 2007; Odegaard et al. 2003).

Manitoulin sub-basin core 596

The lowermost sediments of core 596, from the bottom of the core at ~11.95 to 9.7 m, are greyish brown (2.5Y 5/2), very dense, very hard, and exhibit a large range in grain size. This unit overall is very clay-rich but it also contains abundant sand and larger fragments (pebbles up to ~7 cm in length; Fig. 4.5). Many Paleozoic fossil fragments, similar to those observed in core 146-1 and within the Equality Formation of the South Chippewa sub-basin core (core 101, Chapter 3, this thesis), were present in core 596 sediments, and were particularly plentiful in this lowermost unit. Sediment matching this description has not been previously described for Huron Basin deposits. The two earliest glaciolacustrine units, the Dark Blue (~15.5 – 11.4 ka [18,800 – 13,300 cal] BP) and Dark Green (11.4 – 11.2 ka [13,300 – 13,100 cal] BP) sequences, have been identified in seismic reflection profiles (Moore et al. 1994; Dobson et al. 1995) but have not been sampled by coring. It is likely that this unit belongs to one, or both, of these sedimentary

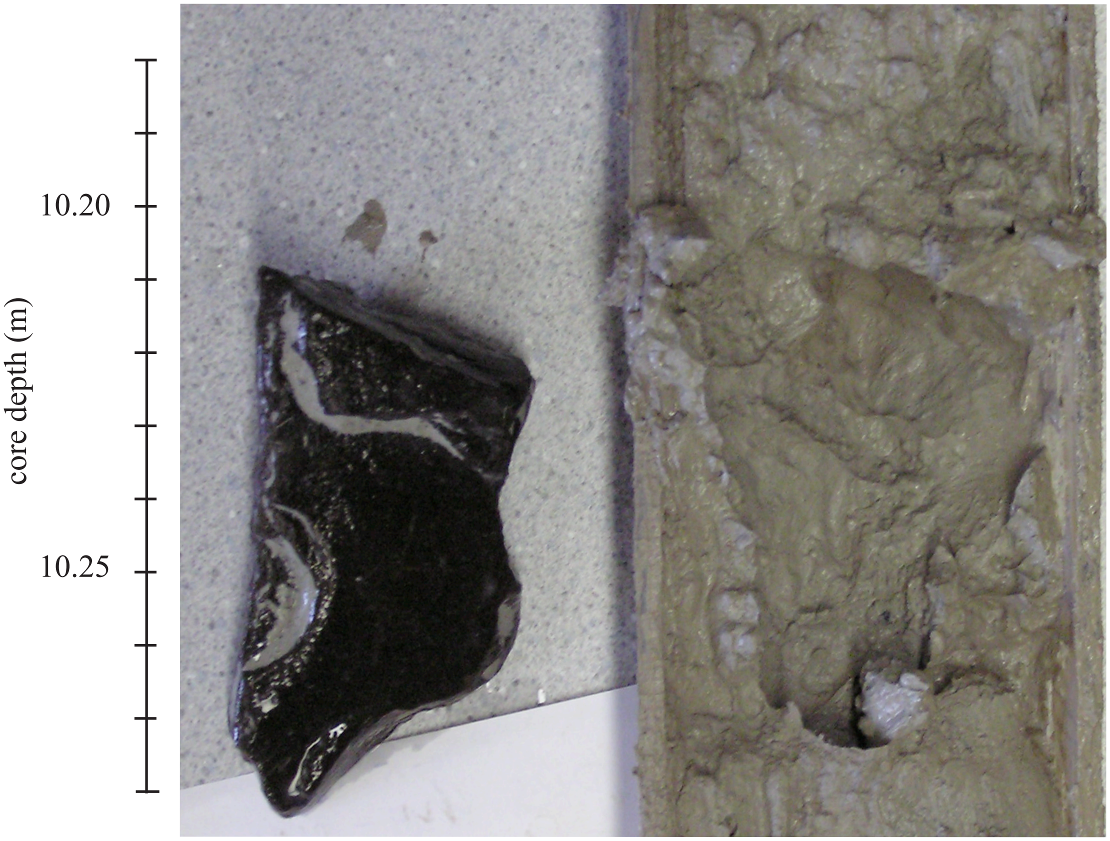

Figure 4.5. Photograph of a pebble-sized clast found in the lowermost sediments of core 596.

sequences. Based on the large range of grain sizes and clay-rich nature of this lowermost unit, we describe this sediment as a stony till.

Sediment from 9.7 – 9.3 m exhibits banding in various shades of reddish (7.5YR 5/1), greyish brown (10YR 5/2) and grey (2.5Y 5/1, 2.5Y 6/1). This sediment is quite sandy and also contains some large pebbles (up to ~1 cm in diameter). This unit is identified as the Orange sequence (11.2 – 10.2 ka [13,100 – 12,000 cal] BP (Moore et al. 1994; Rea et al. 1994a; Dobson et al. 1995), which has been described as very "stiff" sediment with broad reddish and greyish brown horizons and faint banding (Rea et al. 1994a; Dobson et al. 1995).

Sediment from 9.3 – 8.5 m is characterized by thin (~2-3 mm-scale) reddish (10YR 5/2) and grey bands (2.5Y 5/1, 2.5Y 5/2) (Fig. 4.6). Such banding is commonly described as varves (Rea et al. 1994a; Godsey et al. 1999). The sediments of this interval are very compact and very sandy. Red-grey varves are characteristic of the Yellow sequence, which was deposited from 10.2 – 9.9 ka [11,970 – 11,265 cal] BP during a period of falling water levels following the Main Algonquin phase (Lewis et al. 1994; Moore et al. 1994; Rea et al. 1994a; Godsey et al. 1999).

The transition from red-grey varves to the overlying fainter tricolour bedding is subtle but likely occurs at approximately 8.5 m. From this depth to 4.05 m, the sediment undergoes a transition from tricolour banding (grey layer – 7.5YR 5/2; reddish layer – 5YR 5/2, 5YR 5/3, 7.5YR 5/3; darker layer – 10YR 5/2, which is found throughout most of this interval) to more massive red-brown (10YR 5/2) sediment displaying only faint reddish (7.5YR 5/2) banding. Based on the occurrence of characteristic tricolour banding, this interval is interpreted as the Light Green sequence, which was deposited from 9.9 – 9.2 ka [11,300 – 10,300 cal] BP (Lewis et al. 2007; Moore et al. 1994; Rea et al. 1994a; Godsey et al. 1999).

Sediments from 4.05 m to the top of the core are overall grayish brown (10YR 5/2, 10YR 5/3, 2.5Y 5/2) and for the most part exhibit intermittent thin and faint red

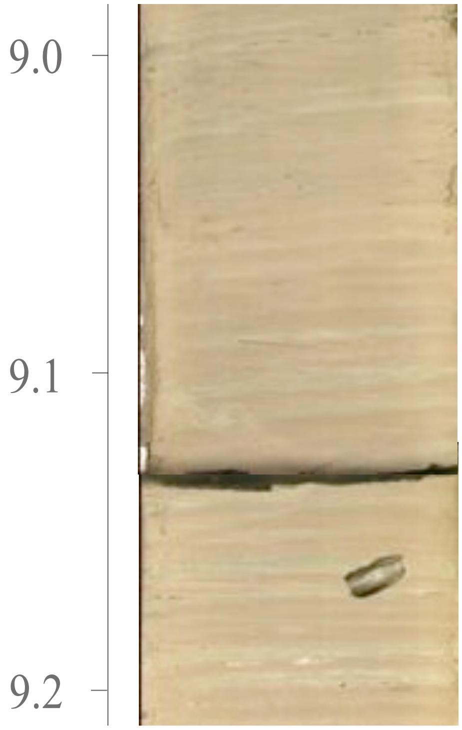

Figure 4.6. Image of the red-grey varves that characterize the Yellow sedimentary sequence (deposited from 10.2 - 9.9 ka [12,000 - 11,300 cal] BP) in the Manitoulin sub-basin core 596.

(7.5YR 5/2) banding. A short sequence of very pronounced red-grey couplets (red layer – 7.5 YR 5/2, 7.5YR 5/3; grey layer – 10YR 5/2, 2.5YR 5/2) occurs between 3.0 – 2.5 m. These couplets are overlain by a distinct, thick grey bed (5Y 5/1) from ~2.4 – 2.0 m, which in turn makes a sharp contact with overlying redder (7.5YR 5/2) sediments. The sediments from ~30 – 20 cm are grey (5Y 5/1) and are sharply overlain by a dark grey bed (2.5Y 4.1) that occurs from ~20 – 7 cm. This dark grey bed originally showed black iron-sulfide banding. The uppermost 2 cm of sediment (from 7 – 5 cm) is black in colour (5Y 2.5/1). These sediments are much softer than the underlying sedimentary units and have become very moldy after ~7 years in storage. The core liner from 5 – 0 cm was devoid of sediment. Based on the overall greyer to browner colour of this interval, together with intermittent yet prominent red banding, this interval is interpreted as the Light Blue sequence, which was deposited from 9.2 – 7.9 ka [10,300 – 8,650 cal] BP (Lewis et al. 2007; Moore et al. 1994; Rea et al. 1994a; Odegaard et al. 2003). Both the lower grey bed at 2.4 – 2.0 m and the upper dark grey bed at 20 – 7 cm are similar in colour, thickness (lower grey bed only), and position within the Light Blue sequence to the beds observed at ~7.2 – 6.8 and 4.6 – 3.8 m in core 146. No sediments from the Surface sequence were observed in core 596.

4.3.3 Radiocarbon Dates

Radiocarbon dates obtained for terrestrial organic matter and shelly material from core 594 are listed in Table 4.1. The dates measured for biogenic carbonates were corrected for the hard-water effect using a value of 438 years as calculated for Lake Huron (Rea and Colman 1995; Moore et al. 1998). Calibrated dates reported here (in square brackets following radiocarbon dates) were obtained using INTCAL04 (Reimer et al. 2004) and ranges on these calibrated dates were obtained using OxCal 4.1.

4.3.4 Pollen Stratigraphy

Pollen stratigraphies prepared by Thane Anderson for cores 594 and 596 are illustrated in Figures 4.7 and 4.8, respectively. The specific pollen zones are based on

Table 4.1. Radiocarbon dates obtained for the Lake Huron cores

Core	Sample Interval (m)	Lab No.	Material	$\delta^{13}C$ (‰, VPBD)	^{14}C Date (year BP)	HWE Correction[1]	Accepted Date	Calibrated Date[2] (cal year BP)	Range[3] (cal year BP)
594	3.4 - 3.6	AA64477	plant/insect fragments	-26.3	6065 ± 47		6065	6925	7155 - 6785
594	6.2 - 6.4	AA64478	plant/insect fragments	-25.1	9169 ± 65		9169	10 270	10 506 - 10 226
594	8.6 - 8.7	AA72071	mixed *Pisidium* clams	-4.5	9946 ± 56	-438	9508	10 745	11 088 - 10 590
594	9.2 - 9.4	AA64479	twigs	-25.9	9489 ± 65		9489	10 730	11 087 - 10 575
594	12.4 - 12.6	AA64480	plant fragments	-27.6	2549 ± 41		2549	2725	2755 - 2488
594	13.4 - 13.5	AA72072	mixed *Pisidium* clams	-5.6	10 343 ± 60	-438	9905	11 265	11 605 - 11 208
594	14.9 - 15.0	AA72073	mixed *Pisidium* clams	-4.3	9716 ± 55	-438	9278	10 475	10 643 - 10 269
594	15.0 - ~15.25	AA64481	plant fragments	-25.2	8626 ± 63		8626	9550	9765 - 9490

[1] hard-water effect correction is from Rea and Colman (1995) and Moore et al. (1998)

[2] radiocarbon dates were converted to calibrated dates using INTCAL04 (Reimer et al. 2004)

[3] ranges on calibrated dates were calculated using OxCal 4.1

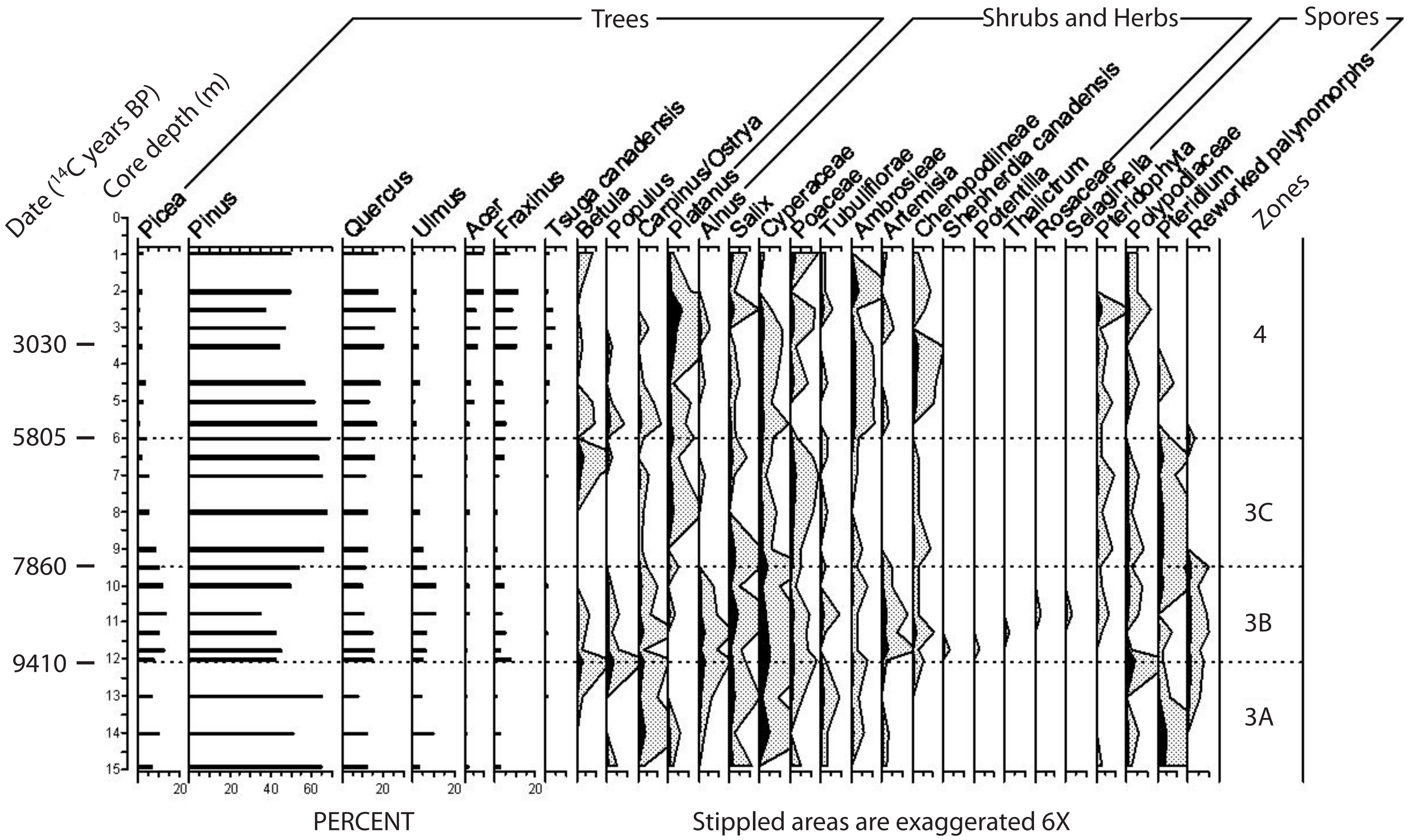

Figure 4.7. Pollen stratigraphy for Goderich sub-basin core 594. The pollen sum is based on 200-250 tree, shrub and herb pollen excluding aquatic pollen; the pollen percentages are calculated on this sum. Pollen analyst: Thane Anderson.

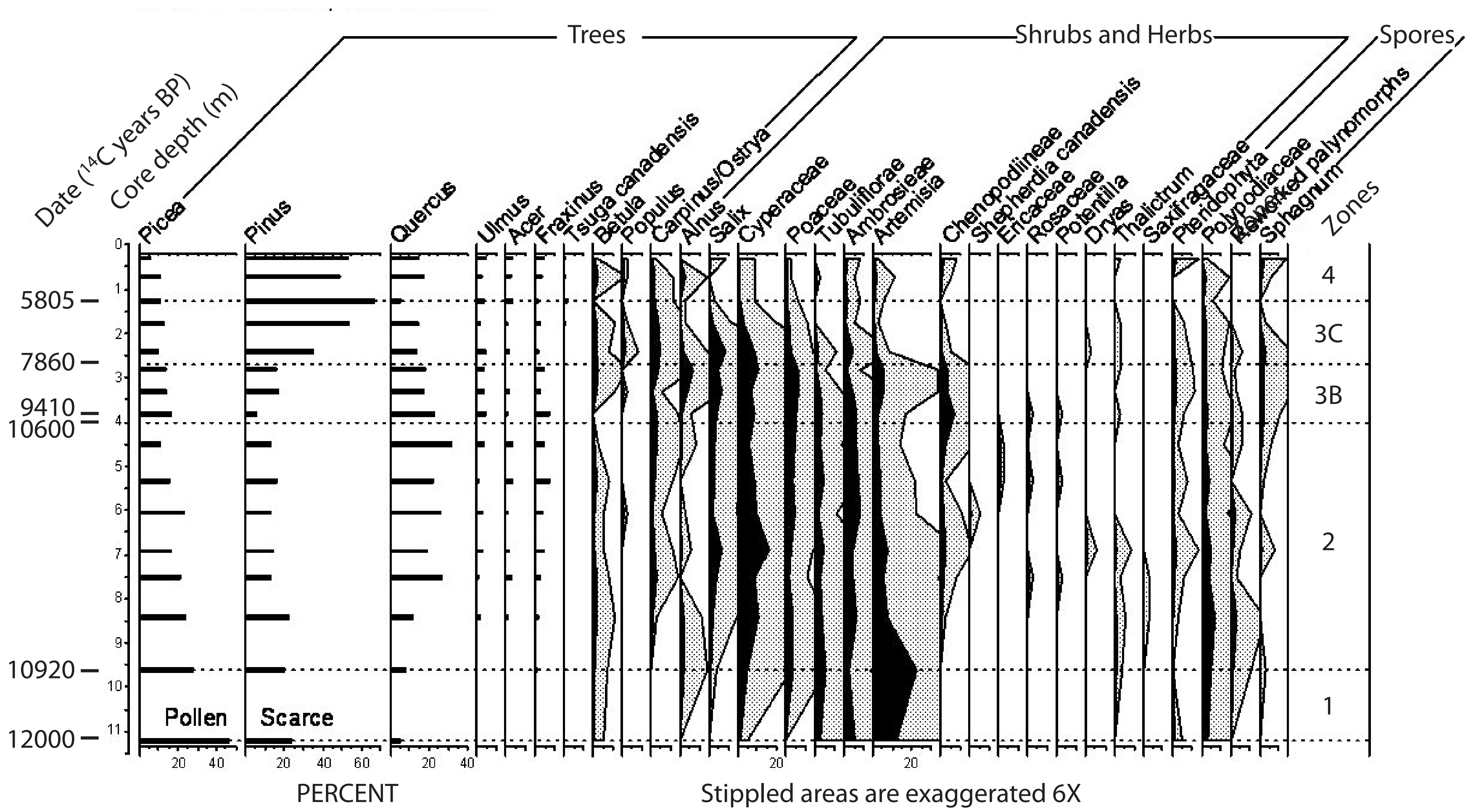

Figure 4.8. Pollen stratigraphy for Manitoulin sub-basin core 596. The pollen sum is based on 200-250 tree, shrub and herb pollen excluding aquatic pollen; the pollen percentages are calculated on this sum. Pollen analyst: Thane Anderson.

changes in the dominant tree taxa. Pollen zone 1 is present only in core 596 and is representative of a tundra landscape based on the peak percentages of *Artemisia* (Daisy) and the overall low abundance of pollen. The high *Picea* (Spruce) percentages are attributed to wind-derived pollen from spruce forests located to the south at this time. The age of 12,000 [13,835 cal] BP assigned to a depth of 11.2 m in core 596 is based on an estimate for the equivalent tundra-*Picea* transition at Twiss Marl Pond, Ontario (Yu 2000), which is located at about the same latitude as southern Lake Huron.

Pollen zone 2, the *Picea* zone, is also present only in core 596. The high percentage of *Quercus* (Oak) pollen is attributed to long distance transport. High amounts of *Quercus* have been previously reported from western Lake Huron (Lewis and Anderson, 1989; their core M17). The age of 10,920 [12,875 cal] BP assigned to 9.6 m is based on an AMS date of 10,920 ± 80 BP for the beginning of the *Picea* pollen zone at Twiss Marl Pond (Yu 2000). The age of 10,600 [12,685 cal] BP assigned to 4.0 m is based on low *Picea* abundances at the top of the *Picea* zone. Similar low *Picea* values occur at 18 Mile River (Karrow et al. 1975) prior to an increase in *Picea* that has been dated to 10,600 ± 160 and 10,500 ± 150 BP at sites 1 and 2 of 18 Mile River (Karrow et al. 1975). The low pollen numbers and dominance of *Artemisia* throughout zones 1 and 2 suggest a tundra landscape with deposition occurring in an ice marginal glacial lake (possibly Early Lake Algonquin). Herbs, which are very prominent throughout this zone, also suggest that this site was proximal to the ice margin at this time.

Pollen zone 3 is the *Pinus*- (Pine-) dominated zone. Subzone 3a represents the initial increase in *Pinus* leading to the *Pinus* maximum of subzone 3c. Subzone 3a is missing from core 596. There, the pollen change from zone 2 to subzone 3b likely signifies an unconformity, possibly amounting to as much as 1200 years (10,600 – 9,410 ka BP). Subzone 3b is present in cores 594 and 596 and is distinguished by a minor but significant increase in *Picea* to peak percentages and a decrease of *Pinus*. This *Picea* peak within the *Pinus*-dominated interval represents a recurrence of spruce and suggests that the northern Lake Huron region was affected by an interval of cooler climate during the early Holocene (9,410-7,860 [10,625-8,620 cal] BP; Anderson 2002; Anderson and

Lewis 2002). The age of 9,410 [10,625 cal] BP was assigned to depths of 12.1 m in core 594 and 3.83 m in core 596, and the age of 7,860 [8,620 cal] BP was assigned to depths of 9.45 m in core 594 and 2.6 m in core 596. This range is based on AMS dates of 9,410 ± 60 and 7,860 ± 50 BP that bracket the *Picea* recurrence at the Sheguiandah PaleoIndian site, Manitoulin Island (Anderson 2002).

Pollen zone 4 is present in both cores and is marked by a decline of *Pinus* and gradual increases in *Acer* (Maple), *Tsuga* (Hemlock) and other hardwoods such as *Quercus, Fraxinus* (Ash), and *Platanus* (Sycamore; core 594 only) to the top of the cores. The age of 5,805 [6,635 cal] BP assigned to 6 m in core 594 and 1.25 m in core 596 is based on a date of 5,805 ± 165 BP for the mid to late Holocene decline of *Pinus*, the first appearance (presumed arrival) of *Tsuga* and increase in *Acer* at Lake Sixteen, northern Michigan adjacent to Lake Huron (Futyma and Miller, 1986). The age of 3,030 [3,210 cal] BP assigned to 3.5 m in core 594 is based on a date of 3,030 ± 70 BP for a second increase in *Tsuga* and decrease in *Pinus*, also at Lake Sixteen, Michigan.

4.3.5 Mineralogy

Twelve bulk sediment samples from core 594, which were examined by XRD, are largely composed of quartz, dolomite and calcite, with minor contributions of clays (illite, kaolinite and chlorite), albite (Na-feldspar) and K-feldspar (Table 4.2, Fig. 4.9). Most samples are dominated by quartz, which increases up-core from a minimum of 29 % at 14.86 m to a maximum of nearly 70 % at 1.98 m. The uppermost sample at 1.98 m contains very little carbonate. Below this depth, the dolomite content is fairly constant at ~20 %. No calcite was detected at depths of 1.98 and 7.0 m but spikes of ~20 – 40 % in calcite content occur at depths of 5.42, 8.6, 13.66 and 14.86 m. The abundances of kaolinite, chlorite, albite and K-feldspar do not vary much throughout the core, each comprising ~5 % of the sediment.

Two core 594 samples of blue-black mineral grains from sediments characterized by black banding (likely iron-sulfide, as described by Rea et al. 1981) were identified as

Table 4.2. Mineral abundances of bulk sediment samples from Goderich sub-basin core 594 as determined by X-Ray Diffraction.

sample depth (m)	**quartz** (%)	**dolomite** (%)	**calcite** (%)	**albite** (%)	**K-feldspar** (%)	**chlorite** (%)	**illite** (%)	**kaolinite** (%)
1.98	68	6	n.d.	6	5	< 5	9	< 5
3.4	54	19	< 5	< 5	< 5	< 5	9	5
4.65	51	22	7	< 5	< 5	< 5	8	< 5
5.42	41	20	18	< 5	< 5	< 5	8	< 5
7.0	58	14	n.d.	8	5	7	n.d.	8
7.8	51	24	< 5	7	< 5	< 5	n.d.	7
8.6	30	16	33	< 5	< 5	< 5	7	< 5
10.44	40	17	9	8	5	< 5	10	7
11.0	42	21	6	7	5	< 5	8	6
12.2	44	13	6	9	6	6	10	7
13.66	38	16	22	< 5	< 5	< 5	10	< 5
14.86	29	13	38	< 5	< 5	< 5	7	< 5

n.d. = not detected

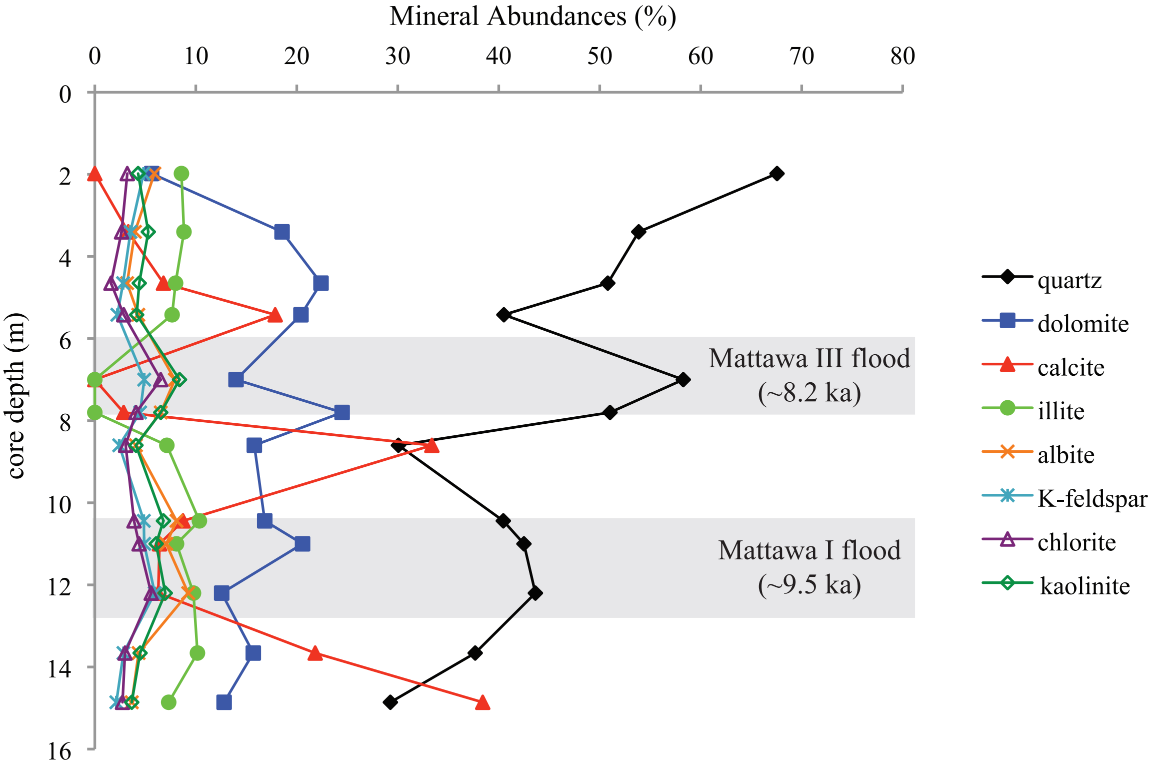

Figure 4.9. Mineral abundances (weighted peak height %) of bulk sediment samples from Goderich sub-basin core 594 as determined using powder X-ray diffraction. The grey shaded regions represent portions of the core that correlate with influxes from Lake Agassiz, as indicated by the oxygen-isotope compositions of biogenic carbonates.

vivianite ($Fe^{2+}_3(PO_4)_2{\bullet}8H_2O$) using XRD. Both the black bands and vivianite grains undergo oxidation within 30 to 60 minutes upon exposure to air. The black bands disappear and vivianite, which is initially colourless, darkens to a blue or blue-black colour (Odegaard et al. 2003; Fagel et al. 2005). Blue-black grains distinctive of vivianite were also identified visually in core 146. Most grains were ~1 mm in diameter, but grains up to 1.5 cm were observed at ~5.5 m in core 594.

4.3.6 Biostratigraphy

Although specific counts of the shells and valves of the various clam and ostracode species within the three Huron Basin cores were not performed, qualitative observations were made of shifts in individual populations. In core 594, *C. subtriangulata* valves were present from the core bottom (15.0 m) to 3.4 m, with abundances dropping substantially between 8.0 – 5.8 m. Shallower-water species (*C. crogmaniana*, *C. rawsoni*, *C. lacustris*, *L. friabilis* and *Pisidium* clams) were present from 15.0 – ~12.8 m and 10.2 – 8.2 m. Valves of *C. crogmaniana*, *C. lacustris* and a few *L. friabilis* individuals were also observed from 5.6 – ~3.6 m.

Ostracode valves and clam shells were less plentiful in core 146 than core 594. *Candona subtriangulata* valves were present from ~11.9 – 3.0 m but had particularly low abundances between 4.6 – 3.6 m. *Candona crogmaniana* valves were present at 7.2 m, 5.2 – 4.4 m and 3.6 m. *Candona rawsoni* valves were present at 8.6 m and 5.2 – 4.6 m. Valves of *C. lacustris* were present from 8.8 – 7.8 m and 5.2 – 4.8 m. Clam shells were scattered throughout the interval 8.8 – 4.4 m.

Only *C. subtriangulata* valves were recovered from core 596. This species was present from 10.7 m to the core top, but no valves were observed between 2.8 – 2.2 m.

4.3.7 Oxygen- and carbon-isotope compositions

The oxygen-isotope compositions of paleolakewater ($\delta^{18}O_{lakewater}$) and $\delta^{13}C$ values of biogenic carbonates are illustrated in Figures 4.10 and 4.11, respectively (see Appendix F for data). The oxygen-isotope compositions of paleolakewater were calculated using the measured oxygen-isotope compositions of the ostracode and clam species and the fractionation factors determined for each species in Chapter 2 (*C. subtriangulata* – 1.0359; *C. crogmaniana* – 1.0338; *C. rawsoni* 1.0341; *C. lacustris* – 1.0323; *Pisidium* clams – 1.0315). In a preliminary report, Macdonald and Longstaffe (2008) used the results for *C. subtriangulata* valves from these cores, the vital effect value reported by von Grafenstein et al. (1999), and the calcite geothermometer of Friedman and O'Neil (1977) to report $\delta^{18}O_{lakewater}$ values. Those results are recalculated here using the fractionation factor described in Chapter 2, and are about ~0.3 ‰ higher.

By utilizing fractionation factors specific to individual species, the ability to estimate the average growth temperatures of individual species is improved. Ostracodes, like many shelly organisms, molt only when their host water reaches a specific temperature (or narrow temperature range; Boomer 2002; Schöne et al. 2006). By calibrating the oxygen-isotope fractionation between water and ostracode samples from modern Lake Huron, we determined that the preferred growth temperatures for the four ostracode species examined here range from 4 – 15 °C (Chapter 2, this thesis).

The paleolakewater oxygen-isotope compositions show very significant variations (Fig. 4.10). The shallower-water ostracode and clam species in cores 594 and 146 are only present in intervals characterized by a generally high and limited range of $\delta^{18}O$ values. Typically, intervals characterized by $\delta^{18}O_{lakewater}$ values lower than -12 ‰ contain only *C. subtriangulata*.

In Goderich sub-basin core 594, $\delta^{18}O_{lakewater}$ values calculated from *C. subtriangulata* valves range from -19.3 to -6.0 ‰, and there are two intervals characterized by low-^{18}O waters, ~12.5 – 10.5 m and 8.0 – 6.0 m (Fig. 4.10). The ranges in $\delta^{18}O_{lakewater}$ values for the other species are: *C. crogmaniana*, -10.9 to -3.9 ‰; *C.*

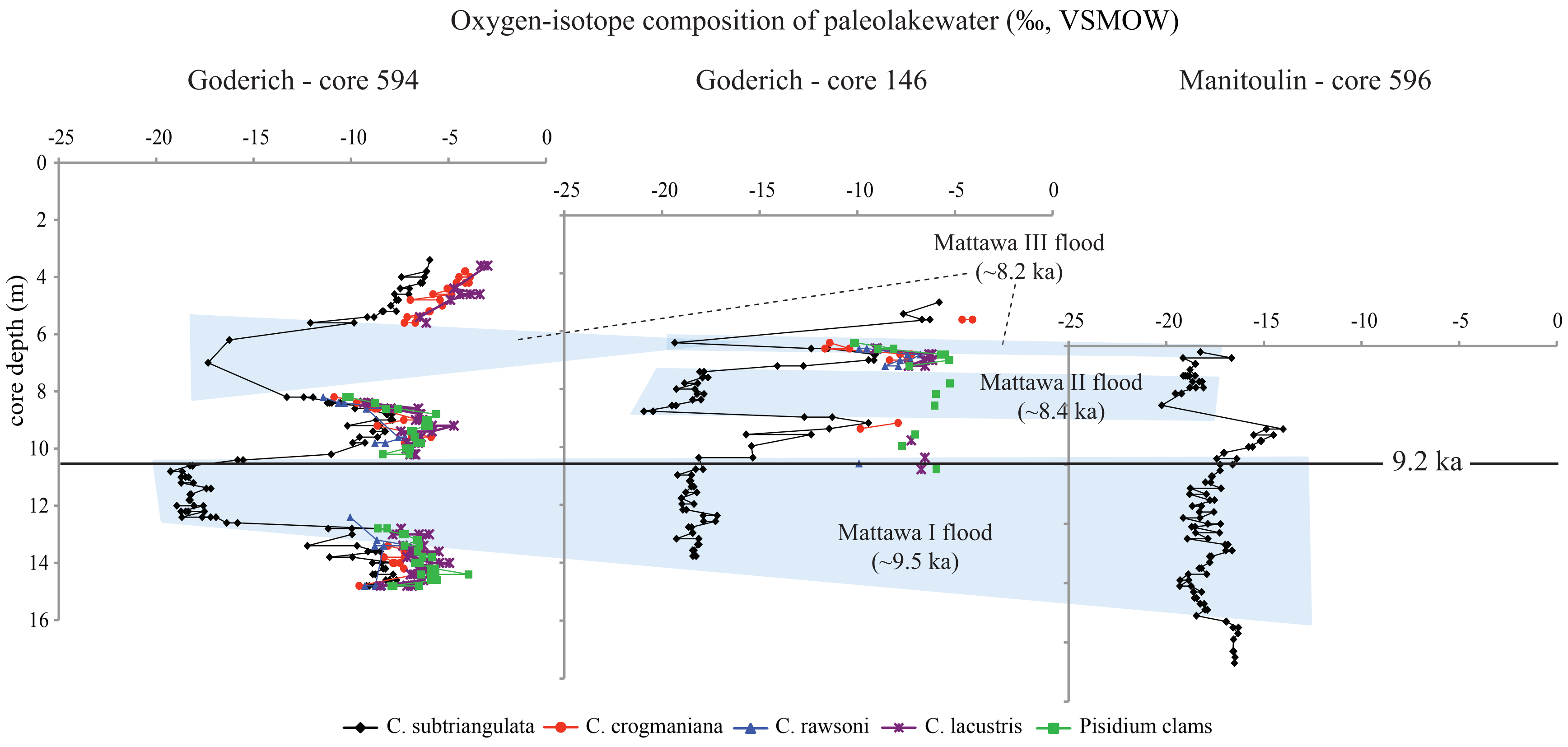

Figure 4.10. Oxygen-isotope composition of paleolakewater as calculated using biogenic carbonates from Goderich sub-basin cores 594 and 146, and Manitoulin sub-basin core 596. The y-axis (core depth in metres) is the same for all three graphs. The graphs are hung at a datum of 9.2 ka [10,300 cal] BP (solid black line), which is the Light Green sedimentary sequence boundary. The blue shaded regions correlate intervals of low $\delta^{18}O$ values associated with floods originating from Lake Agassiz.

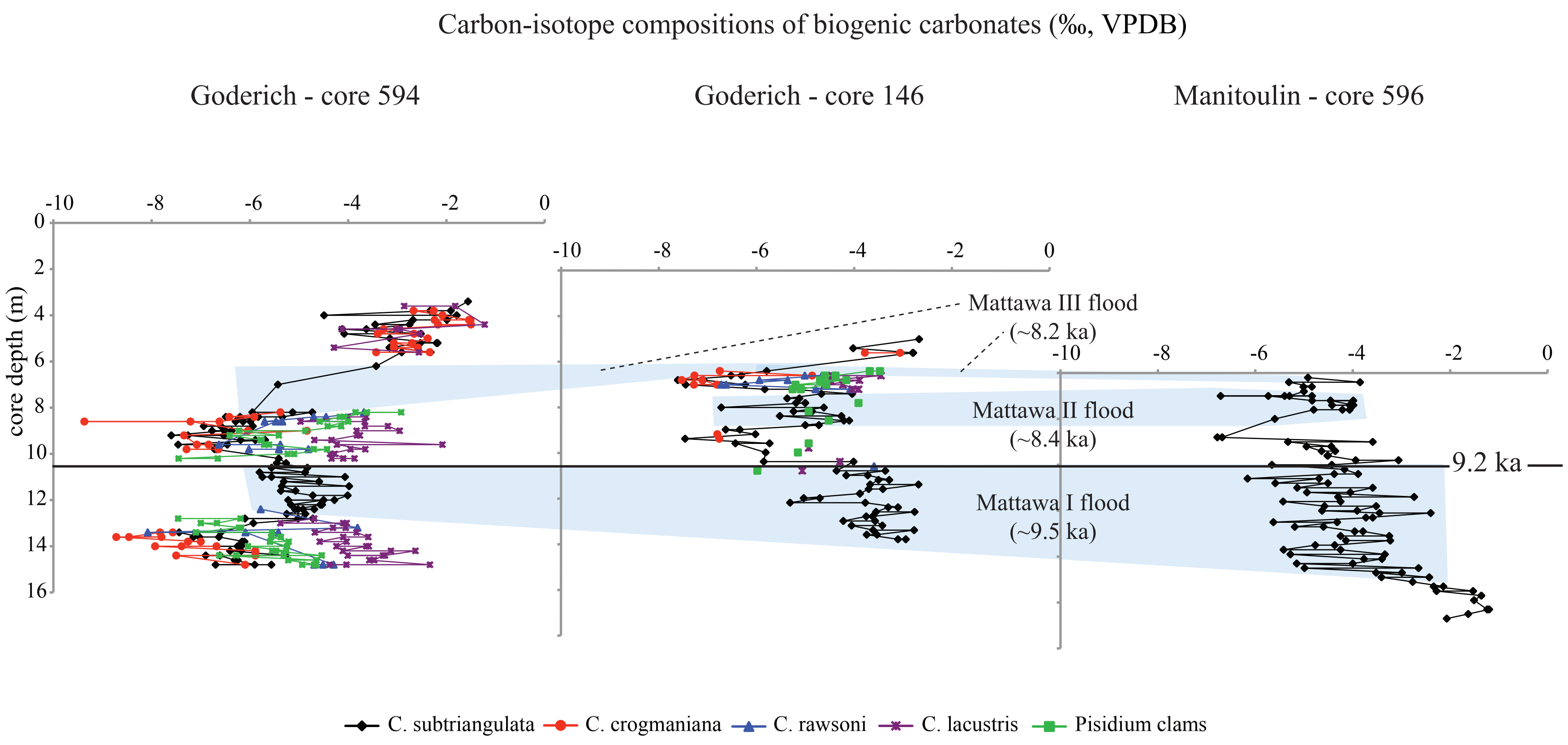

Figure 4.11. Carbon-isotope compositions of biogenic carbonates from Goderich sub-basin cores 594 and 146, and the Manitoulin sub-basin core 596. The y-axis (core depth in metres) is the same for all three graphs. The graphs are hung at a datum of 9.2 ka [10,300 cal] BP (solid black line), which is the Light Green sedimentary sequence boundary. The blue shaded regions correlate intervals of low $\delta^{18}O$ values associated with floods originating from Lake Agassiz.

rawsoni -11.4 to -6.9 ‰; *C. lacustris*, -9.3 to -3.0 ‰, and clams, -10.3 to -4.0 ‰ (Fig. 4.10).

In Goderich sub-basin core 146, $\delta^{18}O_{lakewater}$ values calculated from *C. subtriangulata* valves range from -20.9 to -5.8 ‰. Three intervals are characterized by low-^{18}O waters; 11.8 – 8.4 m, 6.8 – 5.4 m and ~4.5 m. The ranges in $\delta^{18}O_{lakewater}$ values for other species are: *C. crogmaniana*, -11.7 to -4.1 ‰; *C. rawsoni*, -9.9 to -6.8 ‰; *C. lacustris*, -9.1 to -6.2 ‰, and clams -10.2 to -5.3 ‰ (Fig. 4.10). Three clam samples from core depths of 6.6, 6.2 and 5.8 m yield significantly higher $\delta^{18}O_{lakewater}$ values than *C. subtriangulata* from the same intervals. These clam shells were slightly worn and displayed small patches of dissolution, and it is considered likely that they were reworked from older sediments.

In Manitoulin sub-basin core 596, where only *C. subtriangulata* was observed, $\delta^{18}O_{lakewater}$ values range from -20.2 to -14.0 ‰. These values are consistently lower and display a narrower range than observed for the Goderich sub-basin cores (Fig. 4.10).

The ostracode and clam species also show significant variation in the carbon isotopic compositions of their valves and shells (Fig. 4.11). In Goderich sub-basin core 594, the following ranges of $\delta^{13}C$ values were obtained: *C. subtriangulata*, -7.6 to -1.6 ‰; *C. crogmaniana*, -9.4 to -1.5 ‰; *C. rawsoni*, -8.1 to -3.7 ‰; *C. lacustris*, -5.4 to -1.2 ‰, and clams, -7.5 to -2.9 ‰. In Goderich sub-basin core 146, the ranges of $\delta^{13}C$ values are: *C. subtriangulata*, -7.6 to -2.7 ‰; *C. crogmaniana*, -7.5 to -3.0 ‰; *C. rawsoni*, -6.7 to -3.6 ‰; *C. lacustris*, -5.1 to -3.5 ‰, and clams, -6.3 to -3.5 ‰. The $\delta^{13}C$ values of *C. subtriangulata* from Manitoulin sub-basin core 596 range from -6.8 to -1.2 ‰.

A moderately strong negative linear correlation (-0.76; Fig. 4.12) exists between the oxygen- and carbon-isotope compositions of early Holocene (~10 – 8 ka [11,500 – 9,000 cal] BP) *C. subtriangulata* valves from cores 594 and 146. The dominant control on the oxygen-isotope compositions of *C. subtriangulata* during the early Holocene was source water (e.g. glacial meltwater-rich Agassiz inflows versus precipitation); it follows

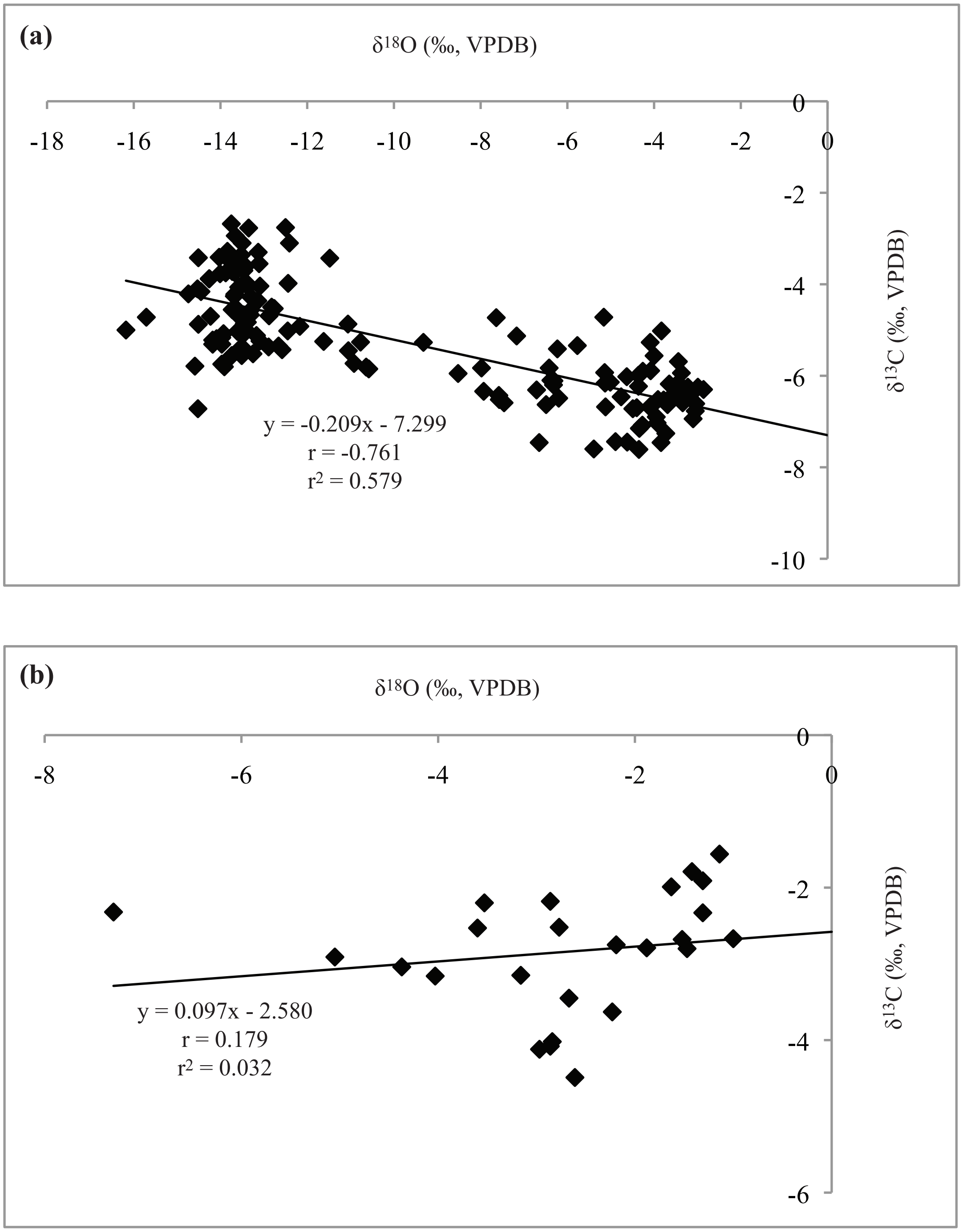

Figure 4.12. Statistical correlation of the carbon- and oxygen-isotope compositions of *C. subtriangulata* valves from Goderich sub-basin cores 594 and 146 during the early Holocene (a) (~10 - 8 ka [11,500 - 9,000 cal] BP) and the mid Holocene (b) (~8 - 6 ka [9,000 - 6,850 cal] BP).

that source water may also have been an important control on the carbon-isotope compositions of *C. subtriangulata* at this time. During the mid Holocene (~8 – 6 ka [9,000 – 6,850 cal] BP), the $\delta^{18}O$ and $\delta^{13}C$ values of *C. subtriangulata* in cores 594 and 146 show only a very weak positive correlation (r = 0.179; Fig 4.12), suggesting that these two isotopic systems were controlled by different factors at this time.

4.4 DISCUSSION

4.4.1 Age of the Sediments

Neither the pollen stratigraphy nor the radiocarbon dates produce an absolute chronology that is entirely consistent with ages assigned to the sequences previously described for the Late Pleistocene-Holocene sediments of the Lake Huron basin. The various sequences were identified in cores 146, 594 and 596 using lithological characteristics. The lack of agreement among the various age indicators makes establishment of chronologies for these three cores especially difficult. For example, it is well documented that radiocarbon dates from Great Lakes sediments, particularly those from Lake Huron, are commonly problematic, with some dates appearing to be too old and other dates being out of sequence (Breckenridge and Johnson 2009). Such limitations exist for the cores studied here, and hence restricts their usefulness for establishing the timing and duration of key events (e.g., the Mattawa floods). To proceed, it has been necessary to identify such key events by other means and to use those markers to establish workable age models for these cores (Fig. 4.13).

Radiocarbon dates

Radiocarbon dates for sediments determined using organic matter can be too old by up to thousands of years if the organic fragments remain on land before being reworked and deposited in lake sediments (Nambudiri et al. 1980; Brown et al. 1989; Colman et al. 1990). Dates for biogenic carbonates can also be erroneously old because the hard water effect (HWE). This is caused by the contribution of radioactively inert

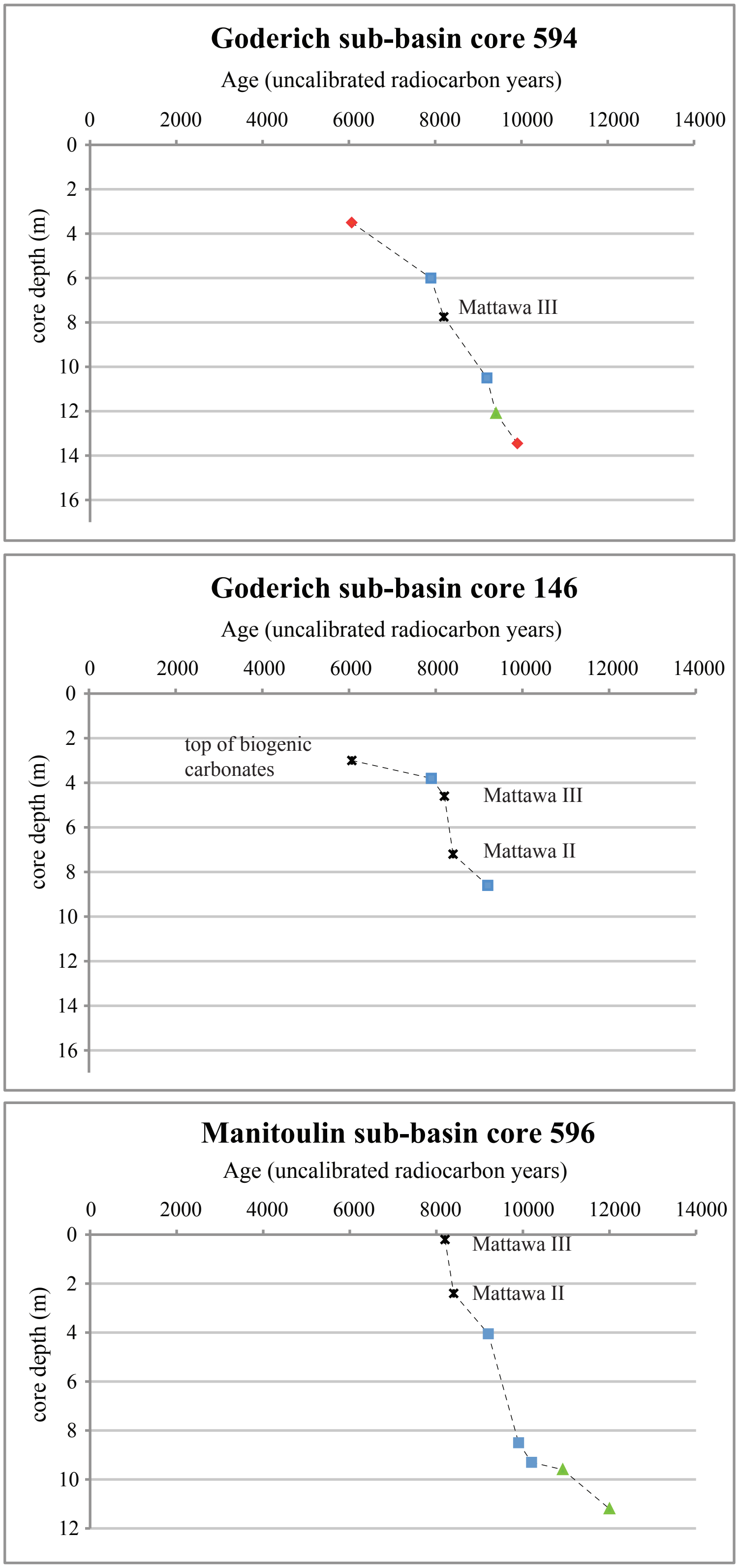

Figure 4.13. Age models for the Lake Huron cores. Radiocarbon dates are denoted by red diamonds, pollen dates by green triangles, dates of sedimentary sequence by blue squares, and dates of key sedimentary features (e.g. floods) by ‘x’.

carbon from carbonate rocks within a lake's catchment, which is then available to organisms when they form their shells (Rea et al. 1994a; Rea and Colman 1995; Moore et al. 1998). This can produce dates that are hundreds of years older than the true age. Bivalves collected from Saginaw Bay, Lake Huron, in the early 1900s were used to calculate a HWE effect of 438 years for Lake Huron (Rea et al. 1994a; Rea and Colman 1995; Moore et al. 1998). This amount has been subtracted from the three dates obtained for bivalves (Table 4.1). Such a correction assumes that the HWE has not varied through time, which is unlikely, but it is presently not possible to estimate the quantity of 'dead' carbon delivered to the Huron Basin at different times.

As discussed further below, most of the radiocarbon dates obtained for core 594 have been excluded from its age model. First, the date of 2,549 [2,725 cal] BP at 12.4 m is too young for the sediment from which it was collected, and has been rejected outright. The AMS Laboratory at The University of Arizona confirmed that all analyses were performed without problem, but it remains difficult to imagine a scenario whereby younger organic materials could be entrained within older sediments at this depth. Second, the relatively young radiocarbon date of 8,626 [9,550 cal] BP obtained for plant fragments from the extruded sediment at the bottom of core 594 (~15.0 – 15.25 m) suggests that a repeated interval from higher in the sediment column was entrained during core retrieval, as described earlier.

The other radiocarbon dates excluded from the age model for this core are likely much closer to the true age of the sediment. We have interpreted the lowermost sediment sequence in core 594 to be the Light Green, which was deposited from 9.9 – 9.2 ka [11,300 – 10,300 cal] BP (Lewis et al. 2007; Moore et al. 1994; Rea et al. 1994a; Godsey et al. 1999). Clams from 14.9 m had an uncorrected radiocarbon age of 9,716 ± 55 years. However, once the HWE correction of 438 years is applied, this date becomes slightly too young for the lower portion of the Light Green sequence. Conversely, clams from 13.45 m have an uncorrected radiocarbon age of 10,343 ± 60 years but a HWE-corrected date of 9,905 [11,265 cal] BP, which is slightly too old for the middle of the Light Green sequence. Sediments between ~14.9 – 13.45 m should have ages somewhere in the range of 9.9 – 9.7 ka [11,175 – 11,265 cal] BP.

The dates of 9,489 [10,730 cal] BP and 9,508 [10,745 cal] BP (HWE-corrected) at 9.3 and 8.65 m, respectively, occur within the Light Blue sequence, which was presumably deposited from 9.2 – 7.9 ka [10,300 – 8,650 cal] BP. These radiocarbon dates are too old – but only by a few hundred years of the lower boundary of the Light Blue sequence. Using sedimentation rates of 1m/400 years (Rea et al. 1994a) to 1m/500 years (Dobson et al. 1995) for the Light Blue sequence, deposition of these two samples was separated by only 260 – 325 years. The similarity between the two radiocarbon dates suggest that (a) the HWE correction is reasonable; and (b) both samples were likely reworked from sediments deposited at ~9.5 ka.

The date of 9,169 [10,270 cal] BP at 6.3 m appears too old for this sediment by a significant amount. The interval from 10.5 – 6.0 m has been interpreted at the Light Blue sequence (9.2 – 7.9 ka [10,300 – 8,650 cal] BP; Lewis et al. 2007; Moore et al. 1994; Rea et al. 1994a; Godsey et al. 1999). Additionally, the thick dark grey bed from 7.75 – 6.0 m is believed to reflect the Mattawa III flood, at 8.4 ka [9,450 cal] BP. This organic matter may have been reworked from shallower regions or a terrestrial source during flooding.

The date of 6,065 [6,925 cal] BP for organic matter at ~3.5 m likely reflects the time of deposition. This date was obtained from near the very top of the preserved biogenic carbonate profile. Biogenic carbonates were not preserved after 6 – 5 ka [6,850 – 5,730 cal] BP. Instead, complete dissolution of shelly material in lake water was facilitated at the sediment-water interface because of the substantial decrease in sedimentation rates (Rea et al. 1994a). The top of the biogenic carbonate-bearing sediment in core 146 likely has a similar age.

Pollen stratigraphy

Pollen dates determined by Thane Anderson for the lowermost portions of cores 596 and 594 yield close matches to dates obtained from other data. Pollen dates for samples from higher in the stratigraphic section, however, do not correlate well with other chronological data for the Huron Basin sediments. In particular, whereas most radiocarbon dates excluded from the age model for core 594 are likely off by only a few hundred years from the true depositional age, some pollen dates differ by several thousands of years.

In core 596, pollen dates of 12,000 [13,835 cal] BP at 11.2 m and 10,920 [12,875 cal] BP at 9.6 m have both been included in the age model. Sediments at ~9.7 – 9.3 m are interpreted as the Orange sequence, which was deposited from 11.2 – 10.2 ka [13,100 – 12,000 cal] BP (Moore et al. 1994; Rea et al. 1994a; Dobson et al. 1995). The pollen date of 10,920 years is consistent with this interpretation. Sediment below a depth of 9.7 m in this core was difficult to interpret in terms of the previously described sequences. This sediment can be described as a stony till and may be quite old, as suggested by these pollen-inferred ages.

The pollen dates of 10,600 [12,685 cal] BP at 4.0 m and 9,410 [10,625 cal] BP at 3.83 m in core 596 perhaps hint at an unconformity, though no features to indicate one (e.g., coarser sediments, an abrupt colour transition) were observed. These pollen dates also occur near the bottom of the Light Blue sequence (9.2 – 7.9 ka [10,300 – 8,650 cal] BP, and thus seem too old by ~200 – 1400 years. Hence these dates were excluded from the age model for core 596.

A pollen date of 7,860 [8,620 cal] BP, assigned to 2.6 m in core 596 (also within the Light Blue sequence), underlies deposits of the Mattawa II flood (~8.4 ka [9,450 cal] BP). Hence, this date is also excluded from the age model for core 596, as it appears too young by as much as ~500 years.

The pollen date of 5,805 [6,635 cal] BP at 1.25 m in core 596 is also questionable. It occurs within the Light Blue sequence (9.2 – 7.9 ka [10,300 – 8,650 cal] BP between flood deposits of the Mattawa II (8.4 ka [9,450 cal] BP) and Mattawa III (8.2 ka [9,100 cal] BP). It is known that low-^{18}O waters derived from Lake Agassiz and the LIS were diverted away from the Upper Great Lakes to Lake Ojibway at ~8.1 ka [9,000 cal] BP (Bajc et al. 1997; Breckenridge et al. 2004, 2010). The pollen date of 5,805 years correlates with a period of very low δ^{18}O values, and would suggest that low-^{18}O waters were present in the Huron Basin more than 2000 years later. Accordingly, this pollen date is excluded from the age model, as it seems to be ~2500 years too young.

In core 594, the pollen date of 9,410 [10,625 cal] BP assigned to 12.1 m correlates well with an influx of low-^{18}O waters, likely the Mattawa I flood at ~9.5 ka [~10,700 cal] BP (Breckenridge and Johnson 2009). This date has been included in the age model.

The pollen date of 7,860 years at 9.45 m in core 594 occurs within the Light Blue sequence (9.2 – 7.9 ka [10,300 – 8,650 cal] BP) and apparently underlies deposits from the Mattawa III flood (~8.2 ka [9,100 cal] BP). This date is excluded from the age model, as it appears too young by as much as ~500 years.

The pollen date of 5,805 [6,635 cal] BP at 6.0 m in core 594 is also questionable. This depth marks the beginning of the Surface sequence, previously dated to 7.9 ka [8,650 cal] BP (Lewis et al. 2007; Moore et al. 1994; Rea et al. 1994a). The pollen date, therefore, appears to be ~2000 years too young and is excluded from the age model.

The pollen date of 3,030 [3,210 cal] BP at 3.5 m in core 594, obtained from sediment in which ostracode valves are preserved, is also excluded from the age model. Sedimentation rates in the Huron Basin decreased to ~ 0.2 mm per year at ~5 ka [~5,730 cal] BP (Kemp et al. 1974; Graham and Rea 1980; Rea et al. 1994a). This resulted in complete dissolution of ostracode valves in sediments younger than ~6 – 5 ka [6,850 – 5,730 cal] BP. The radiocarbon date of 6,065 [6,925 cal] BP for organic matter from this interval is a more reasonable estimate of its age.

As mentioned for the shelly materials and organic matter fragments used for radiocarbon date measurements, the pollen contained in the Huron Basin sediments are likely prone to extensive reworking during periods of large lake-level fluctuations, as were especially pronounced during the early Holocene (~10 – 7.5 ka [11,500 – 8,350 cal] BP). Such movement and redistribution of these grains would have introduced much error into the palynological records for cores 594 and 596, presented here, which may explain why so few of the dates, and in particular the younger dates, are not in agreement with the age models of these cores.

4.4.2 Sediments and Mineralogy

The main source of lacustrine sediment in the Huron Basin is the glacial tills that surround the basin, which are mainly composed of quartz, feldspars, calcite, dolomite and clays (Rea et al. 1981). The mineralogy of lake sediments is therefore very similar to that of the tills, with the exception that carbonates are not well-preserved in sediments of the Surface sequence (Rea et al. 1994a). The earliest glaciolacustrine clays, deposited from ~ 15.5 – 10.2 ka [18,800 – 12,000 cal] BP, have a total carbonate (calcite + dolomite) content of ~10 – 20 % (Lewis et al. 1994). Slightly younger lacustrine sediments, deposited from ~10.2 – 7.9 ka [12,000 – 8,650 cal] BP, including sediments of the Yellow, Light Green and Light Blue sequences, were found by Lewis et al. (1994) to have a carbonate content of 1 – 10 %, by Rea et al. (1994a) to have a total carbonate content of up to 30 %, and by Graham and Rea (1980) to contain up to 40 % carbonate minerals. The sediments of the Surface sequence (deposited more or less continuously since 7.9 ka [8,650 cal] BP) have a carbonate content near 0 % – the result of dissolution associated with the low sedimentation rate since that time (~0.1 – 0.3 mm/yr; Kemp et al. 1974; Graham and Rea 1980; Rea et al. 1981, 1994a; Lewis et al. 1994; Odegaard et al. 2003).

Bulk samples from the Goderich sub-basin core 594 have slightly higher carbonate contents than previously reported. Sediments of the Light Green sequence (15.0 – 10.5 m; 9.9 – 9.2 ka [11,300 – 10,300 cal] BP) contain 19 – 51 % carbonate. A similar range, 14 – 49 %, characterizes the Light Blue sequence (10.5 – 6.0 m; 9.2 – 7.9

ka [10,300 – 8,650 cal] BP) (Fig. 4.9). Within these sequences, intervals with lower total carbonate content (and high quartz content) coincide with periods characterized by low-^{18}O water, and intervals characterized by high-^{18}O water contain higher amounts of carbonate (and lower amounts of quartz; Fig. 4.9). Sediments of the Surface sequence range in total carbonate from 6 – 38 %, with a gradual decrease in carbonate content towards the top of the core. For example, the uppermost sample from a depth of 1.98 m had no detectable calcite but 6 % dolomite, which is more resistant to dissolution. Modern sedimentation rates are so low that the majority of carbonate minerals, particularly calcite, delivered to the lake undergo dissolution in the presence of its carbonate-undersaturated waters (Rea et al. 1981, 1994a; Odegaard et al. 2003). This is common within post-glacial sediments across the Upper Great Lakes (Colman et al. 1994a; Forester et al. 1994; Hyodo and Longstaffe 2011c).

We are unsure about the source of the grey sediments in the Huron Basin cores that mark influxes of low-^{18}O waters represented by the Mattawa II and III Beds. Earlier notions that grey glacial sediments deposited in the Upper Great Lakes, including the A1 (Wilmette) and A2 Beds in the Michigan Basin, were sourced from outflows of Lake Agassiz (Teller 1985; Colman et al. 1990, 1994c; Henderson and Last 1998; Lewis and Todd 1996) have largely been abandoned (Fisher 2003, 2007; Breckenridge et al. 2004; Breckenridge 2007; Hyodo and Longstaffe 2011c). In the Superior Basin, meltwater inflows are indicated by varves in the sedimentary record and exceptionally thick varves are interpreted to reflect relatively large meltwater inputs (Dell 1972; Breckenridge et al. 2004, 2010; Breckenridge 2007; Breckenridge and Johnson 2009; Hyodo and Longstaffe 2011c). Red glacial sediments in the Superior Basin, which have been attributed to deposition when the LIS was within or nearby the basin, have relatively lower carbonate contents than overlying grey glacial sediments, which were deposited after ~9.2 ka [10,400 cal] BP when the LIS was situated further north (Hyodo and Longstaffe 2011c). The mineral abundances (Table 4.2 and Fig. 4.9) within sediments deposited during both the Mattawa I and III floods are remarkably similar, yet the appearance of sediments associated with the Mattawa I flood are not noticeably different from surrounding sediment in core 594, or in cores 146 or 596, for that matter. Further investigations into the source(s) and mineralogy of Huron sediments, particularly the striking grey bed of the Mattawa II flood present in cores 146 and 596, are warranted.

Overall, the sediments of core 594 are significantly less red (more grey) than the sediments of cores 146 and 596, especially within the Light Green sequence. Mothersill and Brown (1982) examined two cores from the Goderich Basin taken ~15 km apart mid-way between cores 594 and 146 (which are nearly 30 km apart). General descriptions of sediment from their cores are similar to core 594, that is, sediment that is less red (more grey) than cores 146 and 596. Additionally, the sediment colours they describe for their more northern core are redder in hue than for the more southerly core. Colour variations between the two Goderich sub-basin cores studied by Mothersill and Brown (1982), together with the descriptions of cores 594 and 146, may indicate that there were different sources of sediment to the northern and southern regions of the Goderich sub-basin, with the northern areas having a redder source, more in line with earlier sediment descriptions from northern areas of the Huron Basin (Rea et al. 1994a; Godsey et al. 1999).

Distinctive black bands of iron sulfide minerals formed in all five of the Great Lakes during the mid to late Holocene as a result of higher organic matter inputs to the sediment as well as reducing conditions within the near-surface sediments (Fig. 4.3; Odegaard et al. 2003). In the present study, vivianite grains were present within intervals characterized by black banding, usually within the black bands themselves.

Vivianite is commonly found in reduced lacustrine sediments, yet its origin and conditions of formation are not very well understood (Fagel et al. 2005). Vivianite is believed to be the most important sink of phosphorus in lakes and is quite stable in reduced lacustrine sediments (Nriagu 1972; Dell 1973; Nriagu and Dell 1974). Its formation is dependent on numerous factors, including (i) reducing and alkaline conditions within the water column, at the sediment-water interface and/or within the sediments, (ii) the availability of dissolved Fe, P, S, Ca, Mg and Mn, (iii) sedimentation rates, and (iv) the amount of organic matter delivered to the sediment (Rosenquist 1970; Manning et al. 1991; Hupfer et al. 1998; Murphy et al. 2001; Sapota et al. 2006). Most studies suggest that vivianite crystallization occurs at shallow depths (<50 cm) below the sediment-water interface (Nriagu and Dell 1974; Deike et al. 1997; Manning et al. 1999; Sapota et al. 2006). In Lake Baikal, vivianite formation is associated with porewater chemistry and relatively slow sedimentation rates and is not a suitable proxy for lacustrine paleoproductivity at that location (Fagel et al. 2005; Sapota et al. 2006). In Lake Huron, the association of vivianite to the black iron-sulfide bands, which are in turn linked to higher amounts of organic matter delivered to the sediment, suggest that primary productivity during the mid Holocene warm period (the Holocene Hypsithermal at ~8 – 4 ka [9,000 – 4,500 cal] BP) was relatively high.

4.4.3 The oxygen-isotope history of Ancient Lake Huron

The late Pleistocene

The cores examined here contain only a short record (~2.1 m) of lakewater composition during the late Pleistocene. According to the age model for core 596, the boundary between the Pleistocene and Holocene epochs (10.0 ka [11,500 cal] BP) occurs at a depth of ~8.8 m (assuming a linear sedimentation rate during deposition of the Yellow sequence). Valves of *C. subtriangulata* were not found below a depth of 10.9 m in this core. Lakewater oxygen-isotope compositions calculated using *C. subtriangulata* from sediments from 10.9 – 9.3 m, representing both the oldest (unidentified) sequence and the Orange sequence (which was deposited until the end of Main Lake Algonquin, at 10.2 ka [12,000 cal] BP) are ~ -17 ‰ (Fig. 4.10), and are similar to those reported previously for the Huron and Erie Basins (~ -18 to -16 ‰) for this time period (Lewis and Anderson 1992; Lewis et al. 1994; Rea et al. 1994a; Moore et al. 2000). A decrease of ~2 ‰ occurs at the onset of the Yellow sequence, which marks the period of dropping water levels following the opening of the North Bay outlet at ~10.3 – 10.2 ka [12,100 – 12,000 cal] BP. This decrease in lakewater oxygen-isotope compositions may reflect increased connectivity to the upstream Superior and Agassiz Basins, which both contained water with very low oxygen-isotope compositions at this time (Last et al. 1994; Remenda et al. 1994; Birks et al. 2007; Breckenridge and Johnson 2009; Hyodo and Longstaffe 2011b).

Records of $\delta^{18}O_{lakewater}$ values from the Michigan Basin during the late Pleistocene, by comparison, vary from -22.5 to -6.0 ‰, with most values ranging from -20 to -15 ‰ (Chapter 3, this thesis). These results show that, during the late Pleistocene, the Huron and Michigan Basins contained a significant proportion of glacial meltwater delivered from upstream basins and/or sourced directly from the LIS.

The striking grey Wilmette (A1) Bed discovered in sediments from the Michigan Basin correlates to a late Pleistocene flood marking the initial drainage of Lake Agassiz eastwards through the Great Lakes Basin at ~10.8 ka [12,800 cal] BP (Colman et al 1994a, 1994c; Teller and Leverington 2004). A Lake Huron bed correlative to this event in Lake Michigan has not been identified, likely because few Lake Huron cores contain sediments old enough to contain such a feature.

The early Holocene (~10 – 8 ka [11,500 – 9,000 cal] BP)

The oxygen-isotope composition of lakewater, as recorded in the cores studied here, are compared to records from the Upper Great Lakes (including Lake Agassiz) during the early to mid Holocene in Figure 4.14. The sediments within cores 594 and 596 that were deposited during the earliest portion of the Holocene, from 10.0 ka [11,500 cal] BP until the Mattawa I flood at ~9.5 ka [10,700 cal] BP, provide substantially different records of lakewater $\delta^{18}O$ values (Fig. 4.14). Lakewater at the site of core 594, in the more southerly Goderich sub-basin, had a fairly high composition of -11 to -8 ‰. Such values are similar to those reported for the Michigan Basin at this time (Chapter 3, this thesis; Colman et al. 1994a, 1994c; Forester et al. 1994). Conversely, lakewater records from core 596, in the more northerly Manitoulin sub-basin, had a much lower composition of -19 to -16 %. Previous records of lakewater from the Huron Basin similarly suggest that $\delta^{18}O_{lakewater}$ values were low, between -21 to -18 ‰, at this time (Fig. 4.14; Lewis et al. 1994; Rea et al. 1994a; Moore et al. 2000; Breckenridge and Johnson 2009). These previous data were largely obtained from Lake Huron's Mackinac and northern Manitoulin sub-basins, which were more proximal to potential sources of low-^{18}O inflow than the Goderich sub-basin.

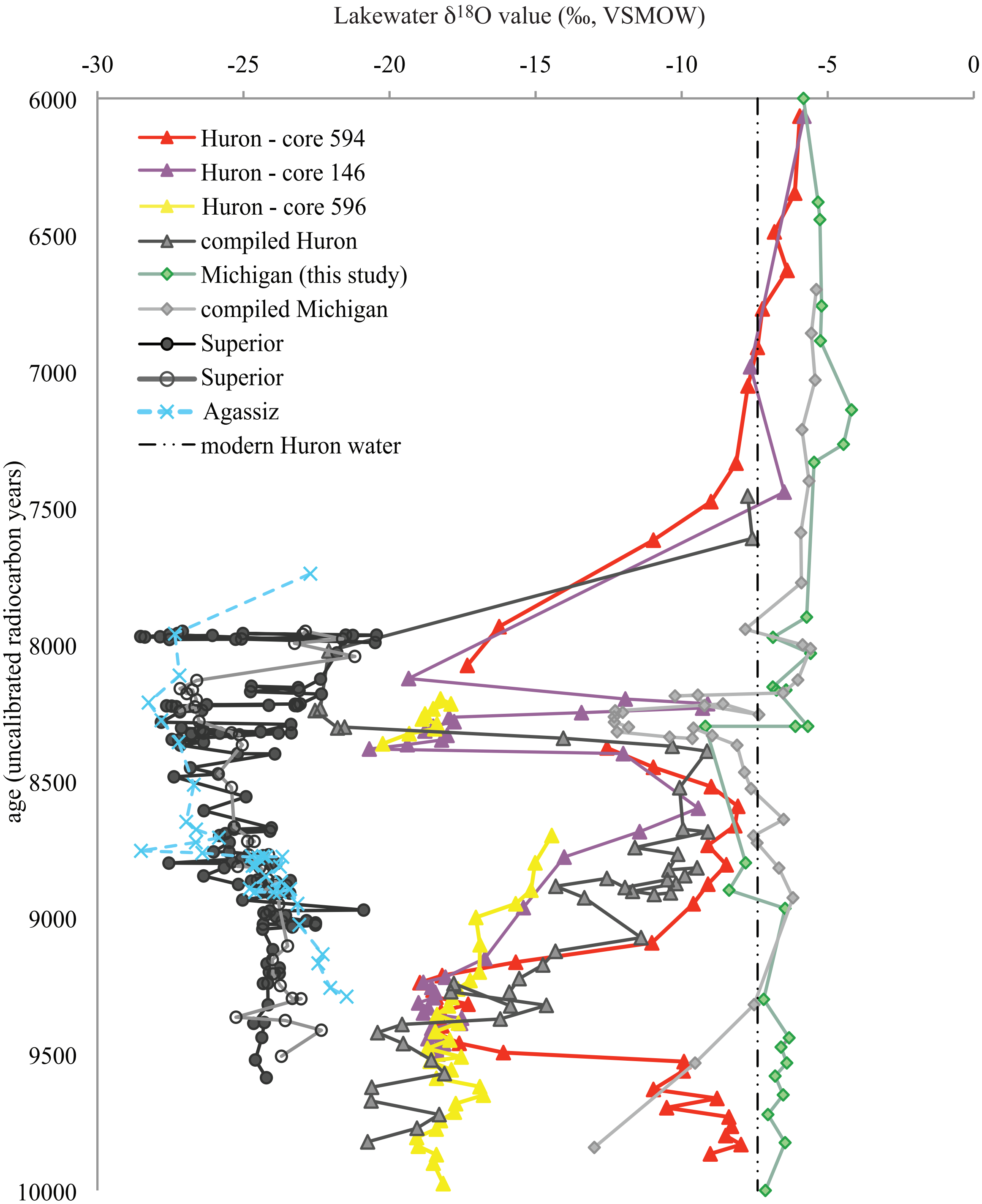

Figure 4.14. Oxygen-isotope compositions of the Great Lakes during the early to mid Holocene (10 - 6 ka [11,500 - 6,850 cal] BP). Oxygen-isotope data for the three cores of this study primarily reflect measurements of *C. subtriangulata* valves. "Compiled" Huron data are from Rea et al. (1994a) and Moore et al. (2000), "compiled" Michigan data are from Colman et al. (1994a, 1994c) and Forester et al. (1994). Records from these two lakes were recalibrated by Breckenridge and Johnson (2009). Superior records are from Hyodo and Longstaffe (2011b; filled circles) and Breckenridge and Johnson (2009; open circles). Lake Agassiz data are from Lewis et al. (2003), as presented in Breckenridge and Johnson (2009). Data for modern Lake Huron water are from Macdonald and Longstaffe (2007).

This difference in the isotopic composition of lakewater suggests a limited hydraulic connection between the northern and southern regions of the Huron Basin. The opening of the North Bay outlet at ~10.3 ka [12,100 cal] BP led to a period of low water levels in the Huron Basin from ~10.0 – 9.5 ka [11,500 – 10,700 cal] BP, which in turn brought about the isolation of many sub-basins (Fig. 4.15; Lewis and Anderson 1989; Lewis et al. 1994, 2007, 2008a; Breckenridge and Johnson 2009). A topographic high, the Six Fathom Scarp, extends in a north-west to south-east direction across the Huron Basin and separates the Manitoulin and Goderich sub-basins (Fig. 4.1). This scarp may have acted as a barrier to the southward movement of low-^{18}O waters into the Goderich sub-basin, which at this time instead contained a higher proportion of ^{18}O-enriched local runoff. A similar situation of localized and reduced mixing has been invoked by Hyodo and Longstaffe (2011b) to explain higher $\delta^{18}O_{lakewater}$ values in the eastern Ile Parisienne sub-basin of Lake Superior during the final influx of glacial meltwater at ~8.1 ka [~9,050 cal] BP relative to the rest of the lake.

Three intervals of low-^{18}O waters (the Mattawa floods) are observed in the Lake Huron cores studied here (Fig. 4.10). In core 594, these are interpreted to be the Mattawa I (12.6 – 10.4 m; ~9.5 ka [10,700 cal] BP) and Mattawa III (7.75 – 6.0 m; ~8.2 ka; [9,100 cal] BP) floods. In core 146, these periods are interpreted as the Mattawa I (bottom of the core at 11.9 – 8.4 m), Mattawa II (7.2 – 6.8 m; 8.4 ka [9,450 cal] BP), and Mattawa III (4.6 – 3.8 m) floods. In core 596, these intervals are interpreted as the Mattawa I (~8.5 – 4.8 m), Mattawa II (2.4 – 2.0 m), and Mattawa III (0.20 – 0.07 m) floods. These flooding events have been identified by their low oxygen-isotope compositions and/or by the presence of darker grey sediment observed in the cores. Teller (1985) examined sediments from northwestern Lake Huron but was unable to identify units that could be attributed to inflows from Lake Agassiz. Sediments deposited during the Mattawa I flood in the cores of this study do not have a noticeably different appearance than surrounding sediments (e.g. colour change), while the Mattawa II Beds are grey (5Y 5/1; Fig. 4.16), and the Mattawa III Beds are dark grey (5Y 4/1, 2.5Y 4.1; Fig. 4.17). Within core 594, both the Mattawa I and III Beds are characterized by a relative decrease in the amount of

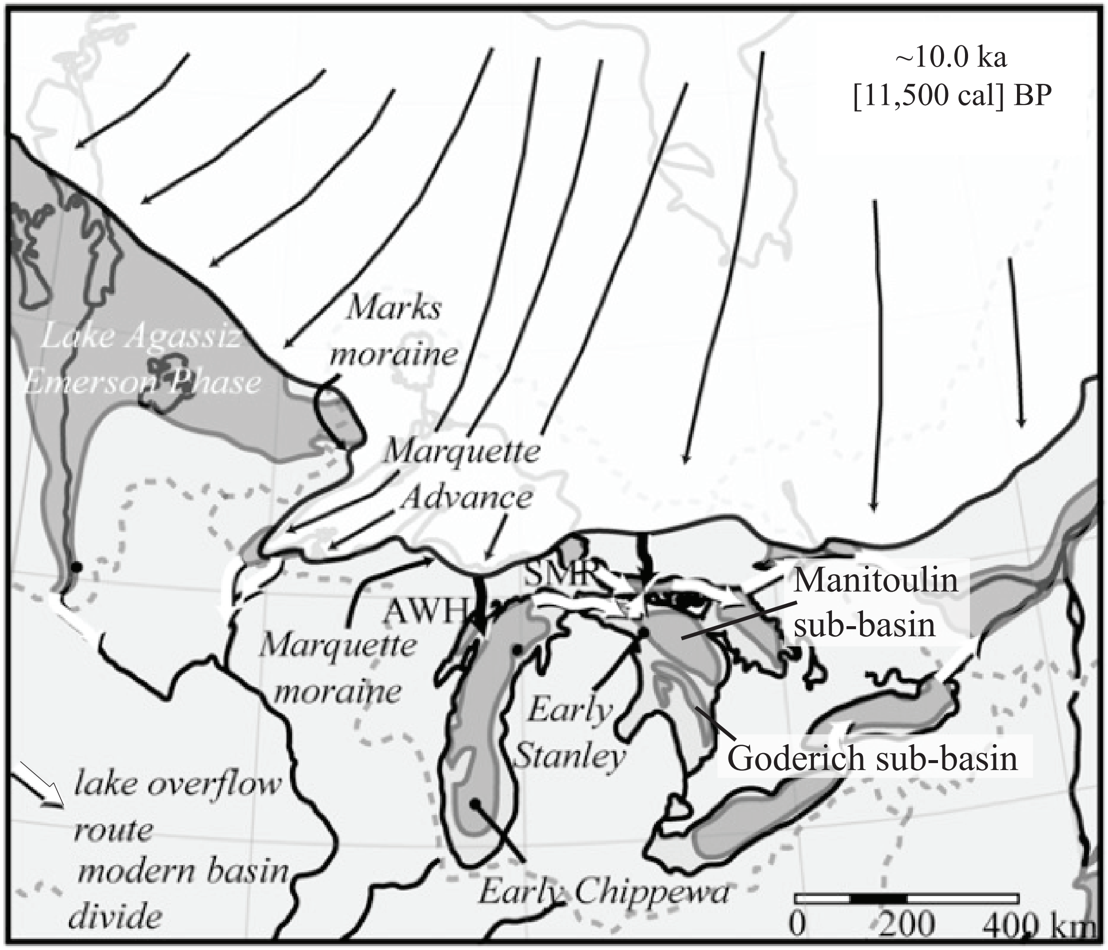

Figure 4.15. Diagram depicting the isolated sub-basins within the Huron Basin during the early Holocene. At this time, the northern Huron Basin received overflow from Lake Minong in the Superior Basin via the St. Mary's River (SMR) and from the Michigan Basin via the Straits of Mackinac. Modified from Breckenridge and Johnson (2009).

Figure 4.16. Images of the Goderich sub-basin core 146 and the Manitoulin sub-basin core 596 showing the grey (5Y 5/1) bed deposited during the Mattawa II flood (~8.4 ka [9,450 cal] BP). This flood is associated with the re-routing of waters from the Superior and Agassiz Basins southwards into the Huron Basin, and it correlates to the initial pulse of the A2 event in the Michigan Basin. Core images are stretched horizontally ~2 times to show detail.

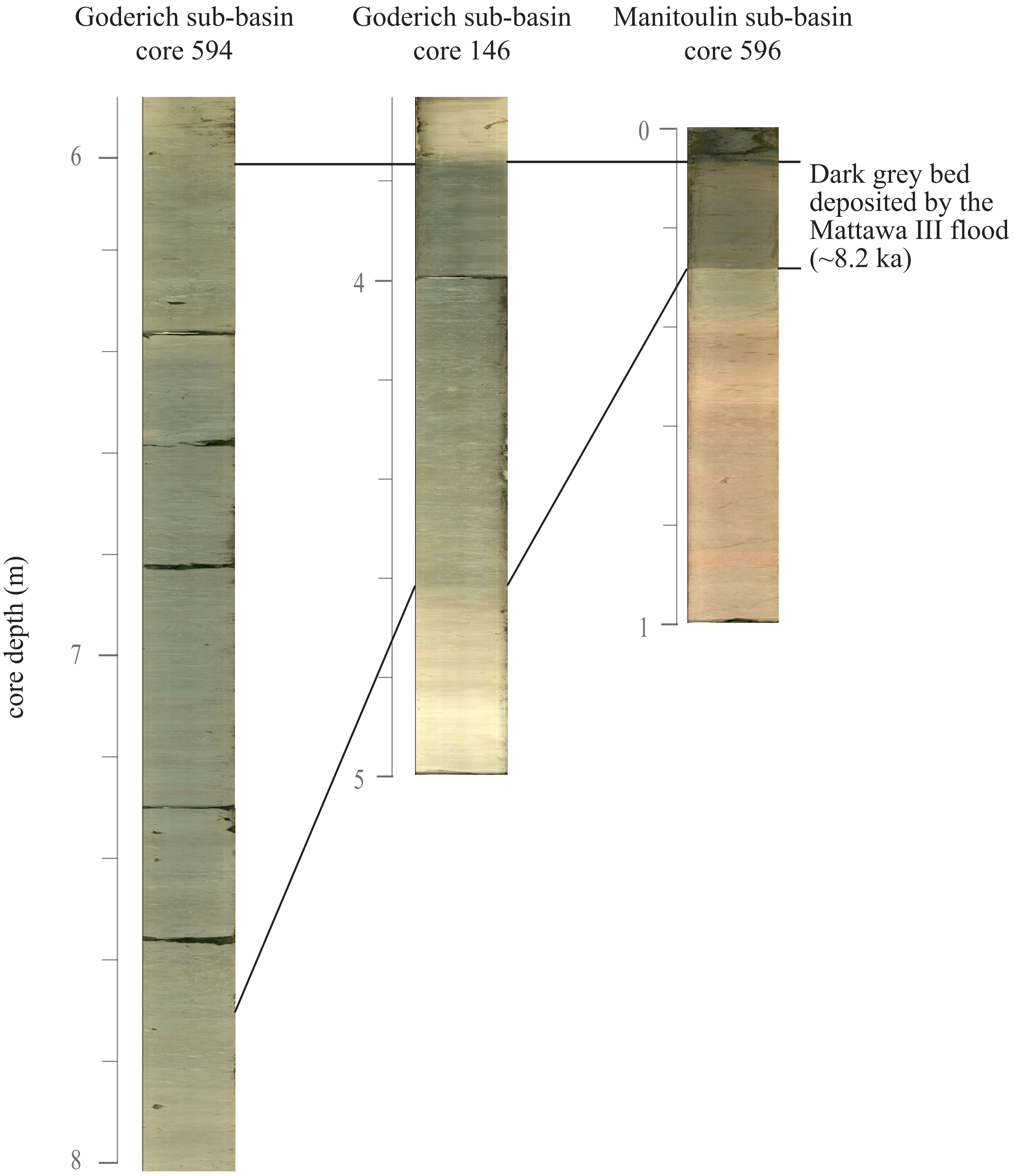

Figure 4.17. Images of Goderich sub-basin cores 594 and 146 and Manitoulin sub-basin core 596 showing the dark grey (5Y 4/1, 2.5Y 4.1) bed deposited during the Mattawa III flood (~8.2 ka [9,100 cal] BP). This flood is associated with the re-routing of water from the Superior and Agassiz Basins southwards into the Huron Basin, and it correlates to the second pulse of the A2 event in the Michigan Basin. Core images are stretched horizontally ~2 times to show detail.

calcite and an increase in the amount of quartz present in the sediment (Fig 4.9). At this time, the source of the darker sediments deposited during the Mattawa II and III floods is unknown.

The oxygen-isotope records for shallower-water species are restricted to intervals characterized by much higher $\delta^{18}O_{\text{lakewater}}$ values than those associated with glacial meltwater (Fig. 4.10). In these intervals, deep- and shallower-water ostracode and clam species in the Goderich sub-basin cores have similarly high $\delta^{18}O$ values. The variety of ostracode and clams species present in the basin during these high-^{18}O intervals suggests that water at this time, dominated by local precipitation and runoff, likely had relatively higher TDS concentrations than glacial meltwater-dominated intervals. Additionally, the TDS content of the lakewater would have increased during low-level intervals for which evaporation has been implicated in increasing $\delta^{18}O_{\text{lakewater}}$ values (i.e., 8.5 ka [9,500 cal] BP and 7.9 ka [8,650 cal] BP; Lewis et al. 2007, 2008b; Brooks et al. 2010; Brooks and Medioli 2010). Conversely, the sole presence of *C. subtriangulata* during periods of low-^{18}O waters, may suggest that glacial meltwater influxes from Lake Agassiz and/or the LIS were characterized by low total dissolved solids (TDS). Indeed, Huron Basin lakewater with low $\delta^{18}O$ values is generally described by Rea et al. (1994a) as “dilute”.

Generally, the source of the Mattawa floods in the Huron Basin, as well as the A1 (Wilmette) and A2 floods in the Michigan Basin, is assumed to be outflows of Lake Agassiz (Lewis and Anderson 1989; Colman et al 1994a, 1994c; Lewis et al. 1994; Rea et al. 1994a, 1994b; Breckenridge and Johnson 2009; Chapter 3, this thesis), and indeed their timing correlates with known periods of eastern Agassiz discharge (Lewis and Anderson 1989; Lewis et al. 1994; Fisher 2003, 2007; Leverington and Teller 2003; Breckenridge et al. 2004; Teller and Leverington 2004; Breckenridge and Johnson 2009). However, low-^{18}O water sourced directly from the LIS is another possibility.

The initial Holocene flood, Mattawa I, is generally considered to have occurred at ~9.5 ka [10,700 cal] BP, during the earliest portion of Lake Agassiz’s Nipigon phase (9.5 – 8.2 ka [10,700 – 9,100 cal] BP. The retreat of the Marquette glacier from the Superior

Basin by ~9.5 ka [10,700 cal] BP allowed Lake Agassiz to drain through its eastern Kaiashk outlet into the Superior Basin via the Nipigon Basin, and then into the Huron Basin via the St. Mary's River (Teller and Thorleifson 1983; Leverington et al. 2000; Teller et al. 2005; Breckenridge 2007, Breckenridge and Johnson 2009; Breckenridge et al. 2010; Hyodo 2010). Oxygen-isotope compositions from the three cores are in agreement during this flooding event, and range from -19 to -17 ‰ (Fig. 4.14). Earlier studies have suggested that this flooding was likely short-lived, with as much as one-third of Lake Agassiz's volume being released in ~2 years (Teller and Thorleifson 1983; Farrand and Drexler 1985; Leverington et al. 2000; Leverington and Teller 2003). That said, sediment cores from the Huron Basin suggest that the connection to the Agassiz Basin via Lake Superior remained open for ~400 years, as indicated by low-^{18}O water until ~9.1 ka [10,200 cal] BP (Fig. 4.14). An alternative to a long and continuous flooding event may lie within sediment records from the Superior Basin, which suggest that the initial Nipigon-aged influx of Lake Agassiz waters into the Great Lakes Basin may have been a two-pulsed event. Within Superior Basin sediments, a sequence of thick red varves deposited at ~9.4 ka [10,600 cal] BP is followed closely by a sequence of thick grey varves deposited from 9.2 – 9.0 ka [10,400 – 10,200 cal] BP (Breckenridge et al. 2004; Breckenridge 2007; Hyodo and Longstaffe 2011c). Hyodo and Longstaffe (2011c) suggest that the change from red to grey varved sediments indicates a change in meltwater-rich sources, from the Agassiz Basin to more distal glaciofluvial discharge. Oxygen-isotope compositions during the Mattawa I flood in the cores examined here all show an increase of ~2 ‰ approximately midway within the low-^{18}O excursion (Fig. 4.10). Such a basin-wide increase in lakewater composition may reflect a temporary cessation in delivery of low-^{18}O waters; this is in agreement with a flood comprised of two closely spaced pulses of water. Unlike in the Superior Basin, no change in sediment colour is observed within sediments attributed to the Mattawa I flood (Fig. 4.2).

While isotopic evidence as well as the regional glacial history indicate a link between the Superior and Huron Basins during the initial Mattawa flooding event, consequences for the Michigan Basins are less clear. In particular, an early Holocene flood correlating to the Mattawa I was not identified in the oxygen-isotope records obtained from the Michigan Basin cores studied here (Chapter 3), although a small change was detected in the South Chippewa sub-basin by earlier investigators (core 9V; Colman et al. 1990, 1994a, 1994b, 1994c; Forester et al. 1994; Breckenridge and Johnson 2009).

Valves of *C. subtriangulata* from both the Manitoulin sub-basin core as well as the Goderich sub-basin core 146 suggest that $\delta^{18}O_{\text{lakewater}}$ values remained low, ~ -17 to -14 ‰, for a few hundred years following the Mattawa I flood (from ~9.1 – 8.7 ka [10,200 – 9,650 cal] BP; Fig. 4.14). Meanwhile, *C. subtriangulata* valves from Goderich sub-basin core 594 indicate that lakewater quickly increased in composition, reaching values of -11 ‰ shortly after 9.1 ka, and further increased to -8 ‰ at ~8.7 ka. Previous records of water composition from the Huron Basin range from -14 to -9 ‰ during this time, which fall between the low values measured for cores 146 and 596 and the higher values measured for core 594 (Fig. 4.14; Lewis et al. 1994; Rea et al. 1994a; Moore et al. 2000; Breckenridge and Johnson 2009).

It has been suggested that the Huron Basin experienced very low lake levels between the Mattawa I and Mattawa II floods, leading to hydraulic closure by ~8.5 ka [9,500 cal] BP (Brooks et al. 2010; Brooks and Medioli 2010). These low lake levels would presumably have isolated the sub-basins and may have allowed low-^{18}O waters, sourced from the north, to pond in the more northern Manitoulin sub-basin but not reach the Goderich sub-basin, as proposed during the early Holocene from 10 – 9.5 ka [11,500 – 10,700 cal] BP. However, isotopic records between the two Goderich sub-basin cores are also not in agreement over the interval from ~9.1 – 8.7 ka [10,200 – 9,650 cal] BP (Fig. 4.14). In core 146, sediment from 8.4 – 6.8 m is relatively coarse-grained (contained abundant sand). The age of this coarser grained interval, ~9.2 – 8.4 ka [10,300 – 9,450 cal] BP, was estimated assuming a constant sedimentation rate between known ages in our age model (Fig. 4.13). However, the Huron Basin experienced rapidly fluctuating lake levels during this time period (Lewis et al. 1994, 2005) and hence assumption of a constant sedimentation rate may be inaccurate. Oxygen-isotope compositions for cores 594 and 146, when plotted versus depth, show a similar trend of increasing $\delta^{18}O$ values following low values associated with the Mattawa I flood (Fig. 4.10). When these oxygen-isotope compositions are plotted versus age (Fig 4.14), however, their lack of correlation following the Mattawa I flood may indicate that our age model for core 146 is too young by ~400 years during the interval from ~9.1 – 8.7 ka [10,200 – 9,650 cal] BP.

Sediment in core 596 deposited from 8.7 – 8.4 ka [9,650 – 9,450 cal] BP was barren of ostracodes, but ostracodes from both Goderich sub-basin cores show that $\delta^{18}O_{lakewater}$ values increased to ~ -10 to -8 ‰ by 8.6 ka [9,550 cal] BP (Fig. 4.14). Previous records spanning the interval from ~8.9 – 8.4 ka [10,000 – 9,450 cal] BP indicate that lakewater in the Huron Basin had $\delta^{18}O$ values of ~ -10 to -9 ‰ (Rea et al. 1994a; Moore 2000; Breckenridge and Johnson 2009), while lakewater in the Agassiz and Superior Basins had $\delta^{18}O$ values of ~ -27 to -25 ‰ (Fig. 4.14; Breckenridge and Johnson 2009; Breckenridge et al. 2010; Hyodo and Longstaffe 2011b).

The discrepancy between the oxygen-isotope compositions of waters in the Superior versus the Huron (and Michigan) Basins between ~8.9 – 8.4 ka [10,000 – 9,450 cal] BP was initially explained by the pathway of Superior outflow through the North Channel onto Georgian Bay and out the North Bay outlet, thus bypassing the main Huron Basin (Teller 1985; Dettman et al. 1995; Lewis et al. 1994; Rea et al. 1994b). Another explanation relies on the stratified lake model of Birks et al. (2007). In this model, the oxygen-isotope records provided by benthic ostracodes from the Superior Basin reflect the composition of turbid, dense meltwater that ponded at great depth whereas outflow into the Huron Basin was dominated by more ^{18}O-rich surface waters derived from precipitation and runoff (Breckenridge and Johnson 2009). However, co-existing benthic and pelagic proxies for $\delta^{18}O_{lakewater}$ in the Superior Basin, which are needed to test this idea, have yet to be obtained.

A third – and perhaps the most likely – explanation for isotopic differences between the Superior and Huron Basins is that outflow from the Superior Basin was diverted through a northeast outlet to Lake Ojibway from ~8.9 – 8.4 ka [10,000 – 9,450 cal] BP until a glacial advance and/or isostatic rebound once again redirected water through the St. Mary’s River into the Huron Basin (Breckenridge and Johnson 2009; Breckenridge et al. 2010). Such a hiatus in the delivery of Superior Basin water into the Huron Basin may have led to hydrologic closure of the Huron Basin by ~8.5 ka [9,500 cal] BP, as proposed by Brooks et al. (2010) and Brooks and Medioli (2010). High $\delta^{18}O_{lakewater}$ values in the Huron Basin at this time also point to a water budget dominated by local precipitation and runoff.

Lakewater records from the Ile Parisienne sub-basin of Lake Superior, the southeastern-most sub-basin, show that water in this region had increasingly high $\delta^{18}O$ values beginning at ~8.9 ka [10,000 cal] BP, a time when other Lake Superior sub-basins recorded very low $\delta^{18}O$ values indicative of large volumes of Lake Agassiz and/or LIS water (Hyodo and Longstaffe 2011b). These differences were interpreted by Hyodo and Longstaffe (2011b) to support the hypothesis of a northern Superior outlet to Lake Ojibway. Such a drainage pattern may have diverted low-^{18}O waters out of the Superior Basin, allowing precipitation and more local runoff to become dominant in the Ile Parisienne sub-basin.

The resumption of Lake Superior outflow into the Huron Basin led to two closely spaced floods, the Mattawa II at 8.4 ka [9,450 cal] BP and Mattawa III at 8.2 ka [9,100 cal] BP. The oxygen-isotope composition of Huron Basin lakewater decreased by ~8 ‰ to values as low as -21 ‰ at ~8.4 ka [9,450 cal] BP (Fig. 4.14). Biogenic carbonates from Goderich sub-basin core 146 provide a very clear record of lakewater composition over the interval from 8.4 – 8.2 ka [9,450 – 9,100 cal] BP. Lakewater $\delta^{18}O$ values increase sharply to -9 ‰ following the Mattawa II flood before the final influx of low-^{18}O waters, the Mattawa III flood at 8.2 ka [9,100 cal] BP, caused a decrease in lakewater $\delta^{18}O$ values to -19 ‰ (Fig. 4.14). These floods have been linked to a temperature decrease of ~2 °C in the North Atlantic centered around 8.3 ka [9,300 cal] BP (Fleitmann et al. 2008; Yu et al. 2010).

Taken together, the Huron Basin cores examined here provide a high-resolution record of $\delta^{18}O_{lakewater}$ fluctuations during the Holocene. The magnitude of these variations is quite high compared to the Superior and Michigan Basins (Fig. 4.14). In particular, individual pulses of low-^{18}O water are clearly resolved into the Mattawa II and III floods (Fig. 4.14). During the interval from 8.4 – 8.2 ka [9,450 – 9,100 cal] BP when the Huron Basin received overflow from the Superior Basin, water residence time in the Huron Basin was likely shorter than the modern value of 22 yrs. This allowed for the individual preservation of both the Mattawa II and III Beds. The Mattawa II and III floods in the Huron Basin correlate to the A2 event in the Michigan Basin, which reflects backflooding through the Straits of Mackinac.

A late surge of low-^{18}O waters into the Superior Basin at ~8.1 ka [9,050 cal] BP is not apparent in the Huron record. This is not surprising; Hyodo and Longstaffe (2011b) note that evidence for this event was found only in the sub-basins most proximal to the source of the floodwaters and is not recorded elsewhere in the Superior Basin.

The mid Holocene (~ 8 – 6 ka [9,000 – 6,850 cal] BP)

Lakewater oxygen-isotope compositions rose steadily after the final Mattawa flood at 8.2 ka [9,100 cal] BP in the Huron Basin from ~ -10 to -5 ‰ at the top of the carbonate fossil record. Biogenic carbonates were not recovered from sediments younger than ~6.1 ka [6,900 cal] BP. Lakewater oxygen-isotope compositions of ~ -5 ‰ are higher than modern Lake Huron water (-7.4 ‰; Macdonald and Longstaffe 2007). Such compositions likely reflect the relatively warm period known as the Holocene Hypsithermal (~8 – 4 ka [9,000 – 4,400 cal] BP), which characterized much of the mid-Holocene throughout North America (Bartlein et al. 1984; Dorale et al. 1992; Wright 1992; Kutzbach and Webb 1993; Krishnamurthy et al. 1995; Dean et al. 1996; Yu et al. 1997; Lovan and Krishnamurthy 2011).

The final Stanley lowstand in the Huron Basin began at ~7.9 ka [8,650 cal] BP (Lewis et al. 2007) soon after Lake Agassiz outflow was diverted away from the Great

Lakes Basin and into Lake Ojibway in the Hudson Bay lowlands (Bajc et al. 1997; Breckenridge et al. 2004, 2010). The relatively warm and dry climate at the time contributed to the lowering of lake levels via evaporative water loss and led to hydrological closure of the Huron, Georgian Bay and Michigan Basins from 7.9 – 7.5 ka [8,650 – 8,350] cal BP (Lewis et al. 2005; 2007, 2008b). The formation of the black Fe-sulfide bands likely began early on during this final low-level phase. Odegaard et al. (2003) hypothesized that the development of these bands was brought on by anoxic conditions caused by a lack of seasonal turnover and continual decay of organic matter (Odegaard et al. 2003). At the very least, these iron-sulfide bands indicate reducing conditions at shallow depths below the sediment-water interface.

The eventual collapse of the ice sheet at ~7.7 ka [8,450 cal] BP (known as the '8.2 ka event') released the immense volume of freshwater stored in Lake Agassiz-Ojibway into Hudson Bay, which may have disrupted ocean circulation patterns and led to a temporary cool period in the North Atlantic region (Stuiver et al. 1995; Alley et al. 1997; Barber et al. 1999; Daley et al. 2009). The collapse of the ice sheet initiated rapid reorganization of atmospheric circulation patterns, causing climate changes across North America (Edwards et al. 1996; Kirby et al. 2002; Shuman et al. 2002). A shift from relatively dry to moist conditions occurred between ~7 – 6 ka [7,800 – 6,800 cal] BP (Bartlein et al. 1984; Edwards et al. 1996; Shuman et al. 2002). The oxygen-isotope composition of precipitation in southern Ontario showed a correlative shift with both temperature and relative humidity, increasing from ~ -10 ‰ to ~ -8 ‰ during this time (Edwards et al. 1999).

Continued isostatic rebound of the Great Lakes Basin caused lake levels to rise during the Nipissing transgression (~7.4 – 5.0 ka [8,200 – 5,700 cal] BP) and eventually shifted drainage to the Port Huron outlet (Thompson and Baedke 1997; Lewis et al. 2007).

In the uppermost biogenic carbonate bearing sediments of the Goderich sub-basin cores there is an apparent difference of ~2-3 ‰ between $\delta^{18}O_{lakewater}$ values calculated from *C. subtriangulata* versus those calculated using clams and *C. lacustris* (Fig. 4.10). This difference may represent inflow of particularly ^{18}O-rich water to the shallower regions of the lakes by tributaries or runoff, or evaporative enrichment of water in the shallow regions. This small but consistent difference between oxygen-isotope compositions may suggest relatively infrequent mixing between waters in the shallow and deep regions of the Huron Basin. This is in agreement with the suggestion made by Odegaard et al. (2003) that regular diurnal turnover of water was halted as a consequence of the climatic conditions during the mid Holocene. Alternatively, these differences may reflect that the fractionation factors calculated using modern Lake Huron species and applied here to calculate lakewater composition overestimate growth temperature and/or the oxygen-isotope vital effect for these mid-Holocene ostracodes.

4.4.4 The carbon-isotope history of Ancient Lake Huron

The carbon-isotope composition of biogenic carbonates is largely controlled by the $\delta^{13}C_{DIC}$ value of dissolved inorganic carbonate (DIC) plus some additions from the organism's diet (referred to as metabolic carbon) and carbon cycling in microenvironments created by these organisms (Tanaka et al. 1986; Dettman et al. 1995, 2005; von Grafenstein et al. 1999; Holmes and Chivas 2002; Leng and Marshall 2004; Decrouy et al. 2011a, 2011b). Most isotopic fractionation within the carbon cycle of freshwater lakes results from primary productivity (photosynthesis) during which the residual DIC pool becomes enriched in ^{13}C as the more ^{12}C-rich organic matter is produced (Lister 1988; Farquhar et al. 1989; Hollander and McKenzie 1991; Leng and Marshall 2004). As organic matter produced from primary productivity is deposited in lake sediments, its decay returns carbon depleted of ^{13}C to the DIC pool (Hayes 1993). The carbon-isotope composition of the DIC pool is also influenced by the composition of atmospheric CO_2 and its degree of exchange with dissolved CO_2, the flux of soil carbon into the lake, and the dissolution of carbonate detritus (Rau 1978; Meyers 1993; Wolfe et al. 1996; Hyodo and Longstaffe 2011a).

In modern Lake Huron, the dominant DIC species is bicarbonate (HCO_3^-), which has a $\delta^{13}C_{DIC}$ value of 0.5 ‰ above the thermocline and -1.0 ‰ below (Rea et al. 1994a: Dettman et al. 1995). Higher $\delta^{13}C_{DIC}$ values above the thermocline likely reflect removal of ^{12}C by photosynthesizing organisms. Lower $\delta^{13}C_{DIC}$ values at greater depths can likely be attributed to the ^{12}C-rich source of carbon provided by oxidizing organic matter on the lake bottom (Dettman et al. 1995). The $\delta^{13}C_{DIC}$ values of porewater (i.e., microenvironment-DIC) are typically lower than lakewater-DIC by ~1-4 ‰ (Decrouy et al. 2011b). Ostracodes live at shallow depths below the sediment-water interface and utilize such a microenvironment-DIC source; this imparts more low-^{13}C into their valves than predicted for equilibrium with lakewater-DIC as their carbon source (Chapter 2, this thesis). Similarly, clams also have lower $\delta^{13}C$ values than expected for precipitation at equilibrium using lakewater-DIC as their carbon source (Chapter 2, this thesis). This results from the incorporation of carbon from low-^{13}C dietary sources, which typically include algae/bacteria and decomposing organic matter with $\delta^{13}C$ values of ~ -30 to -25 ‰ (Meyers and Ishiwatari 1993; Hodell and Schelske 1998; Meyers 2003). Although it may be useful to apply microenvironment or metabolic corrections to calculate the $\delta^{13}C$ value of open lakewater-DIC from shelly fossils, relative changes in $\delta^{13}C_{DIC}$ values are nonetheless still provided, allowing for inferences to be made regarding changes in DIC source(s) and/or productivity through time.

Rea et al. (1994a) and Lewis et al. (1994) noted that excursions to lower $\delta^{13}C_{DIC}$ values coincided with arrival of low-^{18}O waters in the Huron Basin. These studies suggested that the low $\delta^{13}C$ values of biogenic carbonates resulted from sudden additions of dissolved organic carbon (e.g. soil organic matter) to the lake. The Manitoulin sub-basin core 596 examined here shows only small variations in both $\delta^{18}O$ and $\delta^{13}C$ values, and hence cannot be used to explore this idea further. However, the Goderich sub-basin cores 594 and 146 suggest that precipitation and overland runoff (i.e., high $\delta^{18}O$ values), and not Agassiz and/or meltwater inflows, were the dominant source of water during periods characterized by relatively low $\delta^{13}C$ values (Fig. 4.18). In cores 594 and 146, $\delta^{13}C$ values of *C. subtriangulata* increase as $\delta^{18}O$ values decrease (and vice versa) from the bottom of both cores to depths of ~7.0 and 4.4 m, respectively (Figs. 4.18).

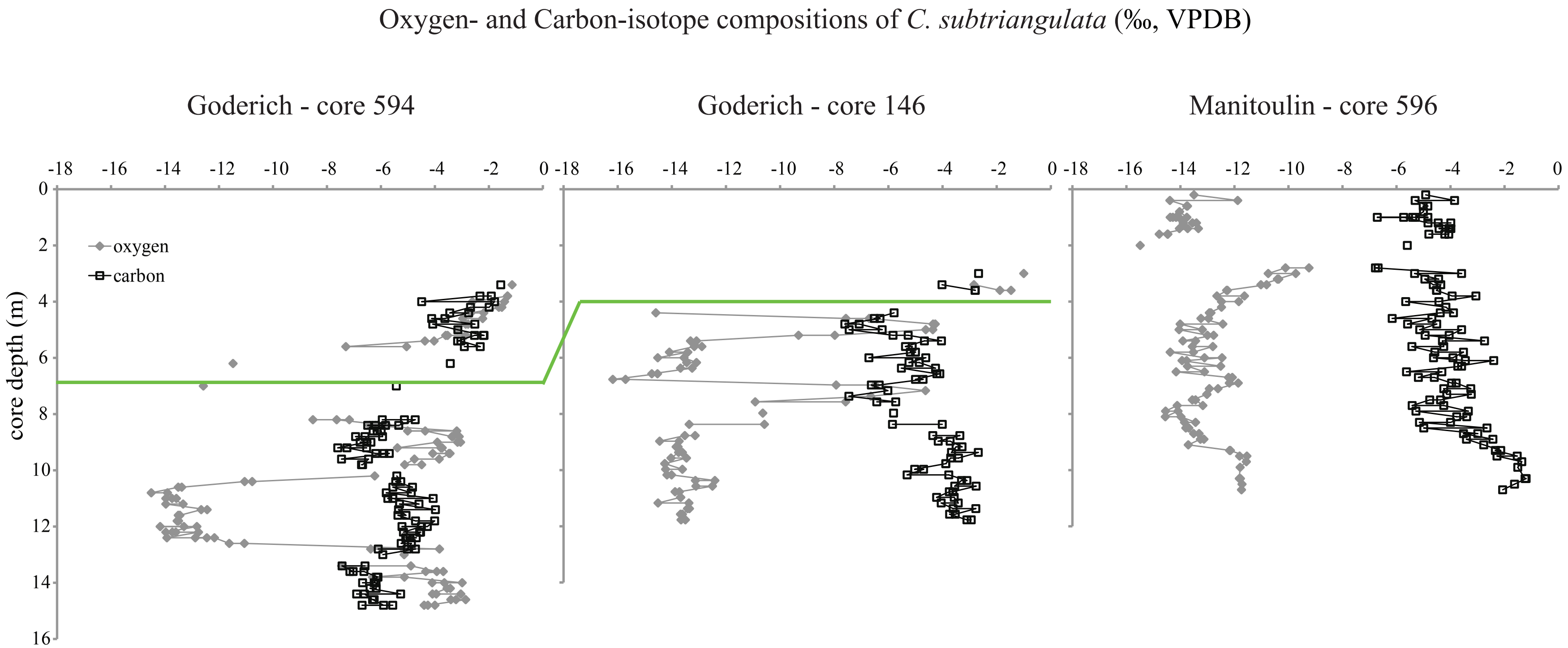

Figure 4.18. Oxygen- and carbon-isotope compositions of *C. subtriangulata* from Goderich sub-basin cores 594 and 146 and Manitoulin sub-basin core 596. The green line across the two Goderich sub-basin graphs marks ~8.0 ka [9,000 cal] BP, the time at which Lake Agassiz water (and/or meltwater) began to bypass the Great Lakes. During the early Holocene (10 - 8 ka [11,500 - 9,000 cal] BP; below the green line), lower $\delta^{18}O$ values are typically associated with higher $\delta^{13}C$ values (and vice-versa) and there is a moderately strong negative correlation between $\delta^{18}O$ and $\delta^{13}C$ values. Conversely, during the mid Holocene (8 - 6 ka [9,000 - 6,850 cal] BP; above the green line), both $\delta^{18}O$ and $\delta^{13}C$ values are typically higher than measured in the early Holocene and are only very weakly positively correlated with each other. Neither relationship is evident for the Manitoulin sub-basin core 596, which shows relatively subtle variations in both $\delta^{18}O$ and $\delta^{13}C$ values.

According to the age models for these cores (Fig. 4.13), sediment at these depths represents ~8.0 ka [9,000 cal] BP, the time at which Agassiz outflow began to bypass the Great Lakes Basin and was directed northeast into Lake Ojibway (Bajc et al. 1997; Barber et al. 1999). This may suggest that Lake Agassiz outflow, which was characterized by low $\delta^{18}O_{lakewater}$ values, also had high $\delta^{13}C_{DIC}$ values relative to local runoff and precipitation.

Potential sources of high-$^{13}C_{DIC}$ material to the Mattawa flood waters may have included Paleozoic carbonates, which surround much of the Huron Basin ($\delta^{13}C$ values = -1 to 4 ‰; Lohmann and Walker 1989), as well as further north in and around the Superior Basin ($\delta^{13}C$ = -2.0 to +1.7 ‰; Chow and Longstaffe 1995). Hyodo and Longstaffe (2011a) suggested that inflows of glacial meltwater likely contained abundant DIC from dissolution of Paleozoic carbonate detritus from the Agassiz and Hudson Bay regions, and found that the amount of DIC delivered to the Superior Basin decreased considerably after the glacial meltwater supply was terminated. Even small contributions of these relatively high-^{13}C sources, together with only limited contributions of terrestrial (e.g. soil) organic matter, would have resulted in inflows from Lake Agassiz with high $\delta^{13}C_{DIC}$ values.

Lower biogenic carbonate $\delta^{13}C$ values during times when local precipitation and runoff were the main water sources to the Huron Basin may reflect decreases in primary productivity. However, it is more likely that the low $\delta^{13}C$ values reflect the delivery of terrestrial (e.g. soil) organic matter, with values of ~ -27 ‰ (Vogel 1993), to the basin. Hyodo and Longstaffe (2011a) attribute soil organic matter adsorbed onto clays to the more or less consistently low $\delta^{13}C$ values of organic matter in Superior Basin glacial sediments.

After 8.0 ka [9,000 cal] BP, biogenic carbonate $\delta^{18}O$ and $\delta^{13}C$ values generally both increase towards the top of the sedimentary section (Fig. 4.18). During the post-glacial period, the $\delta^{13}C$ values of all biogenic carbonate species increase towards maximum values of ~ -3 to -2 ‰ at the top of the profile (Fig. 4.11). Such compositions are very similar to those measured for modern ostracodes from the Huron Basin (Chapter 2, this thesis). This upward increase likely reflects increasing primary productivity within the water column, which would deplete the DIC pool of ^{12}C (Lister 1988; Leng and Marshall 2004). In the Michigan Basin, the δ^{13}C values of ostracodes and clams increase by ~2-3 ‰ following the A2 event, which marked the final influx of Lake Agassiz water, and was attributed to greater rates of primary productivity (Chapter 3, this thesis). The same conclusion of increased primary productivity following the cessation of glacial meltwater inputs was reached for the Superior Basin (Hyodo and Longstaffe 2011a).

4.5 CONCLUSIONS

Efforts to establish reliable chronologies for the three cores examined in this study included radiocarbon dating, pollen assemblage 'dating', identification of previously dated sedimentary sequences, and identification of key units within the sediments for which dates are well known. Several challenges were encountered. First, most of the radiocarbon dates, which were obtained only for Goderich sub-basin core 594, were determined to be too young/old for the enclosing sediment and hence excluded from the age model. That said, many of the excluded dates are likely older than the enclosing sediment by only a few hundred years. Second, the palynological record for cores 594 and 596 was very problematic in that it suggested dates that were too young by up to a few thousand years, if the oxygen isotopic record of glacial meltwater input is to be accepted. It is most likely that large fluctuations in lake level within the Huron Basin, particularly from ~10 – 7.5 ka [11,500 – 8,350 cal] BP, were responsible for reworking the pollen grains, and thus have prevented us from obtaining clear age models using these materials. Over- or under-estimating the hard water effect correction may similarly be preventing us from establishing a clear chronology using the radiocarbon dates; a constant HWE value of 438 years has been used here but it is most likely that the amount of 'dead' carbon delivered to the Huron Basin, and thus true values for the HWE, varied through time.

The Manitoulin sub-basin core 596 samples the oldest sediments of the three cores examined here. Its age ranges from ~12.0 – 8.2 ka [13,800 – 9,100 cal] BP. The Goderich sub-basin core 594 core spans ~9.9 ka [11,300 cal] BP to perhaps ~4.0 ka [4,500 cal] BP. Sediments from Goderich sub-basin core 146 ranges from ~9.5 ka [10,700 cal] to possibly ~4.0 ka [4,500 cal] BP.

Goderich sub-basin sediments, as exemplified by core 594, show large variations in quartz (29 – 68 %) and calcite (0 – 38 ‰) contents, with quartz contents generally increasing towards the top of the core and calcite decreasing. This relationship largely reflects the low sedimentation rates in Lake Huron since ~5 ka [5,730 cal] BP, which facilitates dissolution of carbonate detritus. Calcite contents are also lower (<10 %) during periods when the Huron Basin received inflows of Lake Agassiz water. Such variations during deposition of glacial sediments likely reflect changes in sediment sources to the Huron Basin over time.

Valves of *C. subtriangulata* from core 596 yield $\delta^{18}O_{lakewater}$ values of ~ -19 to -17 ‰ for the Manitoulin sub-basin in the portion of the late Pleistocene sampled here (~11.5 – 10 ka [12,600 – 11,500 cal] BP. These compositions are very similar to values obtained for Lakes Michigan and Erie for this period of time, and suggest a consistent and direct connection to a low-^{18}O water source, such as the LIS or the Agassiz Basin.

Three influxes of low-^{18}O water are present in the isotopic records for the early- to mid-Holocene in Lake Huron. These are attributed to large floods originating from Lake Agassiz: Mattawa I, ~ 9.5 ka [10,700 cal] BP; Mattawa II, ~8.4 ka [9,450 cal] BP and Mattawa III, 8.2 ka [9,100 cal] BP. The Mattawa II flood is recorded by a grey (5Y 5/1) clay-rich bed in core 146 (from 7.2 – 6.8 m) and core 596 (from 2.4 – 2.0 m). The Mattawa III flood is marked by a dark grey (5Y 4/1, 2.5Y 4.1) bed in all three cores (~7.75 – 6.0 m in core 594, 4.6 – 3.8 m in core 146, and 0.2 – 0.07 m in core 596). These beds are similar in appearance to those identified in the Michigan Basin and considered to be associated with Lake Agassiz flooding events.

Differences of up to 11 ‰ are observed in the oxygen-isotope compositions of water in the Goderich and Manitoulin sub-basins during the early Holocene from 10.0 – 9.5 ka [11,500 – 10,700 cal] BP. These sub-basins were dominated by different water sources during this period of low water levels, thus indicating reduced hydraulic connectivity between the northern and southern regions of the Huron Basin.

Relatively high oxygen-isotope compositions at ~8.5 ka [9,500 cal] BP and 7.9 ka [8,700 cal] BP reflect the cessation of glacial meltwater-rich inflows and correlate with times when the Huron Basin was hydrologically closed. After termination of glacial meltwater input to Lake Huron (~8.1 ka [9,000 cal] BP), $\delta^{18}O_{lakewater}$ values in the Goderich sub-basin increased to higher-than-modern values (> -7.4 ‰). Such compositions indicate warmer and drier conditions during the Holocene Hypsithermal (~8 – 4 ka [9,000 – 4,400 cal] BP).

During the early Holocene (~10 – 8 ka [11,500 – 9,000 cal] BP), the carbon-isotope compositions of biogenic carbonates were controlled by Agassiz inflows. Floods originating from Lake Agassiz are associated with higher $\delta^{13}C_{DIC}$ values than regional precipitation and runoff. Lake Agassiz outflows likely contained a smaller proportion of dissolved carbon originating from terrestrial (e.g. soil) organic matter and a larger proportion originating from Paleozoic carbonates derived from the terrain surrounding parts of the Great Lakes Basin. After glacial meltwater input ended until the end of the Holocene fossil record (8.1 - ~6 ka [9,000 – 6,900 cal] BP), the biogenic carbonate $\delta^{13}C$ values gradually increase towards compositions typical of modern biogenic carbonate material in Lake Huron. This increase is suggestive of higher primary productivity towards present time.

4.6 REFERENCES

Alley RB, Shuman CA, Meese DA, Gow AJ, Taylor KC, Cuffey KM, Fitzpatrick JJ, Grootes PM, Zielinski GA, Ram M (1997) Visual-stratigraphic dating of the GISP2 ice core: Basis, reproducibility, and application. J Geophys Res 102: 26367–26381

Anderson TW (2002) Pollen stratigraphy and vegetation history, Sheguiandah

Archaeological Site. In: Julig PJ (ed) The Sheguiandah Site—Archaeological, Geological and Paleobotanical studies at a Paleoindian site on Manitoulin Island, Ontario. Canadian Museum of Civilization, Mercury Series, Archaeol Surv of Can Paper 161, pp 179–194

Anderson TW, Lewis CFM (2002) Upper Great Lakes climate and water-level changes 11 to 7 ka: effect on the Sheguiandah archeological site. In: Julig PJ (ed) The Sheguiandah Site—Archaeological, Geological and Paleobotanical studies at a Paleoindian Site on Manitoulin Island, Ontario. Canadian Museum of Civilization, Mercury Series, Archaeol Surv of Can Paper 161, pp 195–234

Barber DC, Dyke A, Hillaire-Marcel C, Jennings AE, Andrews JT, Kerwin MW, Bilodeau G, McNeely R, Southon J, Morehead MD, Gagnon J-M (1999) Forcing of the cold event of 8,200 years ago by catastrophic drainage of Laurentide lakes. Nature 400: 344–348

Bartlein PJ, Webb T III, Fleri E (1984) Holocene climatic change in the northern Midwest: Pollen-derived estimates. Quat Res 22: 361-374

Birks SJ, Edwards TWD, Remenda VH (2007) Isotopic evolution of Glacial Lake Agassiz: New insights from cellulose and porewater isotopic archives. Palaeogeogr Palaeoclimatol Palaeoecol 246: 8-22

Boomer I (2002) Environmental applications of marine and freshwater ostracoda. In Haslett SK (ed) Quaternary Environmental Micropalaeontology. Arnold, London. pp 115-138

Boyd M (2007) Early postglacial history of the southeastern Assiniboine Delta, glacial Lake Agassiz basin. J Paleolimnol 37: 313–329

Breckenridge A (2007) The Lake Superior varve stratigraphy and implications for eastern Lake Agassiz outflow from 10,700 to 8,900 cal ybp (9.5–8.0 14C ka). Palaeogeogr Palaeoclimatol Palaeoecol 246: 45-61

Breckenridge A, Johnson TC (2009) Paleohydrology of the upper Laurentian Great Lakes from the late glacial to early Holocene. Quat Res 71: 397-408

Breckenridge A, Johnson TC, Beske-Diehl S, Mothersill JS (2004) The timing of regional late glacial events and postglacial sedimentation rates from Lake Superior. Quat Sci Rev 23: 2355-2367

Breckenridge A, Lowell TV, Fisher TG, and Yu S (2010) A late Lake Minong transgression in the Lake Superior basin as documented by sediments from Fenton Lake, Ontario. J Paleolimnol DOI 10.1007/s10933-010-9447-z

Broecker WS, Kennett J, Flower B, Teller JT, Trumbore S, Bonani G, Wolfli W (1989) Routing of meltwater from the Laurentide Ice Sheet during the Younger Dryas cold episode. Nature 341: 318–321

Brooks GR, Medioli BE (2010) Sub-bottom profiling and coring of sub-basins along the lower French River, Ontario: insights into depositional environments within the North Bay outlet. J Paleolimnol DOI 10.1007/s10933-010-9414-8

Brooks GR, Medioli BE, Telka AM (2010) Evidence of early Holocene closed-basin conditions in the Huron-Georgian basins from within the North Bay outlet of the upper Great Lakes. J Paleolimnol DOI 10.1007/s10933-010-9408-6

Brown TA, Nelson DE, Mathewes RW, Vogel JS, Southon JR (1989) Radiocarbon dating of pollen by accelerator mass spectrometry. Quat Res 32: 205-212

Buhay WM, Betcher RN (1998) Paleohydrologic implications of ^{18}O-enriched Lake Agassiz water. J Paleolimnol 19: 285-296

Clark PU, Marshall SJ, Clarke GKC, Hostetler SW, Licciardi JM, Teller JT (2001) Freshwater forcing of abrupt climate change during the last glaciation. Science 293: 283-287

Colman SM, Keigwin LD, Forester RM (1994a) Two episodes of meltwater influx from glacial Lake Agassiz into the Lake Michigan basin and their climatic contrasts. Geology 22: 547-550

Colman SM, Jones GA, Forester RM, Foster DS (1990) Holocene paleoclimate evidence and sedimentation rates from a core in southwestern Lake Michigan. J Paleolimnol 4: 269-284

Colman SM, Clark JA, Clayton L, Hansel AK, Larsen CE (1994b) Deglaciation, lake levels, and meltwater discharge in the Lake Michigan basin. Quat Sci Rev 13: 879-890

Colman SM, Forester RM, Reynolds RL, Sweetkind DS, King JW, Gangemi P, Jones GA, Keigwin LD, Foster DS (1994c) Lake-level history of Lake Michigan for the past 12,000 years: the record from deep lacustrine sediments. J Great Lakes Res 20: 73-92

Coplen TB (1996) New guidelines for reporting stable hydrogen, carbon, and oxygen isotope-ratio data. Geochim et Cosmochim Acta 17: 3359-3360

Couch AG, Eyles N (2008) Sedimentary record of glacial Lake Mackenzie, Northwest Territories, Canada: Implications for Arctic freshwater forcing. Palaeogeogr Palaeoclimatol Palaeoecol 268: 26-38

Daley TJ, Street-Perrott FA, Loader NJ, Barber KE, Hughes PDM, Fisher EH, Marshall JD (2009) Terrestrial climate signal of the "8200 yr B.P. cold event" in the Labrador Sea region. Geology 37: 831-834

Dean WE, Ahlbrandt TS, Anderson RY, Bradbury JP (1996) Regional aridity in North America during the middle Holocene. The Holocene 6: 145-155

Decrouy L, Vennemann TW, Ariztegui D (2011a) Controls on ostracod valve geochemistry, Part 1: Variations of environmental parameters in ostracod (micro-) habitats. Geochim Cosmochim Acta 75: 7364-7359

Decrouy L, Vennemann TW, Ariztegui D (2011b) Controls on ostracod valve geochemistry: Part 2. Carbon and oxygen isotope compositions. Geochim Cosmochim Acta 75: 7380-7399

Deike RG, Granina L, Callender E, McGee JJ (1997) Formation of ferric iron crusts in Quaternary sediments of Lake Baikal, Russia, and implications for paleoclimate. Mar Geol 139: 21-46

Dell CI (1972) The origin and characteristics of the Lake Superior sediments. Programs and Abstracts of the 15th Conference on Great Lake Research, pp 361-370

Dell CI (1973) Vivianite: an authigenic phosphate mineral in Great Lakes sediments. Programs and Abstracts of the 16th Conference on Great Lake Research, pp 1027-1028

Derouin SA, Lowell TV, Hajdas I (2007) Landscape evolution and deglaciation of the Upper Peninsula, Michigan: An examination of chronology and stratigraphy in kettle lake cores. J Great Lakes Res 33: 875-886

Dettman DL, Palacios-Fest MR, Nkotagu HH, Cohen AS (2005) Paleolimnological investigations of anthropogenic environmental change in Lake Tanganyika: VII. Carbonate isotope geochemistry as a record of riverine runoff. J Paleolimnol 34: 93-105

Dettman DL, Smith AJ, Rea DK, Moore TC Jr., Lohmann KC (1995) Glacial meltwater in Lake Huron during early postglacial time as inferred from single-valve analysis of oxygen isotopes in ostracodes. Quat Res 43: 297-310

Dobson DM, Moore TC Jr., Rea DK (1995) The sedimentation history of Lake Huron and Georgian Bay: results from analysis of seismic reflection profiles. J Paleolimnol 13: 231-249

Dorale JA, González LA, Reagan MK, Pickett DA, Murrell MT, Baker RG (1992) A high-resolution record of Holocene climate change in speleothem calcite from Coldwater cave, Northeast Iowa. Science 258: 1626-1630

Edwards TWD, Wolfe BB, MacDonald GM (1996) Influence of changing atmospheric circulation on precipitation $\delta^{18}O$ – temperature relations in Canada during the Holocene. Quat Res 46: 211-218

Eschman DF, Karrow PF (1985) Huron basin glacial lakes: a review. In: Karrow PF, Calkin PE (eds) Quaternary Evolution of the Great Lakes. Geol Assoc Canada Spec Paper 30, pp 79-93

Fagel N, Alleman LY, Granina L, Hatert F, Thamo-Bozso E, Cloots R, Andre L (2005) Vivianite formation and distribution in Lake Baikal sediments. Glob Planet Change 46: 315-336

Farquhar GD, Ehleringer JR, Hubick KT (1989) Carbon isotope discrimination and photosynthesis. Annu Rev Plant Physiol Plant Mol Biol 40: 503-537

Fisher TG (2003) Chronology of glacial Lake Agassiz meltwater routed to the Gulf of Mexico. Quat Res 59: 271-276

Fisher TG (2007) Abandonment chronology of glacial Lake Agassiz's Northwestern outlet. Palaeogeogr Palaeoclimatol Palaeoecol 246: 31-44

Fisher TG, Smith DG (1994) Glacial Lake Agassiz: its northwest maximum extent and outlet in Saskatchewan (Emerson phase). Quat Sci Rev 13: 845-858

Fisher TG, Smith DG, Andrews JT (2002) Preboreal oscillation caused by a glacial Lake Agassiz flood. Quat Sci Rev 21: 873-878

Fisher TG, Weyer KA, Boudreau AM, Martin-Hayden JM, Krantz DE, Breckenridge A (2010) Constraining Holocene lake levels and coastal dune activity in the Lake Michigan basin. J Paleolimnol DOI 10.1007/s10933-010-9460-2

Fleitmann D, Mudelsee M, Burns SJ, Bradley RS, Kramers J, Matter A (2008) Evidence for a widespread climatic anomaly at around 9.2 ka before present. Paleoceanography 23, PA1102 1029/2007PA001519

Forester RM, Colman SM, Reynolds RL, Keigwin LD (1994) Lake Michigan's late Quaternary limnological and climate history from ostracode, oxygen isotope, and magnetic susceptibility. J Great Lakes Res 20: 93-107

Futyma RP, Miller NG (1986) Stratigraphy and genesis of the Lake Sixteen peatland, northern Michigan. Can J Botany 64: 3008-3019

Graham EJ, Rea DK (1980) Grain size and mineralogy of sediment cores from western Lake Huron. J Great Lakes Res 6: 129-140

Godsey HS, Moore TC Jr, Rea DK, Shane LCK (1999) Post-Younger Dryas seasonality in the North American midcontinent region as recorded in Lake Huron varved sediments. Can J Earth Sci 36: 533-547

Hansel AK, Mickelson DM, Schneider AF, Larsen CE (1985) Late Wisconsinan and Holocene history of the lake Michigan basin. In: Karrow PF, Calkin PE (eds)

Quaternary Evolution of the Great Lakes. Geol Assoc Canada Spec Paper 30, pp 39-53

Henderson PJ, Last WM (1998) Holocene sedimentation in Lake Winnipeg, Manitoba, Canada: implications of compositional and textural variations. J Paleolimnol 19: 265-284

Hodell SA, Schelske CL (1998) Production, sedimentation, and isotopic composition of organic matter in Lake Ontario. Limnol Oceanogr 43: 200-214

Hollander DJ, McKenzie JA (1991) CO_2 control on carbon-isotope fractionation during aqueous photosynthesis; a paleo-pCO_2 barometer. Geology 19: 929-932

Holmes JA, Chivas AR (2002) Ostracod shell chemistry – Overview. In: Holmes JA, Chivas AR (eds) The Ostracoda: Applications in Quaternary Research. AGU Monogr 131, pp 185-204

Hough JL (1966) Correlation of glacial lake stages in the Huron-Erie and Michigan basins. J Geol 74: 62-77

Hupfer M, Fischer P, Friese K (1998) Phosphorus retention mechanisms in the sediment of a eutrophic mining lake. Water Air Soil Poll 108: 341–352

Hyodo A (2010) The Holocene paleolimnology of Lake Superior. Ph.D. thesis, The University of Western Ontario, London, pp 330

Hyodo A, Longstaffe FJ (2011a) The paleoproductivity of ancient Lake Superior. Quat Sci Rev 30: 2988-3000

Hyodo A, Longstaffe FJ (2011b) Variations in the oxygen-isotope composition of ancient Lake Superior between 10,600 and 8,800 cal BP. J Paleolimnol, DOI 10.1007/s10933-011-9552-7

Hyodo A, Longstaffe FJ (2011c) The Chronostratigraphy of Holocene sediments from four Lake Superior sub-basins. Can J Earth Sci 48: 1581-1599

Karrow PF, Anderson TW, Clarke AH, Delorme LD, Sreenivasa MR (1975) Stratigraphy, paleontology, and age of Lake Algonquin sediments in southwestern Ontario, Canada. Quat Res 5: 49-87

Kemp ALW, Anderson TW, Thomas RL, Mudrochova A (1974) Sedimentation rates and recent sediment history of Lakes Ontario, Erie and Huron. J Sed Petrology 44: 207-218

Kirby MI, Mullins HT, Patterson WP, Burnett AW (2002) Late glacial – Holocene atmospheric circulation and precipitation in the northeast United States inferred from modern calibrated stable oxygen and carbon isotopes. Geol Soc Am Bull 114: 1326-1340

Krishnamurthy RV, Syrup K, Baskaran M, Long A (1995) Late glacial climate record of Midwestern USA from the hydrogen isotope record of lake organic matter. Science 269: 1565-1567

Kutzbach JE, Webb TI (1993) Conceptual basis for understanding Late-Quaternary climates. In: Wright HEJ, Kutzbach JE, Webb TI, Ruddiman WF, Street-Perrott FA, Bartlein PJ (eds) Global Climates Since the Last Glacial Maximum. University of Minnesota Press, Minneapolis, MN, pp 5-11

Larsen CE (1987) Geological history of glacial Lake Algonquin and the upper Great Lakes. USGS Bull 1801: 1-36

Last WM, Teller JT, Forester RM (1994) Paleohydrology and paleochemistry of Lake Manitoba, Canada: the isotope and ostracode records. J Paleolimnol 12: 269-282

Leng MJ, Marshall JD (2004) Palaeoclimate interpretation of stable isotope data from lake sediment archives. Quat Sci Rev 23: 811-831

Leverington D, Teller J (2003) Paleotopographic reconstructions of the eastern outlets of glacial Lake Agassiz. Can J Earth Sci 40: 1259-1278

Leverington DW, Mann JD, Teller JT (2000) Changes in the bathymetry and volume of glacial Lake Agassiz between 11,000 and 9,300 ^{14}C yr BP. Quat Res 54: 174-181

Lewis CFM, Anderson TW (1989) Oscillations of levels and cool phases of the Laurentian Great Lakes caused by inflows from glacial Lakes Agassiz and Barlow-Ojibway. J Paleolimnol 2: 99-146

Lewis CFM, Anderson TW (1992) Stable isotope (O and C) and pollen trends in eastern Lake Erie, evidence for a locally-induced climatic reversal of Younger Dryas age in the Great Lakes basin. Clim Dynam 6: 241-250

Lewis CFM, Todd BJ (1996) Lithology and seismostratigraphy of long cores, and a reconstruction of Lake Winnipeg water level history. In: Todd BJ, Lewis CFM, Thorleifson LH, Nielsen E (eds) Lake Winnipeg Project: Cruise Report and Scientific Results. Geol Survey of Canada, Open File 3113, pp 161-192

Lewis CFM, Blasco SM, Gareau PL (2005) Glacio-isostatic adjustment of the Laurentian Great Lakes basin: using the empirical record of strandline deformation for reconstruction of early Holocene paleo-lakes and discovery of a hydrologically closed phase. Géog Phys et Quat 59: 171-193

Lewis CFM, Forbes DL, Todd BJ, Thorleifson LH, Matile GLD (2003) Were the oxygen isotopic compositions of Lake Agassiz outflows more enriched than previously thought? Can Quat Assoc/Can Geomorph Res Group, Halifax, Canada, Abstr pp A65

Lewis CFM, Heil Jr CW, Hubeny JB, King JW, Moore Jr TC, Rea DK (2007) The Stanley unconformity in Lake Huron basin: evidence for a climate-driven closed lowstand about 7900 ^{14}C ka BP, with similar implications for the Chippewa lowstand in Lake Michigan basin. J Paleolimnol 37: 435-452

Lewis CFM, Moore Jr TC, Rea DK, Dettman DL, Smith AM, Mayer LA (1994) Lakes of the Huron basin: their record of runoff from the Laurentide Ice Sheet. Quat Sci Rev 13: 891-922

Lewis CFM, Karrow PF, Blasco SM, McCarthy FMG, King JW, Moore Jr TC, Rea DK (2008a) Evolution of lakes in the Huron basin: Deglaciation to present. Aquat Ecosyst Health Manage 11: 127-136

Lewis CFM, King JW, Blasco SM, Brooks GR, Coakley JP, Croley TE II, Dettman DL, Edwards TWD, Heil CW Jr, Hubeny JB, Laird KR, McAndrews JH, McCarthy FMG, Medioli BE, Moore TC Jr, Rea DK, Smith AJ (2008b) Dry Climate Disconnected the Laurentian Great Lakes. EOS 89: 541-542

Lister GS (1988) Stable isotopes from lacustrine ostracoda as tracers for continental palaeoenvironments. In: DeDeckker P, Colin JP, Peypouquet J-P (eds) Ostracoda in the Earth Sciences, Elsevier, Amsterdam, pp 201-218

Lohmann KC, Walker JCG (1989) The δ^{18}O record of Phanerozoic abiotic marine calcite cements. Geophys Res Lett 16: 319-322.

Lovan NA, Krishnamurthy RV (2011) Inferring paleotemperature from the D/H ratio of lacustrine organic matter. Quat International 229: 38-46

Lowell TV, Fisher TG, Comer GC, Hajdas I, Waterson N, Glover K, Loope HM, Schaefer JM, Rinterknecht VR, Broecker W, Denton GH Teller JT (2005) Testing the Lake Agassiz meltwater trigger for the Younger Dryas. EOS 86: 365-372

Macdonald RA, Longstaffe FJ (2007) The oxygen- and hydrogen-isotope compositions of the Great Lakes. Programs and Abstracts of the 50th Conference on Great Lake Research, pp 117-118

Macdonald RM, Longstaffe FJ (2008) The Late Quaternary oxygen-isotope composition of southern Lake Huron. Aquat Ecosyst Health Manage 11: 137-143

Manning PG, Prepas EE, Serediak MS (1999) Pyrite and vivianite intervals in the bottom sediments of eutrophic Baptiste Lake, Alberta, Canada. Can Mineral 37: 593-601

Meyers PA (2003) Application of organic geochemistry to paleolimnological reconstructions: a summary of examples from the Laurentian Great Lakes. Org Geochem 34: 261-289

Meyers PA, Ishiwatari R (1993) Lacustrine organic geochemistry - an overview of indicators of organic matter sources and diagenesis in lake-sediments. Org Geochem 20: 867-900

Moore TC Jr, Rea DK, Godsey H (1998) Regional variation in modern radiocarbon ages and the hard-water effects in Lakes Michigan and Huron. J Paleolimnol 20: 347-351

Moore TC Jr, Rea DK, Mayer LA, Lewis CFM, Dobson DM (1994) Seismic stratigraphy of Lake Huron - Georgian Bay and postglacial lake history. Can J Earth Sci 31: 1606-1617

Moore TC Jr, Walker JCG, Rea DK, Lewis CFM, Shane LCK, Smith AJ (2000) Younger Dryas interval and outflow from the Laurentide ice sheet. Paleoceanography 15: 4-18

Mothersill JS, Brown H (1982) Late Quaternary stratigraphic sequence of the Goderich Basin: Texture, mineralogy, and paleomagnetic record. J Great Lakes Res 8: 578-586

Munsell Color (2000) Munsell Soil Color Charts, Year 2000 Revised Washable Edition. GretagMacbeth, New Windsor, NY

Murphy T, Lawson A, Kumagai M, Nalewajko C (2001) Release of phosphorous from sediments in Lake Biwa. Limnology 2: 119-128

Murton JB, Bateman MD, Dallimore SR, Teller JT, Zhirong Yang (2010) Identification of Younger Dryas outburst flood path from Lake Agassiz to the Arctic Ocean. Nature 464: 740-743

Nambudiri EVM, Teller JT, Last WM (1980) Pre-Quaternary microfossils – A guide to errors in radiocarbon dating. Geology 8: 123-126

Nriagu JO (1972) Stability of vivianite and ion-pair formation in the system $Fe_3(PO_4)_2$ - H_3PO_4 - H_2O. Geochim Cosmochim Acta 36: 459-470

Nriagu, JO, Dell CI (1974) Diagenetic formation of iron phosphates in recent lake sediments. Am Mineral 59: 943-946

Odegaard C, Rea DK, Moore TC (2003) Stratigraphy of the mid-Holocene black bands in Lakes Michigan and Huron: Evidence for possible basin-wide anoxia. J Paleolimnol 29: 221-234

Palacios-Fest MR, Cohen AS, Ruiz J, Blank B (1993) Comparative paleoclimatic interpretations from nonmarine ostracodes using faunal assemblages, trace elements shell chemistry and stable isotope data. In: Swart PK, Lohmann KC, McKenzie JA, Savin S (eds) Climate Change in Continental Isotopic Records. AGU Monogr 78, pp 179-190

Peltier WR (2007) Rapid climate change and Arctic Ocean freshening. Geology 35: 1147–1148

Rasmussen SO, Andersen KK, Svensson AM, Steffensen JP, Vinther BM, Clausen HB, Siggaard-Andersen ML, Johnsen SJ, Larsen LB, Dahl-Jensen D, Bigler M, Röthlisberger R, Fischer H, Goto-Azuma K, Hansson ME, Ruth U (2006) A new Greenland ice core chronology for the last glacial termination. J Geophys Res 111, D06102. doi:10.1029/2005JD006079

Rau GH (1978) Carbon-13 depletion in a subalpine lake: carbon flow implications. Science 201: 901-902

Rea DK, Colman SM (1995) Radiocarbon ages of pre-bomb clams and the hard-water effect in Lakes Michigan and Huron. J Paleolimnol 14: 88-91

Rea DK, Owen RM, Meyers PA (1981) Sedimentary processes in the Great Lakes. Rev Geophys Space Phys 19: 635-648

Rea DK, Moore TC Jr, Lewis CFM, Mayer LA, Dettman DL, Smith AL, Dobson DM (1994a) Stratigraphy and paleolimnologic record of lower Holocene sediments in northern Lake Huron and Georgian Bay. Can J Earth Sci 31: 1586-1605

Rea DK, Moore TC Jr, Anderson TW, Lewis CFM, Dobson DM, Dettman DL, Smith AJ, Mayer LA, (1994b) Great Lakes paleohydrology: complex interplay of glacial meltwater, lake levels and sill depths. Geology 22: 1059-1062

Reimer PJ, Baillie MGL, Bard E, Bayliss A, Beck JW, Bertrand CJH, Blackwell PG, Buck CE, Burr GS, Cutler KB, Damon PE, Edwards RL, Fairbanks RG, Friedrich M, Guilderson TP, Hogg AG, Hughen KA, Kromer B, McCormac G, Manning S, Ramsey CB, Reimer RW, Remmele S, Southon JR, Stuiver M, Talamo S, Taylor FW, van der Plicht J, Weyhenmeyer CE (2004) INTCAL04 Terrestrial radiocarbon age calibration. Radiocarbon 46: 1029-1058

Remenda VH, Cherry JA, Edwards TWD (1994) Isotopic composition of old ground water from Lake Agassiz: implications for late Pleistocene climate. Science 226: 1975-1978

Rooth C (1982) Hydrology and ocean circulation. Prog Oceanogr 11: 131-149

Rosenquist IT (1970) Formation of vivianite in Holocene clay sediments. Lithos 3: 327-334

Sapota T, Aldahan A, Al-Aasm IS (2006) Sedimentary facies and climate control on formation of vivianite and siderite microconcretions in sediments of Lake Baikal, Siberia. J Paleolimnol 36: 245-257

Schöne BR, Rodland DL, Fiebig J, Oschmann W, Goodwin D, Flessa KW, Dettman D (2006). Reliability of multitaxon, multiproxy reconstructions of environmental conditions from accretionary biogenic skeletons. J Geology 114: 267-285

Shuman B, Bartlein P, Logar N, Newby P, Webb T III (2002) Parallel climate and vegetation responses to the early Holocene collapse of the Laurentide Ice Sheet. Quat Sci Rev 21: 1793-1805

Smith DG, Fisher TG (1993) Glacial Lake Agassiz - the northwestern outlet and paleoflood. Geology 21: 9-12

Stuiver M, Grootes PM, Braziunas TF (1995) The GISP2 $\delta^{18}O$ climate record of the past 16,500 years and the role of the sun, ocean, and volcanoes. Quat Res 44: 341-354

Talbot MR, Kelts K (1990) Paleolimnological signatures from carbon and oxygen isotopic ratios in carbonates from organic carbon-rich lacustrine sediments. In: Katz BJ (ed) Lacustrine Basin Exploration: Case Studies and Modern Analogs. The

American Association of Petroleum Geologists Memoir 50, Tulsa, Oklahoma, pp 99-112

Tanaka N, Monaghan MC, Rye DM (1986) Contribution of metabolic carbon to mollusc and barnacle shell carbonate. Nature 320: 520-523

Teller JT (1985) Glacial Lake Agassiz and its influence on the Great Lakes. In: Karrow PF, Calkin PE (eds) Quaternary Evolution of the Great Lakes. Geol Assoc of Canada Spec Paper 30, pp 1-12

Teller JT, Leverington DW (2004) Glacial Lake Agassiz: A 5000 yr history of change and its relationship to the $\delta^{18}O$ record of Greenland. Geol Soc Am Bull 116: 729-742

Teller JT, Thorleifson LH (1983) The Lake Agassiz-Lake Superior connection. In: Teller JT, Clayton L (eds) Glacial Lake Agassiz. Geol Assoc of Canada Spec Paper 26, pp 261-290

Teller JT, Leverington DW, Mann JD (2002) Freshwater outbursts to the oceans from glacial Lake Agassiz and their role in climate change during the last deglaciation. Quat Sci Rev 21: 879-887

Teller JT, Boyd M, Yang ZR, Kor PSG, Fard AM (2005) Alternative routing of Lake Agassiz overflow during the Younger Dryas: new dates, paleotopography, and a re-evaluation. Quat Sci Rev 24: 1890-1905

The Great Lakes Environmental Atlas (1995) The Great Lakes, An Environmental Atlas and Resource Book, Third edition. Government of Canada, Toronto and United States Environmental Protection Agency, Chicago, pp 46

Thomas RL, Kemp AL, Lewis CFM (1973) The Surficial sediments of Lake Huron. Can J Earth Sci 10: 226-271

Thompson TA, Baedke SJ (1997) Standplain evidence for late Holocene lake-level variations in Lake Michigan. Geol Soc Am Bull 109: 666-682

Thorleifson LH, Kristjanson FJ (1993) Quaternary geology and drift prospeting, Beardmose-Geraldton Area, Ontario. Geol Surv Canada Memoir 435, pp 146

Vogel JC (1993) Variability of carbon isotope fractionation during photosynthesis. In: Ehleringer JR, Hall AE, Farquhar GD (eds) Stable Isotopes and Plant Carbon-Water Relations. Academic Press, San Diego, pp 29-46

von Grafenstein U, Erlernkeuser H, Trimborn P (1999) Oxygen and carbon isotopes in modern fresh-water ostracode valves: assessing vital offsets and autecological effects of interest for palaeoclimate studies. Palaeogeogr Palaeoclimatol Palaeoecol 148: 133-152

Wolfe BB, Edwards TWD, Aravena R, MacDonald GM (1996) Rapid Holocene hydrologic change along boreal tree-line revealed by $\delta^{13}C$ and $\delta^{18}O$ in organic lake sediments, Northwest Territories, Canada. J Paleolimnol 15: 171-181

Wright HE Jr (1992) Patterns of Holocene climatic change in the midwestern United States. Quat Res 38: 129-134

Yu S, Colman SM, Lowell TV, Milne GA, Fisher TG, Breckenridge A, Boyd M, Teller JT (2010) Freshwater outburst from Lake Superior as a trigger for the cold event 9300 years ago. Science 328: 1261-1266

Yu Z (2000) Ecosystem response to lateglacial and early Holocene oscillations in the Great Lakes region of North America. Quat Sci Rev 19: 1723-1747

Yu Z, McAndrews JH, Eicher U (1997) Middle Holocene dry climate caused by change in atmospheric circulation patterns: Evidence from lake levels and stable isotopes. Geology 25: 251-254

CHAPTER 5

The Oxygen- and Hydrogen-Isotope Compositions of Porewater from Huron and Michigan Basin Sediments

5.1 INTRODUCTION

Understanding the late Pleistocene and Holocene evolution of the Great Lakes depends in large part on understanding the sources and pathways travelled by meteoric water (glacial meltwater, regional precipitation, groundwater) as the Laurentide Ice Sheet (LIS) retreated. Glacial meltwater input to the ancient Great Lakes is a particularly important part of this record that can be traced using the characteristically very low $\delta^{18}O$ and δD values of this water relative to fresh water from other sources. The oxygen (and sometimes hydrogen) isotopic compositions of ancient lake water can potentially be deduced using proxies such as biogenic carbonates (e.g., ostracodes), aquatic cellulose, diatoms, and porewater trapped in low permeability lacustrine sediments. Here, we focus on the proxy potential of porewater $\delta^{18}O$ and δD values for four sediment cores from Lakes Huron and Michigan. We evaluate whether or not original lakewater oxygen-isotope compositions were preserved in the porewater through comparison with the paleo-lakewater oxygen isotopic compositions calculated using *Candona subtriangulata*, a common cold-water ostracode species (see Chapters 3 and 4). *Candona subtriangulata* was by far the most common species in these cores and showed large fluctuations in its oxygen isotopic composition through time.

The usefulness of porewater as an archive of original lakewater oxygen- and hydrogen-isotope compositions in glaciolacustrine sediments depends on a hydrogeological setting that preserves connate water trapped during lacustrine sedimentation (Desaulniers et al. 1981; Remenda et al. 1994; Birks et al. 2007). Sedimentary sub-basins underlying the Great Lakes are clay-rich and thus should have very low permeability (Desualniers et al. 1981; Kolak et al. 1999). Lacustrine clays in the Great Lakes region can serve as confining units and are reported to be effective barriers to fluid flow and solute transport (McIntosh and Walter 2006). As such, these units have the potential to retain connate waters captured during different glacial lake phases. However, post-depositional interaction (mixing, diffusion) with water from other sources (e.g., modern lakewater, groundwater) may have modified the isotopic composition of porewater now contained in these lacustrine mud deposits.

Many studies have examined the oxygen- and hydrogen-isotope compositions of sedimentary porewater from locations within or adjacent to the Great Lakes Basin (Paleozoic carbonates: McIntosh and Walter 2006; Pleistocene tills: Desaulniers et al. 1981; Hendry and Wassenaar 1999; Hendry et al. 2004; Pleistocene-Holocene lacustrine sediments: Drimmie et al. 1994; Remenda et al. 1994; Cumming and Al-Aasm 1999; Kolak et al. 1999; Birks et al. 2007). Most of these studies report that the original isotopic composition of porewater was modified over time by downward mixing and/or diffusion, but some reports conclude that connate water is present at greater depths (Desaulniers et al. 1981; Remenda et al. 1994; Cumming and Al-Aasm 1999; Birks et al. 2007). In particular, Remenda et al. (1994) and Birks et al. (2007) suggest that ancient water compositions were preserved by porewater in Lake Agassiz sediments deposited from ~10 – 8 ka [11,000 – 9,000 cal] BP.

Groundwater discharge into the Great Lakes through lake-bottom sediments could also lead to modification of porewater compositions. Such contributions are generally assumed to be limited (Hoaglund et al. 2002; Croley and Hunter 2004). However, a few studies have reported significant upwelling of groundwater through bottom sediments of the Great Lakes (e.g., Cherkauer and McKereghan 1991; Drimmie et al. 1992, 1994; Kolak et al. 1999; Hoaglund et al. 2004; Ruberg et al. 2005) and nearby Lake Simcoe (Longstaffe et al. 2008; Macdonald et al. 2009). Recognition of numerous ‘sinkholes’ in karstic formations underlying western Lake Huron, through which groundwater is discharging (Biddanda et al. 2006, 2009), indicates that such contributions to the Great Lakes, and their potential impact on porewater compositions, should not be overlooked.

Results for ostracodes from Great Lake sediments have shown that late Pleistocene and early Holocene lake waters exhibited large fluctuations in oxygen isotope composition arising from variations in glacial meltwater input (Chapters 3 and 4, this thesis; Colman et al. 1990, 1994a; Forester et al. 1994; Lewis et al. 1994; Rea et al. 1994a, 1994b; Dettman et al. 1995; Macdonald and Longstaffe 2008; Breckenridge and Johnson 2009; Breckenridge et al. 2010; Hyodo 2010; Hyodo and Longstaffe 2011b). When the influence of meltwater ended (~8.0 ka [9,000 cal] BP), regional climate factors including air temperature, precipitation and humidity began to control the isotopic composition of the Great Lakes (Dean et al. 1996; Edwards et al. 1996) and in general caused their δ^{18}O values to increase towards compositions typical of these lakes today. If porewater contained in the cores examined here is connate – that is, reflective of original lake water – we expect fluctuations in its oxygen-isotope compositions that are correlative with the *C. subtriangulata* record. Primary porewater records would afford us the opportunity to examine mid to late Holocene climate-induced changes in lakewater composition, given that the oxygen-isotope record provided by biogenic carbonates ends at ~6 ka [6,850 cal] BP (Chapters 3 and 4). However, downward mixing, diffusion, advection and upwelling of groundwater may have modified original porewaters, producing oxygen-isotope compositions that differ from the *C. subtriangulata* record, and which no longer record conditions at the time of their entrapment.

5.2 MATERIALS AND METHODS

Porewater was examined from three Lake Huron cores and one Lake Michigan core (Fig. 5.1); all cores were collected during cruises of the *CCGS Limnos*. Coring sites in Lake Huron were selected for their clay-rich nature, as identified by Thomas et al. (1973). Core 146, which is made up of two piston cores taken within 17 m of each other, was collected in 2003 from the Goderich sub-basin (net core length, ~15 m). The liner of the first core retrieved at this site (core 146-1, 15 m in length) cracked during collection, and so a second core (core 146-2, nearly 12 m in length) was retrieved. The first core (146-1) was used to examine sediments from 12.14 to 14.8 m, and the second core (146-2) was used to examine sediments from 11.88 m to the core top. Core 594, also from the

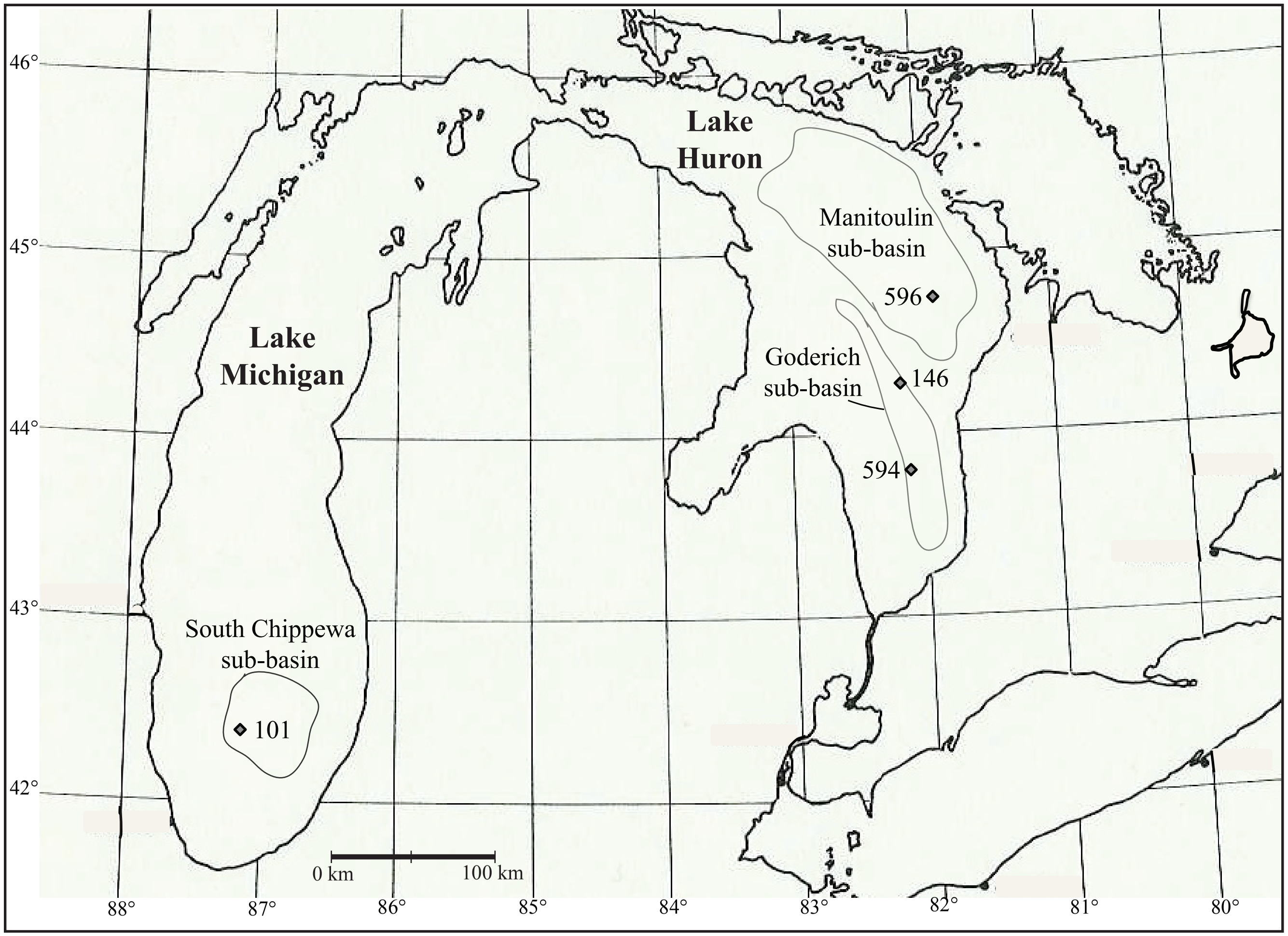

Figure 5.1. Map showing core locations in Lakes Michigan and Huron. Coordinates are: core 101 - 42° 33' 53" N and 87° 13' 54" W (water depth 134 m); core 146-1 - 44° 14' 55" N and 82° 15' 16" W, and core 146-2: 44° 14' 42" N and 82° 15' 48" W (water depth 92.4 m); core 594 - 43° 48' 02" N and 82° 06' 57" W (water depth 88.5 m); core 596 - 44° 41' 13" N and 81° 54' 42" W (water depth 120 m).

Goderich sub-basin (core length, ~15 m) and core 596 from the Manitoulin sub-basin (core length, ~12 m) were collected in 2004. The piston core from Lake Michigan (core 101, core length, ~17 m) was collected from the South Chippewa sub-basin in 2006. Clay-rich cores had previously been collected successfully from nearby locations (Colman et al. 1990, 1994a, 1994b; Forester et al. 1994). Following retrieval, the plastic liners of each piston core were sub-sectioned into ~1 m-long segments, capped and then sealed with black vinyl tape (see Chapters 3 and 4 for core descriptions).

Lakewater was collected by the staff and crew of the *CCGS Limnos*. Samples were collected in 15 or 30 ml HDPE Nalgene bottles with no headspace, sealed with parafilm to prevent evaporation and leakage, and kept refrigerated prior to isotopic analysis. Lake Huron and Georgian Bay were sampled during various spring, summer and fall cruises over the period 2004-2007 at various depths ranging from 1 to 192 m. Lake Michigan water was sampled during May-June 2006 at various depths ranging from 1 to 257 m.

Porewater was extracted from all cores within six weeks of collection except for core 146, which was sampled following two years of storage. The ~1 m-long core sections were split lengthwise; one half of each core was immediately sealed and returned to refrigerated ‘archive’ at The University of Western Ontario. The other half was sub-sampled immediately at 10 cm intervals and porewater extracted. Thirty-five to forty grams of sediment was scooped from the center of the core into centrifuge tubes and weighed. The tubes were then capped and centrifuged at 15,000 rpm and 4 °C for 20 minutes using a Beckman Coulter high-speed centrifuge. The amount of porewater extracted by centrifugation ranged from 5 to 18 mL.

The oxygen- and hydrogen-isotope results for lakewater and porewater are reported in the normal delta (δ) notation in parts per thousand (‰) relative to Vienna Standard Mean Ocean Water (VSMOW) (Coplen 1996). The oxygen-isotope compositions of the water were determined by equilibration with CO_2 (Epstein and Mayeda 1953) and analyzed in continuous flow mode using a GasBench® attached to a ThermoFinnigan Delta^{Plus} XL® stable isotope ratio mass spectrometer. One ml of water was placed in vials and equilibrated with CO_2 for at least 18 hours at 30 °C. The CO_2 in the headspace of each vial was then transferred in a He-stream to the mass spectrometer via a Valco® sampling port for measurement of the oxygen-isotope ratios. Four laboratory standards (HEAVEN, EDT, MID, LSD), calibrated to VSMOW and SLAP, were measured with each set of samples. HEAVEN and LSD were used to provide a calibration curve, and EDT and LSD were used to assess precision and accuracy. Over the course of porewater analysis, a value of -7.3 ± 0.1 ‰ (1σ; n = 55) was obtained for EDT, which compares well with its accepted value of -7.3 ‰, and a value of -13.1 ± 0.1 ‰ (1σ; n = 15) was obtained for MID, which compares well with its accepted value of -13.1 ‰. The standard deviation for replicate analysis of unknown samples was better than ± 0.1 ‰ (1σ; n = 43).

Hydrogen-isotope measurements were made by reduction of H_2O to H_2 gas over hot metallic zinc (Coleman et al. 1982). Two μl of water were injected into an evacuated Pyrex tube containing 60 mg of Indiana® zinc. The samples were then reacted for 30 min at 400 °C to release H_2 gas. The δD values were measured in dual inlet mode using a Micromass PRISM II stable isotope ratio mass spectrometer. The standardization and calibration approach was similar to that used for oxygen, and performed using the same laboratory standards. Over the course of porewater analysis, a value of -55 ± 1 ‰ (1σ; n = 29) was obtained for EDT, which compares well with its accepted value of -56 ‰, and a value of -107 ± 1 ‰ (1σ; n = 28) was obtained for MID, which compares well with its accepted value of -108 ‰. The standard deviation for replicate analysis of unknown samples was better than ± 1 ‰ (1σ; n = 40).

5.3 RESULTS

Water from Lake Huron and Georgian Bay sampled during this study has average $\delta^{18}O$ and δD values of -7.4 ± 0.4 ‰ (n = 379) and -59 ± 4.0 ‰ (n = 195), respectively (Fig. 5.2, Macdonald and Longstaffe 2004, 2007; Longstaffe et al. 2011). Lake Michigan water has average $\delta^{18}O$ and δD values -5.9 ± 0.2 ‰ (n = 93) and -45 ± 1.9 ‰ (n = 91), respectively (Fig. 5.3, Macdonald and Longstaffe 2007, Macdonald et al. 2007; Longstaffe et al. 2011).

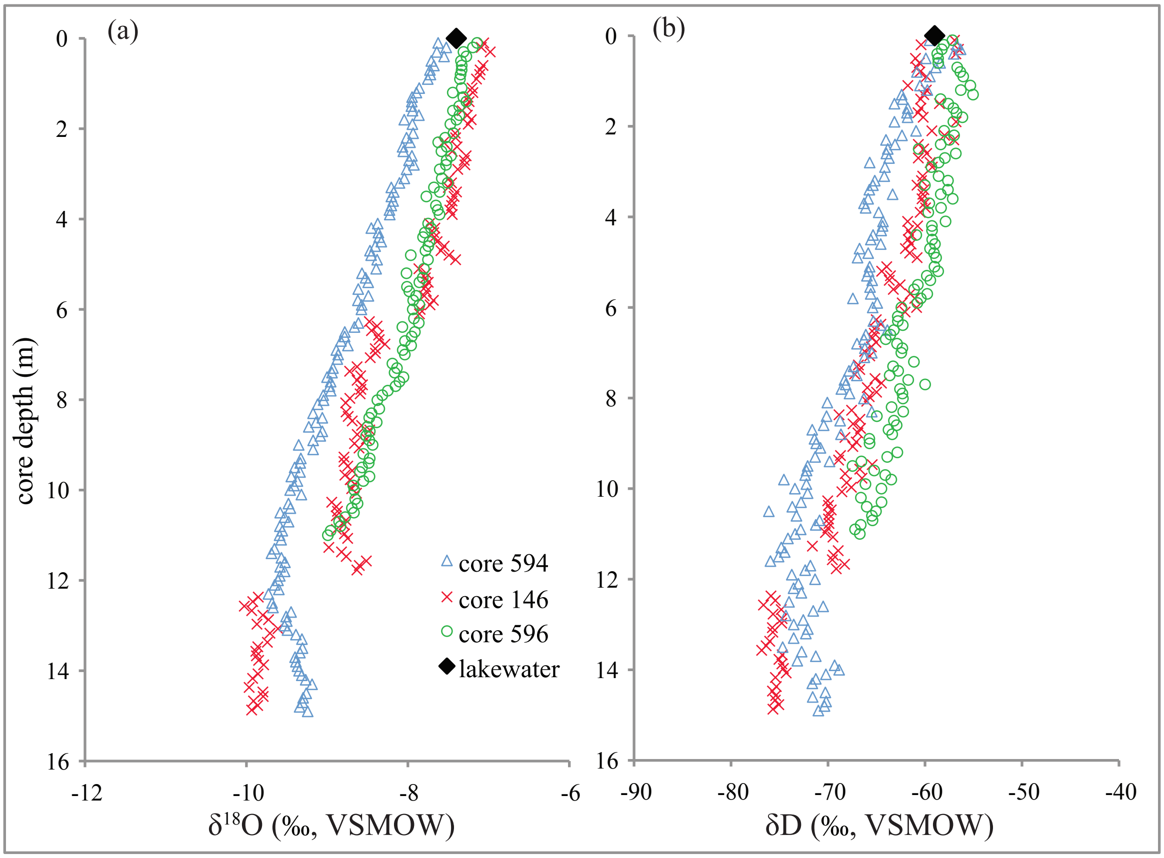

Figure 5.2. Depth versus oxygen- (a) and hydrogen- (b) isotope compositions of pore-water for Lake Huron cores 594, 146 and 596. The average isotopic composition of modern Lake Huron is also shown.

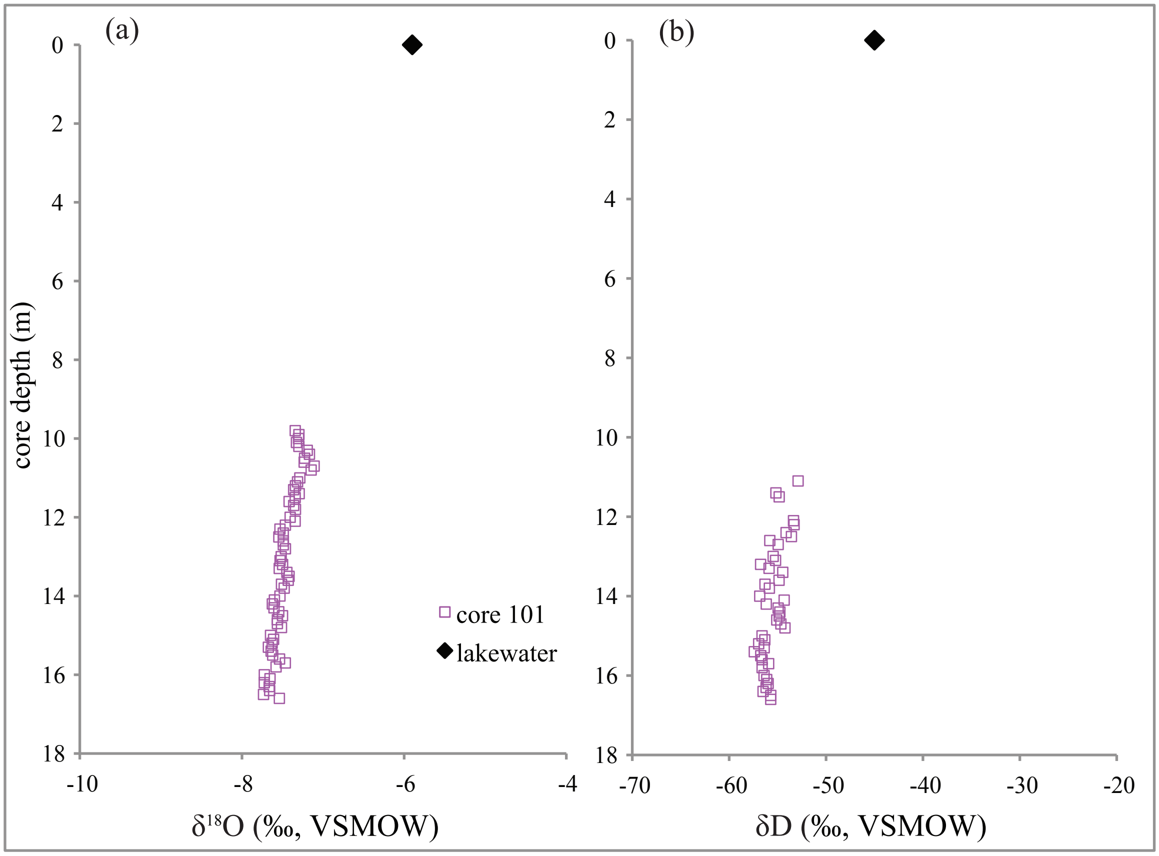

Figure 5.3. Depth versus oxygen- (a) and hydrogen- (b) isotope compositions of pore-water from Lake Michigan core 101. The average isotopic composition of modern Lake Michigan is also shown.

Porewater oxygen- and hydrogen-isotope compositions are listed in Appendix G. The porewater $\delta^{18}O$ and δD values from Lake Huron core 596 decrease systematically from -7.1 and -57 ‰, respectively, near its top to -9.0 and -67 ‰ near the profile bottom at 12 m (Fig. 5.2). The maximum ranges in $\delta^{18}O$ and δD values are 1.8 and 12 ‰, respectively. Porewater $\delta^{18}O$ and δD values from Lake Huron core 594 decrease gradually from ~ -7.6 and -60 ‰, respectively, near the core top to -9.7 and -76 ‰ near 12 m and then increase slightly to –9.2 and -70 ‰ towards the core bottom at 14.9 m (Fig. 5.2). The maximum ranges in $\delta^{18}O$ and δD values are 2.2 and 20 ‰, respectively.

Porewater $\delta^{18}O$ and δD values from Lake Huron core 146-2 decrease with depth, ranging from -7.1 and -57 ‰, respectively, at its top to -8.6 and -69 ‰ at its bottom (11.8 m) (Fig. 5.2). The maximum ranges in $\delta^{18}O$ and δD values are 2.0 and 15 ‰, respectively. Core 146-2 does not show the gradual sample-to-sample change in δ-values with depth as observed for cores 594 and 596 (Fig. 5.2). Instead, porewater δ-values have only limited variability within each 1 m core segment. This pattern is likely an artifact of horizontal core storage for almost two years prior to porewater extraction. The results suggest rapid porewater mixing within core segments following recovery and sub-sectioning, and hence the need to extract porewater as soon as possible after collection in order to obtain the *in situ* distribution of porewater δ-values.

In core 146-1 (12.3 to 14.8 m), porewater $\delta^{18}O$ and δD values are more or less constant at -9.8 and -75 ‰, respectively. Its sediments exhibit features characteristic of coring disturbance (e.g., absence of lamination, vertical streaking) (see Chapter 4). Similarly disturbed sediment from the Superior Basin also displayed invariant $\delta^{18}O$ and δD values (Hyodo 2010). Those compositions were attributed to lateral suction of sediment and associated porewater into the bottom of the piston core (Hyodo and Longstaffe 2011a, 2011b, 2011c). Given the disturbed nature of similar sediment in core 146-1, we have set aside the porewater isotopic results from further consideration. That said, this disturbed interval has average porewater compositions consistent with a linear continuation of the depth-δ trend from higher in the section (Fig. 5.2).

Porewater isotopic analyses were made only for lower portions of Lake Michigan core 101 (oxygen, 9.8 to 16.6 m; hydrogen, 11.1 to 16.6 m) (Fig. 5.3). Porewater $\delta^{18}O$ and δD values show very gradual but systematic variation, from -7.3 and -53 ‰, respectively, at the top of the profile to -7.7 and -56 ‰ at the bottom. Given this small range, porewater analysis was discontinued for the remainder of the core.

5.4 DISCUSSION

5.4.1 End-member compositions

Possible sources of porewater in Great Lakes sediments include original (connate) lakewater, modern lakewater, groundwater and precipitation, and deep formation water, which is a product of its source(s) and water-rock interaction at elevated temperatures. Each potential source has an identifiable range of $\delta^{18}O$ and δD values.

Ancient lakewater

The oxygen isotopic compositions of connate porewater can be calculated using ostracode valves. Their $\delta^{18}O$ values reflect lakewater composition and the temperature of valve formation (Dettman et al. 1995; Boomer 2002; Holmes and Chivas 2002; Leng and Marshall 2004). *Candona subtriangulata* is the most common ostracode species recovered from Great Lakes sediments and lives in the deepest regions of the lakes where temperature remains at ~1 – 4 °C (Dettman et al. 1995). As a result, variations in its oxygen-isotope compositions more-or-less reflect changes in lakewater oxygen-isotope composition ($\alpha^{18}O_{shell-water}$ = 1.0359; Chapters 2 – 4, this thesis; Macdonald and Longstaffe 2008).

In Lake Huron core 594, $\delta^{18}O_{lakewater}$ values calculated from *C. subtriangulata* valves range from -19.3 to -6.0 ‰; two intervals are characterized by particularly low-^{18}O water, ~12.5 – 10.5 m and 8.0 – 6.0 m (Fig. 5.4). In core 146, calculated $\delta^{18}O_{lakewater}$

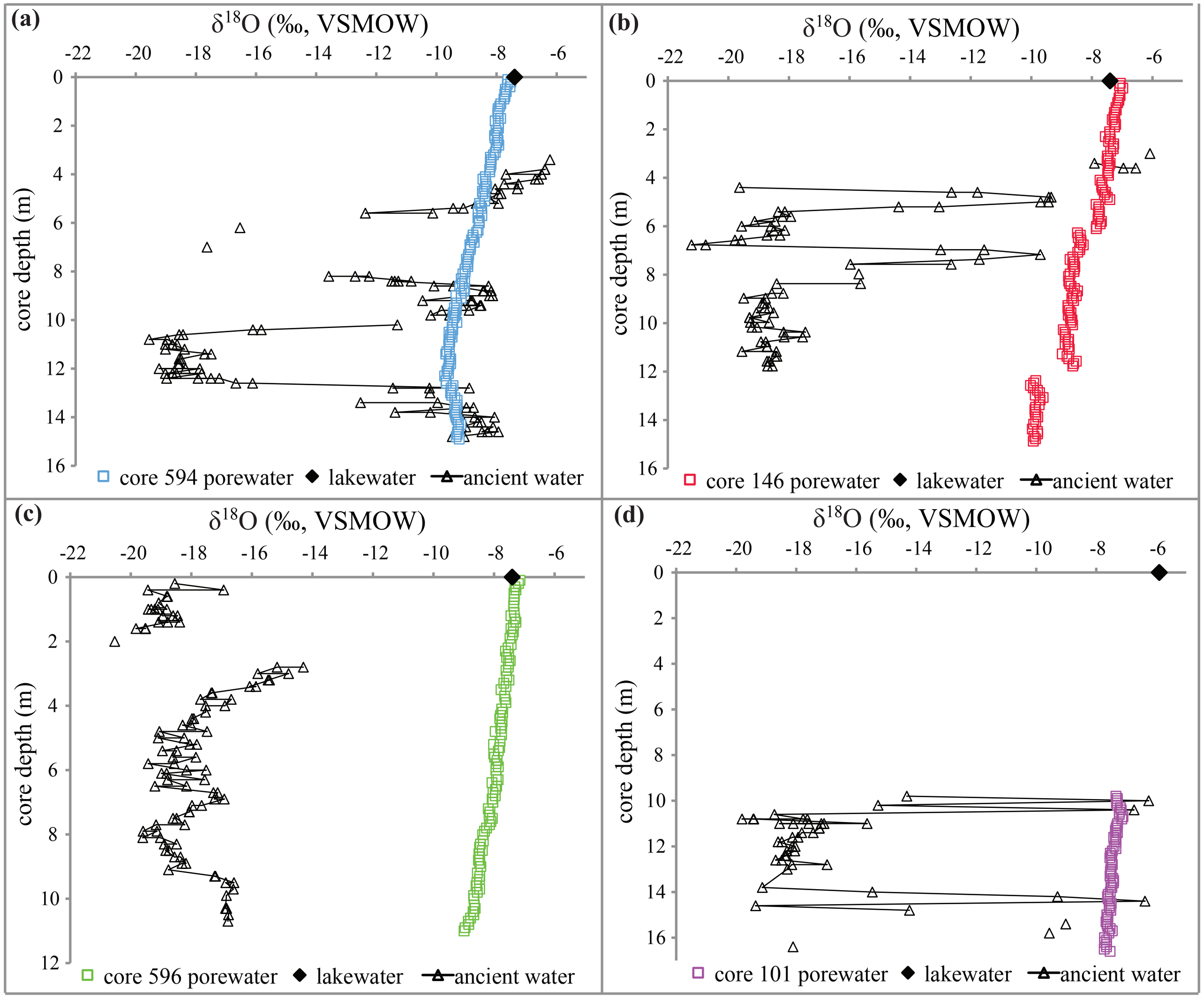

Figure 5.4. Depth versus oxygen-isotope compositions of ancient lakewater, calculated using *C. subtriangulata*, compared with present porewater for: (a) Lake Huron core 594, (b) Lake Huron core 146, (c) Lake Huron core 596, and (d) Lake Michigan core 101. The average $\delta^{18}O$ values of modern Lakes Huron and Michigan are also shown.

values range from -20.9 to -5.8 ‰, and three intervals are characterized by low-^{18}O water (11.8 – 8.4 m, 6.8 – 5.4 m, ~4.5 m) (Fig. 5.4). The ostracode record for core 596 has $\delta^{18}O_{lakewater}$ values ranging from -20.2 to -14.0 ‰ (Fig. 5.4). As described in Chapter 4, several water sources for ancient Lake Huron are reflected by this variation: (i) late Pleistocene and early Holocene mixing among inflows from upstream proglacial lakes (e.g., Agassiz and Superior) (~ -28 to -20 ‰; Last et al. 1994; Lewis et al. 2003; Birks et al. 2007; Breckenridge and Johnson 2009; Hyodo and Longstaffe 2011b); (ii) meltwater sourced directly from the LIS (~ -30 to -28 ‰; Sima et al. 2006), and (iii) the regional watershed ~ -18 to -15 ‰; Desaulniers et al. 1981; Long et al. 1988; Edwards et al. 1999; Kolak et al. 1999; Hoaglund et al. 2004;).

In Lake Michigan core 101, ostracodes indicate that late Pleistocene (~11.7 ka [13,600 cal] BP; see Chapter 3) lakewater had δ^{18}O values of -20 to -14 ‰, with a few excursions to -6 ‰ (Fig. 5.4). As described in Chapter 3, several sources for ancient Lake Michigan are reflected by this variation: (i) direct meltwater input from the LIS (~ -30 ‰; Sima et al. 2006) until ~11.1 ka [13,000 cal] BP (Hansel et al. 1985; Colman et al. 1994a, 1994b); (ii) flows of lakewater (~ -18 to -16 ‰) from the Huron and Erie Basins via the Grand River Valley from 13 – 12.2 ka [15,300 – 14,050 cal] BP (Hansel et al. 1985; Kehew 1993; Lewis and Anderson 1992; Lewis et al. 1994; Rea et al. 1994a; Moore et al. 2000); and (iii) the regional watershed (~ -13 ‰, based on a 5 ‰ difference between late Pleistocene and modern precipitation in southern Ontario; Edwards et al. 1996). Much higher δ^{18}O values indicate periods of evaporative enrichment, and/or precipitation during warmer periods.

Modern lakewater

Modern Lakes Huron and Michigan have average δ-values (-7.4 and -5.9 ‰ for oxygen, -59 and -45 ‰ for hydrogen) that are higher than average annual precipitation in these basins. This enrichment in ^{18}O and D largely reflects evaporation from the lakes and their catchments (Patterson et al. 1993; Edwards et al. 2004; Macdonald and Longstaffe 2007).

Groundwater and precipitation

Annual average $\delta^{18}O$ and δD values of modern precipitation range from ~ -12 and -90 ‰, respectively, in the northern regions of the Great Lakes Basin to ~ -7 and -50 ‰ in the south (Desaulniers et al. 1981; Eberts and George 2000; IAEA/WMO 2006; Longstaffe et al. 2011). Precipitation near Lake Huron has average annual $\delta^{18}O$ and δD values of about -9.5 and -66 ‰, respectively, with significant seasonal variation (avg. winter $\delta^{18}O$ = -13.7 ‰; avg. summer $\delta^{18}O$ = -6.4 ‰) (Longstaffe et al. unpublished data). Precipitation from two locations within the catchment of Lake Michigan (Chicago, Illinois; Kalamazoo, Michigan) has average annual $\delta^{18}O$ and δD values of -7.8 and -55 ‰, respectively (IAEA/WMO 2006).

This precipitation replenishes groundwater, which is largely contained within shallow unconfined glacial drift aquifers in the Great Lakes region. Modern groundwater has $\delta^{18}O$ and δD values within the range of modern precipitation (McIntosh and Walter 2006), but because of preferential recharge by snowmelt, groundwater δ-values are typically skewed towards the lower end of the annual range (Longstaffe et al. unpublished data). Some deeper groundwater represents Pleistocene recharge and has lower $\delta^{18}O$ values (-25 to -11 ‰; Clayton et al. 1966; Desaulniers et al. 1981; Long et al. 1988; Husain et al. 2004), reflecting glacial meltwater and cooler-climate precipitation (Kolak et al. 1999; Hoaglund et al. 2002, 2004; McIntosh and Walter 2006; Person et al. 2007; Lemieux et al. 2008).

Formation water

Older formation water (brines to relatively fresh water) is present in Paleozoic sedimentary strata underlying the Great Lakes Basin. This water has $\delta^{18}O$ and δD values ranging from -17.1 to 3.2 ‰, and -120 to -20 ‰, respectively (McNutt et al. 1987; Weaver et al. 1995).

5.4.2 Porewater Records in the Great Lakes Cores

In the Lake Huron cores, porewater $\delta^{18}O$ (and δD) values increase steadily towards the sediment-water interface, reaching compositions very similar to modern Lake Huron (Fig. 5.2). Porewater δ-values for Lake Michigan core 101 also show gradual upward enrichment in ^{18}O and D (Fig. 5.3). While lower porewater δ-values at greater depths are consistent with higher contributions of glacial meltwater and/or cooler climate precipitation, the extent of ^{18}O-depletion is much smaller than shown by the ostracode proxy record (Fig. 5.4). Connate (ancient) water $\delta^{18}O$ values calculated for Lake Huron core 594 range from ~10 ‰ lower to 2 ‰ higher than its porewater, with multiple excursions in both directions (Fig. 5.4a). Three intervals in Lake Huron core 146 (11.8 – 8.4 m, 6.8 – 5.4 m, 4.4 m) are characterized by ancient waters with $\delta^{18}O$ values up to ~15 ‰ lower than porewater from these depths (Fig. 5.4b). In Lake Huron core 596, ancient lakewater $\delta^{18}O$ values are much lower (by ~7 to 13 ‰) than recorded in porewater (Fig. 5.4c). Likewise, in Lake Michigan core 101, connate water $\delta^{18}O$ values range from ~12 ‰ lower than coexisting porewater in most cases to 1 to 2 ‰ higher in a few cases (Fig. 5.4d).

Porewater isotopic results for the various Lake Huron cores display minor differences. The porewater $\delta^{18}O$ value at the top of core 594 is slightly lower (-7.6 ‰), and at the tops of cores 146 and 596, slightly higher (-7.1 ‰) than modern Lake Huron (-7.4 ‰) (Fig 5.2). Porewater δD values follow the same pattern (core 594, -60 ‰; cores 146 and 596, -57 ‰; modern Lake Huron, -59 ‰). While at the boundary of natural variation in modern Lake Huron (oxygen, ±0.2 ‰; hydrogen, ±3 ‰), these differences extend to greater core depths. Why porewater δ-values in core 594 in general are slightly lower than in cores 146 and 596 remains unexplained. In contrast, the ancient lakewater record for core 594 is on average the most ^{18}O-rich of the three cores examined whereas core 596 is the most ^{18}O-poor (Figs. 5.2 and 5.4). What is apparent is that ancient lakewater signals do not define porewater composition at any particular depth.

Given that they do not directly reflect connate water compositions, what information is carried by the porewater $\delta^{18}O$ and δD values? Figure 5.5 illustrates the isotopic compositions of Lake Huron porewater and average Lake Huron surface water, relative to the Great Lakes Meteoric Water Line (GLMWL, $\delta D = 7.4 * \delta^{18}O + 5.1$). The GLMWL line describes the relationship between the hydrogen and oxygen isotopic compositions of precipitation at five stations within the Great Lakes Basin, as recorded from 1960 – 1993 (IAEA/WMO 2006). As the result of evaporation, modern Lake Huron plots to the right of the GLMWL. During evaporation, lighter molecular masses (e.g., $H_2{}^{16}O$) are preferentially removed into the vapour phase whereas heavier molecules (e.g., $HD^{16}O$, $H_2{}^{18}O$) preferentially remain in the liquid phase (Dansgaard 1964). An analogous plot for Lake Michigan porewater produced a pattern qualitatively similar to of Lake Huron. However, the small range in Lake Michigan porewater δ-values led to large errors in defining the Michigan Porewater Line (MPL), and it is not considered further.

Linear regression of the porewater $\delta^{18}O$ and δD values produces a line (Huron Porewater Line, HPL, $\delta D = 6.6 * \delta^{18}O -10.1$) that, at one end, intersects modern Lake Huron, and at the other end, intercepts the GLMWL at $\delta^{18}O = -19.0 \pm 2.4$ ‰ and $\delta D = -136 \pm 16$ ‰ (Fig. 5.5). The oxygen isotopic intercept with the GLMWL is similar to the median composition of ancient Lake Huron (-18.4 ‰) during its periods of glacial meltwater domination (Fig. 5.4). Whether the GLMWL then was exactly the same as at present, or whether climatic conditions and lakewater residence times led to evaporative ^{18}O-enrichment similar to today are difficult to assess. Notwithstanding those caveats, the HPL can be most easily explained by mixing between modern Lake Huron and water typical of its early glacial meltwater-dominated phases, with additional minor process – as yet undefined – accounting for small core-to-core differences. The distribution of porewater $\delta^{18}O$ and δD values between these two end-members likely was driven by downward molecular diffusion from the overlying column of younger Lake Huron water. Values of hydraulic conductivity (*K*) for unfractured clay-rich deposits within the Great Lakes Basin range from 10^{-8} to 10^{-9} cm/s (Desaulniers et al. 1981; Kolak et al. 1999). Such low K values lead to such low groundwater flow rates (0.00016 to 0.0016 m/yr) that advection becomes negligible and molecular diffusion becomes the dominant mode of

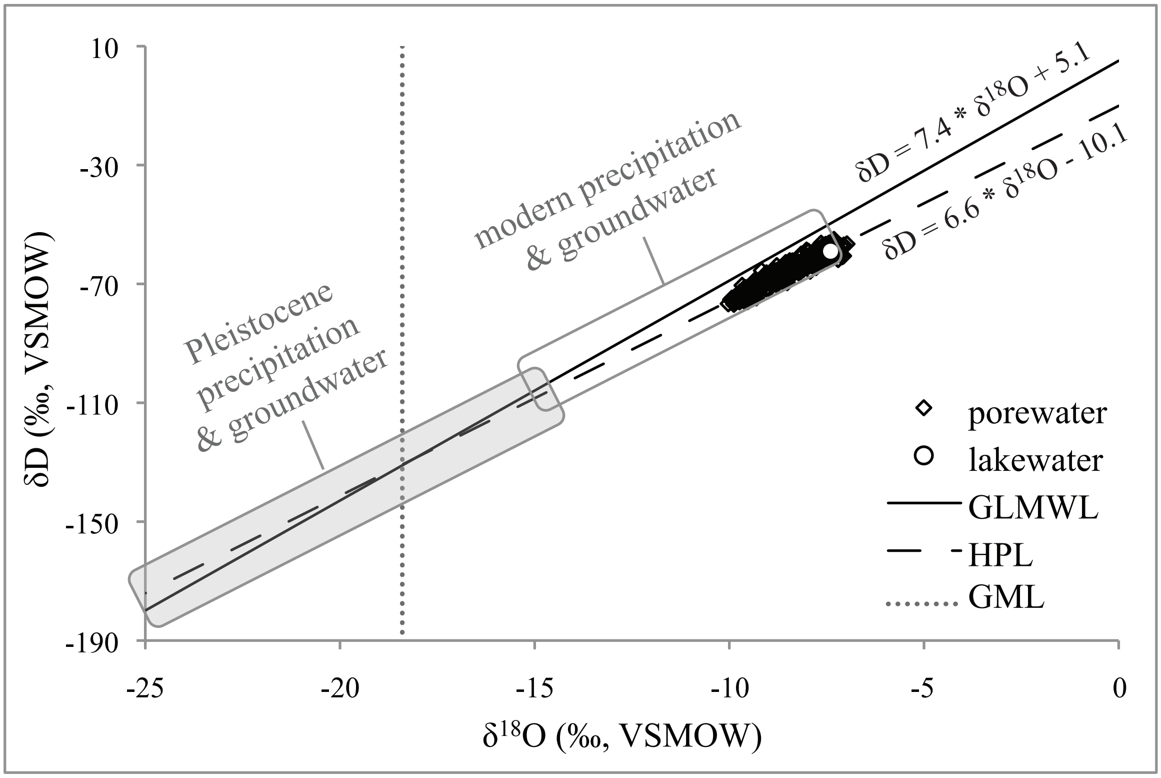

Figure 5.5. Hydrogen- versus oxygen-isotope compositions of Lake Huron porewater and lakewater. GLMWL = Great Lakes Meteoric Water Line; HPL = Huron Porewater Line; GML = Glacial Meltwater line, the median $\delta^{18}O$ value of glacial meltwater in the Huron Basin, ~ -18.4 ‰.

solute transport (Desaulniers et al. 1981; Remenda et al. 1994; Hendry and Wassenaar 1999; Kolak et al. 1999; Hendry et al. 2004; Hoaglund et al. 2004).

The above model focuses on downward flow, and discounts upward groundwater movement. A role for upward-moving modern groundwater in this deep lake situation is unlikely but cannot be ruled out based on the isotopic data alone. Upward migration of low-^{18}O Pleistocene groundwater in response to ice unloading and isostatic rebound remains possible but is also improbable in the current hydrodynamic setting. Likewise, it is unlikely that formation waters originating from underlying Paleozoic sedimentary rocks played a role in replacing connate waters in these offshore, clay-rich sub-basins of Lake Huron. However, porewater chemical analyses are required to confirm the presence or absence of a contribution from basinal brines that underlie the region.

Porewater in lacustrine units located closer to the present shoreline may indeed be affected by groundwater originating from freshwater glacial drift aquifers and/or brines from the underlying Paleozoic units, depending on the local geological setting. Kolak et al. (1999) simulated transport of ^{18}O and Cl^- in porewaters from both terrestrial and lacustrine cores collected around and within Saginaw Bay, southwestern Lake Huron. Their results suggested that while the solute profiles in the terrestrial cores developed slowly, over a period of ~8,000 years, profiles in the lacustrine cores developed much more quickly, within 15 to 250 years. Kolak et al. (1999) noted that the focusing of regional groundwater flow towards Saginaw Bay could explain faster transport rates of solutes in the lacustrine cores.

5.5 CONCLUSIONS

Sediment porewater from Lake Huron cores 146, 594 and 596 and Lake Michigan core 101 has not retained δ^{18}O and δD values characteristic of connate water. Instead, an upward increase in porewater δ-values reflects downward diffusion of modern lake water. This process has largely erased the original (low-^{18}O) isotopic signals of glacial meltwater-dominated lakewater. However, the end-member composition for ancient

Lake Huron (~ -18 ‰) during periods of significant glacial meltwater inflow is estimated reasonably well by the intersection between the Lake Huron Porewater Line (HPL) and the modern Great Lakes Meteoric Water Line (GLMWL).

5.6 REFERENCES

Biddanda BA, Nold SC, Ruberg SA, Kendall ST, Sanders TG, Gray JJ (2009) Great Lakes sinkholes: A microbiogeochemical frontier. EOS 90: 61-62

Biddanda BA, Coleman DF, Johengen TH, Ruberg SA, Meadows GA, Van Sumeren HW, Rediske RR, Kendall ST (2006) Exploration of a submerged sinkhole ecosystem in Lake Huron. Ecosystems 9: 828-842

Birks SJ, Edwards TWD, Remenda VH (2007) Isotopic evolution of Glacial Lake Agassiz: New insights from cellulose and porewater isotopic archives. Palaeogeogr Palaeoclimatol Palaeoecol 246: 8-22

Boomer I (2002) Environmental applications of marine and freshwater ostracoda. In: Haslett SK (ed) Quaternary Environmental Micropalaeontology. Arnold, London, pp 115-138

Breckenridge A, Johnson TC (2009) Paleohydrology of the upper Laurentian Great Lakes from the late glacial to early Holocene. Quat Res 71: 397-408

Breckenridge A, Lowell TV, Fisher TG, and Yu S (2010) A late Lake Minong transgression in the Lake Superior basin as documented by sediments from Fenton Lake, Ontario. J Paleolimnol DOI 10.1007/s10933-010-9447-z

Cherkauer DS, McKereghan PF (1991) Ground-water discharge to lakes: Focusing in embayments. Ground Water 29: 72-80

Clayton RN, Friedman I, Graf DL, Mayeda TK, Meents WF, Shimp NF (1966) The origin of saline formation waters. 1. Isotopic composition. J Geophys Res 71: 3869-3882

Coleman ML, Shepherd TJ, Durham JJ, Rouse JE, Moore GR (1982) Reduction of water with zinc for hydrogen isotope analysis. Anal Chem 54: 993-995

Colman SM, Keigwin LD, Forester RM (1994a) Two episodes of meltwater influx from glacial Lake Agassiz into the Lake Michigan basin and their climatic contrasts. Geology 22: 547-550

Colman SM, Jones GA, Forester RM, Foster DS (1990) Holocene paleoclimate evidence and sedimentation rates from a core in southwestern Lake Michigan. J Paleolimnol 4: 269-284

Colman SM, Forester RM, Reynolds RL, Sweetkind DS, King JW, Gangemi P, Jones GA, Keigwin LD, Foster DS (1994b) Lake-level history of Lake Michigan for the past 12,000 years: the record from deep lacustrine sediments. J Great Lakes Res 20: 73-92

Coplen TB (1996) New guidelines for reporting stable hydrogen, carbon, and oxygen isotope-ratio data. Geochim Cosmochim Acta 60: 3359-3360

Croley TE II, Hunter TS (1994) Great Lakes monthly hydrologic data. NOAA Technical Memorandum GLERL-83. Ann Arbor, Michigan: Great Lake Environmental Research Laboratory

Cumming JD, Al-Aasm IS (1999) Sediment characterization and porewater isotope chemistry of Quaternary deposits from the St. Clair Delta, Ontario, Canada. Quat Res 51: 174-186

Dean WE, Ahlbrandt TS, Anderson RY, Bradbury JP (1996) Regional aridity in North America during the middle Holocene. The Holocene 6: 145-155

Dansgaard W (1964) Stable isotopes in precipitation. Tellus 16*:* 436-468

Desaulniers DE, Cherry JA, Fritz P (1981) Origin, age and movement of pore water in argillaceous Quaternary deposits at four sites in Southwestern Ontario. J Hydrol 50: 231-257

Dettman DL, Smith AJ, Rea DK, Moore TC Jr., Lohmann KC (1995) Glacial meltwater in Lake Huron during early postglacial time as inferred from single-valve analysis of oxygen isotopes in ostracodes. Quat Res 43: 297–310

Drimmie RJ, Frape SK, Thomas RL, Terry SM (1994) Stable isotope signature of glacial melt water in the sediments of Lake Erie and Lake Ontario. Program with Abstracts – Geol Assoc Canada:Mineral Assoc Canada Joint Annual Meeting 19, pp 30

Drimmie RJ, Frape SK, Morden MJ, Thomas RL, McNutt RH, Bowins RJ (1992) Chemical inputs to Lake Ontario from saline formation water below the sediments. Programs and Abstracts of the 35th Conference on Great Lake Research, pp 90

Eberts SM, George LL (2000) Regional ground-water flow and geochemistry in the midwestern basins and arches aquifer system in parts of Indiana, Ohio, Michigan, and Illinois. Regional Aquifer-System Analysis-Midwestern Basins and Arches, USGS Professional Paper 1423-C: C1-C103

Edwards TWD, Wolfe BB, MacDonald GM (1996) Influence of changing atmospheric circulation on precipitation δ^{18}O – temperature relations in Canada during the Holocene. Quat Res 46: 211-218

Edwards TWD, Wolfe BB, Gibson JJ, Hammarlund D (2004) Use of water isotope tracers in high latitude hydrology and paleohydrology. In: Pienitz R, Douglas MSV, Smol JP (eds) Long Term Environmental Change in Arctic and Antarctic Lakes, Springer, Dordrecht, pp 187-207

Epstein S, Mayeda T (1953) Variation of ^{18}O content of waters from natural sources. Geochim Cosmochim Acta 4: 213-22

Forester RM, Colman SM, Reynolds RL, Keigwin LD (1994) Lake Michigan's Late Quaternary limnological and climate history from ostracode, oxygen isotope, and magnetic susceptibility. J Great Lakes Res 20: 93-107

Hansel AK, Mickelson DM, Schneider AF, Larsen CE (1985) Late Wisconsinan and Holocene history of the Lake Michigan basin. In: Karrow PF, Calkin PE (eds) Quaternary Evolution of the Great Lakes. Geol Assoc Canada Spec Paper 30, pp 39-53

Hendry MJ, Wassenaar LI (1999) Implications of the transport of δD and δ^{18}O in porewaters on groundwater flow and the timing of geologic events in a thick aquitard system. Water Resources Res 35: 1751-1760

Hendry MJ, Kelln CJ, Wassenaar LI, Shaw J (2004) Characterizing the hydrogeology of a complex clay-rich aquitard system using detailed vertical profiles of the stable isotopes of water. J Hydrol 293: 47-56

Hoaglund JR III, Huffman GC, Grannemann NG (2002) Michigan Basin regional ground water flow to three Great Lakes. Ground Water 40: 390-406

Hoaglund JR III, Kolak JJ, Long DT, Larson GJ (2004) Analysis of modern and Pleistocene hydrologic exchange between Saginaw Bay (Lake Huron) and the Saginaw Lowlands area. Geol Soc Am Bull 116: 3-15

Holmes JA, Chivas AR (2002) Ostracod shell chemistry – Overview. In: Holmes JA, Chivas AR (eds) The Ostracoda: Applications in Quaternary Research. AGU Monogr 131, pp 185-204

Husain MM, Cherry JA, Frape SK (2004) The persistence of a large stagnatin zone in a developed regional aquifer, southwestern Ontario. Can Geotech J 41: 943-958

Hyodo A (2010) The Holocene paleolimnology of Lake Superior. PhD thesis, The University of Western Ontario, London, pp 330

Hyodo A, Longstaffe FJ (2011a) The paleoproductivity of ancient Lake Superior. Quat Sci Rev 30: 2988-3000

Hyodo A, Longstaffe FJ (2011b) Variations in the oxygen-isotope composition of ancient Lake Superior between 10,600 and 8,800 cal BP. J Paleolimnol, DOI 10.1007/s10933-011-9552-7

Hyodo A, Longstaffe FJ (2011c) The chronostratigraphy of Holocene sediments from four Lake Superior sub-basins. Can J Earth Sci 48: 1581-1599

IAEA/WMO (2006) Global Network of Isotopes in Precipitation. The GNIP Database. Accessible at: http://isohis.iaea.org

Kehew AE (1993) Glacial-lake outburst erosion of the Grand Valley, Michigan, and impacts on glacial lakes in the Lake Michigan Basin. Quat Res 39: 36-44

Kolak JJ, Long DT, Matty JM, Larson GJ, Sibley DF, Councell TB (1999) Ground-water, large-lake interactions in Saginaw Bay, Lake Huron: A geochemical and isotopic approach. Geol Soc Am Bull 111: 177-188

Last WM, Teller JT, Forester RM (1994) Paleohydrology and paleochemistry of Lake Manitoba, Canada: the isotope and ostracode records. J Paleolimnol 12: 269-282

Lemieux J-M, Sudicky EA, Peltier WR, Tarasov L (2008) Dynamics of groundwater recharge and seepage over the Canadian landscape during the Wisconsinian glaciation. J Geophys Res 113: F01011, DOI 10.1029/2007JF000838

Leng MJ, Marshall JD (2004) Palaeoclimate interpretation of stable isotope data from lake sediment archives. Quat Sci Rev 23: 811-831

Lewis CFM, Anderson TW (1992) Stable isotope (O and C) and pollen trends in eastern Lake Erie, evidence for a locally-induced climatic reversal of Younger Dryas age in the Great Lakes basin. Clim Dynam 6: 241-250

Lewis CFM, Forbes DL, Todd BJ, Thorleifson LH, Matile GLD (2003) Were the oxygen isotopic compositions of Lake Agassiz outflows more enriched than previously thought? Can Quat Assoc/Can Geomorph Research Group, Halifax, Canada, Abstr pp A65

Lewis CFM, Moore Jr TC, Rea DK, Dettman DL, Smith AM, Mayer LA (1994) Lakes of the Huron basin: their record of runoff from the Laurentide Ice Sheet. Quat Sci Rev 13: 891-922

Longstaffe FJ, Lewis CFM, King JW, Heil CW Jr, Hubeny JB, Goodyear DR, Slattery SR, Macdonald RA (2008). Stable isotope evidence for groundwater seepage into Kempenfelt Bay, Lake Simcoe. Programs and Abstracts of the 51st Conference on Great Lake Research, pp 91

Longstaffe FJ, Ayalon A, Bumstead NL, Crowe AS, Hladyniuk R, Hornibrook PA, Hyodo A, Macdonald RA (2011) The oxygen-isotope evolution of the North American Great Lakes. Geol Soc Am Abstracts with Programs 43, pp 57

Macdonald RA, Longstaffe FJ (2004) The oxygen and hydrogen isotope composition of Lake Huron. EOS Trans 85: PP43A-0621

Macdonald RA, Longstaffe FJ (2007) The oxygen and hydrogen isotope compositions of the Great Lakes. Programs and Abstracts of the 50th Conference on Great Lake Research, pp 117-118

Macdonald RM, Longstaffe FJ (2008) The Late Quaternary oxygen-isotope composition of southern Lake Huron. Aquat Ecosyst Health Manage 11: 137-143

Macdonald RA, Longstaffe FJ, Crowe AS (2007) The Late Quaternary oxygen isotope composition of Lake Michigan. EOS Trans 88: PP13B-1283

Macdonald RA, Longstaffe FJ, Crowe AJ, Lewis CFM, King JW (2009). Stable isotope compositions of Great Lake porewaters and evidence for groundwater seepage into Kempenfelt Bay, Lake Simcoe. SIMSYN 2009, pp 12-13

McIntosh JC, Walter LM (2006) Paleowaters in Silurian-Devonian carbonate aquifers: Geochemical evolution of groundwater in the Great Lakes region sine the Lake Pleistocene. Geochim Cosmochim Acta 70: 2454-2479

McNutt RH, Frape SK, Dollar P (1987) A strontium, oxygen and hydrogen isotopic composition of brines, Michigan and Appalachian Basins, Ontario and Michigan. Appl Geochem 2: 495-505

Moore TC Jr, Walker JCG, Rea DK, Lewis CFM, Shane LCK, Smith AJ (2000) Younger Dryas interval and outflow from the Laurentide ice sheet. Paleoceanography 15: 4-18

Rea DK, Moore TC Jr, Lewis CFM, Mayer LA, Dettman DL, Smith AL, Dobson DM (1994a) Stratigraphy and paleolimnologic record of lower Holocene sediments in northern Lake Huron and Georgian Bay. Can J Earth Sci 31: 1586-1605

Rea DK, Moore TC Jr, Anderson TW, Lewis CFM, Dobson DM, Dettman DL, Smith AJ, Mayer LA, (1994b) Great Lakes paleohydrology: complex interplay of glacial meltwater, lake levels and sill depths. Geology 22: 1059-1062

Remenda VH, Cherry JA, Edwards TWD (1994) Isotopic composition of old ground water from Lake Agassiz: implications for late Pleistocene climate. Science 226: 1975-1978

Ruberg S, Coleman D, Johengen T, Meadows G, VanSumeren H, Land G, Biddanda B (2005) Groundwater plume mapping in a submerged sinkhole in Lake Huron. Mar Technol Soc J 39: 65-9

Sima A, Paul A, Schulz M, Oerlemans J (2006) Modeling the oxygen-isotopic composition of the North American Ice Sheet and its effect on the isotopic composition of the ocean during the last glacial cycle. Geophys Res Lett, DOI 10.1029/2006GL026923

Patterson WP, Smith GR, Lohmann KC (1993) Continental paleothermometry and seasonality using the isotopic composition of aragonitic otoliths of freshwater fishes. In: Swart PK, McKenzie J, Lohmann KC, Savin S (eds) Climate Change in Continental Isotopic Records. AGU Monogr 78, pp 191-202

Person M, McIntosh J, Bense V, Remenda VH (2007) Pleistocene hydrology of North America: The role of ice sheets in reorganizing groundwater flow systems. Rev

Geophys 45: RG3007

Thomas RL, Kemp AL, Lewis CFM (1973) The surficial sediments of Lake Huron. Can J Earth Sci 10: 226-271

Weaver TR, Frape SK, Cherry JA (1995) Recent cross-formational fluid flow and mixing in the shallow Michigan Basin. Geol Soc Am Bull 107: 697-707

CHAPTER 6

Conclusions

Isotopic records contained in sediment cores retrieved from the Huron and Michigan Basins contain information about the fluctuations in source water and water chemistry at the end of the last glacial period. The main findings from our reading of this archive are summarized below.

6.1 CONTRIBUTIONS TO BIOGENIC CARBONATE ISOTOPIC CALIBRATIONS

The oxygen- and carbon-isotope compositions of modern ostracodes, bivalves and gastropods collected from Lake Huron were compared to the average oxygen-isotope composition of Lake Huron water and the average carbon-isotope composition of lakewater-DIC to assess the extent of non-equilibrium isotopic fractionation. The species examined are common within the sediments of the Great Lakes Basin. Hence, better understanding how ancient isotopic signals are recorded in their shells is helpful in interpretation of such data. Ostracode species are enriched in ^{18}O by 2.2 ‰ relative to equilibrium precipitation from lakewater. Bivalves and gastropods (except for one lung-breathing gastropod species, *S. elodes*) precipitate their shells in oxygen isotopic equilibrium with lake water.

A lack of carbon isotopic equilibrium between modern ostracode, bivalve and gastropod shells from Lake Huron and modern, open lakewater-DIC is suggested by their $\delta^{13}C$ values. However, the ostracodes examined here are infaunal; DIC within their microenvironment can be expected to be a few permil lower than open lakewater-DIC as a result of decaying organic matter within the sediment. These organisms (with the exception of *C. rawsoni*) likely form their valves in carbon-isotope equilibrium with the DIC present in the microenvironment. By comparison, the bivalves and gastropods incorporate some metabolic (i.e., dietary) carbon during shell formation. Given that their dietary organic matter sources typically have very low $\delta^{13}C$ values (~ -30 to -25 ‰;

Meyers and Ishiwatari 1993; Hodell and Schelske 1998; Meyers 2003), a low-^{13}C signal is imparted to their shells. Once they are better defined, it will be useful to apply microenvironment or metabolic corrections when calculating the δ^{13}C value of open lakewater-DIC. However, even without such corrections, relative changes in $\delta^{13}C_{DIC}$ values should still be apparent in the shelly archives from Great Lakes sediments, allowing for reasonable inferences regarding changes in productivity and/or DIC source(s).

6.2 CONTRIBUTIONS TO GREAT LAKES PALEOLIMNOLOGY

Differences between the oxygen-isotope compositions of deep-water ostracodes (*C. subtriangulata*) and shallower-water ostracodes and clams from the Michigan Basin cores suggest isotopic stratification of lakewater during much of the late Pleistocene. Such stratification has been previously reported for Lake Agassiz (Birks et al. 2007), and tentatively suggested for Lake Superior (Breckenridge and Johnson 2009). However, the present study presents the first evident for such a process within the Great Lakes Basin.

The three Michigan Basin cores, together with a short portion of Huron Basin core 596, record lakewater oxygen isotopic compositions during the late Pleistocene. In the Michigan Basin, oxygen-isotope results for *C. subtriangulata* (~ -23 to -6 ‰ with an average of ~ -15 ‰) indicate a more-or-less continuous supply of low-^{18}O glacial meltwater from ~13 – 10 ka [15,300 – 11,500 cal] BP. Oxygen-isotope results for the shallower-water ostracodes and clams (typically ~ -5 to -2 ‰) are more indicative of regional precipitation and runoff, and hence more local climatic conditions. Large oscillations in the Pleistocene $\delta^{18}O_{lakewater}$ values, as calculated using *C. subtriangulata*, are commonly observed, particularly in the South Chippewa and Chippewa sub-basins of the Michigan Basin. These changes are indicative of a very dynamic system, involving some combination of mixing between ^{18}O-poor bottom water and ^{18}O-rich surface water, intermittent inflows from the Huron and Erie basins, and/or rapid advances and retreats of the Michigan Lobe of the Laurentide Ice Sheet (LIS). In Huron Basin core 596, *C. subtriangulata* yields consistently low $\delta^{18}O_{lakewater}$ values of ~ -19 to -17 ‰ during the late Pleistocene record available here (~11.5 – 10 ka [12,600 – 11,500 cal] BP). Such compositions suggest a consistent and direct connection to a low-^{18}O water source, such as the LIS or the Agassiz Basin.

Results for the Huron Basin indicate that during the earliest stages of the Holocene (10 – 9.5 ka [11,500 – 10,700 cal] BP), $\delta^{18}O_{lakewater}$ values in the Goderich and Manitoulin sub-basins differed by up to 11 ‰. Such a disparity can be explained by different dominating water sources in the two sub-basins, which suggests reduced hydraulic connectivity between the northern and southern regions of the Huron Basin during this period of low water levels.

The Holocene record from the Huron Basin contains large fluctuations in $\delta^{18}O_{lakewater}$ values. Three influxes of low-^{18}O water during the early- to mid-Holocene are recorded primarily by *C. subtriangulata* valves, and are attributed to large floods originating from the Agassiz Basin: Mattawa I, ~9.5 ka [10,700 cal] BP; Mattawa II, ~8.4 ka [9,450 cal] BP and Mattawa III, 8.2 ka [9,100 cal] BP. Relatively high $\delta^{18}O_{lakewater}$ values at ~8.5 ka [9,500 cal] BP and 7.9 ka [8,700 cal] BP reflect cessation of glacial meltwater-rich inflow during periods when the basin was hydrologically closed. Following the final termination of glacial meltwater input at ~8.0 ka [9,000 cal] BP, $\delta^{18}O_{lakewater}$ values in the Goderich sub-basin increased to higher-than-modern values (> -7.4 ‰). Such an increase is reflective of warmer and drier conditions during the Holocene Hypsithermal (~8 – 4 ka [9,000 – 4,400 cal] BP). Valves of *C. subtriangulata* from the Michigan Basin also record a substantial increase in $\delta^{18}O_{lakewater}$ values, from ~ -15 to ~ -7 ‰, although this increase begins at the onset of the Holocene, that is, earlier than in the Huron Basin. Biogenic carbonates from the Michigan Basin cores do not record large variations in $\delta^{18}O_{lakewater}$ values during the Holocene; most species only vary by ~3 ‰.

Two distinctive sedimentary units within the Michigan Basin cores, the Wilmette and A2 Beds, and two distinctive beds within the Huron Basin cores, the Mattawa II and III Beds, are correlated to major flooding events originating from Lake Agassiz. A third flooding event, the Mattawa I, is recorded in the isotopic compositions of shelly fauna from the Huron Basin but is not marked by noticeably different sediments. The Wilmette Bed was deposited by the A1 flood, likely at ~10.9 – 10.8 ka [12,900 – 12,800 cal] BP, as Agassiz outflow was rerouted from the northwest outlet eastwards towards the Great Lakes Basin (Teller et al. 2005; Murton et al. 2010). Biogenic carbonates from sediment immediately overlying the Wilmette Bed in the South Chippewa and Milwaukee sub-basin cores of the Michigan Basin likely record the isotopic signature of the floodwaters, and indicate that $\delta^{18}O_{lakewater}$ values decreased to nearly -20 ‰ at this time.

The Mattawa I flood (~9.5 ka [10,700 cal] BP) occurred after Lake Agassiz's eastern Kaiashk outlet was opened by retreat of the Marquette glacier from the Superior Basin, which allowed drainage through the Great Lakes Basin (Teller and Thorleifson 1983; Leverington et al. 2000; Teller et al. 2005; Breckenridge 2007, Breckenridge and Johnson 2009; Breckenridge et al. 2010; Hyodo 2010; Hyodo and Longstaffe 2011a, 2011b). Biogenic carbonates from the Huron cores indicate that $\delta^{18}O_{lakewater}$ values were -19 to -17 ‰ during this event.

Two closely spaced yet discrete floods at 8.4 and 8.2 ka [9,450 and 9,100 cal] BP are identified in the Huron Basin record (Mattawa II and III, respectively), but are recorded as one event, the A2 event, in the Michigan Basin. These floods were most likely caused by the return of outflow to the Huron and Michigan Basins from the Superior Basin following a temporary northwards diversion (Breckenridge et al. 2010; Breckenridge and Johnson 2009). At this time, $\delta^{18}O_{lakewater}$ values in the Huron Basin decrease by ~12 ‰, whereas $\delta^{18}O_{lakewater}$ values in the Michigan Basin show a much smaller decrease of ~2-3 ‰. This is likely an effect of low-^{18}O waters spilling more directly into the Huron Basin through the St. Mary's River while the Michigan Basin received only backflooded waters through the Straits of Mackinac, which would have mixed with lakewater already present in the Huron Basin.

Major flooding events recorded in the Michigan and Huron Basin sediments, and attributed to floods from the upstream Agassiz and/or Superior Basins, correlate with major global climatic cooling events. Specifically, onset of the Younger Dryas (11-10 ka

[12,900 – 11,500 cal] BP) corresponds fairy closely with deposition of the Wilmette Bed in the Michigan Basin. The A2 Bed in the Michigan Basin and Mattawa II and III Beds in the Huron Basin match well with the unnamed ~8.3 ka [9,300 cal] BP event. Each of these beds is associated with low-^{18}O water. This observation supports the previously hypothesized linkage between large-scale movement of glacial meltwater through the Great Lakes Basin and the effect of such water on ocean circulation patterns and global climate (Peltier 2007; Fleitmann et al. 2008; Daley et al. 2009; Yu et al. 2010).

The δ^{13}C values of biogenic carbonate from the Michigan and Huron Basins during the late Pleistocene to mid Holocene suggest that primary lacustrine productivity was low. During this time, the carbon-isotope composition of shelly material was likely controlled by DIC and/or allochthonous carbonate delivered by incoming source waters. Following the cessation of glacial meltwater input (~8.0 ka [9,000 cal] BP), the carbon-isotope compositions of biogenic carbonates gradually increase in both basins, suggesting increasing primary productivity.

The difficulties experienced in establishing a reliable age model for the Huron Basin cores highlight the likelihood that potentially useful materials, such as fragments of organic matter fragments and pollen were reworked by lake-level fluctuations. Likewise, porewater from the cores did not retain original lakewater compositions, despite the clay-rich nature of these sediments. Instead, porewater isotopic compositions describe a diffusion gradient between modern lakewater and connate water.

6.3 FUTURE RESEARCH DIRECTIONS

The following recommendations are made for continuance of the research presented here:

1. A more robust chronology is required to more fully interpret the paleolimnological records contained within the Michigan and Huron Basin cores. These cores did not contain much organic matter suitable for radiocarbon dating, making it necessary

for other dating techniques to be pursued. In particular, paleomagnetic secular variation (PSV) measurements, which correlates variations in the inclination, declination and intensity of magnetic minerals contained within sediment to other regional, well-dated records (Mothersill and Brown 1982; King and Peck 2001; Breckenridge and Johnson 2009) should be employed. This method has been used successfully on other (often difficult to date) Great Lakes Basin cores.

2. To obtain a greater understanding of the oxygen-isotope evolution of Lakes Michigan and Huron, the $\delta^{18}O$ values of proxies formed in the upper portion of the water column – such as diatoms, algal cellulose or chara encrustations – should be measured and compared with those of *C. subtriangulata* valves. Such materials conceivably are present in sediment intervals devoid of shallow-water biogenic carbonates. Such analysis would allow for identification of lake phases characterized by isotopic stratification, and may allow inferences to be made about how such a process can occur.
3. The significance of the ubiquitous black iron-sulfide bands in mid Holocene to recent Great Lakes Basin sediments needs to be explored more fully. What are the conditions necessary for their formation? Are they indicative of anoxic conditions? Did such conditions occur only below the sediment-water interface, or were bottom waters of the lakes affected as well? Such understanding may be particularly relevant, given current and projected future increases in global temperature. Increased water temperature may have prevented regular turnover and mixing of the water column, facilitating formation of these black bands.
4. The mineralogy and chemistry of the flood beds (Wilmette and A2 Beds in the Michigan Basin, the Mattawa I, II and III Beds in the Huron Basin) should be investigated to help evaluate whether the detritus was from proximal sources or distal sources, and whether or not such source(s) – and hence the pathway of the flood waters – changed over time.

6.4. REFERENCES

Birks SJ, Edwards TWD, Remenda VH (2007) Isotopic evolution of Glacial Lake Agassiz: New insights from cellulose and porewater isotopic archives. Palaeogeogr Palaeoclimatol Palaeoecol 246: 8-22

Breckenridge A (2007) The Lake Superior varve stratigraphy and implications for eastern Lake Agassiz outflow from 10,700 to 8,900 cal ybp (9.5–8.0 14C ka). Palaeogeogr Palaeoclimatol Palaeoecol 246: 45-61

Breckenridge A, Johnson TC (2009) Paleohydrology of the upper Laurentian Great Lakes from the late glacial to early Holocene. Quat Res 71: 397-408

Breckenridge A, Lowell TV, Fisher TG, and Yu S (2010) A late Lake Minong transgression in the Lake Superior basin as documented by sediments from Fenton Lake, Ontario. J Paleolimnol DOI 10.1007/s10933-010-9447-z

Daley TJ, Street-Perrott FA, Loader NJ, Barber KE, Hughes PDM, Fisher EH, Marshall JD (2009) Terrestrial climate signal of the “8200 yr B.P. cold event” in the Labrador Sea region. Geology 37: 831-834

Fleitmann D, Mudelsee M, Burns SJ, Bradley RS, Kramers J, Matter A (2008) Evidence for a widespread climatic anomaly at around 9.2 ka before present. Paleoceanography 23, PA1102 1029/2007PA001519

Hodell SA, Schelske CL (1998) Production, sedimentation, and isotopic composition of organic matter in Lake Ontario. Limnol Oceanogr 43: 200-214

Hyodo A (2010) The Holocene paleolimnology of Lake Superior. Ph.D. thesis, The University of Western Ontario, London, pp 330

Hyodo A, Longstaffe FJ (2011a) Variations in the oxygen-isotope composition of ancient Lake Superior between 10,600 and 8,800 cal BP. J Paleolimnol, DOI 10.1007/s10933-011-9552-7

Hyodo A, Longstaffe FJ (2011b) The chronostratigraphy of Holocene sediments from four Lake Superior sub-basins. Can J Earth Sci 48: 1581-1599

King JW, Peck J (2001) Use of paleomagnetism in studies of lake sediments. In: Last WM, Smol JP (eds) Tracking environmental change using lake sediments. Volume 1: Basin analysis, coring and chronological techniques. Kluwer Academic Publishers, Dordrecht, pp 371-389

Leverington DW, Mann JD, Teller JT (2000) Changes in the bathymetry and volume of glacial Lake Agassiz between 11,000 and 9,300 ^{14}C yr BP. Quat Res 54: 174-181

Meyers PA (2003) Application of organic geochemistry to paleolimnological reconstructions: a summary of examples from the Laurentian Great Lakes. Org Geochem 34: 261-289

Meyers PA, Ishiwatari R (1993) Lacustrine organic geochemistry - an overview of indicators of organic matter sources and diagenesis in lake-sediments. Org Geochem 20: 867-900

Mothersill JS, Brown H (1982) Late Quaternary stratigraphic sequence of the Goderich Basin: Texture, mineralogy, and paleomagnetic record. J Great Lakes Res 8: 578-586

Murton JB, Bateman MD, Dallimore SR, Teller JT, Zhirong Yang (2010) Identification of Younger Dryas outburst flood path from Lake Agassiz to the Arctic Ocean. Nature 464: 740-743

Peltier WR (2007) Rapid climate change and Arctic Ocean freshening. Geology 35: 1147–1148

Teller JT, Thorleifson LH (1983) The Lake Agassiz-Lake Superior connection. In:

Teller JT, Clayton L (eds) Glacial Lake Agassiz. Geol Assoc of Canada Spec Paper 26, pp 261-290

Teller JT, Boyd M, Yang ZR, Kor PSG, Fard AM (2005) Alternative routing of Lake Agassiz overflow during the Younger Dryas: new dates, paleotopography, and a re-evaluation. Quat Sci Rev 24: 1890-1905

Yu S, Colman SM, Lowell TV, Milne GA, Fisher TG, Breckenridge A, Boyd M, Teller JT (2010) Freshwater outburst from Lake Superior as a trigger for the cold event 9300 years ago. Science 328: 1261-1266

Appendix A – Taxonomic information for ostracode and mollusc species

Class Ostracoda
Subclass Podocopa
Order Podocopida (Sars, 1866)
Suborder Podocopina (Sars, 1866)
- Superfamily Cypridoidea (Baird, 1845)
  - Family Canoniidae Kaufman, 1900
    - Subfamily Candoninae Daday, 1900
      - Genus *Candona* Baird, 1845
        - *Candona acuta* Hoff, 1942
        - *Candona crogmaniana* Turner, 1894
        - *Candona rawsoni* Tressler, 1957
        - *Candona subtriangulata* Benson and Macdonald, 1963
      - Genus *Fabaeformiscandona* (Krstic, 1972)
        - *Fabaeformiscandona caudata* (Kaufman, 1900)
- Superfamily Cytheroidea (Baird, 1845)
  - Family Neocytherideidae (Puri, 1957)
    - Subfamily Neocytherideidinae (Puri, 1957)
      - Genus *Cytherissa* (Sars, 1863)
        - *Cytherissa lacustris* (Sars, 1863)

Class Bivalvia (Pelecypoda)
Order Veneroida
- Superfamily Corbiculacea
  - Family Sphaeriidae
    - Subfamily Sphaeriinae (Fingernail Clams)
      - Genus *Sphaerium* (Scopoli, 1777)
        - *Sphaerium rhomboideum* (Say, 1822)
        - *Sphaerium simile* (Say, 1816)
        - *Sphaerium striatinum* (Lamarck, 1818)

    - Subfamily Pisidiinae (Pea Clams)
      - Genus *Pisidium* Pfeiffer, 1821
        - *Pisidium amnicum* (Müller, 1774)
        - *Pisidium casertanum* (Poli, 1795)
        - *Pisidium compressum* Prime, 1852
        - *Pisidium fallax* Sterki, 1890
        - *Pisidium nitidum* Jenyns, 1832
        - *Pisidium ventricosum* Prime, 1851

Class Gastropoda
Subclass Prosobrancia
Order Mesogastropoda
  - Family Valvatidae (Valve Snails)
    - Genus *Valvata*

        - *Valvata perdepressa* Walker, 1906
        - *Valvata piscinalis* (Müller, 1774)
        - *Valvata sincera sincera* Say, 1824
        - *Valvata tricarinata* (Say, 1817)
    - Family Hydrobiidae (Spire Snails)
        - *Amnicum limosa* (Say, 1817)
        - *Marstonia decepta* (Baker, 1928)
        - *Probythinella lacustris* (Baker, 1928)
- Subclass Pulmonata
- Order Basommatophora
    - Family Lymnaeidae (Pond Snails)
        - *Stagnicola elodes* (Say, 1821)

Appendix B – Ecological information for ostracode and mollusc species

Candona subtriangulata: The most common ostracode species over the past ~10,000 years in the Great Lakes has been, and still is, *C. subtriangulata*. Many studies suggest that *C. subtriangulata* lives at a mean water temperature of ~4-5 °C, but can tolerate waters from 2.6 to 19.2 °C (Delorme 1978, 1991, 2001; Colman et al. 1990; Dettman et al. 1995). This species is common in Lakes Superior, Huron and Ontario where the bottom-water temperature does not fluctuate much throughout the year (Dettman et al. 1995; Delorme 2001). *Candona subtriangulata* is restricted to cold, low-salinity and deep lakes and has the highest minimum dissolved oxygen requirement of common ostracodes found in Canada; few other ostracode species are as productive under these conditions (Colman et al. 1990; Delorme 2001).

Candona crogmaniana: Very little information is available on the ecology of *C. crogmaniana*. Colman et al. (1990) observed this species at similar stratigraphic intervals in sediment cores as *C. subtriangulata* and suggested that these two species may have similar environmental responses. However, and perhaps in challenge to this assumption, *C. crogmaniana* is not nearly as common as *C. subtriangulata* in the fossil record. *Candona crogmaniana* has been found in small numbers in Lakes Huron (this study), Michigan (Buckley 1975) and Erie (Delorme 1978), and in smaller water bodies in Northern Ontario (Delorme 1970a).

Candona rawsoni: This species can tolerate a wide range of chemical and physical conditions (Delorme 1989). When cultured in the laboratory, Xia et al. (1997) found *C. rawsoni* to prefer temperatures above 15 °C. Delorme (1991, 2001) reported a tolerance range of 5 to 25 °C for this species, with a mean of ~17.5 °C. This species is common in both permanent and temporary lakes and in prairie wetlands (Delorme 1970a). Colman et al. (1990) suggested that *C. rawsoni* is not very productive in the modern Great Lakes. However, *C. rawsoni* was the most common ostracode found in the Pinery Beach samples collected in the current study, which suggests that modern Lake Huron supports a healthy population of this species.

Candona acuta: *Candona acuta* tolerates water temperatures of 7 to 27 °C, living at a mean temperature of 18 °C (Delorme 1991, 2001). This species has adapted to both flowing and standing waters and is thus well-suited to large lakes with bottom currents (Delorme 2001) and is most commonly found in the sluggish parts of streams (Delorme 1970a). Within Lake Michigan, *C. acuta* likely lives in the littoral or supralittoral zone (Colman et al. 1990).

Fabaeformiscandona caudata: This species can tolerate water temperatures ranging from 3 to 27 °C but generally lives at a mean temperature of 12 °C (Delorme 1991, 2001). *Fabaeformiscandona caudata* is able to survive through the summer months in Lake Erie – a period when the hypolimnion waters have very low dissolved oxygen; this species has a short life cycle that allows it to lay eggs before anoxia occurs (Delorme 2001). Like *C. acuta*, *F. caudata* has adapted to living in large lakes with bottom currents (Delorme 2001). *Fabaeformiscandona caudata* is commonly found in streams and at great depths in lakes (Delorme 1970a).

Cytherissa lacustris: This species is common in deeper lakes (>3 m depth) in the boreal forests of Canada (Delorme, 1970b). It generally lives at a mean water temperature of ~10 °C, although this species can tolerate temperatures ranging from 3 to 23 °C (Delorme 1991, 2001). Like *C. subtriangulata*, *C. lacustris* is adapted and restricted to permanent lake habitats (Delorme, 2001). *Cytherissa lacustris* was second in abundance of the ostracodes found in the Pinery Beach samples; it too is apparently thriving in modern Lake Huron.

Pisidium casertanum: *Pisidium casertanum*, the most abundant species of *Pisidium* in Canada and the world (G. Mackie, pers. commun.), is present in all of the Great Lakes. It is common in water depths to 25 m but has been collected as deep as 100 m (Mackie et al. 1980). This species is also found in ponds, rivers, streams, ditches, swamps and temporary-water habitats (Clarke 1981). Because this species is very tolerant to a wide range of environmental conditions (Kerr-Lawson et al. 1992), its presence in a sedimentary record does not offer specific ecological information.

Pisidium compressum: This common bivalve species usually lives among vegetation in shallow water within permanent water bodies, such as lakes, ponds, rivers and streams (Clarke 1981). *Pisidium compressum* lives in the upper few centimeters of the sediment column and thus is less likely than other bivalve species to be reworked; this feature is useful in paleoclimate studies where transportation of fossils can pose a problem (Kerr-Lawson et al. 1992).

Pisidium nitidum: *Pisidium nitidum* lives in all types of permanent water habitats and is currently found throughout the Great Lakes (Mackie et al. 1980). It is commonly associated with shallow-water and sandy substrates (Clarke 1981; Kerr-Lawson et al. 1992).

Pisidium amnicum: This species was introduced from Europe in the late 1800s (G. Mackie, pers. commun.) and thus should not be found in Late Quaternary to Holocene records from the Great Lakes. Within North America, this species inhabits only large lakes or rivers (Clarke 1981).

Pisidium fallax: This species lives in all the Great Lakes except Lake Superior and is most common at depths of less than 10 m (Kerr-Lawson et al. 1992). *Pisidium fallax* is not a common species, but can be found in lakes, rivers and streams (Clarke 1981). Its preferred habitat is coarse sand to gravel substrates (Mackie et al. 1980).

Pisidium ventricosum: *Pisidium ventricosum*, like *P. fallax*, also occurs in all Great Lakes except for Lake Superior (Kerr-Lawson et al. 1992). This species is also found in ponds, rivers and streams of all sizes (Clarke 1981). Its preferred habitats are shallow, quiet waters with muddy to sandy subtrates (Mackie et al. 1980).

Sphaerium striatinum: This is a common species in Canadian rivers, streams and large lakes and occurs in all of the Great Lakes (Clarke 1981; Kerr-Lawson et al. 1992). *Sphaerium striatinum* lives on a variety of substrates at depths from 0-30 m (Mackie et al. 1980).

Sphaerium rhomboideum: This species prefers quiet, more protected habitats and can be found in lakes, ponds and streams on vegetation or muddy substrates (Clarke, 1981; Kerr-Lawson et al. 1992).

Sphaerium simile: *Sphaerium simile* is common in all types of Canadian perennial-water habitats and prefers living on muddy or sandy bottoms. This species is commonly associated with submerged vegetation (Clarke 1981; Kerr-Lawson et al. 1992).

Valvata perdepressa: *V. perdepressa* is found from Lake Michigan to Lake Ontario, typically from beach drift on the shores of these lakes (Clarke 1981). According to Kerr-Lawson et al. (1992), this species is typically associated with abundant submerged vegetation.

Valvata tricarinata: This species lives among vegetation in perennial-water habitats, such as lakes, rivers and streams (Clarke 1981; Kerr-Lawson et al. 1992).

Valvata sincera: *V. sincera* is commonly found in large lakes, often at considerable depths, and is usually found on mud associated with abundant submerged vegetation (Clark 1981; Kerr-Lawson et al. 1992).

Valvata piscinalis: This European gastropod was introduced to Canada in the early 1900s (Clarke, 1981) and has since spread through much of the lower Great Lakes (Grigorovich et al. 2005).

Probythinella lacustris: *P. lacustris* lives in perennial-water lakes, ponds and rivers of various sizes. It prefers muddy to sandy substrates and is usually found among submerged vegetation (Clarke 1981; Kerr-Lawson et al. 1992). This species, along with *Marstonia decepta* and *Stagnicola elodes*, are members of the family *Hydrobiidae*. Hydrobiidae are gill-breathing, aquatic gastropods and most genera of this family live at water temperatures ranging from 22 to 35 °C (Herschler 1998; Shanahan et al. 2005).

Amnicola limosa: *A. limosa* is an indicator species for eutrophic lake conditions (Clarke 1979). This species is found in many types of perennial-water habitats among submerged aquatic vegetation (Clarke 1981).

Marstonia decepta: This species lives throughout the Great Lakes-St. Lawrence system. *M. decepta* is commonly found with *A. limosa* in permanent lakes, ponds and slow-moving streams (Clarke 1981).

Stagnicola elodes: *S. elodes* is a lung-breathing snail that is ubiquitous throughout Canada in all types of aquatic habitats, especially on muddy substrates and among thick vegetation (Clarke 1981).

Plate 1 *Candona acuta*: (a) female right valve, (b) female left valve

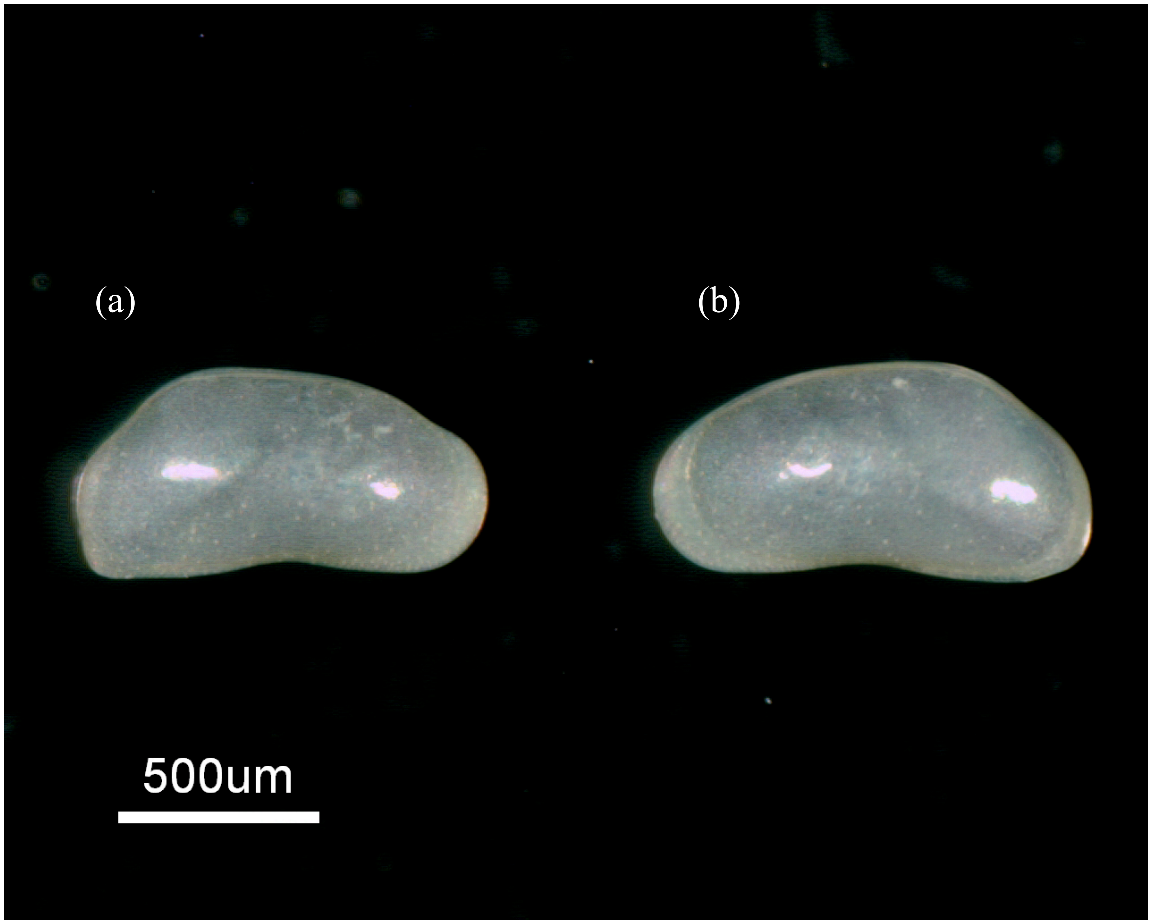

Plate 2 *Candona crogmaniana*: (a) female right valve, (b) male right valve, (c) female left valve, (d) male left valve

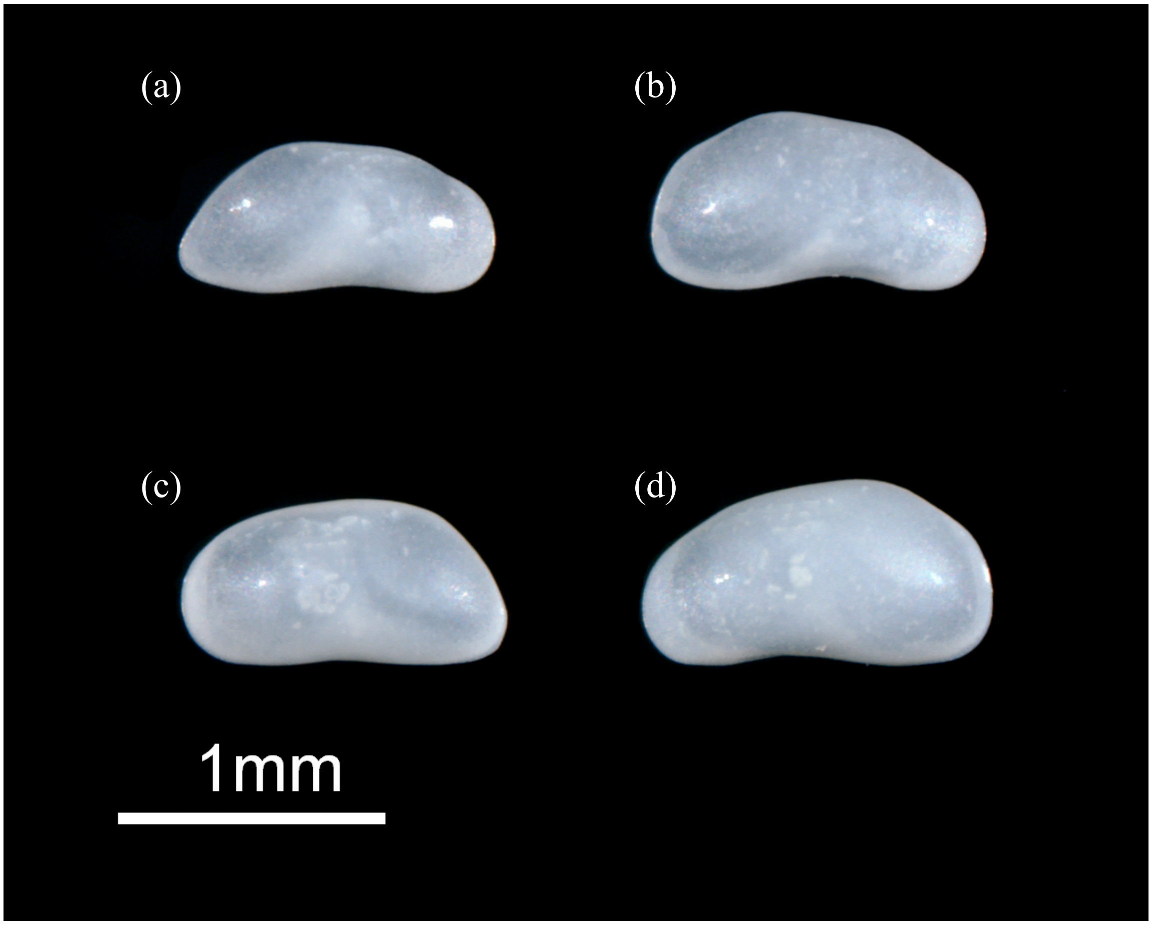

Plate 3 *Candona rawsoni*: (a) female right valve, (b) male right valve, (c) female left valve, (d) male left valve

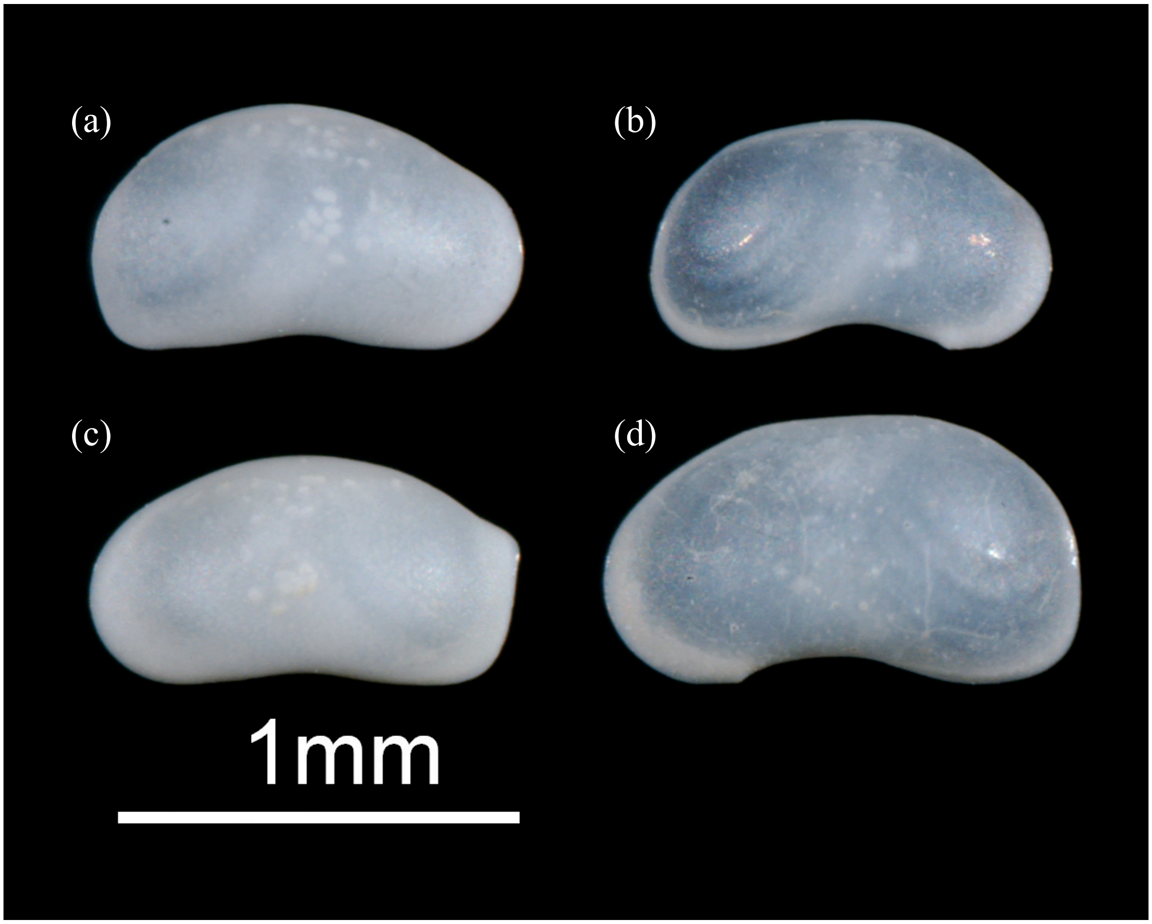

Plate 4 *Candona subtriangulata*: (a) female right valve, (b) male right valve, (c) female left valve, (d) male left valve

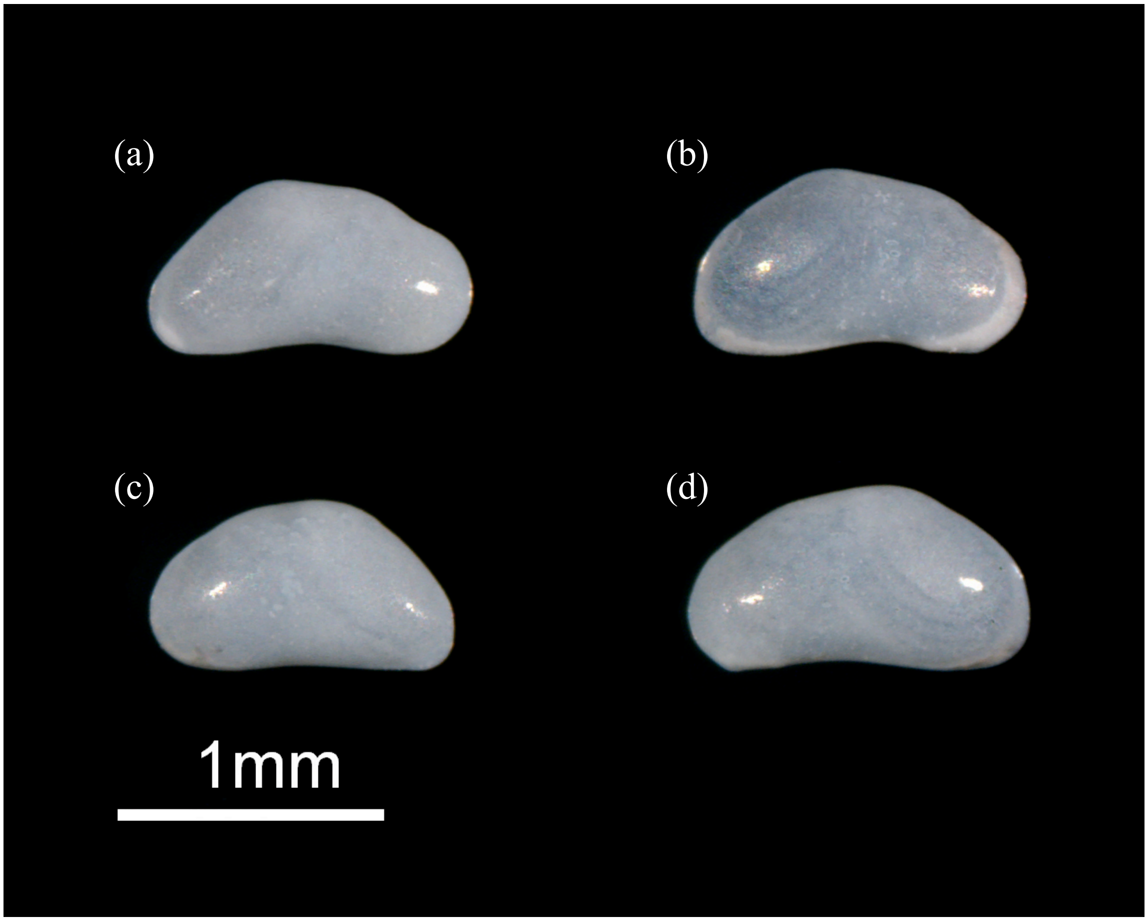

Plate 5 *Cytherissa lacustris*: (a) unsexed right valve, (b) unsexed right valve, (c) unsexed left valve

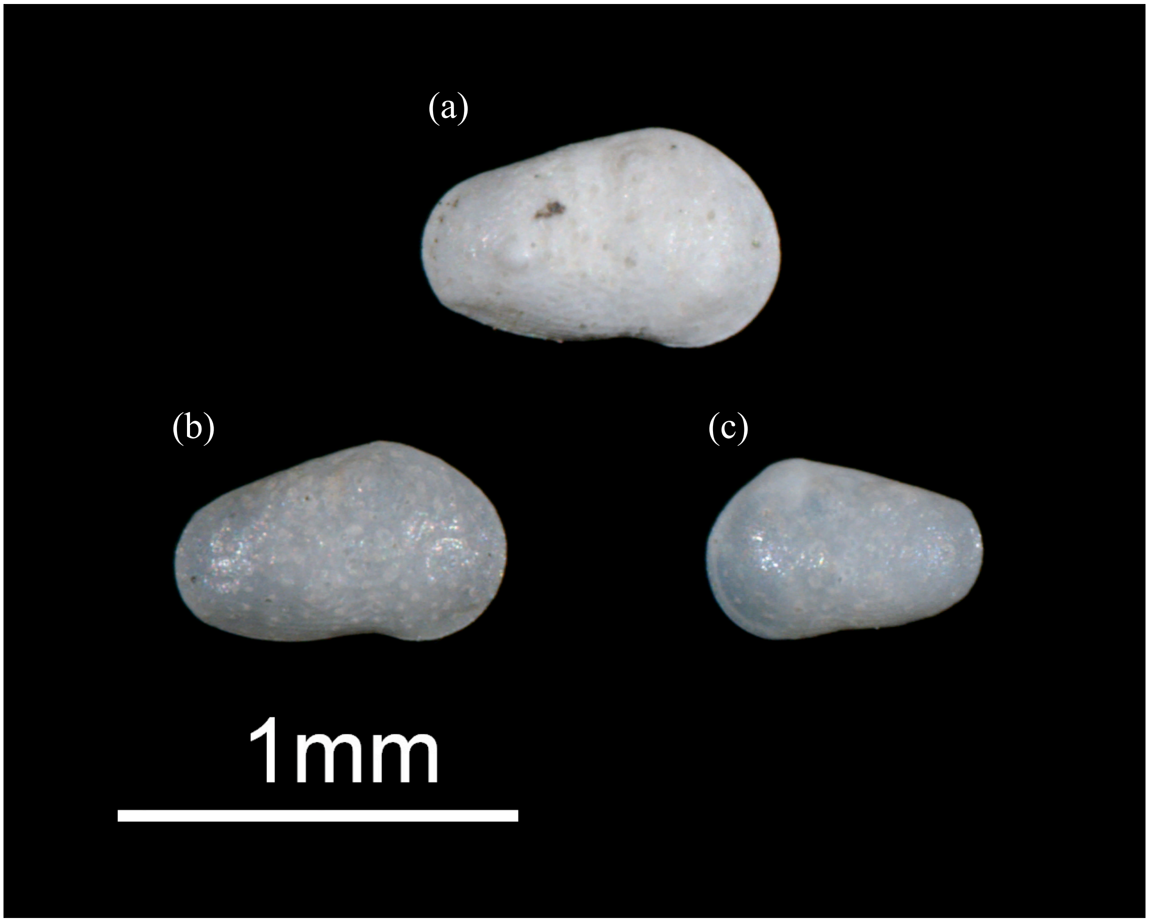

Plate 6 *Fabaeformiscandona caudata*: (a) female right valve, (b) female left valve, (c) male right valve, (d) male left valve

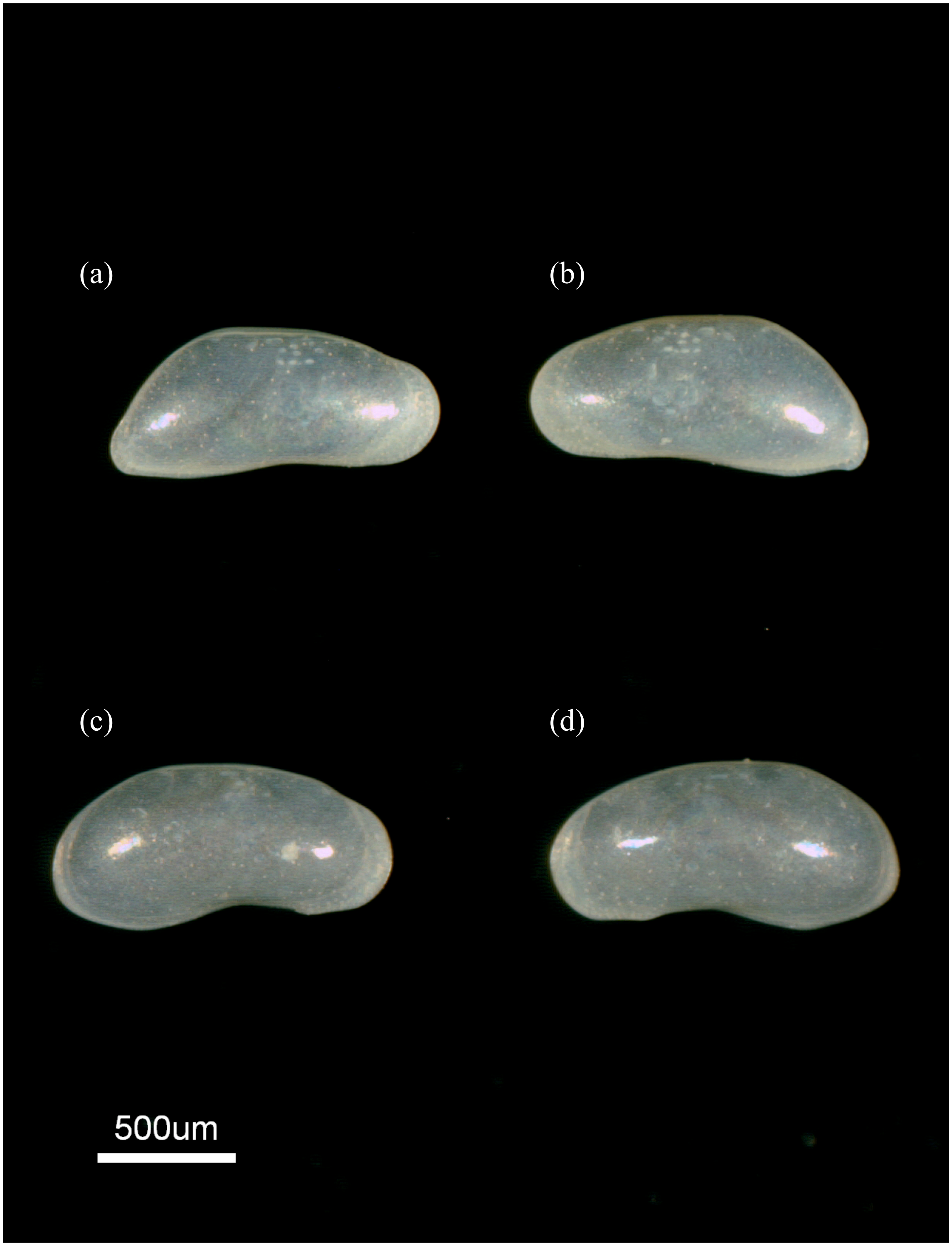

Plate 7 Unidentified *Pisidium* clams

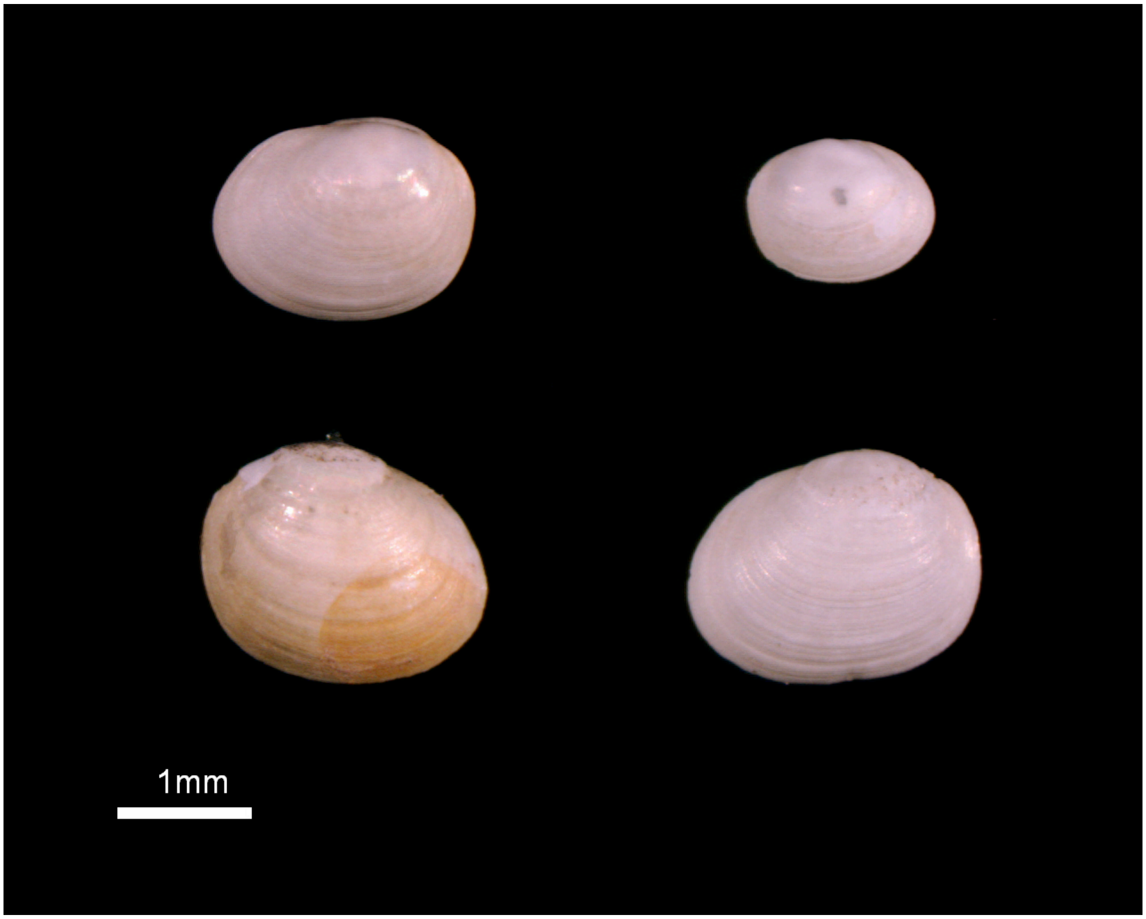

Appendix D - Ostracode and clam populations from the Michigan Basin cores

South Chippewa sub-basin - Core 101

sediment depth (m)	sediment weight (g)	*C. subtriangulata* (# valves)	*C. subtriangulata* (valves/g)	*Pisidium* clams (# valves)	*Pisidium* clams (valves/g)	*C. crogmaniana* (# valves)	*C. crogmaniana* (valves/g)	*C. rawsoni* (# valves)	*C. rawsoni* (valves/g)	*C. lacustris* (# valves)	*C. lacustris* (valves/g)	total (# valves)	total (valves/g)
0.0	116.4	37	0.32			12	0.10	15	0.13			64	0.55
0.2	141.1	635	4.50	12	0.09	364	2.58	803	5.69			1814	12.86
0.4	162.1	1960	12.09	36	0.22	1245	7.68	585	3.61			3826	23.60
0.6	182.3	2008	11.01	56	0.31	614	3.37	469	2.57	8	0.04	3155	17.31
0.8	208.6	1797	8.61	76	0.36	709	3.40	392	1.88	66	0.32	3040	14.57
1.0	166.9	75	0.45	46	0.28	19	0.11	20	0.12			160	0.96
1.2	183.2	2157	11.77	183	1.00	380	2.07	2	0.01	14	0.08	2736	14.93
1.4	175.1	2010	11.48	68	0.39	59	0.34			48	0.27	2185	12.48
1.6	170.7	1459	8.55	16	0.09	12	0.07			116	0.68	1603	9.39
1.8	173.9	654	3.76	4	0.02	16	0.09	4	0.02	1	0.01	679	3.90
2.0	148.2	337	2.27			2	0.01	1	0.01			340	2.29
2.2	151.2	190	1.26	1	0.01							191	1.26
2.4	160.2	163	1.02			4	0.02					167	1.04
2.6	129.5	145	1.12	15	0.12	45	0.35	10	0.08	3	0.02	218	1.68
2.8	156	52	0.33			1	0.01	2	0.01			55	0.35
3.0	122.9	4	0.03			2	0.02					6	0.05
3.8	144.3	55	0.38	1	0.01			1	0.01	1	0.01	58	0.40
4.0	165.2	101	0.61	1	0.01	5	0.03	1	0.01	1	0.01	109	0.66
4.2	165.8	73	0.44			2	0.01		0.00			75	0.45
4.4	164.4	45	0.27			1	0.01	1	0.01			47	0.29
4.6	199.6	21	0.11									21	0.11
4.7	112.6	7	0.06					1	0.01			8	0.07
4.8	121.6	183	1.50	1	0.01	2	0.02					186	1.53
4.9	151.4	194	1.28	4	0.03	1	0.01	1	0.01			200	1.32
5.0	154.6	282	1.82	1	0.01	5	0.03	2	0.01			290	1.88
5.1	141.4	57	0.40	9	0.06	4	0.03					70	0.50
5.2	119	98	0.82	3	0.03	6	0.05	2	0.02			109	0.92
5.3	153.9	240	1.56			2	0.01					242	1.57
5.4	113.4	119	1.05			4	0.04	5	0.04			128	1.13
5.5	143.5	279	1.94			7	0.05	1	0.01			287	2.00
5.6	141.9	230	1.62			4	0.03			1	0.01	235	1.66
5.7	139	490	3.53					1	0.01			491	3.53
5.8	135.4	460	3.40									460	3.40
5.9	124.4	270	2.17									270	2.17
6.0	117.4	243	2.07	2	0.02	1	0.01					246	2.10
6.1	116.8	222	1.90									222	1.90
6.2	106.6	16	0.15									16	0.15
6.3	104.7	178	1.70									178	1.70
6.4	120.8	421	3.49									421	3.49
6.5	107.2	254	2.37									254	2.37

Appendix D - (continued) Ostracode and clam populations from the Michigan Basin cores

South Chippewa sub-basin - Core 101

sediment depth (m)	sediment weight (g)	*C. subtriangulata* (# valves)	*C. subtriangulata* (valves/g)	*Pisidium* clams (# valves)	*Pisidium* clams (valves/g)	*C. crogmaniana* (# valves)	*C. crogmaniana* (valves/g)	*C. rawsoni* (# valves)	*C. rawsoni* (valves/g)	*C. lacustris* (# valves)	*C. lacustris* (valves/g)	total (# valves)	total (valves/g)
6.6	95.4	210	2.20									210	2.20
6.7	202.8	197	0.97									197	0.97
6.8	167.3	801	4.79									801	4.79
6.9	170.9	669	3.91									669	3.91
7.0	171.1	148	0.86	5	0.03	5	0.03					158	0.92
7.1	177.6	141	0.79	2	0.01	1	0.01			1	0.01	145	0.82
7.2	207.3	139	0.67	2	0.01	1	0.00			2	0.01	144	0.69
7.3	190.4	96	0.50	6	0.03	1	0.01					103	0.54
7.4	185.3	32	0.17	3	0.02	4	0.02					39	0.21
7.5													
7.6	163.2	9	0.06			2	0.01					11	0.07
7.7	189.3	18	0.10	1	0.01							19	0.10
7.8	162.1	24	0.15			1	0.01			1	0.01	26	0.16
8.0	152.6	23	0.15	3	0.02	3	0.02			1	0.01	30	0.20
8.2	174.2	42	0.24	3	0.02	1	0.01			2	0.01	48	0.28
8.4	167.4	26	0.16	1	0.01					1	0.01	28	0.17
8.6	144	16	0.11	2	0.01	1	0.01	1	0.01			20	0.14
8.8	162.8	23	0.14	3	0.02			1	0.01			27	0.17
9.0	170.3	21	0.12			1	0.01	1	0.01			23	0.14
9.2	171.2	15	0.09			1	0.01			1	0.01	17	0.10
9.4	159.8	12	0.08			1	0.01					13	0.08
9.6	165	5	0.03	1	0.01			1	0.01			7	0.04
9.8	169.1	7	0.04			1	0.01					8	0.05
10.0	174.3	1	0.01									1	0.01
10.2	178.3	4	0.02									4	0.02
10.4	174.3	6	0.03					1	0.01			7	0.04
10.6	182.3	7	0.04									7	0.04
10.8	146.7	180	1.23									180	1.23
11.0	174.9	140	0.80									140	0.80
11.2	201.5	150	0.74									150	0.74
11.4	208.3	166	0.80									166	0.80
11.6	206.1	146	0.71									146	0.71
11.8	146.4	28	0.19									28	0.19
12.0	186.5	93	0.50									93	0.50
12.2	204.6	80	0.39									80	0.39
12.4	222.8	74	0.33									74	0.33
12.6	210.5	84	0.40									84	0.40
12.8	181.5	59	0.33									59	0.33
13.0	164.4	10	0.06									10	0.06
13.2	187.5	1	0.01									1	0.01
13.4	186	1	0.01									1	0.01

Appendix D - (continued) Ostracode and clam populations from the Michigan Basin cores

South Chippewa sub-basin - Core 101

sediment depth (m)	sediment weight (g)	*C. subtriangulata* (# valves)	*C. subtriangulata* (valves/g)	*Pisidium* clams (# valves)	*Pisidium* clams (valves/g)	*C. crogmaniana* (# valves)	*C. crogmaniana* (valves/g)	*C. rawsoni* (# valves)	*C. rawsoni* (valves/g)	*C. lacustris* (# valves)	*C. lacustris* (valves/g)	total (# valves)	total (valves/g)
13.6	167.1					1	0.01					1	0.01
13.8	169.1	2	0.01									2	0.01
14.0	168.6	3	0.02									3	0.02
14.2	168.6	4	0.02									4	0.02
14.4	153	1	0.01	1	0.01							2	0.01
14.6	160.1	2	0.01					1	0.01			3	0.02
14.8	168.3	2	0.01									2	0.01
15.0	128.6												
15.2	158.1												
15.4	156.9	1	0.01									1	0.01
15.6	158.3												
15.8	154.6	1	0.01									1	0.01
16.0	155.3												
16.2	147.7												
16.4	156.5	9	0.06									9	0.06

Appendix D - (continued) Ostracode and clam populations from the Michigan Basin cores

Milwaukee sub-basin - Core 102

sediment depth (m)	sediment weight (g)	*C. subtriangulata* (# valves)	*C. subtriangulata* (valves/g)	*Pisidium* clams (# valves)	*Pisidium* clams (valves/g)	*C. crogmaniana* (# valves)	*C. crogmaniana* (valves/g)	*C. rawsoni* (# valves)	*C. rawsoni* (valves/g)	*C. lacustris* (# valves)	*C. lacustris* (valves/g)	total (# valves)	total (valves/g)
0.0	106.9												
0.2	129												
0.4	134.2												
0.6	136.6												
0.8	154.9												
1.0	153.1												
1.2	162.6	9	0.06			2	0.01	26	0.16			37	0.23
1.4	169.1	15	0.09			13	0.08	12	0.07			40	0.24
1.6	178.6	19	0.11	7	0.04	18	0.10	11	0.06	2	0.01	57	0.32
1.8	200	18	0.09	8	0.04	18	0.09	15	0.08	1	0.01	60	0.30
2.0	157.8	14	0.09	4	0.03	14	0.09	12	0.08	4	0.03	48	0.30
2.2	173	3	0.02			1	0.01					4	0.02
2.4	180.4	17	0.09	24	0.13	6	0.03			14		61	0.34
2.6	170.9	11	0.06	16	0.09	14	0.08			17	0.10	58	0.34
2.8	176.9	15	0.08	12	0.07	12	0.07			12	0.07	51	0.29
3.0	188.7	13	0.07	16	0.08	6	0.03			12	0.06	47	0.25
3.2	203.2	12	0.06	28	0.14	9	0.04			17	0.08	66	0.32
3.4	177.5	50	0.28	3	0.02					30	0.17	83	0.47
3.6	178.9	420	2.35	2	0.01							422	2.36
3.8	260	152	0.58	1	0.00							153	0.59
4.0	188.9	696	3.68									696	3.68
4.2	186.4	141	0.76	1	0.01	1	0.01					143	0.77
4.4	182.5	365	2.00									365	2.00
4.6	188.4	180	0.96									180	0.96
4.8	263.8	149	0.56									149	0.56
5.0	154.6	41	0.27									41	0.27
5.2	164.1	3	0.02			2	0.01					5	0.03
5.4	162.6	5	0.03									5	0.03
5.6	195.4	3	0.02									3	0.02
5.8	149.9	9	0.06									9	0.06
6.0	156.5	8	0.05	2	0.01							10	0.06
6.2	163.1	83	0.51									83	0.51
6.4	159.2	62	0.39									62	0.39
6.6	121.1	62	0.51									62	0.51
6.8	155.9	101	0.65									101	0.65
7.0	164.3	93	0.57									93	0.57
7.2	168.7	69	0.41									69	0.41
7.4	178.9	90	0.50									90	0.50
7.6	142	55	0.39									55	0.39
7.8	156.8	98	0.63									98	0.63
8.0	168.5	94	0.56									94	0.56

Appendix D - (continued) Ostracode and clam populations from the Michigan Basin cores

Milwaukee sub-basin - Core 102

sediment depth (m)	sediment weight (g)	*C. subtriangulata* (# valves)	*C. subtriangulata* (valves/g)	*Pisidium* clams (# valves)	*Pisidium* clams (valves/g)	*C. crogmaniana* (# valves)	*C. crogmaniana* (valves/g)	*C. rawsoni* (# valves)	*C. rawsoni* (valves/g)	*C. lacustris* (# valves)	*C. lacustris* (valves/g)	total (# valves)	total (valves/g)
8.2	179.1	90	0.50									90	0.50
8.4	168.2	72	0.43									72	0.43
8.6	119.3	34	0.28									34	0.28
8.8	167.2	77	0.46									77	0.46
9.0	178.6	55	0.31									55	0.31
9.2	181.7	112	0.62									112	0.62
9.4	177.8	135	0.76									135	0.76
9.6	149.5	61	0.41									61	0.41
9.8	168.6	109	0.65									109	0.65
10.0	188.8	305	1.62									305	1.62
10.2	195	199	1.02									199	1.02
10.4	188.6	64	0.34									64	0.34
10.6	168.2	17	0.10									17	0.10
10.8	181.5	76	0.42									76	0.42
11.0	181.5	156	0.86									156	0.86
11.2	181.5	76	0.42									76	0.42
11.4	187.1	135	0.72									135	0.72
11.6	176.5	48	0.27			2	0.01					50	0.28
11.8	149.8	65	0.43									65	0.43
12.0	171.4	35	0.20									35	0.20
12.2	175	95	0.54									95	0.54
12.4	183.1	76	0.42									76	0.42
12.6	182.4	91	0.50									91	0.50
12.8	134.5	51	0.38									51	0.38
13.0	176.1	79	0.45									79	0.45
13.2	185.2	64	0.35									64	0.35
13.4	191.8	38	0.20									38	0.20
13.6	194.2	36	0.19									36	0.19
13.8	136.5	32	0.23									32	0.23
14.0	176.5	51	0.29									51	0.29
14.2	172.4	55	0.32									55	0.32
14.4	174.2	64	0.37									64	0.37

Appendix D - (continued) Ostracode and clam populations from the Michigan Basin cores

Chippewa sub-basin - Core 100

sediment depth (m)	sediment weight (g)	*C. subtriangulata* (# valves)	*C. subtriangulata* (valves/g)	*Pisidium* clams (# valves)	*Pisidium* clams (valves/g)	*C. crogmaniana* (# valves)	*C. crogmaniana* (valves/g)	*C. rawsoni* (# valves)	*C. rawsoni* (valves/g)	*C. lacustris* (# valves)	*C. lacustris* (valves/g)	total (# valves)	total (valves/g)
0.0	75.6	121	1.60	5	0.07	3	0.04	4	0.05	1	0.01	134	1.77
0.2	88.5	17	0.19	6	0.07					6	0.07	29	0.33
0.4	109.2	2	0.02					2	0.02			4	0.04
0.6	57.2	2	0.03			2	0.03					4	0.07
0.8	141.4	56	0.40	1	0.01	4	0.03	1	0.01			62	0.44
1.0	159.2	227	1.43			234	1.47	252	1.58			713	4.48
1.2	158.6	800	5.04	12	0.08	225	1.42	175	1.10			1212	7.64
1.4	170.2	1860	10.93	60	0.35	500	2.94	375	2.20	5	0.03	2800	16.45
1.6	120.2	660	5.49	40	0.33	75	0.62	55	0.46	7	0.06	837	6.96
1.8	153.9	14	0.09	13	0.08	11	0.07	23	0.15	1	0.01	62	0.40
2.0	146.6	15	0.10	6	0.04	18	0.12	13	0.09			52	0.35
2.2	142	42	0.30	1	0.01	17	0.12	7	0.05			67	0.47
2.4	148.7	21	0.14									21	0.14
2.6	107.4	753	7.01	28	0.26	21	0.20			5	0.05	807	7.51
2.8	161	1611	10.01	72	0.45	33	0.20	1	0.01	32	0.20	1749	10.86
3.0	147.8	1101	7.45	49	0.33	26	0.18			24	0.16	1200	8.12
3.2	158.6	1794	11.31	64	0.40	35	0.22			57	0.36	1950	12.30
3.4	168.3	1491	8.86	7	0.04					27	0.16	1525	9.06
3.6	111.1	45	0.41									45	0.41
3.8	182.6	34	0.19	4	0.02							38	0.21
4.0	170.7	8	0.05					2	0.01			10	0.06
4.2	155.1	75	0.48	3	0.02	1	0.01			1	0.01	80	0.52
4.4	177.2	80	0.45			2	0.01			2	0.01	84	0.47
4.6													
4.8	203.7	17	0.08			1	0.00					18	0.09
5.0	204.8	18	0.09	1	0.00							19	0.09
5.2	208.5	13	0.06			2	0.01	1	0.00			16	0.08
5.4	185.5	17	0.09	2	0.01	3	0.02	1	0.01			23	0.12
5.6	116.6	23	0.20									23	0.20
5.8	195.8	6	0.03	3	0.02							9	0.05
6.0	209.9	12	0.06			1	0.00					13	0.06
6.2	207.3	12	0.06			1						13	0.06
6.4	213	5	0.02			1	0.00	1	0.00	1	0.00	8	0.04
6.6	279.6	12	0.04			1		3	0.01			16	0.06
6.8	237.2	2	0.01									2	0.01
7.0													
7.2	241.9	9	0.04							1	0.00	10	0.04
7.4	235.9	5	0.02									5	0.02
7.6	249.2	6	0.02									6	0.02
7.8	237.2	2	0.01									2	0.01
8.0	239.6	6	0.03	1	0.00							7	0.03

Appendix D - (continued) Ostracode and clam populations from the Michigan Basin cores

Chippewa sub-basin - Core 100

sediment depth (m)	sediment weight (g)	*C. subtriangulata* (# valves)	*C. subtriangulata* (valves/g)	*Pisidium* clams (# valves)	*Pisidium* clams (valves/g)	*C. crogmaniana* (# valves)	*C. crogmaniana* (valves/g)	*C. rawsoni* (# valves)	*C. rawsoni* (valves/g)	*C. lacustris* (# valves)	*C. lacustris* (valves/g)	total (# valves)	total (valves/g)
8.2	204.6	1	0.00					1	0.00			2	0.01
8.4	229.4	2	0.01									2	0.01
8.6	264.9	6	0.02									6	0.02
8.8	236.2	8	0.03									8	0.03
9.0	194.9	5	0.03					1	0.01			6	0.03
9.2	176.2	3	0.02					2	0.01			5	0.03
9.4	216	2	0.01									2	0.01
9.6	217.8	14	0.06									14	0.06
9.8	211.6	4	0.02									4	0.02
10.0	199	4	0.02			1	0.01					5	0.03
10.2	114.1	28	0.25									28	0.25
10.4	204.6	17	0.08			1	0.00	1	0.00	1	0.00	20	0.10
10.6	223.5	85	0.38					2	0.01			87	0.39
10.8	221.4	20	0.09	3	0.01	1	0.00	2	0.01			26	0.12
11.0	216.3	35	0.16	1								36	0.17
11.2	163.7	28	0.17									28	0.17
11.4	204.7	6	0.03	1	0.00							7	0.03
11.6	209.4	56	0.27									56	0.27
11.8	216.5	52	0.24	1								53	0.24
12.0	214.5	17	0.08									17	0.08
12.3	303.7	33	0.11									33	0.11
12.5	214.6	19	0.09									19	0.09
12.7	224.1	9	0.04									9	0.04
12.9	244.4	8	0.03									8	0.03
13.1	342.5	16	0.05									16	0.05
13.2	92.7	25	0.27									25	0.27
13.4	206.3	32	0.16									32	0.16
13.6	223.4	31	0.14									31	0.14
13.8	213.7	8	0.04									8	0.04
14.0	218.9	7	0.03									7	0.03
14.2	179.4	2	0.01									2	0.01
14.4	211.6	6	0.03									6	0.03
14.6	219.4	13	0.06									13	0.06
14.8	230.8	2	0.01									2	0.01
15.0	249.9	27	0.11									27	0.11
15.2	143.2	5	0.03									5	0.03
15.4	195.9	3	0.02									3	0.02
15.6	210.8	0	0.00										
15.8	210.6	8	0.04									8	0.04

Appendix E - Oxygen- and carbon-isotope compositions of ostracode valves and clam shells from the Michigan Basin cores

South Chippewa sub-basin - Core 101

sediment depth (m)[a]	species	$\delta^{13}C$ (VPDB)	$\delta^{18}O$ (VSMOW)	$\delta^{18}O_{lakewater}$ (VSMOW)[b]
0.0	*C. subtriangulata*	-2.2	29.3	-6.4
0.0	*C. subtriangulata*	-2.8	30.5	-5.2
0.2	*C. subtriangulata*	-2.3	30.4	-5.3
0.2	*C. subtriangulata*	-3.0	30.4	-5.3
0.4	*C. subtriangulata*	-3.0	30.5	-5.2
0.6	*C. subtriangulata*	-2.7	30.2	-5.5
0.7	*C. subtriangulata*	-2.5	30.1	-5.6
0.8	*C. subtriangulata*	-2.8	30.3	-5.4
0.8	*C. subtriangulata*	-2.7	30.3	-5.4
1.0	*C. subtriangulata*	-3.4	30.0	-5.7
1.2	*C. subtriangulata*	-4.1	29.3	-6.3
1.2	*C. subtriangulata*	-2.5	29.3	-6.4
1.2	*C. subtriangulata*	-4.4	29.0	-6.6
1.4	*C. subtriangulata*	-2.9	29.4	-6.2
1.4	*C. subtriangulata*	-3.7	29.1	-6.6
1.6	*C. subtriangulata*	-3.7	29.4	-6.3
1.6	*C. subtriangulata*	-4.6	29.1	-6.5
1.8	*C. subtriangulata*	-3.7	25.0	-10.6
1.8	*C. subtriangulata*	-2.9	24.5	-11.1
2.0	*C. subtriangulata*	-4.7	17.1	-18.1
2.2	*C. subtriangulata*	-4.1	22.4	-13.0
2.4	*C. subtriangulata*	-5.6	19.3	-16.0
2.6	*C. subtriangulata*	-4.3	28.6	-7.0
2.8	*C. subtriangulata*	-3.5	27.4	-8.2
3.0	*C. subtriangulata*	-5.6	22.6	-12.8
3.8	*C. subtriangulata*	-3.1	18.3	-17.0
4.0	*C. subtriangulata*	-3.2	17.8	-17.5
4.0	*C. subtriangulata*	-2.7	21.2	-14.2
4.2	*C. subtriangulata*	-3.4	17.9	-17.4
4.2	*C. subtriangulata*	-4.1	17.9	-17.3
4.4	*C. subtriangulata*	-4.3	23.9	-11.6
4.6	*C. subtriangulata*	-3.4	17.2	-18.1
4.7	*C. subtriangulata*	-4.1	29.3	-6.4
4.8	*C. subtriangulata*	-5.6	18.9	-16.4
4.8	*C. subtriangulata*	-4.1	18.0	-17.3
4.9	*C. subtriangulata*	-4.8	20.0	-15.4
4.9	*C. subtriangulata*	-4.7	21.1	-14.3
5.0	*C. subtriangulata*	-4.6	21.5	-13.9
5.0	*C. subtriangulata*	-3.9	20.7	-14.7
5.1	*C. subtriangulata*	-4.9	22.5	-13.0
5.2	*C. subtriangulata*	-6.2	18.0	-17.3
5.2	*C. subtriangulata*	-5.4	17.4	-17.8
5.3	*C. subtriangulata*	-3.8	16.7	-18.5
5.3	*C. subtriangulata*	-4.3	17.2	-18.0
5.4	*C. subtriangulata*	-4.2	23.1	-12.3
5.4	*C. subtriangulata*	-4.9	24.3	-11.2

Appendix E - (continued) Oxygen- and carbon-isotope compositions of ostracode valves and clam shells from the Michigan Basin cores

South Chippewa sub-basin - Core 101

sediment depth (m)[a]	species	$\delta^{13}C$ (VPDB)	$\delta^{18}O$ (VSMOW)	$\delta^{18}O_{lakewater}$ (VSMOW)[b]
5.5	*C. subtriangulata*	-3.3	18.8	-16.5
5.5	*C. subtriangulata*	-4.3	19.3	-16.0
5.6	*C. subtriangulata*	-4.6	18.2	-17.1
5.6	*C. subtriangulata*	-4.5	18.0	-17.2
5.7	*C. subtriangulata*	-4.2	17.7	-17.6
5.7	*C. subtriangulata*	-3.9	18.3	-17.0
5.8	*C. subtriangulata*	-3.9	17.3	-18.0
5.8	*C. subtriangulata*	-3.3	17.1	-18.2
5.9	*C. subtriangulata*	-4.0	17.4	-17.9
5.9	*C. subtriangulata*	-4.6	17.1	-18.2
6.0	*C. subtriangulata*	-4.1	16.9	-18.4
6.0	*C. subtriangulata*	-3.6	16.8	-18.4
6.1	*C. subtriangulata*	-4.8	17.8	-17.5
6.1	*C. subtriangulata*	-5.5	18.9	-16.4
6.2	*C. subtriangulata*	-3.1	20.6	-14.8
6.2	*C. subtriangulata*	-4.1	17.5	-17.8
6.3	*C. subtriangulata*	-3.8	17.0	-18.2
6.3	*C. subtriangulata*	-2.9	19.1	-16.3
6.4	*C. subtriangulata*	-4.2	19.8	-15.5
6.4	*C. subtriangulata*	-4.3	19.5	-15.8
6.5	*C. subtriangulata*	-4.0	19.3	-16.0
6.5	*C. subtriangulata*	-4.0	19.1	-16.2
6.6	*C. subtriangulata*	-3.7	21.0	-14.4
6.6	*C. subtriangulata*	-3.6	17.7	-17.6
6.7	*C. subtriangulata*	-3.9	17.7	-17.6
6.7	*C. subtriangulata*	-4.5	18.0	-17.3
6.8	*C. subtriangulata*	-4.6	19.7	-15.6
6.8	*C. subtriangulata*	-3.3	18.8	-16.5
6.9	*C. subtriangulata*	-3.8	19.4	-15.9
6.9	*C. subtriangulata*	-4.2	20.0	-15.4
7.0	*C. subtriangulata*	-4.1	23.2	-12.3
7.0	*C. subtriangulata*	-4.6	19.3	-16.0
7.1	*C. subtriangulata*	-3.7	18.3	-17.0
7.1	*C. subtriangulata*	-3.3	17.3	-17.9
7.2	*C. subtriangulata*	-3.0	17.6	-17.7
7.2	*C. subtriangulata*	-3.1	20.4	-15.0
7.3	*C. subtriangulata*	-4.0	18.1	-17.2
7.3	*C. subtriangulata*	-3.5	16.7	-18.5
7.4	*C. subtriangulata*	-3.6	27.8	-7.8
7.4	*C. subtriangulata*	-3.7	24.8	-10.7
7.6	*C. subtriangulata*	-3.8	20.5	-14.8
7.7	*C. subtriangulata*	-4.5	20.8	-14.6
7.8	*C. subtriangulata*	-3.5	23.5	-12.0
7.8	*C. subtriangulata*	-3.2	25.9	-9.7
8.0	*C. subtriangulata*	-3.3	22.4	-13.0
8.2	*C. subtriangulata*	-3.2	20.7	-14.7

Appendix E - (continued) Oxygen- and carbon-isotope compositions of ostracode valves and clam shells from the Michigan Basin cores

South Chippewa sub-basin - Core 101

sediment depth (m)[a]	species	$\delta^{13}C$ (VPDB)	$\delta^{18}O$ (VSMOW)	$\delta^{18}O_{lakewater}$ (VSMOW)[b]
8.2	*C. subtriangulata*	-3.9	22.1	-13.3
8.4	*C. subtriangulata*	-3.9	25.6	-10.0
8.4	*C. subtriangulata*	-3.4	24.2	-11.3
8.6	*C. subtriangulata*	-2.8	22.8	-12.6
8.6	*C. subtriangulata*	-4.4	22.7	-12.7
8.8	*C. subtriangulata*	-3.2	27.5	-8.1
8.8	*C. subtriangulata*	-3.7	24.0	-11.5
9.0	*C. subtriangulata*	-4.4	23.1	-12.4
9.2	*C. subtriangulata*	-3.2	18.6	-16.7
9.2	*C. subtriangulata*	-4.5	25.4	-10.1
9.4	*C. subtriangulata*	-2.7	22.0	-13.5
9.6	*C. subtriangulata*	-4.1	23.6	-11.8
9.8	*C. subtriangulata*	-4.3	21.4	-14.0
10.0	*C. subtriangulata*	-4.9	29.7	-6.0
10.2	*C. subtriangulata*	-2.5	20.4	-15.0
10.4	*C. subtriangulata*	-2.4	29.2	-6.5
10.6	*C. subtriangulata*	-4.7	16.8	-18.4
10.8	*C. subtriangulata*	-2.8	17.8	-17.5
10.8	*C. subtriangulata*	-2.5	17.9	-17.3
10.8	*C. subtriangulata*	-3.9	15.7	-19.5
10.8	*C. subtriangulata*	-4.3	16.1	-19.1
10.8	*C. subtriangulata*	-2.5	16.1	-19.1
11.0	*C. subtriangulata*	-4.8	20.0	-15.4
11.0	*C. subtriangulata*	-1.9	18.0	-17.3
11.0	*C. subtriangulata*	-1.9	17.5	-17.8
11.0	*C. subtriangulata*	-2.5	17.0	-18.3
11.0	*C. subtriangulata*	-2.6	18.5	-16.8
11.0	*C. subtriangulata*	-2.7	18.4	-16.9
11.2	*C. subtriangulata*	-2.5	18.3	-16.9
11.2	*C. subtriangulata*	-1.9	18.3	-16.9
11.4	*C. subtriangulata*	-2.3	18.1	-17.1
11.4	*C. subtriangulata*	-1.9	17.7	-17.5
11.6	*C. subtriangulata*	-2.4	17.6	-17.6
11.6	*C. subtriangulata*	-1.9	17.4	-17.8
11.8	*C. subtriangulata*	-2.8	17.1	-18.2
11.8	*C. subtriangulata*	-3.2	16.9	-18.3
12.0	*C. subtriangulata*	-2.9	17.5	-17.7
12.0	*C. subtriangulata*	-2.7	17.4	-17.8
12.2	*C. subtriangulata*	-2.7	17.2	-18.0
12.2	*C. subtriangulata*	-2.4	17.5	-17.8
12.4	*C. subtriangulata*	-2.5	17.2	-18.1
12.4	*C. subtriangulata*	-3.3	17.2	-18.0
12.6	*C. subtriangulata*	-2.8	16.8	-18.4
12.6	*C. subtriangulata*	-2.6	17.1	-18.2
12.8	*C. subtriangulata*	-2.3	18.6	-16.7
12.8	*C. subtriangulata*	-3.2	17.4	-17.9

Appendix E - (continued) Oxygen- and carbon-isotope compositions of ostracode valves and clam shells from the Michigan Basin cores

South Chippewa sub-basin - Core 101

sediment depth (m)[a]	species	$\delta^{13}C$ (VPDB)	$\delta^{18}O$ (VSMOW)	$\delta^{18}O_{lakewater}$ (VSMOW)[b]
13.0	*C. subtriangulata*	-3.5	17.2	-18.0
13.8	*C. subtriangulata*	-2.8	16.4	-18.8
14.0	*C. subtriangulata*	-3.7	20.2	-15.2
14.2	*C. subtriangulata*	-3.4	26.6	-9.0
14.4	*C. subtriangulata*	-3.8	29.6	-6.1
14.6	*C. subtriangulata*	-3.4	16.2	-19.1
14.8	*C. subtriangulata*	-3.6	21.5	-13.9
15.4	*C. subtriangulata*	-3.4	26.8	-8.7
15.8	*C. subtriangulata*	-4.3	26.3	-9.3
16.4	*C. subtriangulata*	-3.3	17.4	-17.8
0.0	*C. crogmaniana*	-1.6	30.4	-3.3
0.2	*C. crogmaniana*	-0.9	30.2	-3.5
0.2	*C. crogmaniana*	-1.3	30.4	-3.3
0.4	*C. crogmaniana*	-1.1	30.6	-3.1
0.4	*C. crogmaniana*	0.1	29.8	-3.9
0.6	*C. crogmaniana*	-2.2	30.0	-3.6
0.6	*C. crogmaniana*	-1.9	29.8	-3.9
0.8	*C. crogmaniana*	-2.7	30.1	-3.6
0.8	*C. crogmaniana*	-1.8	28.5	-5.2
1.0	*C. crogmaniana*	-1.3	30.2	-3.5
1.2	*C. crogmaniana*	-5.5	29.5	-4.2
1.2	*C. crogmaniana*	-4.7	29.4	-4.2
1.2	*C. crogmaniana*	-4.9	29.0	-4.7
1.4	*C. crogmaniana*	-2.7	29.2	-4.5
1.4	*C. crogmaniana*	-3.6	29.3	-4.4
1.6	*C. crogmaniana*	-4.0	29.4	-4.3
1.6	*C. crogmaniana*	-4.3	29.4	-4.3
1.8	*C. crogmaniana*	-2.9	29.6	-4.1
2.0	*C. crogmaniana*	-2.8	30.0	-3.7
2.4	*C. crogmaniana*	-1.9	30.4	-3.3
2.6	*C. crogmaniana*	-2.4	29.7	-4.0
3.0	*C. crogmaniana*	-1.4	29.9	-3.8
4.0	*C. crogmaniana*	-2.6	29.1	-4.5
4.2	*C. crogmaniana*	-1.0	30.1	-3.6
5.0	*C. crogmaniana*	-3.4	29.7	-3.9
5.1	*C. crogmaniana*	-2.9	29.5	-4.2
5.2	*C. crogmaniana*	-4.2	29.0	-4.6
5.5	*C. crogmaniana*	-2.0	30.2	-3.4
5.6	*C. crogmaniana*	-5.1	29.2	-4.5
7.0	*C. crogmaniana*	-2.3	28.9	-4.7
7.8	*C. crogmaniana*	-4.1	28.4	-5.2
8.0	*C. crogmaniana*	-4.2	28.3	-5.3
8.2	*C. crogmaniana*	-5.6	26.4	-7.1
8.6	*C. crogmaniana*	-4.6	26.8	-6.8
9.4	*C. crogmaniana*	-2.0	28.3	-5.3

Appendix E - (continued) Oxygen- and carbon-isotope compositions of ostracode valves and clam shells from the Michigan Basin cores

South Chippewa sub-basin - Core 101

sediment depth (m)[a]	species	$\delta^{13}C$ (VPDB)	$\delta^{18}O$ (VSMOW)	$\delta^{18}O_{lakewater}$ (VSMOW)[b]
9.8	*C. crogmaniana*	-0.6	31.0	-2.7
0.0	*C. rawsoni*	1.3	30.8	-3.2
0.0	*C. rawsoni*	0.5	31.0	-3.0
0.2	*C. rawsoni*	1.8	31.0	-3.0
0.2	*C. rawsoni*	1.8	30.6	-3.4
0.4	*C. rawsoni*	0.4	31.6	-2.4
0.4	*C. rawsoni*	-0.3	31.0	-3.0
0.6	*C. rawsoni*	-0.1	30.6	-3.4
0.6	*C. rawsoni*	0.6	30.8	-3.2
0.8	*C. rawsoni*	-0.1	27.9	-6.0
0.8	*C. rawsoni*	0.6	29.2	-4.8
1.0	*C. rawsoni*	0.5	30.9	-3.1
1.2	*C. rawsoni*	0.3	30.5	-3.5
2.6	*C. rawsoni*	0.5	31.0	-3.0
2.8	*C. rawsoni*	-0.4	30.6	-3.4
5.0	*C. rawsoni*	-0.8	30.4	-3.5
5.4	*C. rawsoni*	0.8	30.0	-3.9
5.7	*C. rawsoni*	-0.7	29.9	-4.0
8.8	*C. rawsoni*	0.1	29.6	-4.3
9.0	*C. rawsoni*	-1.0	28.5	-5.5
9.6	*C. rawsoni*	1.8	31.0	-3.0
10.4	*C. rawsoni*	-3.7	17.0	-16.5
14.6	*C. rawsoni*	-1.9	24.4	-9.3
0.6	*C. lacustris*	-0.9	29.3	-2.9
0.8	*C. lacustris*	-1.1	29.5	-2.7
1.2	*C. lacustris*	-2.3	28.6	-3.6
1.4	*C. lacustris*	-1.8	28.5	-3.7
1.4	*C. lacustris*	-2.3	28.6	-3.6
1.6	*C. lacustris*	-1.6	28.4	-3.8
1.6	*C. lacustris*	-0.6	28.5	-3.7
2.6	*C. lacustris*	-1.2	29.8	-2.4
7.8	*C. lacustris*	-1.8	26.5	-5.6
8.2	*C. lacustris*	-2.3	27.8	-4.3
0.2	*Pisidium* clams	-0.8	26.9	-4.5
0.2	*Pisidium* clams	-1.0	28.5	-2.9
0.4	*Pisidium* clams	1.6	29.8	-1.7
0.4	*Pisidium* clams	1.6	29.8	-1.7
0.6	*Pisidium* clams	-0.4	29.0	-2.4
0.6	*Pisidium* clams	0.6	29.2	-2.2
0.8	*Pisidium* clams	-0.1	29.6	-1.8
0.8	*Pisidium* clams	0.2	29.1	-2.3
1.0	*Pisidium* clams	-0.6	22.0	-9.2
1.2	*Pisidium* clams	-0.3	28.8	-2.6

Appendix E - (continued) Oxygen- and carbon-isotope compositions of ostracode valves and clam shells from the Michigan Basin cores

South Chippewa sub-basin - Core 101

sediment depth (m)[a]	species	$\delta^{13}C$ (VPDB)	$\delta^{18}O$ (VSMOW)	$\delta^{18}O_{lakewater}$ (VSMOW)[b]
1.2	*Pisidium* clams	-0.9	28.0	-3.4
1.2	*Pisidium* clams	-0.2	28.8	-2.6
1.4	*Pisidium* clams	-1.2	28.4	-3.0
1.4	*Pisidium* clams	-2.0	28.6	-2.8
1.6	*Pisidium* clams	-2.4	28.2	-3.2
1.6	*Pisidium* clams	-1.5	28.1	-3.3
1.8	*Pisidium* clams	-0.2	28.5	-2.9
1.8	*Pisidium* clams	0.7	29.6	-1.8
2.6	*Pisidium* clams	1.4	29.3	-2.1
2.6	*Pisidium* clams	-0.1	27.5	-3.9
3.8	*Pisidium* clams	0.6	29.6	-1.9
4.0	*Pisidium* clams	-1.7	28.2	-3.2
4.6	*Pisidium* clams	-0.7	28.4	-3.0
4.9	*Pisidium* clams	-1.9	28.2	-3.2
4.9	*Pisidium* clams	-1.9	28.4	-3.0
5.1	*Pisidium* clams	0.7	29.4	-2.0
5.1	*Pisidium* clams	0.6	29.4	-2.0
5.2	*Pisidium* clams	0.6	29.6	-1.8
6.0	*Pisidium* clams	-0.4	26.3	-5.1
6.8	*Pisidium* clams	-0.6	28.4	-3.0
6.8	*Pisidium* clams	-1.1	28.4	-3.0
7.0	*Pisidium* clams	0.7	29.1	-2.3
7.0	*Pisidium* clams	-1.0	28.5	-2.9
7.3	*Pisidium* clams	0.0	26.9	-4.5
7.3	*Pisidium* clams	-0.7	28.4	-3.0
7.4	*Pisidium* clams	-0.5	29.6	-1.9
7.4	*Pisidium* clams	0.2	29.5	-1.9
7.7	*Pisidium* clams	-0.4	29.5	-1.9
8.0	*Pisidium* clams	-1.0	28.4	-3.0
8.0	*Pisidium* clams	-1.2	28.4	-3.0
8.2	*Pisidium* clams	0.1	29.4	-2.0
8.4	*Pisidium* clams	-0.4	29.9	-1.6
8.6	*Pisidium* clams	-0.3	27.1	-4.3
8.6	*Pisidium* clams	-0.3	27.4	-4.0
8.8	*Pisidium* clams	-0.3	27.4	-4.0
8.8	*Pisidium* clams	-1.4	28.2	-3.2
9.6	*Pisidium* clams	-1.1	28.4	-3.0
14.4	*Pisidium* clams	0.2	26.5	-4.8

Appendix E - (continued) Oxygen- and carbon-isotope compositions of ostracode valves and clam shells from the Michigan Basin cores

Milwaukee sub-basin - Core 102

sediment depth (m)[a]	species	$\delta^{13}C$ (VPDB)	$\delta^{18}O$ (VSMOW)	$\delta^{18}O_{lakewater}$ (VSMOW)[b]
1.4	*C. subtriangulata*	-3.4	31.3	-4.5
1.6	*C. subtriangulata*	0.2	29.4	-6.3
1.8	*C. subtriangulata*	-4.3	28.8	-6.9
2.0	*C. subtriangulata*	-4.5	28.8	-6.9
2.4	*C. subtriangulata*	-4.4	27.2	-8.4
2.6	*C. subtriangulata*	-4.1	28.8	-6.9
2.6	*C. subtriangulata*	-4.2	29.3	-6.4
2.8	*C. subtriangulata*	-3.5	29.4	-6.3
3.0	*C. subtriangulata*	-3.8	29.2	-6.5
3.0	*C. subtriangulata*	-4.5	28.6	-7.1
3.2	*C. subtriangulata*	-4.3	28.6	-7.0
4.0	*C. subtriangulata*	-3.0	20.2	-15.2
4.0	*C. subtriangulata*	-3.5	20.0	-15.4
4.2	*C. subtriangulata*	-3.5	20.1	-15.2
4.2	*C. subtriangulata*	-3.9	21.5	-13.9
4.4	*C. subtriangulata*	-5.2	19.5	-15.8
4.4	*C. subtriangulata*	-4.9	19.5	-15.8
4.6	*C. subtriangulata*	-4.3	19.8	-15.6
4.6	*C. subtriangulata*	-4.1	19.8	-15.6
4.6	*C. subtriangulata*	-4.6	19.6	-15.7
4.8	*C. subtriangulata*	-4.9	18.3	-17.0
4.8	*C. subtriangulata*	-3.8	18.5	-16.8
5.0	*C. subtriangulata*	-4.2	16.1	-19.1
5.0	*C. subtriangulata*	-5.1	15.7	-19.5
5.4	*C. subtriangulata*	-5.1	20.4	-14.9
5.6	*C. subtriangulata*	-4.8	24.8	-10.7
5.8	*C. subtriangulata*	-5.1	24.4	-11.1
5.8	*C. subtriangulata*	-6.7	19.9	-15.4
6.0	*C. subtriangulata*	-4.5	24.9	-10.6
6.2	*C. subtriangulata*	-3.2	18.0	-17.3
6.2	*C. subtriangulata*	-3.9	17.9	-17.4
6.4	*C. subtriangulata*	-5.4	17.6	-17.6
6.6	*C. subtriangulata*	-3.3	18.4	-16.8
6.8	*C. subtriangulata*	-5.0	18.7	-16.6
6.8	*C. subtriangulata*	-4.2	18.5	-16.8
7.0	*C. subtriangulata*	-3.7	18.4	-16.9
7.0	*C. subtriangulata*	-3.9	18.4	-16.9
7.2	*C. subtriangulata*	-3.2	18.2	-17.1
7.2	*C. subtriangulata*	-3.9	18.1	-17.2
7.4	*C. subtriangulata*	-3.2	17.8	-17.5
7.4	*C. subtriangulata*	-3.8	18.3	-17.0
7.6	*C. subtriangulata*	-4.3	17.8	-17.5
7.6	*C. subtriangulata*	-3.9	17.9	-17.4
7.8	*C. subtriangulata*	-3.8	18.0	-17.2
7.8	*C. subtriangulata*	-4.5	17.8	-17.5
8.0	*C. subtriangulata*	-4.4	17.6	-17.7

Appendix E - (continued) Oxygen- and carbon-isotope compositions of ostracode valves and clam shells from the Michigan Basin cores

Milwaukee sub-basin - Core 102

sediment depth (m)[a]	species	$\delta^{13}C$ (VPDB)	$\delta^{18}O$ (VSMOW)	$\delta^{18}O_{lakewater}$ (VSMOW)[b]
8.0	*C. subtriangulata*	-6.1	17.0	-18.2
8.2	*C. subtriangulata*	-3.7	17.7	-17.6
8.2	*C. subtriangulata*	-4.6	17.9	-17.3
8.4	*C. subtriangulata*	-2.5	18.0	-17.3
8.4	*C. subtriangulata*	-3.6	17.8	-17.4
8.6	*C. subtriangulata*	-3.3	17.5	-17.7
8.6	*C. subtriangulata*	-3.4	17.2	-18.1
8.8	*C. subtriangulata*	-3.2	16.9	-18.3
8.8	*C. subtriangulata*	-4.2	16.9	-18.4
9.0	*C. subtriangulata*	-4.4	16.7	-18.5
9.0	*C. subtriangulata*	-4.3	17.0	-18.2
9.2	*C. subtriangulata*	-3.9	16.9	-18.3
9.2	*C. subtriangulata*	-4.4	16.7	-18.6
9.4	*C. subtriangulata*	-4.1	17.1	-18.2
9.4	*C. subtriangulata*	-4.6	17.0	-18.2
9.6	*C. subtriangulata*	-5.0	16.7	-18.5
9.6	*C. subtriangulata*	-5.1	17.2	-18.0
9.8	*C. subtriangulata*	-4.1	16.6	-18.6
10.0	*C. subtriangulata*	-6.2	15.9	-19.3
10.0	*C. subtriangulata*	-4.0	16.2	-19.0
10.2	*C. subtriangulata*	-4.4	16.2	-19.0
10.2	*C. subtriangulata*	-4.7	16.5	-18.7
10.4	*C. subtriangulata*	-3.0	16.0	-19.2
10.4	*C. subtriangulata*	-4.2	15.8	-19.4
10.6	*C. subtriangulata*	-4.8	15.3	-19.9
10.6	*C. subtriangulata*	-4.5	15.3	-19.8
10.8	*C. subtriangulata*	-4.5	15.4	-19.8
10.8	*C. subtriangulata*	-5.4	14.5	-20.6
11.0	*C. subtriangulata*	-5.0	16.2	-19.0
11.0	*C. subtriangulata*	-4.2	16.0	-19.2
11.2	*C. subtriangulata*	-5.0	17.0	-18.3
11.2	*C. subtriangulata*	-4.8	16.7	-18.6
11.4	*C. subtriangulata*	-6.1	15.5	-19.7
11.4	*C. subtriangulata*	-5.1	15.3	-19.9
11.6	*C. subtriangulata*	-6.0	17.0	-18.3
11.8	*C. subtriangulata*	-4.3	17.2	-18.0
11.8	*C. subtriangulata*	-4.4	17.2	-18.1
12.0	*C. subtriangulata*	-4.8	17.2	-18.0
12.2	*C. subtriangulata*	-4.2	17.6	-17.7
12.2	*C. subtriangulata*	-4.8	17.8	-17.4
12.4	*C. subtriangulata*	-4.8	17.0	-18.3
12.6	*C. subtriangulata*	-6.4	16.0	-19.2
12.8	*C. subtriangulata*	-5.1	16.3	-18.9
13.0	*C. subtriangulata*	-4.6	15.9	-19.3
13.2	*C. subtriangulata*	-4.3	16.0	-19.2
13.4	*C. subtriangulata*	-5.5	16.0	-19.2

Appendix E - (continued) Oxygen- and carbon-isotope compositions of ostracode valves and clam shells from the Michigan Basin cores

Milwaukee sub-basin - Core 102

sediment depth (m)[a]	species	$\delta^{13}C$ (VPDB)	$\delta^{18}O$ (VSMOW)	$\delta^{18}O_{lakewater}$ (VSMOW)[b]
13.4	*C. subtriangulata*	-3.3	15.8	-19.4
13.6	*C. subtriangulata*	-6.3	15.3	-19.9
13.6	*C. subtriangulata*	-6.5	15.6	-19.6
13.8	*C. subtriangulata*	-5.4	15.4	-19.8
14.0	*C. subtriangulata*	-5.2	15.4	-19.8
14.0	*C. subtriangulata*	-6.5	15.6	-19.6
14.2	*C. subtriangulata*	-7.7	14.5	-20.6
14.4	*C. subtriangulata*	-4.9	15.6	-19.6
14.4	*C. subtriangulata*	-5.0	15.6	-19.6
14.4	*C. subtriangulata*	-5.7	15.5	-19.7
1.4	*C. crogmaniana*	-2.3	31.2	-2.6
1.6	*C. crogmaniana*	-2.5	30.3	-3.4
1.8	*C. crogmaniana*	-3.4	29.1	-4.6
2.0	*C. crogmaniana*	-3.0	28.1	-5.5
2.4	*C. crogmaniana*	-5.6	26.0	-7.6
2.6	*C. crogmaniana*	-4.0	28.5	-5.1
2.6	*C. crogmaniana*	-4.0	28.6	-5.1
2.8	*C. crogmaniana*	-6.1	28.9	-4.8
3.0	*C. crogmaniana*	-5.0	28.1	-5.6
3.0	*C. crogmaniana*	-4.6	28.1	-5.5
3.2	*C. crogmaniana*	-4.4	28.3	-5.3
11.6	*C. crogmaniana*	-4.0	28.8	-4.9
1.2	*C. rawsoni*	0.7	30.9	-3.1
1.4	*C. rawsoni*	0.6	31.8	-2.3
1.8	*C. rawsoni*	0.4	28.8	-5.2
2.0	*C. rawsoni*	-0.8	28.9	-5.0
1.6	*C. lacustris*	-0.8	29.6	-2.6
1.8	*C. lacustris*	-1.5	26.8	-5.4
2.0	*C. lacustris*	-0.4	26.9	-5.2
2.4	*C. lacustris*	-1.0	27.0	-5.1
2.6	*C. lacustris*	-1.3	28.7	-3.5
2.6	*C. lacustris*	-1.6	28.7	-3.5
2.8	*C. lacustris*	-1.3	28.8	-3.4
3.0	*C. lacustris*	-1.5	28.3	-3.9
3.0	*C. lacustris*	-0.5	28.3	-3.8
3.2	*C. lacustris*	-2.0	28.4	-3.8
1.6	*Pisidium* clams	0.7	30.9	-0.6
1.6	*Pisidium* clams	-2.5	30.3	-1.2
1.8	*Pisidium* clams	-0.3	27.2	-4.2
2.0	*Pisidium* clams	1.3	28.3	-3.1
2.4	*Pisidium* clams	-0.1	26.5	-4.9
2.4	*Pisidium* clams	0.0	26.9	-4.5

Appendix E - (continued) Oxygen- and carbon-isotope compositions of ostracode valves and clam shells from the Michigan Basin cores

Milwaukee sub-basin - Core 102

sediment depth (m)[a]	species	$\delta^{13}C$ (VPDB)	$\delta^{18}O$ (VSMOW)	$\delta^{18}O_{lakewater}$ (VSMOW)[b]
2.6	*Pisidium* clams	-0.4	28.3	-3.1
2.6	*Pisidium* clams	-0.5	28.4	-3.0
2.8	*Pisidium* clams	-1.1	28.4	-3.0
3.0	*Pisidium* clams	-1.1	27.9	-3.5
3.0	*Pisidium* clams	-0.6	28.2	-3.2
3.2	*Pisidium* clams	-1.7	27.9	-3.5
3.2	*Pisidium* clams	-1.0	28.0	-3.4
4.2	*Pisidium* clams	1.1	31.5	0.0
4.4	*Pisidium* clams	0.8	29.2	-2.2
6.0	*Pisidium* clams	-0.9	28.2	-3.2
6.0	*Pisidium* clams	-0.3	28.1	-3.3

Appendix E - (continued) Oxygen- and carbon-isotope compositions of ostracode valves and clam shells from the Michigan Basin cores

Chippewa sub-basin - Core 100

sediment depth (m)[a]	species	$\delta^{13}C$ (VPDB)	$\delta^{18}O$ (VSMOW)	$\delta^{18}O_{lakewater}$ (VSMOW)[b]
0.0	*C. subtriangulata*	-3.3	29.4	-6.3
0.2	*C. subtriangulata*	-4.6	28.6	-7.1
0.8	*C. subtriangulata*	-3.3	29.8	-5.9
1.0	*C. subtriangulata*	-3.2	30.5	-5.3
1.0	*C. subtriangulata*	-1.7	30.3	-5.4
1.2	*C. subtriangulata*	-2.3	30.4	-5.3
1.2	*C. subtriangulata*	-2.4	30.6	-5.1
1.4	*C. subtriangulata*	-3.0	30.9	-4.8
1.4	*C. subtriangulata*	-2.5	32.7	-3.1
1.4	*C. subtriangulata*	-1.9	31.1	-4.6
1.6	*C. subtriangulata*	-2.1	30.2	-5.5
1.6	*C. subtriangulata*	-2.4	30.2	-5.5
1.8	*C. subtriangulata*	-2.8	30.1	-5.6
1.8	*C. subtriangulata*	-3.3	29.8	-5.9
2.0	*C. subtriangulata*	-3.0	29.2	-6.4
2.0	*C. subtriangulata*	-2.7	28.9	-6.8
2.2	*C. subtriangulata*	-4.7	29.6	-6.1
2.4	*C. subtriangulata*	-4.6	27.8	-7.8
2.6	*C. subtriangulata*	-4.1	27.7	-7.9
2.6	*C. subtriangulata*	-4.4	28.0	-7.6
2.8	*C. subtriangulata*	-4.2	29.1	-6.6
2.8	*C. subtriangulata*	-3.6	29.1	-6.5
3.0	*C. subtriangulata*	-4.5	29.1	-6.5
3.0	*C. subtriangulata*	-4.1	29.3	-6.4
3.2	*C. subtriangulata*	-4.3	29.2	-6.5
3.2	*C. subtriangulata*	-4.6	29.3	-6.4
3.4	*C. subtriangulata*	-4.6	27.9	-7.7
3.4	*C. subtriangulata*	-4.5	27.6	-8.0
3.6	*C. subtriangulata*	-4.8	26.8	-8.8
3.6	*C. subtriangulata*	-4.7	13.5	-21.6
3.8	*C. subtriangulata*	-3.7	18.6	-16.7
3.8	*C. subtriangulata*	-5.0	13.8	-21.3
4.0	*C. subtriangulata*	-4.4	27.7	-7.9
4.0	*C. subtriangulata*	-3.6	25.3	-10.2
4.2	*C. subtriangulata*	-4.4	25.1	-10.4
4.2	*C. subtriangulata*	-3.5	25.3	-10.2
4.4	*C. subtriangulata*	-4.6	18.2	-17.1
4.4	*C. subtriangulata*	-5.3	18.2	-17.1
4.8	*C. subtriangulata*	-4.7	24.1	-11.4
4.8	*C. subtriangulata*	-4.4	14.0	-21.1
4.8	*C. subtriangulata*	-5.6	25.5	-10.1
5.0	*C. subtriangulata*	-4.7	13.9	-21.2
5.0	*C. subtriangulata*	-4.2	23.6	-11.8
5.2	*C. subtriangulata*	-4.9	29.1	-6.6
5.2	*C. subtriangulata*	-4.5	28.8	-6.8
5.4	*C. subtriangulata*	-4.4	23.8	-11.7

Appendix E - (continued) Oxygen- and carbon-isotope compositions of ostracode valves and clam shells from the Michigan Basin cores

Chippewa sub-basin - Core 100

sediment depth (m)[a]	species	$\delta^{13}C$ (VPDB)	$\delta^{18}O$ (VSMOW)	$\delta^{18}O_{lakewater}$ (VSMOW)[b]
5.6	*C. subtriangulata*	-4.7	12.6	-22.5
5.8	*C. subtriangulata*	-4.0	25.0	-10.6
6.2	*C. subtriangulata*	-4.7	26.7	-8.9
6.2	*C. subtriangulata*	-4.6	26.0	-9.6
6.4	*C. subtriangulata*	-3.8	27.4	-8.2
6.6	*C. subtriangulata*	-3.9	29.4	-6.3
6.6	*C. subtriangulata*	-3.2	23.8	-11.7
7.2	*C. subtriangulata*	-5.0	28.8	-6.8
7.2	*C. subtriangulata*	-4.8	27.2	-8.4
7.4	*C. subtriangulata*	-3.9	16.3	-18.9
7.6	*C. subtriangulata*	-3.1	12.8	-22.3
8.0	*C. subtriangulata*	-3.5	26.6	-9.0
8.4	*C. subtriangulata*	-6.6	18.6	-16.7
8.6	*C. subtriangulata*	-6.8	18.6	-16.7
8.8	*C. subtriangulata*	-5.8	20.0	-15.4
8.8	*C. subtriangulata*	-5.8	19.9	-15.4
9.0	*C. subtriangulata*	-4.9	20.5	-14.8
9.2	*C. subtriangulata*	-6.2	21.2	-14.2
9.6	*C. subtriangulata*	-5.9	18.2	-17.1
9.6	*C. subtriangulata*	-5.9	18.7	-16.6
9.8	*C. subtriangulata*	-5.0	21.2	-14.2
10.2	*C. subtriangulata*	-3.4	20.8	-14.6
10.2	*C. subtriangulata*	-3.7	20.7	-14.7
10.4	*C. subtriangulata*	-3.8	23.2	-12.3
10.4	*C. subtriangulata*	-4.8	20.9	-14.5
10.6	*C. subtriangulata*	-5.8	21.2	-14.1
10.6	*C. subtriangulata*	-4.5	21.1	-14.2
10.8	*C. subtriangulata*	-5.4	22.9	-12.6
10.8	*C. subtriangulata*	-4.5	25.3	-10.2
11.0	*C. subtriangulata*	-5.1	20.7	-14.6
11.0	*C. subtriangulata*	-3.7	22.4	-13.0
11.2	*C. subtriangulata*	-5.1	23.4	-12.1
11.2	*C. subtriangulata*	-3.6	26.1	-9.5
11.6	*C. subtriangulata*	-5.5	20.6	-14.8
11.8	*C. subtriangulata*	-4.1	21.4	-14.0
11.8	*C. subtriangulata*	-4.7	21.3	-14.1
12.0	*C. subtriangulata*	-5.7	22.7	-12.7
12.3	*C. subtriangulata*	-5.1	19.9	-15.4
12.3	*C. subtriangulata*	-3.9	21.2	-14.2
12.5	*C. subtriangulata*	-5.9	20.0	-15.3
12.5	*C. subtriangulata*	-4.2	21.0	-14.4
12.7	*C. subtriangulata*	-2.4	20.6	-14.8
12.7	*C. subtriangulata*	-3.8	21.9	-13.5
12.9	*C. subtriangulata*	-3.9	19.2	-16.1
13.1	*C. subtriangulata*	-4.2	19.4	-16.0
13.1	*C. subtriangulata*	-4.1	20.1	-15.2

Appendix E - (continued) Oxygen- and carbon-isotope compositions of ostracode valves and clam shells from the Michigan Basin cores

Chippewa sub-basin - Core 100

sediment depth (m)[a]	species	$\delta^{13}C$ (VPDB)	$\delta^{18}O$ (VSMOW)	$\delta^{18}O_{lakewater}$ (VSMOW)[b]
13.2	*C. subtriangulata*	-5.3	20.8	-14.6
13.2	*C. subtriangulata*	-4.2	20.2	-15.1
13.4	*C. subtriangulata*	-4.9	19.1	-16.2
13.4	*C. subtriangulata*	-2.5	20.0	-15.3
13.6	*C. subtriangulata*	-3.0	19.9	-15.4
13.6	*C. subtriangulata*	-2.3	19.8	-15.5
13.8	*C. subtriangulata*	-5.9	16.3	-18.9
14.0	*C. subtriangulata*	-4.3	24.8	-10.7
14.4	*C. subtriangulata*	-6.3	19.4	-15.9
14.6	*C. subtriangulata*	-3.5	20.6	-14.8
14.6	*C. subtriangulata*	-3.1	20.2	-15.2
15.0	*C. subtriangulata*	-4.0	19.1	-16.2
15.0	*C. subtriangulata*	-4.4	18.5	-16.8
15.8	*C. subtriangulata*	-2.2	20.6	-14.8
15.8	*C. subtriangulata*	-3.5	23.3	-12.1
0.6	*C. crogmaniana*	-4.4	28.7	-5.0
0.8	*C. crogmaniana*	-3.5	29.6	-4.1
1.0	*C. crogmaniana*	-2.1	30.4	-3.3
1.2	*C. crogmaniana*	-2.1	30.8	-2.9
1.2	*C. crogmaniana*	-2.7	30.4	-3.3
1.4	*C. crogmaniana*	-3.1	30.6	-3.1
1.4	*C. crogmaniana*	-2.1	30.6	-3.1
1.4	*C. crogmaniana*	-2.0	30.8	-2.9
1.6	*C. crogmaniana*	-2.3	30.3	-3.4
1.6	*C. crogmaniana*	-2.5	30.3	-3.4
1.8	*C. crogmaniana*	-2.4	30.3	-3.4
1.8	*C. crogmaniana*	-3.0	29.4	-4.2
2.0	*C. crogmaniana*	-4.3	28.2	-5.4
2.0	*C. crogmaniana*	-4.4	29.4	-4.2
2.2	*C. crogmaniana*	-5.1	29.2	-4.5
2.2	*C. crogmaniana*	-4.7	29.9	-3.8
2.6	*C. crogmaniana*	-4.0	27.2	-6.4
2.6	*C. crogmaniana*	-4.5	27.3	-6.3
2.8	*C. crogmaniana*	-4.4	29.2	-4.4
2.8	*C. crogmaniana*	-5.0	28.9	-4.8
3.0	*C. crogmaniana*	-4.0	29.3	-4.4
3.0	*C. crogmaniana*	-5.1	29.1	-4.5
3.2	*C. crogmaniana*	-4.6	29.3	-4.4
6.0	*C. crogmaniana*	-3.2	29.7	-3.9
0.0	*C. rawsoni*	-0.7	30.0	-3.9
0.0	*C. rawsoni*	1.2	30.8	-3.2
0.4	*C. rawsoni*	0.0	30.6	-3.4
0.8	*C. rawsoni*	-0.2	31.3	-2.7
1.0	*C. rawsoni*	1.5	30.9	-3.1

Appendix E - (continued) Oxygen- and carbon-isotope compositions of ostracode valves and clam shells from the Michigan Basin cores

Chippewa sub-basin - Core 100

sediment depth (m)[a]	species	$\delta^{13}C$ (VPDB)	$\delta^{18}O$ (VSMOW)	$\delta^{18}O_{lakewater}$ (VSMOW)[b]
1.0	*C. rawsoni*	1.7	30.9	-3.1
1.2	*C. rawsoni*	1.1	31.1	-2.9
1.2	*C. rawsoni*	0.3	30.9	-3.1
1.4	*C. rawsoni*	-0.3	31.2	-2.8
1.4	*C. rawsoni*	0.5	31.7	-2.3
1.4	*C. rawsoni*	0.3	31.5	-2.5
1.6	*C. rawsoni*	0.2	31.1	-2.9
1.6	*C. rawsoni*	0.4	31.0	-3.0
1.8	*C. rawsoni*	0.0	30.1	-3.8
1.8	*C. rawsoni*	-0.2	30.0	-4.0
2.0	*C. rawsoni*	0.2	29.9	-4.1
2.0	*C. rawsoni*	0.1	29.4	-4.5
2.2	*C. rawsoni*	-0.1	30.0	-4.0
2.2	*C. rawsoni*	0.0	27.6	-6.3
6.6	*C. rawsoni*	0.5	30.5	-3.5
1.6	*C. lacustris*	-1.7	28.9	-3.3
1.8	*C. lacustris*	0.6	29.3	-2.9
2.6	*C. lacustris*	-1.8	27.5	-4.6
2.8	*C. lacustris*	-2.3	28.7	-3.5
2.8	*C. lacustris*	-2.5	28.8	-3.4
3.0	*C. lacustris*	-2.3	28.5	-3.7
3.0	*C. lacustris*	-2.5	28.5	-3.7
3.2	*C. lacustris*	-2.1	28.2	-4.0
3.2	*C. lacustris*	-1.4	28.5	-3.7
3.4	*C. lacustris*	-3.0	26.9	-5.2
3.4	*C. lacustris*	-2.1	27.5	-4.6
0.0	*Pisidium* clams	-0.5	28.6	-2.8
0.0	*Pisidium* clams	-0.7	28.5	-2.9
0.2	*Pisidium* clams	-0.9	28.0	-3.4
0.8	*Pisidium* clams	-0.1	29.1	-2.4
1.4	*Pisidium* clams	1.1	29.9	-1.6
1.4	*Pisidium* clams	1.0	32.9	1.4
1.6	*Pisidium* clams	0.0	29.3	-2.1
1.6	*Pisidium* clams	0.3	29.3	-2.1
1.8	*Pisidium* clams	0.7	29.2	-2.3
1.8	*Pisidium* clams	-0.4	28.4	-3.0
2.0	*Pisidium* clams	0.0	29.5	-2.0
2.0	*Pisidium* clams	-0.7	28.5	-2.9
2.6	*Pisidium* clams	-1.3	27.0	-4.4
2.6	*Pisidium* clams	-0.6	27.2	-4.1
2.8	*Pisidium* clams	-1.1	28.3	-3.1
2.8	*Pisidium* clams	-0.8	28.4	-3.0
3.0	*Pisidium* clams	-2.3	28.2	-3.2
3.0	*Pisidium* clams	-1.7	27.7	-3.7

Appendix E - (continued) Oxygen- and carbon-isotope compositions of ostracode valves and clam shells from the Michigan Basin cores

Chippewa sub-basin - Core 100

sediment depth (m)[a]	species	$\delta^{13}C$ (VPDB)	$\delta^{18}O$ (VSMOW)	$\delta^{18}O_{lakewater}$ (VSMOW)[b]
3.2	*Pisidium* clams	-2.0	28.2	-3.2
3.2	*Pisidium* clams	-1.4	28.5	-2.9
3.4	*Pisidium* clams	-1.8	27.0	-4.4
3.4	*Pisidium* clams	-2.6	27.3	-4.0
3.8	*Pisidium* clams	-0.8	28.4	-3.0
3.8	*Pisidium* clams	0.0	26.6	-4.7
3.8	*Pisidium* clams	-1.3	27.7	-3.7
4.2	*Pisidium* clams	0.0	29.0	-2.4
4.2	*Pisidium* clams	-0.7	28.4	-3.0
5.0	*Pisidium* clams	-1.6	28.2	-3.2
5.4	*Pisidium* clams	-1.5	28.0	-3.4
5.4	*Pisidium* clams	0.6	28.9	-2.5
5.8	*Pisidium* clams	-1.6	27.9	-3.5
8.0	*Pisidium* clams	-0.5	27.9	-3.5
10.8	*Pisidium* clams	-0.3	28.5	-2.9
11.0	*Pisidium* clams	0.6	28.6	-2.8
11.4	*Pisidium* clams	-1.3	28.6	-2.8
11.8	*Pisidium* clams	0.2	29.0	-2.4

[a] Top of 10-cm sediment interval

[b] as calculated using measured fractionation factors for each species, see text

Appendix F - Oxygen- and carbon-isotope compositions of ostracode valves and clam shells from the Huron Basin cores

Goderich sub-basin - Core 594

sediment depth (m)[a]	species	δ^{13}C (VPDB)	δ^{18}O (VSMOW)	$\delta^{18}O_{lakewater}$ (VSMOW)[b]
3.4	*C. subtriangulata*	-1.6	29.7	-6.0
3.8	*C. subtriangulata*	-1.9	29.6	-6.1
3.8	*C. subtriangulata*	-2.3	29.6	-6.1
4.0	*C. subtriangulata*	-4.5	28.2	-7.4
4.0	*C. subtriangulata*	-1.8	29.4	-6.2
4.2	*C. subtriangulata*	-2.0	29.2	-6.4
4.2	*C. subtriangulata*	-2.7	29.3	-6.3
4.4	*C. subtriangulata*	-3.5	28.2	-7.5
4.4	*C. subtriangulata*	-2.8	28.7	-7.0
4.6	*C. subtriangulata*	-3.6	28.6	-7.0
4.6	*C. subtriangulata*	-4.1	27.9	-7.8
4.8	*C. subtriangulata*	-2.5	28.1	-7.6
4.8	*C. subtriangulata*	-4.1	28.0	-7.7
5.0	*C. subtriangulata*	-3.2	27.7	-8.0
5.2	*C. subtriangulata*	-2.2	28.0	-7.7
5.2	*C. subtriangulata*	-2.2	27.3	-8.3
5.2	*C. subtriangulata*	-2.5	27.2	-8.4
5.4	*C. subtriangulata*	-3.2	26.8	-8.8
5.4	*C. subtriangulata*	-3.0	26.4	-9.2
5.6	*C. subtriangulata*	-2.3	23.4	-12.1
5.6	*C. subtriangulata*	-2.9	25.7	-9.8
6.2	*C. subtriangulata*	-3.4	19.1	-16.2
7.0	*C. subtriangulata*	-5.4	17.9	-17.3
8.2	*C. subtriangulata*	-6.0	22.1	-13.3
8.2	*C. subtriangulata*	-5.1	23.5	-12.0
8.2	*C. subtriangulata*	-4.7	23.0	-12.4
8.4	*C. subtriangulata*	-5.3	25.0	-10.6
8.4	*C. subtriangulata*	-6.2	24.4	-11.1
8.4	*C. subtriangulata*	-6.5	24.5	-11.0
8.4	*C. subtriangulata*	-5.8	24.3	-11.2
8.6	*C. subtriangulata*	-6.3	27.6	-8.0
8.6	*C. subtriangulata*	-6.1	25.8	-9.8
8.6	*C. subtriangulata*	-6.0	26.4	-9.2
8.8	*C. subtriangulata*	-5.9	27.4	-8.2
8.8	*C. subtriangulata*	-6.9	27.7	-7.9
8.8	*C. subtriangulata*	-6.6	27.5	-8.1
9.0	*C. subtriangulata*	-6.4	27.7	-8.0
9.0	*C. subtriangulata*	-6.8	27.8	-7.9
9.0	*C. subtriangulata*	-6.5	26.9	-8.7
9.2	*C. subtriangulata*	-7.6	25.4	-10.2
9.2	*C. subtriangulata*	-6.5	27.0	-8.6
9.2	*C. subtriangulata*	-7.3	27.1	-8.5
9.4	*C. subtriangulata*	-6.2	27.3	-8.3
9.4	*C. subtriangulata*	-5.9	26.7	-8.9
9.4	*C. subtriangulata*	-5.7	27.4	-8.2
9.6	*C. subtriangulata*	-7.5	27.0	-8.6

Appendix F - (continued) Oxygen- and carbon-isotope compositions of ostracode valves and clam shells from the Huron Basin cores

Goderich sub-basin - Core 594

sediment depth (m)[a]	species	$\delta^{13}C$ (VPDB)	$\delta^{18}O$ (VSMOW)	$\delta^{18}O_{lakewater}$ (VSMOW)[b]
9.6	*C. subtriangulata*	-6.5	26.0	-9.6
9.8	*C. subtriangulata*	-6.7	25.6	-9.9
9.8	*C. subtriangulata*	-6.7	26.3	-9.3
10.2	*C. subtriangulata*	-5.4	24.5	-11.0
10.4	*C. subtriangulata*	-5.3	19.8	-15.5
10.4	*C. subtriangulata*	-5.5	19.5	-15.8
10.6	*C. subtriangulata*	-4.8	17.1	-18.1
10.6	*C. subtriangulata*	-5.6	17.0	-18.3
10.8	*C. subtriangulata*	-4.9	15.9	-19.3
10.8	*C. subtriangulata*	-5.8	16.6	-18.7
11.0	*C. subtriangulata*	-4.1	16.9	-18.3
11.0	*C. subtriangulata*	-5.7	16.5	-18.7
11.0	*C. subtriangulata*	-5.6	16.7	-18.5
11.2	*C. subtriangulata*	-4.6	17.2	-18.1
11.2	*C. subtriangulata*	-5.3	16.5	-18.7
11.4	*C. subtriangulata*	-4.0	18.1	-17.2
11.4	*C. subtriangulata*	-5.4	17.9	-17.4
11.6	*C. subtriangulata*	-5.1	17.0	-18.2
11.6	*C. subtriangulata*	-5.4	17.0	-18.3
11.8	*C. subtriangulata*	-4.7	16.9	-18.3
11.8	*C. subtriangulata*	-4.0	17.0	-18.3
12.0	*C. subtriangulata*	-4.3	17.2	-18.1
12.0	*C. subtriangulata*	-5.2	16.3	-18.9
12.0	*C. subtriangulata*	-4.5	17.7	-17.6
12.2	*C. subtriangulata*	-5.2	16.5	-18.7
12.2	*C. subtriangulata*	-4.6	16.9	-18.4
12.2	*C. subtriangulata*	-4.6	16.7	-18.5
12.2	*C. subtriangulata*	-4.5	17.7	-17.5
12.4	*C. subtriangulata*	-5.1	16.6	-18.7
12.4	*C. subtriangulata*	-5.0	18.1	-17.2
12.4	*C. subtriangulata*	-4.7	17.6	-17.6
12.4	*C. subtriangulata*	-4.9	18.4	-16.9
12.6	*C. subtriangulata*	-5.3	18.9	-16.4
12.6	*C. subtriangulata*	-4.9	19.5	-15.8
12.8	*C. subtriangulata*	-5.0	27.0	-8.6
12.8	*C. subtriangulata*	-6.1	24.3	-11.2
12.8	*C. subtriangulata*	-4.7	25.6	-10.0
13.0	*C. subtriangulata*	-5.9	25.6	-9.9
13.4	*C. subtriangulata*	-6.6	23.2	-12.2
13.4	*C. subtriangulata*	-7.4	25.9	-9.7
13.6	*C. subtriangulata*	-7.0	26.9	-8.7
13.6	*C. subtriangulata*	-7.2	26.4	-9.1
13.6	*C. subtriangulata*	-6.6	27.1	-8.5
13.8	*C. subtriangulata*	-6.1	24.4	-11.1
13.8	*C. subtriangulata*	-6.2	25.6	-9.9
14.0	*C. subtriangulata*	-6.3	27.8	-7.8

Appendix F - (continued) Oxygen- and carbon-isotope compositions of ostracode valves and clam shells from the Huron Basin cores

Goderich sub-basin - Core 594

sediment depth (m)[a]	species	$\delta^{13}C$ (VPDB)	$\delta^{18}O$ (VSMOW)	$\delta^{18}O_{lakewater}$ (VSMOW)[b]
14.0	*C. subtriangulata*	-6.7	26.7	-8.9
14.0	*C. subtriangulata*	-6.2	27.2	-8.4
14.2	*C. subtriangulata*	-6.2	27.4	-8.2
14.2	*C. subtriangulata*	-6.4	27.3	-8.3
14.4	*C. subtriangulata*	-5.3	26.7	-8.9
14.4	*C. subtriangulata*	-6.9	26.8	-8.8
14.4	*C. subtriangulata*	-6.6	27.8	-7.8
14.6	*C. subtriangulata*	-6.3	27.4	-8.2
14.6	*C. subtriangulata*	-6.3	27.6	-8.0
14.6	*C. subtriangulata*	-6.3	28.0	-7.7
14.8	*C. subtriangulata*	-5.9	26.5	-9.1
14.8	*C. subtriangulata*	-6.7	26.4	-9.2
14.8	*C. subtriangulata*	-5.6	26.8	-8.8
3.8	*C. crogmaniana*	-2.3	29.5	-4.2
3.8	*C. crogmaniana*	-2.7	29.5	-4.1
4.0	*C. crogmaniana*	-2.1	29.2	-4.5
4.0	*C. crogmaniana*	-2.1	29.8	-3.9
4.2	*C. crogmaniana*	-1.5	29.5	-4.1
4.2	*C. crogmaniana*	-1.5	29.1	-4.6
4.2	*C. crogmaniana*	-2.2	29.7	-3.9
4.4	*C. crogmaniana*	-2.2	28.6	-5.1
4.4	*C. crogmaniana*	-1.5	28.9	-4.7
4.6	*C. crogmaniana*	-3.3	27.8	-5.8
4.6	*C. crogmaniana*	-3.0	28.8	-4.8
4.8	*C. crogmaniana*	-3.4	26.6	-7.0
4.8	*C. crogmaniana*	-2.7	28.2	-5.4
5.0	*C. crogmaniana*	-2.4	28.3	-5.3
5.2	*C. crogmaniana*	-2.7	27.6	-6.0
5.2	*C. crogmaniana*	-3.1	27.7	-5.9
5.4	*C. crogmaniana*	-2.6	26.4	-7.1
5.4	*C. crogmaniana*	-3.1	27.0	-6.6
5.6	*C. crogmaniana*	-2.3	26.9	-6.7
5.6	*C. crogmaniana*	-3.4	26.3	-7.3
8.2	*C. crogmaniana*	-5.4	22.6	-10.9
8.4	*C. crogmaniana*	-6.4	24.5	-9.0
8.4	*C. crogmaniana*	-5.9	23.8	-9.7
8.6	*C. crogmaniana*	-6.6	24.3	-9.2
8.6	*C. crogmaniana*	-9.4	24.7	-8.8
8.6	*C. crogmaniana*	-7.2	24.9	-8.6
9.0	*C. crogmaniana*	-6.0	27.1	-6.5
9.0	*C. crogmaniana*	-4.8	26.3	-7.3
9.2	*C. crogmaniana*	-7.3	24.9	-8.7
9.6	*C. crogmaniana*	-7.1	27.7	-5.9
9.6	*C. crogmaniana*	-6.8	26.7	-6.9
9.8	*C. crogmaniana*	-6.6	27.0	-6.6

Appendix F - (continued) Oxygen- and carbon-isotope compositions of ostracode valves and clam shells from the Huron Basin cores

Goderich sub-basin - Core 594

sediment depth (m)[a]	species	$\delta^{13}C$ (VPDB)	$\delta^{18}O$ (VSMOW)	$\delta^{18}O_{lakewater}$ (VSMOW)[b]
9.8	*C. crogmaniana*	-7.3	26.3	-7.3
13.4	*C. crogmaniana*	-7.6	26.2	-7.4
13.4	*C. crogmaniana*	-7.8	25.4	-8.1
13.6	*C. crogmaniana*	-8.5	26.7	-6.9
13.6	*C. crogmaniana*	-7.8	27.2	-6.4
13.6	*C. crogmaniana*	-8.7	26.3	-7.3
13.8	*C. crogmaniana*	-7.0	26.3	-7.3
13.8	*C. crogmaniana*	-7.3	25.2	-8.3
14.0	*C. crogmaniana*	-7.4	25.8	-7.8
14.0	*C. crogmaniana*	-6.7	26.1	-7.5
14.0	*C. crogmaniana*	-7.9	25.7	-7.9
14.2	*C. crogmaniana*	-5.9	26.3	-7.3
14.4	*C. crogmaniana*	-5.9	26.8	-6.8
14.4	*C. crogmaniana*	-7.5	27.0	-6.6
14.8	*C. crogmaniana*	-6.1	23.9	-9.6
8.2	*C. rawsoni*	-3.7	22.3	-11.4
8.4	*C. rawsoni*	-4.5	23.1	-10.6
8.4	*C. rawsoni*	-4.7	23.4	-10.3
8.6	*C. rawsoni*	-5.7	25.7	-8.1
8.6	*C. rawsoni*	-5.3	26.2	-7.6
8.6	*C. rawsoni*	-5.5	24.6	-9.2
9.6	*C. rawsoni*	-6.6	26.3	-7.6
9.6	*C. rawsoni*	-5.4	26.6	-7.2
9.8	*C. rawsoni*	-5.4	25.6	-8.2
9.8	*C. rawsoni*	-4.8	25.0	-8.8
9.8	*C. rawsoni*	-6.0	25.6	-8.2
12.4	*C. rawsoni*	-5.8	23.7	-10.0
13.2	*C. rawsoni*	-3.8	25.1	-8.7
13.4	*C. rawsoni*	-8.1	26.9	-6.9
13.4	*C. rawsoni*	-5.4	25.0	-8.8
13.4	*C. rawsoni*	-6.1	25.5	-8.3
14.8	*C. rawsoni*	-4.3	25.0	-8.8
14.8	*C. rawsoni*	-4.5	25.4	-8.4
14.8	*C. rawsoni*	-4.7	24.5	-9.3
3.6	*C. lacustris*	-2.9	28.9	-3.3
3.6	*C. lacustris*	-1.8	29.2	-3.0
4.4	*C. lacustris*	-1.2	27.4	-4.7
4.6	*C. lacustris*	-3.0	28.8	-3.4
4.6	*C. lacustris*	-4.1	27.7	-4.4
4.6	*C. lacustris*	-3.0	28.3	-3.9
4.8	*C. lacustris*	-2.5	27.2	-4.9
5.4	*C. lacustris*	-4.3	25.6	-6.5
5.6	*C. lacustris*	-2.6	26.0	-6.1
8.4	*C. lacustris*	-3.6	22.9	-9.1

Appendix F - (continued) Oxygen- and carbon-isotope compositions of ostracode valves and clam shells from the Huron Basin cores

Goderich sub-basin - Core 594

sediment depth (m)[a]	species	$\delta^{13}C$ (VPDB)	$\delta^{18}O$ (VSMOW)	$\delta^{18}O_{lakewater}$ (VSMOW)[b]
8.4	*C. lacustris*	-4.0	22.7	-9.3
8.6	*C. lacustris*	-5.0	25.5	-6.5
8.6	*C. lacustris*	-3.7	24.1	-8.0
8.8	*C. lacustris*	-3.7	25.7	-6.4
8.8	*C. lacustris*	-3.2	25.6	-6.5
9.0	*C. lacustris*	-3.0	25.4	-6.7
9.0	*C. lacustris*	-3.8	25.8	-6.3
9.2	*C. lacustris*	-3.8	26.3	-5.8
9.2	*C. lacustris*	-3.8	27.4	-4.7
9.4	*C. lacustris*	-4.3	26.3	-5.8
9.4	*C. lacustris*	-4.7	24.6	-7.4
9.6	*C. lacustris*	-2.1	25.5	-6.6
9.6	*C. lacustris*	-4.2	25.7	-6.4
9.8	*C. lacustris*	-3.7	25.6	-6.5
9.8	*C. lacustris*	-4.0	24.9	-7.1
10.0	*C. lacustris*	-4.4	24.9	-7.2
10.0	*C. lacustris*	-4.3	25.0	-7.0
10.2	*C. lacustris*	-4.1	25.3	-6.7
10.2	*C. lacustris*	-3.9	25.1	-7.0
10.2	*C. lacustris*	-4.3	25.4	-6.7
12.8	*C. lacustris*	-4.7	24.6	-7.4
13.0	*C. lacustris*	-5.4	24.2	-7.9
13.0	*C. lacustris*	-4.0	25.6	-6.5
13.0	*C. lacustris*	-4.1	26.1	-6.0
13.2	*C. lacustris*	-4.1	25.7	-6.4
13.2	*C. lacustris*	-4.3	25.7	-6.4
13.4	*C. lacustris*	-4.7	25.8	-6.3
13.4	*C. lacustris*	-3.8	24.7	-7.3
13.6	*C. lacustris*	-3.6	25.1	-7.0
13.6	*C. lacustris*	-4.1	26.6	-5.5
13.8	*C. lacustris*	-4.6	25.0	-7.1
13.8	*C. lacustris*	-4.0	25.3	-6.7
14.0	*C. lacustris*	-4.2	26.2	-5.9
14.0	*C. lacustris*	-3.6	26.7	-5.5
14.0	*C. lacustris*	-3.6	27.2	-5.0
14.2	*C. lacustris*	-4.1	25.9	-6.2
14.2	*C. lacustris*	-3.1	25.5	-6.6
14.2	*C. lacustris*	-2.6	25.8	-6.3
14.4	*C. lacustris*	-3.3	25.7	-6.4
14.4	*C. lacustris*	-4.0	25.1	-6.9
14.4	*C. lacustris*	-3.3	25.1	-7.0
14.6	*C. lacustris*	-3.5	25.8	-6.3
14.6	*C. lacustris*	-3.6	25.8	-6.3
14.8	*C. lacustris*	-2.3	23.5	-8.5
14.8	*C. lacustris*	-4.4	25.2	-6.9
14.8	*C. lacustris*	-4.0	24.9	-7.1

Appendix F - (continued) Oxygen- and carbon-isotope compositions of ostracode valves and clam shells from the Huron Basin cores

Goderich sub-basin - Core 594

sediment depth (m)[a]	species	$\delta^{13}C$ (VPDB)	$\delta^{18}O$ (VSMOW)	$\delta^{18}O_{lakewater}$ (VSMOW)[b]
8.2	*Pisidium* clams	-3.9	21.1	-10.1
8.2	*Pisidium* clams	-2.9	20.9	-10.2
8.2	*Pisidium* clams	-3.6	21.0	-10.2
8.4	*Pisidium* clams	-4.1	22.5	-8.8
8.4	*Pisidium* clams	-4.2	22.4	-8.8
8.6	*Pisidium* clams	-4.6	23.0	-8.2
8.6	*Pisidium* clams	-4.0	23.7	-7.6
8.8	*Pisidium* clams	-4.4	25.7	-5.7
8.8	*Pisidium* clams	-4.1	25.7	-5.6
9.0	*Pisidium* clams	-4.9	25.3	-6.1
9.0	*Pisidium* clams	-6.2	25.2	-6.2
9.2	*Pisidium* clams	-5.4	25.3	-6.0
9.2	*Pisidium* clams	-6.4	25.1	-6.2
9.4	*Pisidium* clams	-5.8	24.4	-6.9
9.4	*Pisidium* clams	-5.8	24.5	-6.8
9.6	*Pisidium* clams	-5.7	24.6	-6.7
9.6	*Pisidium* clams	-5.6	24.5	-6.8
9.8	*Pisidium* clams	-4.7	24.7	-6.6
9.8	*Pisidium* clams	-4.4	24.9	-6.4
10.0	*Pisidium* clams	-5.1	24.3	-7.0
10.0	*Pisidium* clams	-5.2	24.1	-7.2
10.2	*Pisidium* clams	-7.4	22.9	-8.4
10.2	*Pisidium* clams	-6.7	24.3	-7.0
12.8	*Pisidium* clams	-7.5	23.1	-8.2
12.8	*Pisidium* clams	-6.2	22.6	-8.6
13.0	*Pisidium* clams	-6.7	24.0	-7.3
13.0	*Pisidium* clams	-7.0	24.0	-7.2
13.2	*Pisidium* clams	-6.2	24.7	-6.6
13.2	*Pisidium* clams	-6.2	24.7	-6.6
13.4	*Pisidium* clams	-7.1	24.0	-7.3
13.4	*Pisidium* clams	-5.6	24.8	-6.5
13.6	*Pisidium* clams	-5.4	24.7	-6.6
13.6	*Pisidium* clams	-5.6	24.7	-6.6
13.8	*Pisidium* clams	-5.2	25.5	-5.9
13.8	*Pisidium* clams	-5.6	25.0	-6.3
14.0	*Pisidium* clams	-5.2	24.8	-6.5
14.0	*Pisidium* clams	-6.0	24.6	-6.7
14.2	*Pisidium* clams	-5.3	25.6	-5.7
14.2	*Pisidium* clams	-5.5	25.4	-5.9
14.2	*Pisidium* clams	-5.6	25.6	-5.7
14.4	*Pisidium* clams	-4.5	27.4	-4.0
14.4	*Pisidium* clams	-5.3	25.7	-5.7
14.4	*Pisidium* clams	-6.3	24.9	-6.4
14.4	*Pisidium* clams	-6.6	25.4	-5.9
14.6	*Pisidium* clams	-4.7	25.4	-5.9
14.6	*Pisidium* clams	-5.2	25.8	-5.6

Appendix F - (continued) Oxygen- and carbon-isotope compositions of ostracode valves and clam shells from the Huron Basin cores

Goderich sub-basin - Core 594

sediment depth (m)[a]	species	$\delta^{13}C$ (VPDB)	$\delta^{18}O$ (VSMOW)	$\delta^{18}O_{lakewater}$ (VSMOW)[b]
14.8	*Pisidium* clams	-4.7	23.3	-7.9
14.8	*Pisidium* clams	-4.9	24.8	-6.5
14.8	*Pisidium* clams	-4.7	23.4	-7.8

Appendix F - (continued) Oxygen- and carbon-isotope compositions of ostracode valves and clam shells from the Huron Basin cores

Goderich sub-basin - Core 146

sediment depth (m)[a]	species	$\delta^{13}C$ (VPDB)	$\delta^{18}O$ (VSMOW)	$\delta^{18}O_{lakewater}$ (VSMOW)[b]
3.00	*C. subtriangulata*	-2.7	29.9	-5.8
3.40	*C. subtriangulata*	-4.0	28.0	-7.6
3.60	*C. subtriangulata*	-2.8	29.0	-6.7
3.60	*C. subtriangulata*	-2.8	29.4	-6.3
4.40	*C. subtriangulata*	-5.8	15.9	-19.3
4.60	*C. subtriangulata*	-6.5	23.1	-12.4
4.60	*C. subtriangulata*	-6.3	24.0	-11.5
4.80	*C. subtriangulata*	-7.6	26.4	-9.2
4.80	*C. subtriangulata*	-7.1	26.5	-9.1
5.00	*C. subtriangulata*	-6.2	26.4	-9.2
5.00	*C. subtriangulata*	-7.5	26.1	-9.4
5.20	*C. subtriangulata*	-5.8	22.7	-12.8
5.20	*C. subtriangulata*	-5.3	21.3	-14.1
5.40	*C. subtriangulata*	-4.0	17.4	-17.8
5.40	*C. subtriangulata*	-4.7	17.2	-18.1
5.60	*C. subtriangulata*	-5.4	17.6	-17.6
5.60	*C. subtriangulata*	-5.1	17.3	-17.9
5.80	*C. subtriangulata*	-5.2	16.4	-18.8
5.80	*C. subtriangulata*	-5.0	17.1	-18.2
6.00	*C. subtriangulata*	-6.7	15.9	-19.3
6.00	*C. subtriangulata*	-4.6	16.9	-18.3
6.17	*C. subtriangulata*	-5.2	17.4	-17.8
6.17	*C. subtriangulata*	-4.9	17.0	-18.2
6.37	*C. subtriangulata*	-4.3	16.8	-18.4
6.37	*C. subtriangulata*	-5.5	17.3	-18.0
6.57	*C. subtriangulata*	-4.2	15.7	-19.5
6.57	*C. subtriangulata*	-4.1	15.9	-19.3
6.77	*C. subtriangulata*	-5.0	14.2	-20.9
6.77	*C. subtriangulata*	-4.7	14.7	-20.5
6.97	*C. subtriangulata*	-6.3	22.7	-12.7
6.97	*C. subtriangulata*	-6.6	24.2	-11.3
7.17	*C. subtriangulata*	-6.0	26.1	-9.4
7.37	*C. subtriangulata*	-7.5	24.1	-11.4
7.57	*C. subtriangulata*	-5.7	19.7	-15.7
7.57	*C. subtriangulata*	-6.4	23.1	-12.4
7.97	*C. subtriangulata*	-5.8	19.9	-15.4
8.37	*C. subtriangulata*	-5.9	20.0	-15.3
8.37	*C. subtriangulata*	-4.0	17.1	-18.1
8.77	*C. subtriangulata*	-4.4	17.4	-17.9
8.77	*C. subtriangulata*	-3.4	17.0	-18.3
8.97	*C. subtriangulata*	-4.2	16.0	-19.2
8.97	*C. subtriangulata*	-3.7	16.8	-18.5
9.17	*C. subtriangulata*	-3.3	16.6	-18.6
9.17	*C. subtriangulata*	-3.5	16.7	-18.5
9.37	*C. subtriangulata*	-3.7	16.9	-18.4
9.37	*C. subtriangulata*	-2.7	16.7	-18.5

Appendix F - (continued) Oxygen- and carbon-isotope compositions of ostracode valves and clam shells from the Huron Basin cores

Goderich sub-basin - Core 146

sediment depth (m)[a]	species	$\delta^{13}C$ (VPDB)	$\delta^{18}O$ (VSMOW)	$\delta^{18}O_{lakewater}$ (VSMOW)[b]
9.57	*C. subtriangulata*	-3.4	16.4	-18.8
9.57	*C. subtriangulata*	-3.7	17.0	-18.2
9.77	*C. subtriangulata*	-3.9	16.2	-19.0
9.77	*C. subtriangulata*	-3.9	16.2	-19.0
9.97	*C. subtriangulata*	-5.0	16.9	-18.4
9.97	*C. subtriangulata*	-4.7	16.2	-19.0
10.17	*C. subtriangulata*	-5.3	16.3	-18.9
10.17	*C. subtriangulata*	-3.8	16.5	-18.8
10.37	*C. subtriangulata*	-3.1	18.1	-17.2
10.37	*C. subtriangulata*	-3.3	17.4	-17.9
10.57	*C. subtriangulata*	-3.6	17.4	-17.9
10.57	*C. subtriangulata*	-2.8	18.0	-17.3
10.77	*C. subtriangulata*	-3.6	16.8	-18.5
10.77	*C. subtriangulata*	-3.8	16.6	-18.6
10.97	*C. subtriangulata*	-4.2	16.8	-18.4
10.97	*C. subtriangulata*	-3.6	16.8	-18.4
11.17	*C. subtriangulata*	-3.4	16.0	-19.3
11.17	*C. subtriangulata*	-4.1	17.1	-18.1
11.37	*C. subtriangulata*	-3.6	17.1	-18.2
11.37	*C. subtriangulata*	-2.8	17.1	-18.1
11.57	*C. subtriangulata*	-3.5	16.9	-18.4
11.57	*C. subtriangulata*	-3.7	16.8	-18.4
11.77	*C. subtriangulata*	-3.1	17.0	-18.3
11.77	*C. subtriangulata*	-2.9	16.8	-18.4
3.60	*C. crogmaniana*	-3.1	29.0	-4.6
3.60	*C. crogmaniana*	-3.8	29.6	-4.1
4.40	*C. crogmaniana*	-6.8	22.0	-11.4
4.60	*C. crogmaniana*	-4.9	23.1	-10.4
4.60	*C. crogmaniana*	-7.3	21.8	-11.7
4.80	*C. crogmaniana*	-7.5	26.3	-7.2
4.80	*C. crogmaniana*	-7.1	25.7	-7.8
5.00	*C. crogmaniana*	-6.8	26.1	-7.4
5.00	*C. crogmaniana*	-7.3	25.2	-8.3
7.17	*C. crogmaniana*	-6.8	25.6	-7.9
7.37	*C. crogmaniana*	-6.8	23.6	-9.8
4.6	*C. rawsoni*	-5.0	23.9	-9.9
4.6	*C. rawsoni*	-4.7	24.3	-9.5
4.8	*C. rawsoni*	-5.9	26.4	-7.4
4.8	*C. rawsoni*	-5.4	27.1	-6.8
5.0	*C. rawsoni*	-6.6	26.6	-7.3
5.0	*C. rawsoni*	-6.7	26.0	-7.8
5.2	*C. rawsoni*	-4.1	25.2	-8.6
5.2	*C. rawsoni*	-4.8	25.9	-7.9
8.57	*C. rawsoni*	-3.6	23.9	-9.9

Appendix F - (continued) Oxygen- and carbon-isotope compositions of ostracode valves and clam shells from the Huron Basin cores

Goderich sub-basin - Core 146

sediment depth (m)[a]	species	$\delta^{13}C$ (VPDB)	$\delta^{18}O$ (VSMOW)	$\delta^{18}O_{lakewater}$ (VSMOW)[b]
4.6	*C. lacustris*	-4.5	22.9	-9.1
4.6	*C. lacustris*	-3.5	23.0	-9.0
4.8	*C. lacustris*	-4.5	25.9	-6.2
4.8	*C. lacustris*	-3.9	25.8	-6.3
5.0	*C. lacustris*	-4.6	26.0	-6.2
5.0	*C. lacustris*	-4.2	25.5	-6.6
5.2	*C. lacustris*	-3.9	24.7	-7.4
5.2	*C. lacustris*	-4.0	25.6	-6.5
7.77	*C. lacustris*	-4.9	24.8	-7.2
8.37	*C. lacustris*	-4.3	25.6	-6.5
8.77	*C. lacustris*	-5.1	25.4	-6.7
4.40	*Pisidium* clams	-3.5	21.0	-10.2
4.40	*Pisidium* clams	-3.7	21.1	-10.1
4.60	*Pisidium* clams	-4.4	23.1	-8.1
4.60	*Pisidium* clams	-4.6	22.3	-9.0
4.80	*Pisidium* clams	-4.7	25.6	-5.7
4.80	*Pisidium* clams	-4.2	25.8	-5.5
5.00	*Pisidium* clams	-5.2	26.0	-5.3
5.00	*Pisidium* clams	-4.6	26.1	-5.3
5.20	*Pisidium* clams	-5.1	23.9	-7.3
5.20	*Pisidium* clams	-5.3	23.9	-7.3
5.80	*Pisidium* clams	-3.9	26.1	-5.3
6.17	*Pisidium* clams	-4.9	25.4	-6.0
6.57	*Pisidium* clams	-4.5	25.3	-6.0
7.57	*Pisidium* clams	-4.9	24.3	-7.0
7.97	*Pisidium* clams	-5.2	23.6	-7.7
8.77	*Pisidium* clams	-6.0	25.4	-5.9

Appendix F - (continued) Oxygen- and carbon-isotope compositions of ostracode valves and clam shells from the Huron Basin cores

Manitoulin sub-basin - Core 596

sediment depth (m)[a]	species	$\delta^{13}C$ (VPDB)	$\delta^{18}O$ (VSMOW)	$\delta^{18}O_{lakewater}$ (VSMOW)[b]
0.2	*C. subtriangulata*	-4.9	17.0	-18.3
0.4	*C. subtriangulata*	-3.9	18.7	-16.7
0.4	*C. subtriangulata*	-5.3	16.1	-19.1
0.6	*C. subtriangulata*	-4.8	16.7	-18.5
0.6	*C. subtriangulata*	-5.0	16.7	-18.5
0.8	*C. subtriangulata*	-5.0	16.4	-18.8
1.0	*C. subtriangulata*	-5.3	16.7	-18.5
1.0	*C. subtriangulata*	-4.8	16.3	-18.9
1.0	*C. subtriangulata*	-6.7	16.1	-19.1
1.0	*C. subtriangulata*	-5.4	16.4	-18.8
1.0	*C. subtriangulata*	-5.7	16.2	-19.0
1.2	*C. subtriangulata*	-4.8	16.6	-18.7
1.2	*C. subtriangulata*	-4.0	17.1	-18.2
1.2	*C. subtriangulata*	-4.5	16.9	-18.3
1.4	*C. subtriangulata*	-4.0	17.2	-18.1
1.4	*C. subtriangulata*	-4.4	16.4	-18.8
1.4	*C. subtriangulata*	-4.1	16.7	-18.5
1.6	*C. subtriangulata*	-4.1	15.7	-19.5
1.6	*C. subtriangulata*	-4.2	16.0	-19.2
1.6	*C. subtriangulata*	-4.8	16.0	-19.2
2.0	*C. subtriangulata*	-5.6	14.9	-20.2
2.8	*C. subtriangulata*	-6.7	21.4	-14.0
2.8	*C. subtriangulata*	-6.8	20.5	-14.9
3.0	*C. subtriangulata*	-3.6	19.8	-15.5
3.0	*C. subtriangulata*	-5.3	20.9	-14.5
3.2	*C. subtriangulata*	-4.4	20.2	-15.2
3.2	*C. subtriangulata*	-5.0	20.2	-15.1
3.4	*C. subtriangulata*	-4.6	19.6	-15.8
3.4	*C. subtriangulata*	-4.4	19.8	-15.6
3.6	*C. subtriangulata*	-4.5	18.2	-17.1
3.6	*C. subtriangulata*	-4.5	18.3	-17.0
3.8	*C. subtriangulata*	-3.9	17.9	-17.4
3.8	*C. subtriangulata*	-3.1	18.9	-16.4
4.0	*C. subtriangulata*	-4.4	18.7	-16.6
4.0	*C. subtriangulata*	-5.7	18.0	-17.2
4.2	*C. subtriangulata*	-4.2	18.0	-17.2
4.4	*C. subtriangulata*	-3.9	17.6	-17.7
4.4	*C. subtriangulata*	-4.4	17.6	-17.6
4.6	*C. subtriangulata*	-6.2	17.5	-17.7
4.6	*C. subtriangulata*	-4.7	17.3	-18.0
4.8	*C. subtriangulata*	-5.6	18.1	-17.2
4.8	*C. subtriangulata*	-4.5	16.5	-18.8
5.0	*C. subtriangulata*	-5.1	17.3	-17.9
5.0	*C. subtriangulata*	-3.6	16.4	-18.8
5.2	*C. subtriangulata*	-4.1	17.5	-17.8
5.2	*C. subtriangulata*	-4.9	17.7	-17.5

Appendix F - (continued) Oxygen- and carbon-isotope compositions of ostracode valves and clam shells from the Huron Basin cores

Manitoulin sub-basin - Core 596

sediment depth (m)[a]	species	$\delta^{13}C$ (VPDB)	$\delta^{18}O$ (VSMOW)	$\delta^{18}O_{lakewater}$ (VSMOW)[b]
5.4	*C. subtriangulata*	-2.7	16.6	-18.7
5.4	*C. subtriangulata*	-4.3	17.1	-18.2
5.6	*C. subtriangulata*	-4.3	16.9	-18.3
5.6	*C. subtriangulata*	-5.4	17.7	-17.6
5.8	*C. subtriangulata*	-4.6	17.0	-18.3
5.8	*C. subtriangulata*	-3.5	16.1	-19.1
6.0	*C. subtriangulata*	-3.9	17.4	-17.9
6.0	*C. subtriangulata*	-4.6	18.1	-17.2
6.1	*C. subtriangulata*	-3.5	16.7	-18.5
6.1	*C. subtriangulata*	-2.4	16.5	-18.7
6.3	*C. subtriangulata*	-3.7	18.0	-17.3
6.3	*C. subtriangulata*	-3.6	16.7	-18.5
6.5	*C. subtriangulata*	-5.6	17.4	-17.9
6.5	*C. subtriangulata*	-4.3	16.3	-18.9
6.7	*C. subtriangulata*	-5.2	18.3	-17.0
6.7	*C. subtriangulata*	-4.6	18.5	-16.8
6.9	*C. subtriangulata*	-4.0	18.3	-17.0
6.9	*C. subtriangulata*	-3.8	18.7	-16.6
7.1	*C. subtriangulata*	-3.3	17.6	-17.7
7.1	*C. subtriangulata*	-4.3	17.5	-17.8
7.3	*C. subtriangulata*	-4.1	17.5	-17.8
7.3	*C. subtriangulata*	-3.2	17.5	-17.8
7.5	*C. subtriangulata*	-4.4	16.9	-18.3
7.5	*C. subtriangulata*	-4.8	17.1	-18.2
7.7	*C. subtriangulata*	-5.4	17.3	-17.9
7.7	*C. subtriangulata*	-4.3	16.4	-18.9
7.9	*C. subtriangulata*	-3.3	15.9	-19.3
7.9	*C. subtriangulata*	-5.3	16.4	-18.8
8.1	*C. subtriangulata*	-3.8	15.9	-19.3
8.1	*C. subtriangulata*	-3.4	16.5	-18.7
8.3	*C. subtriangulata*	-4.0	17.1	-18.2
8.3	*C. subtriangulata*	-5.2	16.6	-18.6
8.5	*C. subtriangulata*	-2.7	16.8	-18.4
8.5	*C. subtriangulata*	-5.0	16.7	-18.6
8.7	*C. subtriangulata*	-3.0	17.0	-18.3
8.7	*C. subtriangulata*	-3.5	17.2	-18.1
8.9	*C. subtriangulata*	-2.4	17.4	-17.9
8.9	*C. subtriangulata*	-3.4	17.2	-18.0
9.1	*C. subtriangulata*	-2.8	16.8	-18.5
9.3	*C. subtriangulata*	-2.1	18.4	-16.9
9.3	*C. subtriangulata*	-2.3	18.4	-16.9
9.5	*C. subtriangulata*	-1.5	19.0	-16.3
9.5	*C. subtriangulata*	-2.3	18.7	-16.6
9.7	*C. subtriangulata*	-1.4	19.0	-16.3
9.9	*C. subtriangulata*	-1.5	18.8	-16.6
10.3	*C. subtriangulata*	-1.2	18.7	-16.6

Appendix F - (continued) Oxygen- and carbon-isotope compositions of ostracode valves and clam shells from the Huron Basin cores

Manitoulin sub-basin - Core 596

sediment depth (m)[a]	species	$\delta^{13}C$ (VPDB)	$\delta^{18}O$ (VSMOW)	$\delta^{18}O_{lakewater}$ (VSMOW)[b]
10.3	*C. subtriangulata*	-1.2	18.8	-16.5
10.5	*C. subtriangulata*	-1.6	18.8	-16.5
10.7	*C. subtriangulata*	-2.1	18.8	-16.5

[a] Top of 20-cm sediment interval

[b] as calculated using measured fractionation factors for each species, see text

Appendix G - Oxygen- and hydrogen-isotope compositions of porewater samples

Goderich sub-basin core 594

sediment depth (m)	$\delta^{18}O$ (VSMOW)	δD (VSMOW)
0.10	-7.6	-60
0.20	-7.5	-57
0.30	-7.6	-56
0.40	-7.6	-57
0.50	-7.7	-60
0.60	-7.7	-58
0.70	-7.7	-59
0.80	-7.7	-61
0.90	-7.8	-59
1.10	-7.9	-61
1.20	-7.9	-60
1.30	-7.9	-62
1.40	-8.0	-62
1.50	-8.0	-63
1.60	-7.9	-62
1.70	-7.9	-62
1.80	-8.0	-62
1.90	-7.9	-63
2.10	-7.9	-61
2.20	-8.0	-62
2.30	-8.0	-64
2.40	-8.1	-63
2.50	-8.1	-64
2.60	-8.0	-64
2.70	-8.0	-64
2.80	-7.9	-66
2.90	-8.0	-64
3.10	-8.0	-64
3.20	-8.1	-65
3.30	-8.2	-65
3.40	-8.2	-66
3.50	-8.2	-63
3.60	-8.2	-66
3.70	-8.2	-66
3.80	-8.2	-66
3.90	-8.2	-65
4.10	-8.4	-64
4.20	-8.5	-64
4.30	-8.4	-65
4.40	-8.4	-65
4.50	-8.3	-66
4.60	-8.4	-65
4.70	-8.5	-67
4.80	-8.5	-66
4.90	-8.4	-67
5.10	-8.4	-66
5.20	-8.6	-66
5.30	-8.5	-66
5.40	-8.5	-65
5.55	-8.6	-66
5.70	-8.5	-66
5.80	-8.6	-67
5.90	-8.6	-65
6.00	-8.6	-65
6.30	-8.6	-65
6.39	-8.7	-65
6.50	-8.8	-64
6.60	-8.8	-66
6.70	-8.8	-66
6.80	-8.7	-67
6.90	-8.9	-66
7.00	-8.9	-65
7.10	-8.9	-66
7.30	-8.9	-67
7.40	-8.9	-68
7.50	-9.0	-67
7.60	-9.0	-68
7.70	-9.0	-68
7.80	-9.0	-69
7.90	-9.0	-68
8.01	-9.0	-66
8.10	-9.1	-70
8.30	-9.2	-65
8.40	-9.1	-70
8.50	-9.1	-69
8.60	-9.2	-70
8.70	-9.1	-72
8.80	-9.1	-69
8.90	-9.2	-71
9.00	-9.4	-71
9.10	-9.2	-71
9.30	-9.3	-71
9.40	-9.3	-70
9.50	-9.4	-72

Appendix G - (continued) Oxygen- and hydrogen-isotope compositions of porewater samples

Goderich sub-basin core 594

sediment depth (m)	$\delta^{18}O$ (VSMOW)	δD (VSMOW)
9.60	-9.3	-72
9.70	-9.4	-72
9.80	-9.4	-75
9.90	-9.4	-72
10.00	-9.5	-73
10.10	-9.3	-72
10.30	-9.5	-73
10.40	-9.5	-74
10.50	-9.6	-76
10.60	-9.5	-73
10.70	-9.5	-71
10.80	-9.6	-71
10.90	-9.6	-73
11.00	-9.6	-73
11.10	-9.6	-74
11.30	-9.7	-75
11.40	-9.7	-74
11.50	-9.6	-75
11.60	-9.5	-76
11.70	-9.6	-72
11.80	-9.5	-72
11.90	-9.6	-74
12.00	-9.6	-71
12.10	-9.7	-73
12.20	-9.6	-74
12.30	-9.7	-73
12.50	-9.7	-74
12.60	-9.7	-70
12.70	-9.4	-72
12.80	-9.5	-74
12.90	-9.5	-73
13.00	-9.5	-74
13.10	-9.5	-72
13.20	-9.4	-72
13.30	-9.3	-74
13.50	-9.3	-75
13.60	-9.3	-73
13.70	-9.4	-71
13.80	-9.4	-73
13.90	-9.4	-69
14.00	-9.3	-69
14.10	-9.3	-70
14.20	-9.3	-71
14.30	-9.2	-72
14.50	-9.3	-70
14.60	-9.3	-72
14.70	-9.3	-70
14.80	-9.3	-70
14.90	-9.2	-71

Appendix G - (continued) Oxygen- and hydrogen-isotope compositions of porewater samples

Goderich sub-basin core 146-2

sediment depth (m)	$\delta^{18}O$ (VSMOW)	δD (VSMOW)
0.10	-7.1	-57
0.20	-7.1	-60
0.30	-7.0	-57
0.40	--	-57
0.50	--	-61
0.60	-7.1	-61
0.70	-7.1	-61
0.80	-7.1	-61
0.90	-7.2	-60
1.10	-7.2	-62
1.20	-7.2	-60
1.30	-7.3	-60
1.40	-7.2	-60
1.50	-7.3	-59
1.60	-7.3	-60
1.70	-7.3	-61
1.80	-7.2	-60
1.90	-7.3	-57
2.10	-7.4	-59
2.20	-7.4	-58
2.30	-7.6	-57
2.40	-7.4	-61
2.50	-7.5	-60
2.60	-7.3	-60
2.70	-7.3	-61
2.80	-7.3	-59
2.90	-7.4	-59
3.10	-7.5	-60
3.20	-7.5	-60
3.30	-7.5	-61
3.40	-7.4	-60
3.50	-7.4	-60
3.60	-7.5	-60
3.70	-7.5	-60
3.80	-7.5	-60
3.90	-7.5	-60
4.10	-7.7	-62
4.20	-7.7	-61
4.30	-7.7	-62
4.40	-7.7	-61
4.50	-7.6	-62
4.60	-7.6	-61
4.70	-7.6	-62
4.80	-7.5	-62
4.90	-7.4	-61
5.10	-7.9	-64
5.20	-7.8	-64
5.30	-7.8	-64
5.40	-7.7	-64
5.50	-7.8	-63
5.60	-7.8	-63
5.70	-7.8	-62
5.80	-7.7	-61
5.90	-7.7	-62
6.00	-7.8	-61
6.10	-7.9	-62
6.27	-8.5	-65
6.37	-8.4	-65
6.47	-8.5	-65
6.57	-8.4	-65
6.67	-8.4	-65
6.77	-8.3	-65
6.87	-8.4	-66
6.97	-8.4	-66
7.07	-8.5	-66
7.27	-8.6	-67
7.37	-8.7	-67
7.47	-8.6	-67
7.57	-8.6	-65
7.67	-8.6	-64
7.77	-8.6	-66
7.87	-8.6	-65
7.97	-8.7	-66
8.07	-8.8	-66
8.27	-8.8	-68
8.37	-8.7	-69
8.47	-8.7	-67
8.57	-8.6	-67
8.67	-8.5	-67
8.77	-8.6	-67
8.87	-8.5	-68
8.97	-8.7	-67
9.07	-8.6	-67
9.27	-8.8	-69

Appendix G - (continued) Oxygen- and hydrogen-isotope compositions of porewater samples

Goderich sub-basin core 146-2

sediment depth (m)	δ^{18}O (VSMOW)	δD (VSMOW)
9.37	-8.8	-69
9.47	-8.7	-65
9.57	-8.7	-67
9.67	-8.8	-68
9.77	-8.7	-66
9.87	-8.7	-68
9.97	-8.7	-68
10.07	-8.6	-69
10.27	-8.9	-70
10.37	-8.9	-70
10.47	-8.9	-70
10.57	-8.9	-70
10.67	-8.8	-70
10.77	-8.8	-70
10.87	-8.9	-70
10.97	-8.8	-70
11.07	-8.7	-69
11.27	-9.0	-72
11.37	-8.8	-69
11.47	-8.8	-69
11.57	-8.5	-70
11.67	-8.6	-68
11.77	-8.6	-69

Goderich sub-basin core 146-1

sediment depth (m)	δ^{18}O (VSMOW)	δD (VSMOW)
12.37	-9.9	-76
12.47	-9.9	-75
12.57	-10.0	-77
12.67	-9.9	-75
12.77	-9.8	-76
12.87	-9.7	-75
12.97	-9.9	-75
13.07	-9.6	-76
13.17	-9.7	-76
13.37	-9.7	-76
13.47	-9.9	-76
13.57	-9.9	-77
13.67	-9.9	-75
13.77	-9.8	-75
13.87	-9.8	-75
13.97	--	-75
14.07	-9.9	-74
14.17	-9.9	-75
14.37	-10.0	-75
14.47	-9.8	-76
14.57	-9.8	-75
14.67	-9.9	-75
14.77	-9.9	-75
14.87	-9.9	-76

Appendix G - (continued) Oxygen- and hydrogen-isotope compositions of porewater samples

Manitoulin sub-basin core 596

sediment depth (m)	$\delta^{18}O$ (VSMOW)	δD (VSMOW)
0.10	-7.1	-57
0.20	-7.2	-58
0.30	-7.3	-58
0.40	-7.3	-59
0.50	-7.3	-59
0.60	-7.3	-59
0.70	-7.3	-57
0.80	-7.3	-56
0.90	-7.4	-56
1.10	-7.3	-55
1.20	-7.4	-56
1.30	-7.3	-55
1.40	-7.3	-58
1.50	-7.4	-58
1.60	-7.4	-57
1.70	-7.4	-57
1.80	-7.4	-56
1.90	-7.5	-57
2.10	-7.4	-58
2.20	-7.5	-57
2.30	-7.6	-57
2.40	-7.5	-58
2.50	-7.6	-61
2.60	-7.5	-57
2.70	-7.5	-58
2.80	-7.5	-59
2.90	-7.6	-59
3.10	-7.6	-59
3.20	-7.5	-58
3.30	-7.7	-60
3.40	-7.6	-58
3.50	-7.8	-58
3.60	--	-57
3.70	-7.7	-60
3.80	-7.6	-58
3.90	-7.6	-60
4.10	-7.7	-58
4.20	-7.7	-59
4.30	-7.8	-59
4.40	-7.8	-61
4.50	-7.7	-59
4.60	-7.7	-59
4.70	-7.8	-59
4.80	-8.0	-59
4.90	-7.8	-59
5.10	-7.8	-59
5.20	-8.0	-59
5.30	-7.8	-60
5.40	-7.9	-59
5.50	-8.0	-61
5.60	-8.0	-61
5.70	-7.9	-60
5.80	-7.9	-60
5.90	-7.9	-61
6.00	-7.9	-62
6.20	-7.9	-63
6.30	-7.9	-63
6.39	-8.1	-62
6.50	-7.9	-63
6.60	-8.0	-64
6.70	-8.0	-64
6.80	-8.0	-63
6.90	-8.1	-62
7.00	-8.0	-62
7.20	-8.2	-61
7.30	-8.1	-63
7.40	-8.2	-63
7.50	-8.1	-64
7.60	-8.1	-62
7.70	-8.2	-60
7.80	-8.2	-63
7.90	-8.3	-62
8.01	-8.4	-62
8.20	-8.4	-63
8.30	-8.5	-62
8.40	-8.5	-65
8.50	-8.4	-63
8.60	-8.5	-63
8.70	-8.5	-64
8.80	-8.5	-63
8.90	-8.5	-66
9.00	-8.4	-66
9.20	-8.6	-63
9.30	-8.5	-64

Appendix G - (continued) Oxygen- and hydrogen-isotope compositions of porewater samples

Manitoulin sub-basin core 596

sediment depth (m)	$\delta^{18}O$ (VSMOW)	δD (VSMOW)
9.40	-8.5	-67
9.50	-8.6	-67
9.60	-8.6	-65
9.70	-8.5	-64
9.80	-8.6	-63
9.90	-8.7	-66
10.00	-8.7	-64
10.20	-8.7	-67
10.30	-8.6	-64
10.40	-8.7	-66
10.50	-8.7	-65
10.60	-8.8	-65
10.70	-8.9	-65
10.80	-8.8	-67
10.90	-9.0	-67
11.00	-9.0	-67

Appendix G - (continued) Oxygen- and hydrogen-isotope compositions of porewater samples

<u>South Chippewa sub-basin core 101</u>

sediment depth (m)	$\delta^{18}O$ (VSMOW)	δD (VSMOW)
9.80	-7.3	--
9.90	-7.3	--
10.00	-7.3	--
10.10	-7.3	--
10.20	-7.3	--
10.30	-7.2	--
10.40	-7.2	--
10.50	-7.2	--
10.60	-7.2	--
10.70	-7.1	--
10.80	-7.1	--
11.00	-7.3	--
11.10	-7.3	-53
11.20	-7.3	--
11.30	-7.4	--
11.40	-7.3	-55
11.50	-7.3	-55
11.60	-7.4	--
11.70	-7.4	--
11.80	-7.3	--
12.00	-7.4	--
12.10	-7.3	-53
12.20	-7.5	-53
12.30	-7.5	--
12.40	-7.5	-54
12.50	-7.5	-54
12.60	-7.5	-56
12.70	-7.5	-55
12.80	-7.5	--
13.00	-7.5	-55
13.10	-7.5	-55
13.20	-7.5	-57
13.30	-7.5	-56
13.40	-7.4	-54
13.50	-7.4	--
13.60	-7.4	-55
13.70	-7.5	-56
13.80	-7.5	-56
14.00	-7.5	-57
14.10	-7.6	-54
14.20	-7.6	-56
14.30	-7.6	-55
14.40	-7.5	-55
14.50	-7.5	-55
14.60	-7.6	-55
14.70	-7.6	-55
14.80	-7.5	-54
15.00	-7.6	-57
15.10	-7.6	-56
15.20	-7.6	-57
15.30	-7.7	-56
15.40	-7.6	-57
15.50	-7.6	-57
15.60	-7.5	-57
15.70	-7.5	-56
15.80	-7.6	-57
16.00	-7.7	-56
16.10	-7.7	-56
16.20	-7.7	-56
16.30	-7.7	-56
16.40	-7.7	-57
16.50	-7.7	-56
16.60	-7.5	-56

CURRICULUM VITAE

Name:	Rebecca Amy Macdonald
Post-Secondary Education and Degrees:	The University of Western Ontario, London, Ontario, Canada 1999 – 2003 Hons. B.Sc. in Geology with Environmental Science The University of Western Ontario, London, Ontario, Canada 2003 – 2012 Ph.D. in Geology
Honours and Awards:	Dean's Honours List, 2002 – 2003, 2003 – 2004 Western Graduate Research Scholarship, 2003 – 2007 The Lumsden Award in Earth Sciences – 2004, 2005, 2006, 2011, 2012 Michigan Basin Geological Society Scholarship, 2006 Ontario Graduate Scholarship in Science & Technology, 2007 – 2008
Related Work Experience:	Teaching Assistant The University of Western Ontario 2003 – 2008 Sessional Lecturer The University of Western Ontario, Isotope Geochemistry in Earth and Environmental Sciences Fall term 2010 Sessional Lecturer The University of Western Ontario, Waters and Geochemical Cycles Winter term 2012

Publications:

Macdonald RA, Longstaffe FJ (2008) The Late Quaternary oxygen isotope composition of Lake Huron. Aquatic Ecosystem Health and Management 11: 137-143

Abstracts and Presentations:

Macdonald RA, Longstaffe FJ (2012) A stable isotope investigation of the Late Quaternary evolution of Lake Michigan. Ontario-Québec Paleolimnology Symposium (PALS), The University of Western Ontario, London, Ontario.

St. Amour NA, Longstaffe FJ, **Macdonald RA**, Crowe AS (2012) Factors influencing variability in Great Lakes water isotope compositions. Ontario-Québec Paleolimnology Symposium (PALS), The University of Western Ontario, London, Ontario.

Longstaffe FJ, Ayalon A, Crowe A, Hladyniuk R, Huddart P, Hyodo A, **Macdonald R** (2011) Climate Change and the Oxygen-Isotope Evolution of the North American Great Lakes. International Atomic Energy Agency, Monaco.

Longstaffe FJ, Ayalon A, Bumstead N, Crowe A, Hladyniuk R, Huddart P, Hyodo A, **Macdonald R** (2011) The Oxygen-Isotope Evolution of the North American Great Lakes. Geological Society of America, Pittsburgh, Pennsylvania.

North RL, Barton D, Bhavsar S, Borwick J, Bumstead N, Crowe AS, Dillon PJ, Dolson R, Evans DO, Gee K, Gewurtz S, Ginn B, Hakanson L, Hawryshyn J, Helm P, Hiriart-Baer V, Jarjanazi H, Kelly N, King JW, Landre A, La Rose J, Lewis CFM, Lin ZH, Longstaffe FJ, **Macdonald RA,** Metcalfe B, Milne J, Moles M, Molot L, Ozersky T, Quinlan R, Rennie MD, Robillard M, Rodé D, Rühland KM, Smol JP, Soliman C, Stainsby E, Weseloh C, Willox C, Winter JG, Yan N, Young JD (2010) State of Lake Simcoe. International Association of Great Lakes Research, University of Toronto, Toronto, Ontario.

Macdonald RA, Longstaffe FJ, Crowe AS, Lewis CFM, King JW (2009) Stable Isotope Compositions of Great Lake Porewaters and Evidence for Groundwater Seepage into Kempenfelt Bay, Lake Simcoe. SIMSYN 2009, Toronto, Ontario. [oral presentation]

Macdonald RA, Hyodo A, Hladyniuk R, Bumstead NL, Longstaffe FJ, Crowe AJ (2009) Current Great Lakes (Paleo-) Research at The University of Western Ontario. SIMSYN 2009, Toronto, Ontario. [poster presentation]

Bumstead NL, Longstaffe FJ, **Macdonald RA** (2009) Paleolimnology of Lake Simcoe using Stable Isotopes and Assemblages. SIMSYN 2009, Toronto, Ontario.

Longstaffe FJ, Lewis CFM, King JW, Heil CW Jr, Hubeny JB, Goodyear DR, Slattery SR, **Macdonald RA** (2008) Stable Isotope Evidence for Groundwater Seepage into Kempenfelt Bay, Lake Simcoe. International Association of Great Lakes Research, Trent University, Peterborough, Ontario. [oral presentation]

Lewis CFM, King JW, Heil CW JR, Hubeny JB, **Macdonald RA**, Shumchenia EJ, Goodyear DR, Slattery SR (2008) Lake Simcoe Sediment Architecture: Evidence for a

Lowstand During Early Holocene Dry Climate. International Association of Great Lakes Research, Trent University, Peterborough, Ontario.

Macdonald RA, Longstaffe FJ, Crowe AS (2007) The Late Quaternary oxygen isotope composition of Lake Michigan. EOS Trans 88: PP13B-1283. AGU, San Francisco. [poster presentation]

Macdonald RA, Longstaffe FJ (2007) The oxygen and hydrogen isotope compositions of the Great Lakes. Programs and Abstracts of the 50th Conference on Great Lake Research, pp 117-118. Pennsylvania State University, University Park, Pennsylvania. [oral presentation]

Macdonald RA, Longstaffe FJ (2006) The Late Quaternary oxygen isotope composition of Lake Huron. The State of Lake Huron conference, Honey Harbour, Ontario. [oral presentation]

Macdonald RA (2005) Paleoclimatic reconstructions of the Lake Huron Basin using stable isotopes. ERW Colloquium. UWO Environmental Sciences Program. The University of Western Ontario, London Ontario. [oral presentation]

Macdonald RA, Longstaffe FJ (2004) The oxygen and hydrogen isotope composition of Lake Huron. EOS Trans 85: PP43A-0621. AGU, San Francisco. [poster presentation]